THERMODYNAMIC ENVIRONMENTAL FATE MODELLING

By

Daniel Vorenberg

A dissertation submitted in the
School of Chemical Engineering
University of Natal
Durban

In fulfillment of the requirements for the degree
Master of Science in Engineering (Chemical)

January 2002
Prof. D. Ramjugernath

Declaration

The work presented in this dissertation was performed at the University of Natal, Durban at the School of Chemical Engineering, from January 2001 to December 2002, under the supervision of Prof. D. Ramjugernath and Prof. C.A. Buckley.

This dissertation is submitted as full requirement for the degree of Master of Science in Engineering (Chemical). All the work that is presented in this dissertation is my own, except as otherwise specifically acknowledged in the text. This work has not been submitted in part, or in whole to any other University.

_____

D. Vorenberg

As the candidate's supervisor I have approved this thesis for submission

Signed: _____

Name: _____

Date: _____

Acknowledgements

I am indebted to my supervisors, Prof. D. Ramjugernath and Prof. C.A. Buckley, for their guidance, advice and assistance during the duration of this project.

I would also like to express my appreciation and gratitude to the following persons:

To Prof. J.D. Raal, Prof. T.M. Letcher and Mr. T. Leske, University of Natal, for their advice and assistance.

To Prof. S.I. Sandler, University of Delaware (USA), for his kindness and hospitability, and for the use of his laboratories to conduct some of the measurements undertaken in this project.

To Prof. D. Mackay, Dr. M. MacLeod and Mr. T. Gouin, at Trent University (Canada), for their thought provoking discussions and comments.

To Dr. L. Phillips from SASOL for her efforts relating to this project.

To SASOL and THRIP for their financial assistance.

To my loving parents; brothers, Grant and Paul; and my sister, Jo-anne; for being an endless source of love, encouragement and support.

Abstract

The labelling of methyl tertiary butyl ether (MTBE), an oxygenate additive used extensively in gasoline blending, as an environmentally harmful chemical has led to the banning and subsequent phasing-out of this additive in California (USA). In response, the global petroleum industry is currently considering replacement strategies, which include the use of tertiary amyl methyl ether (TAME) or ethanol. Subsequently, SASOL (South African Coal and Oil Limited), a local petrochemical company, in its capacity as an environmentally responsible player in the global petroleum and aligned chemical markets, has commissioned this investigation into the environmental fate of the fuel oxygenates: TAME, ethanol and MTBE.

In order to evaluate the environmental fate of the oxygenates, this dissertation has formed a three-tiered approach, using MTBE as a benchmark. The first tier assessed the general fate behaviour of the oxygenates using an evaluative model. A generic evaluative model, developed by Mackay et al. (1996a), called the Equilibrium Criterion (EQC) model was used for this purpose. This fugacity based multimedia model showed MTBE and TAME to have similar affinities for the water compartment. Ethanol was demonstrated to have a pre-disposition for the air compartment. Parameterisation of the EQC model to South African conditions resulted in the development of ChemSA, which reiterated the EQC findings.

The second tier quantified the persistence (P), bioaccumulation (B) and long-range transport (LRT) potential of the additives. This tier also included a brief toxicity (T) review. MTBE and ethanol were demonstrated to be persistent and non-persistent, respectively, according to three threshold limit protocols (Convention on the Long Range Trans-boundary Air Pollution Persistent Organic Chemical Protocol; the United Nations Environment Programme Global Initiative; and the Track 1 criteria as defined by the Canadian Toxic Substances Management Policy, as referred to by the Canadian Environmental Protection Act 1999). These protocols were not unanimous in the persistence classification of TAME. Further investigation of persistence was conducted using a persistence and long-range transport multimedia model, called TaPL3, developed by Webster et al. (1998) and extended by Beyer et al. (2000). TaPL3 reiterated the conclusions drawn from the threshold limit protocols, indicating that TAME's classification worsened from non-persistent to persistent on moving from an air emission to a water emission scenario. This served to emphasise the negative water

compartment affinity associated with TAME. Using classification intervals defined by Beyer et al. (2000), TaPL3 demonstrated that the long-range transport potential of the oxygenates increased in the order of TAME, ethanol and MTBE; however, it was concluded that none of the oxygenates were expected to pose a serious long-range transport threat. Bioaccumulation was not expected to be a pertinent environmental hazard. As expected, the oxygenates were dismissed as potential bioaccumulators by the first level of a screening method developed by Mackay and Fraser (2000); as well as by the threshold limit protocols listed above. Simulation of biomagnification, using an equilibrium food chain model developed by Thomann (1989), demonstrated that none of the oxygenates posed a biomagnification threat. A review of toxicity data confirmed that none of the three oxygenates are considered particularly toxic. LD_{50} values indicated the following order of increasing toxicity: ethanol, MTBE and TAME.

The third tier focussed on oxygenate aqueous behaviour. A simple equilibrium groundwater model was used to analyse the mobility of the oxygenates in groundwater. TAME was found to be 21 % less mobile than MTBE. Ethanol was shown to be very mobile; however, the applicability of the equilibrium model to this biodegradable alcohol was limited. An analysis of liquid-liquid equilibria comprised of oxygenate, water and a fuel substitution chemical was performed to investigate fuel-aqueous phase partitioning and the co-solvency effects of the oxygenates. Ethanol was shown to partition appreciably into an associated water phase from a fuel-phase. Moreover, this alcohol was shown to act as a co-solvent drawing fuel chemicals into the water phase. MTBE was found to partition sparingly into the water phase from a fuel-phase, with TAME partitioning less than MTBE. Neither ether was shown to act as a co-solvent.

It was concluded that TAME and ethanol pose less of a burden to the environment than MTBE. Ethanol was assessed to be environmentally benign; however, it was concluded that ethanol's air compartment affinity and the extent of its co-influence on secondary solutes justified the need for further investigation before its adoption as a fuel additive. This project showed sufficient variation in the environmental behaviour of TAME and MTBE to justify the abandonment of the axiom that MTBE and TAME behave similarly in the environment. However, as MTBE is a significant water pollutant, and TAME has been shown to share a similar water affinity, it is cautiously recommended that the assumption of environmental similarity be discarded, except for the water compartment.

Table of contents

List of figures

List of tables

Nomenclature

Symbols

a	Fitted Langmuir isotherm constant in Equation (4-37) [-] or fitted constant to pressure-composition data in Equation (D-3) [kPa]
a_{ij}	Fate parameter in Equation (3-3) indicating transfer from compartment i to compartment j [s^{-1}]
a_η	Parameter (See Table 11-1) for species η in food assimilation coefficient correlation of Thomann (1989) in Equation (11-1) [-]
A	Interfacial area in the direction of flow [m^2]
$\underline{\underline{A}}$	State matrix defined with respect to concentration in Equation (3-5) [s^{-1}] and with respect to fugacity in Equation (B-1) [s^{-1}]
b	Fitted Langmuir isotherm constant in Equation (4-37) [-]or fitted constant to pressure-composition data in Equation (D-3) [kPa]
b_i	Fate parameter in Equation (3-3) representing input source term into compartment I [mol/m^3/s]
b_η	Parameter (See Table 11-1) for species η in food assimilation coefficient correlation of Thomann (1989) in Equation (11-1) [-]
B_{ij}	Second virial coefficient between solute i and solute j [m^3/mol]
$\underline{B}$	Control vector defined with respect to concentration in Equation (3-5) [mol/m3/s] and with respect to fugacity in Equation (B-1) [Pa/s]
$\underline{B}(t)$	Time varying control vector, as defined in Equation (3-5) [mol/(m^3.s)] and used in Equation (A-8) [mol/(m^3.s)]
BAF_η	Bioaccumulation factor of a chemical in a biotic species η [-]
BCF_η	Bioconcentration factor of a chemical in a biotic species η [-]
BMF_η	Biomagnification factor of a chemical in a biotic species η [-]
c	Constant in Junge adsorption model defined in Equation (5-4) [Pa..cm]
c_η	Parameter (See Table 11-1) for species η in food assimilation coefficient correlation of Thomann (1989) in Equation (11-1) [-]
C	Concentration [mol/m^3]

C_D	Drag coefficient [-]
C_i	Concentration of chemical in compartment i [mol/m^3]
C_i^j	Concentration of solute i in compartment j or concentration of component i in bulk compartment j [mol/m^3]
C_i^{bulk}	Concentration of species i in the bulk phase [mol/m^3]
C_i^{sorbed}	Concentration of species i adsorbed to the adsorbent [mol/m^3]
C_{diet}^{η}	Concentration of a chemical in the diet of a biota species η [mol/m^3]
C_{sat}^{w}	Water solubility of chemical [mol/m^3]
$\underline{C}(t)$	Concentration state vector defined in Equation (3-5) [mol/m^3]
Cf	Confidence factor [-]
CTD_i	Characteristic travel distance in compartment i [km]
d_p	Particle diameter [m]
D	Diffusivity [m^2/s]or Mackay transfer coefficient [mol/(Pa.s)]
$D_{ad,i}$	Mackay transfer coefficient describing advection from compartment i [mol/(Pa.s)]
D_{ij}	Mackay transfer coefficient describing transfer from compartment i to j [mol/(Pa.s)]
$D_{r,i}$	Mackay transfer coefficient describing reaction in compartment i [mol/(Pa.s)]
E_i	Emission into compartment i [mol/s]
$\underline{E}$	Emission vector [mol/s]
$\underline{f}$	Fugacity state vector defined in Equation (B-1) [Pa]
$\underline{\dot{f}}$	Fugacity derivative vector defined in Equation (B-1) [Pa/s]
$\hat{f}_i$	Fugacity of chemical in compartment i [Pa]
$\hat{f}_i^j$	Fugacity of solute i in compartment j [Pa]
F	Force [N]
F_η	Rate of consumption of prey species by predator species η [s^{-1}]
g	Gravitational acceleration [9.81 m/s^2]
g_{ij}	NRTL energy interaction parameter between solute i and solute j [J/mol]
G	Volumetric flow rate [m^3/s] or Gibb's molar free energy [J/mol]

G_i	Advection volumetric flow rate in compartment i [m^3/s]
H	Height [m]
H_i^j	Concentration based Henry's constant of solute i in phase or solvent j [$Pa/(m^3.mol)$]
$\hat{H}_i^j$	Mole fraction based Henry's constant of solute i in phase or solvent j [Pa]
$H_i^{E,\infty}$	Infinite dilution excess partial molar enthalpy of solute i [J/mol]
ΔH_d	Heat of desorption [J/mol]
ΔH_v	Heat of vaporisation [J/mol]
I	Input variable
$\underline{\underline{I}}$	Identity (n x n) matrix
I_k	Input variable k
J_z	Molar transport rate in the z direction [mol/s]
$J_{\alpha\rightarrow\beta}$	Molar transport rate from a phase α to a phase β [mol/s]
k_i	First order reaction rate constant for phase or mechanism i [s^{-1}]
$k_{\eta,e}$	Rate constant for decomposition and excretion of chemical from biota species η [s^{-1}]
$k_{\eta,j}$	Rate constant for elimination or uptake mechanism j in biota species η [s^{-1}]
$k_{\eta,w}$	Rate constant for uptake of chemical from water into biota species η [s^{-1}]
k_{OH}	Pseudo-first order hydroxyl radical reaction rate constant [s^{-1}]
k'_{OH}	Second order hydroxyl radical reaction rate constant [$cm^3/(s.molecules)$]
$k_{overall}$	Overall multimedia system first order reaction rate constant [s^{-1}]
K_{aw}	Air-water partition coefficient [-]
K_{bw}	Biota-water partition coefficient [-]
K_d	Sorption coefficient [L/kg]
K_F	Fitted Freundlich isotherm proportionality constant in Equation (4-37) [-]
$K_{i,j}$	Partition coefficient relating phase i to phase j
K_{MM}	Fitted Michaelis-Menten constant in Equation (4-43) [-]
K_{oa}	Octanol-air partition coefficient [-]
K_{oc}	Organic carbon-water partition coefficient [L/kg]

K_{ow}	Octanol-water partition coefficient [-]
K_p	Particle-gas partition coefficient [$m^3/\mu g$]
K_{pa}	Particle-air partition coefficient [-]
K_{va}	Vegetation-air partition coefficient [-]
$K_{\alpha\beta,i}$	Partition coefficients of solute i between compartments α and β respectively [-]
L_η	Lipid fraction (by volume) of biota species η [-]
LC_{50}	Lethal concentration to kill 50 % of a biota population [mg/L]
LD_{50}	Lethal dosage to kill 50 % of a biota population [mL/kg]
m_1, m_2	Constants in Equation (5-7) reported in Bidleman and Harner (2000) [-]
m_j	Mobility of compartment j [m/s]
M	Molar mass of air [g/mol]
M_j	Molar mass of solute or component j [g/mol]
n_i^j	Moles of solute i in phase j [mol]
N_i	Molar inventory in compartment i [mol]
N_s	Number of moles of sorption sites [mol]
O	Output variable
p_i^a	Partial pressure of solute i in the air phase [Pa]
P	Pressure [Pa or kPa] or precipitation rate [mm/a]
$[P]$	Concentration of biological product from enzyme catalysis [mol/m^3]
$P(z)$	Pressure at height z [m]
P_i^{sat}	Saturated vapour pressure of solute i [Pa, kPa or bar]
P_0	Pressure at ground level [kPa]
P_{tot}	Total atmospheric pressure [Pa]
r	Reaction rate [$mol/(m^3.s)$]
R	Ideal gas constant [8.314 J/(mol.K)]
R_j	Compartment-specific spatial range with respect to compartment j [km]
R^2	Linear correlation index
Re_p	Particle Reynolds number defined in Equation (4-39) [-]
S	Sensitivity or molar entropy [J/mol]
$[S]$	Concentration of biological substrate depleted from enzyme catalysis [mol/m^3]

$S_{I,k}$	Sensitivity of model output to the input variable k
t	Time or GC retention time [s]
$t_{1/2,i}$	Half-life of chemical in compartment i [h]
$t_{1/2,overall}$	Overall half-life of chemical in a multimedia system [h]
T	Temperature [K]
TSP	Total suspended particulates [μg/m^3]
u	Fluid velocity [m/s]
u_d	Dry deposition velocity [mm/s]
$u_{d,g}$	Dry gas deposition velocity [mm/s]
$u_{d,p}$	Dry particle deposition velocity [mm/s]
u_i	Velocity of compartment i [m/s]
u_{ij}	UNIQUAC energy interaction parameter between solute i and solute j [J/mol]
u_p	Particle velocity [mm/s]
u_w	Overall wet deposition velocity [mm/a] or groundwater velocity [m/s]
U	Mass transfer coefficient [m/s]
U_i	Mass transfer coefficient in phase i or transport coefficient of mechanism i [m/h]
$U^i_{overall}$	Overall mass transfer coefficient with respect to phase i [m/h]
V_i	Volume of compartment i [m^3]
$\underline{V_i}$	Eigenvector (n x 1)
V_i^L	Liquid molar volume of species i [m^3/mol]
V_{tot}^j	Total volume of phase j [m^3]
$\tilde{V}_w$	Molar volume of water [m^3/mol]
VP_i	Vapour pressure constant in Equation (7-1) for i = 1, 2, 3 and 4 [-]
W	Atmospheric washout ratio [-]
W_g	Wet gas washout ratio [-]
W_p	Wet particle washout ratio [-]
x_i	Mole fraction of chemical in compartment i [-]
x_i^j	Mole fraction of solute i in compartment j [-]

y_i	Vapour phase mole fraction of solute i [-]
y_i	Mass fraction of component i in a solid sorbing medium [-]
Y_i	Fractional distribution of chemical in compartment i [-]
z	Displacement in the z-axis direction [m]
Δz	Stagnant film thickness [m]
Z_i	Fugacity capacity factor of chemical in compartment or sub-compartment i [mol/(m^3.Pa)]
Z_i^j	Fugacity capacity factor of solute i in compartment j [mol/(m^3.Pa)]
$\underline{0}$	Null (n x 1) vector

Greek letters

α	Constant in NRTL activity coefficient model [-]
α_i	Constant in Equation (A-6) [-]
α_i^{ss}	Constant in Equation (A-7) [-]
α_η	Assimilation efficiency of food consumed by biota species η [-]
α_{BA}	Net retention ratio of solute B with respect to solute A [-]
β_j	Vapour phase non-ideality constant defined in Equation (D-2) [-]
$\beta_{i,j}$	Selectivity factor of chemical between phase i and phase j [-]
δ_η	Food assimilation coefficient for species η as defined by Thomann (1989) [-]
Δ	Difference between calculated property and experimental property
ε_i	Volumetric fraction of phase i in bulk soil [-]
ε_i^∞	Vapour phase non-ideality constant defined in Equation (D-2) [-]
ϕ	Fraction of chemical sorbed to sorbent [-]
ϕ_i^a	Fugacity coefficient of solute i in the air phase [-]
γ_i^j	Activity coefficient of component or solute i in phase j [-]
$\gamma_i^{j,\infty}$	Infinite dilution activity coefficient of solute i in phase j [-]
λ_i	Eigenvalue

λ_{ij}	Wilson (1964) activity coefficient model interaction parameter between solute *i* and solute *j* [J/mol]
μ	Fluid viscosity [Pa.s]
μ_i^j	Chemical potential of solute *i* in phase *j* [J/mol]
μ_{MM}	Fitted Michaelis-Menten constant in Equation (4-43) [s^{-1}]
v_i^j	Volume fraction of sub-compartment *i* in bulk compartment *j* [-]
θ	Surface area per unit volume [cm^2 aerosol/cm^3 air]
θ_η	Baseline biomagnification factor for species η defined with respect to the primary producer species [-]
$\Theta(t)$	Integration constant in Equation (A-22) [J/mol]
ρ	Fluid density [kg/m^3]
ρ_p	Particle density [kg/m^3]
ρ_{tot}^j	Total density of phase *j* [kg/m^3]
σ	Standard deviation
σ^2	Variance
$\sigma_{I,k}^2$	Variance of input variable *k*
τ	Overall persistence [h]
τ_{ad}	Advection persistence defined in Equation (B-2) [h]
τ_r	Reaction persistence defined in Equation (B-3) [h]
ξ	Dispersion coefficient [m^2/s]

Superscripts

a	air
abs	absorption
b	biota
dep	deposition
diff	diffusion
eq	equilibrium
or	octanol-rich
p	aerosol particulate matter

rain	rain dissolution
resusp	resuspension
s	soil
sat	saturated
sed	sediment
ss	steady state or suspended solids
v	vegetation
vol	volatilisation
w	water
wr	water-rich
∞	infinite dilution

Subscripts

a	air
c	critical property
I	input
NO_3	nitrate radicals
oc	organic carbon
om	organic matter
oxy	oxygenate
O	output
O_3	ozone
OH	hydroxyl radicals
p	aerosol particulate matter
photo	photolysis
ref	reference
tot	total
tropo	troposphere
w	water
0	initial
η	biota species

Abbreviations

ASOG	Analytical Solution Of Groups group contribution model
B	Bioaccumulation
BAF	Bioaccumulation factor
BCF	Bioconcentration factor
BMF	Biomagnification factor
BTEX	Benzene, toluene, ethylbenzene and xylenes
CART	Classification and Regression Tree
Cf	Confidence factor
CLRTAP POP	Convention on Long Range Trans-boundary Air Pollution Persistent Organic Chemical
CTD	Characteristic travel distance
EDB	Ethylene dibromide
EPICS	Equilibrium Partitioning In Closed Systems
EQC	Equilibrium Criterion model developed by Mackay et al (1996a)
EUSES	European Union System for the Evaluation of Substances
FID	Flame ionisation detector
GC	Gas chromatogrpahy
GLC	Gas-Liquid Chromatography
HPLC	High Pressure Liquid Chromatography
HSC	Headspace Chromatography
IGS	Inert Gas Stripping
LLE	Liquid-liquid equilibrium
LOAEL	Lowest-observed-adverse-effects level
LRAT	Long-range air transport
LRT	Long-range transport
LSER	Linear solvation energy relationship
MTBE	Methyl tertiary butyl ether or 2-methoxy-2-methylpropane
MTC	Mass transfer coefficient
NO_3	Nitrate radical
NOAEL	No-observed-adverse-effects level
NO_x	Nitrogen oxide
NRTL	Non-random Two liquid activity coefficient model
OH	Hydroxyl radical
ppb	Parts per billion
ppm	Parts per million

P	Persistence
PAH	Polyaromatic hydrocarbons
PCB	Polychlorinated biphenyls
PBT-LRT	Persistence, bioaccumulation, toxicity and long-range transport profile
PDD	Activity coefficient correlation of Pierotti, Deal and Derr (Pierotti et al., 1959)
POP	Persistent organic pollutants
QSAR	Quantitative structure-activity relationship
PRI	Pollution Release Inventory
RFG	Reformulated gasoline
RGLC	Relative Gas Liquid Chromatography
RP HPLC	Reverse Phase High Pressure Liquid Chromatography
STP	Standard temperature and pressure
SVOC	Semi-volatile organic compounds
T	Toxicity
TAME	Tertiary amyl methyl ether or 2-methoxy-2-methylbutane
TaPL3	Level III transport and persistence model developed by Webster et al. (1998)
TCD	Thermal conductivity detector
TEL	Tetraethyl lead
TMP	i-octane or 2,2,4-trimethylpentane
TSMP	Toxic Substances Management Policy
TSP	Total suspended particulates
UNEP	United Nations Environment Programme
UNIFAC	UNIQUAC Functional group Activity Coefficient model
UNIQUAC	Universal quasi-chemical activity coefficient model
US EPA	United States Environmental Protection Agency
vol	Volume
VLE	Vapour-liquid equilibrium
VOC	Volatile organic compound
wt	Weight

Preface

The significant problems we face cannot be solved at the same level of thinking we were at when we created them.

Albert Einstein (1879-1955)

This dissertation is comprised of thirteen chapters. The first two chapters are introductory in nature. The middle five chapters review the relevant theory and literature pertaining to the environment and environmental fate modelling. Lastly, the remaining six chapters present the results and conclusions generated from the three-tiered investigation used to assess the environmental fate of the gasoline oxygenates: methyl tertiary butyl ether (MTBE), tertiary amyl methyl ether (TAME) and ethanol.

Chapter 1 outlines the objectives and nature of this dissertation indicating the evaluation techniques used to assess environmental fate. Chapter 2 provides background information establishing perspective to the environmental problems facing current additives. Included in this chapter is a recount of the history of fuel additives and a description of the benefits and drawbacks of the gasoline oxygenates investigated in this study.

Chapter 3 introduces environmental fate modelling and assessment from its general classification to its mass-balance foundation. In Chapter 4, the equilibrium partitioning of solutes in the environment is explored. This chapter also expands upon environmental processes that are significant to the fate of a chemical in the environment. Chapter 5 elucidates the various media and compartments, which comprise the environment, and elaborates on current methodology used to model these compartments. Chapter 6 expatiates on the numerous multimedia models available in literature. Chapter 7 discusses and presents a compilation of the oxygenate properties, which are relevant in the assessment of their environmental fate behaviour.

In Chapter 8, the general fate characteristics of the oxygenates using a generic multimedia model are examined. Additionally, this chapter includes a fate assessment performed using a

multimedia model parameterised to South African conditions, named ChemSA. Chapter 9 evaluates the persistence and long-range transport potential of the three oxygenates. In Chapter 10, the bioaccumulation and biomagnification tendencies of the oxygenates are investigated. Chapter 11 reviews toxicity data available for the three oxygenates, completing their PBT-LRT (persistence, bioaccumulation, toxicity and long-range transport) profile. Chapter 12 explores the thermodynamic behaviour of the water-soluble oxygenates associated with the aqueous phase investigating groundwater mobility, aqueous-fuel phase partitioning and co-solvency tendencies. Chapter 13 integrates the fate assessment results and conclusions obtained in preceding chapters and presents the overall environmental assessment of the oxygenates, including recommendations gleamed from the project.

CHAPTER 1

Introduction

Every year, hundreds of new compounds, as well as approximately 250 million metric tons of synthetic organic chemicals (Korte, 1992), are introduced into the chemical market. It is inevitable that a fraction of these chemicals will breach the boundary separating the technosphere and the biosphere. Consequently, in order to market and steward new products or continue to sell existing high production volume chemicals, accurate understanding and determination of the possible pathways of biosphere contamination need to be presented to the governing environmental agencies. Accordingly, a new branch of environmental science has been founded to describe and quantify the behaviour of chemicals in the environment. This branch of environmental science is termed environmental fate modelling or chemodynamics.

As environmental agencies learn from the anthropogenic problems of the past, the control, regulations and restrictions on new and existing chemical products are becoming more stringent. The responsibility of safeguarding our environment does not rest solely on government: Three important players, comprised of the governing authority, the environmentally-responsible company, and the surrounding communities, each with its own objectives and needs, have a role to play in ensuring the protection of our planet.

In recent years, attention has been drawn to methyl tertiary butyl ether (MTBE, 2-methoxy-2-methylpropane), a synthetic organic compound that was introduced as a technological solution to a technology-derived problem. MTBE was added to gasoline with the intent to reduce air emissions, making the fuel burn more cleanly. Ironically, the use of this additive has alleviated air pollution at the expense of creating a widespread water pollution problem.

In March 2000, the United States Environmental Protection Agency (US EPA) issued a recommendation for the phasing-out and the ultimate ban of MTBE as a fuel additive used in reformulated and oxygenated gasoline. Numerous strategies exist for the replacement of MTBE, ranging from no oxygenate addition to mixtures of oxygenates blended to gasoline

(Nadim et al., 2001). Two possible replacement additives for the banned oxygenate include tertiary amyl methyl ether (TAME, 2-methoxy-2-methylbutane) and ethanol.

The recent commitment of the state of California (USA) to begin the phasing-out of MTBE (Jacobs et al., 2001) has pre-empted SASOL (South African Coal and Oil Limited), a local petrochemical company, in its capacity as an environmentally responsible player in the global petroleum and aligned chemical markets, to commission an investigation into the environmental fate of the fuel oxygenates: TAME, ethanol and MTBE. This is in line with a current international call for the collection of research on fuel additives, in particular, regarding TAME [US EPA (1996)].

This above investigation was undertaken at the University of Natal, Durban's School of Chemical Engineering in the form of a research project towards an MScEng degree. The project involved the following objectives:

- To perform an extensive literature survey on the topic of environmental fate modelling, reviewing models and fate analysis methods available.
- Collection of all relevant physical and chemical data required as inputs in the fate analysis and the measurement of outstanding thermodynamic data.
- Formulation of an environmental thermodynamic fate multimedia model customised to South African conditions.
- Evaluation of the environmental fate of TAME and ethanol using MTBE as a benchmark.

In order to evaluate the environmental fate of the three oxygenates, this dissertation has formed a three-tiered approach. The first tier evaluates the fate behaviour of the oxygenates in a generic environment and, subsequently, in a model parameterised to South African conditions. This tier identifies the general fate characteristics of the oxygenates in the environment. The second tier evaluates the persistence (P), bioaccumulation (B) and long-range transport (LRT) potential of MTBE, TAME and ethanol. This tier includes a brief toxicity (T) review. Lastly, the third tier, focuses on the aqueous medium, investigating the groundwater mobility of the three oxygenates and the thermodynamic behaviour of three-component systems consisting of oxygenate, water and a pseudo-fuel chemical. The latter investigation is included to account for a simplifying

assumption evoked in environmental models that compounds found in a mixture do not interact with each other.

The three-tiered investigation of this dissertation was formulated to address three issues pertaining to oxygenates and the environment. The environmental issues were identified with respect to the benchmark species, MTBE, and have been selected to highlight areas of significant gravity pertaining to the environmental behaviour of the banned oxygenate and its possible replacements. Firstly, MTBE has been classified as a recalcitrant species, especially in water, owing to its low environmental degradation rates. The applicability of this issue to the other oxygenates is addressed in the second-tier of this investigation which quantifies the oxygenates' persistence and other important environmental markers. Secondly, MTBE partitions rapidly into groundwater without any natural attenuation. This concern is addressed by the third tier of the investigation which analyses the aqueous behaviour of the oxygenates including a groundwater mobility simulation. The third issue addressed in this dissertation is the accepted axiom that TAME will behave similarly to MTBE in the environment (Pankow et al., 1997; Nadim et al., 2001). This matter is addressed by all three tiers of the assessment. Combined, this dissertation forms an unmitigated environmental assessment of MTBE, TAME and ethanol, evaluating their complete environmental fate and their PBT-LRT profiles.

CHAPTER 2

Background

2.1 History of fuel additives

In the early 20th century, automotive engineers discovered that engines operating in the absence of knock effects performed more efficiently and considerably smoother. In 1916, Thomas Midgely, a research scientist employed at the Dayton Research Laboratories (Ohio) discovered that the addition of iodine to gasoline greatly reduced the knock effects. He related engine knocks to low fuel combustion quality, which was later defined as the fuel octane. Iodine blended into gasoline raised the octane, eliminating the knock effects; however, this additive suffered from two drawbacks: it was corrosive and relatively expensive (Nadim et al., 2001).

Midgely, in a collaborative research project with Charles Kettering in 1917, blended grain alcohol with gasoline, proclaiming this alcohol additive had many advantages over other additives. The advantages included: burning more cleanly, increased octane, and higher engine compression ratios. In February 1920, Midgely applied for a patent for the blend of alcohol and gasoline as an anti-knock fuel (Lincoln, 2000).

During his research on gasoline additives, Midgely discovered the anti-knock properties of tetraethyl lead (TEL) in December 1921. Research on alcohol-gasoline blends continued until August 1925, when Kettering announced the discovery of a new fuel called "Synthol", a mixture of alcohol and gasoline, which purportedly could double gas mileage. Oil companies preferred TEL to other alcohol additives, as the reduction of a vehicles' gasoline use would have left cars less dependent on petroleum products (Nadim et al., 2001).

In 1923, well-known public health and medical authorities including Reid Hunt of Harvard, Yandell Henderson of Yale and Erik Krause of the Institute of Technology (Postdam, Germany) communicated their concerns to Midgely, regarding TEL and its toxic characteristics (Lincoln, 2000). William Mansfield Clark, a laboratory director in the United States Public

Health Service wrote to his superior, A.M. Stimson, the Surgeon General, warning him that the widespread usage of TEL as a gasoline additive would have accumulative toxic effects. Disregarding the warnings, the Surgeon General decided to rely solely on industry to supply the relevant investigative data. Unwittingly, this decision made at this time did not allow a comprehensive understanding of the drawbacks of TEL till many decades after its discovery (Nadim et al., 2001).

The Clean Air Act was ratified by US President Nixon in December 1970 and the phasing-out of leaded gasoline began in December 1973. The primary phase of this program was completed in 1986. A complete ban on the use of leaded gasoline for highway vehicles was implemented in the United States as of 1 January 1996. Substantial reduction in average blood lead levels in the United States was reported between the years, 1976 to 1990; corresponding to the period of leaded fuel use, from its peak usage to near zero levels (Thomas, 1995).

The early 1970's had borne witness to the brief use of ethylene dibromide (EDB) as an additive to reduce the damaging effects of lead on car engines. With the phasing-out of leaded gasoline, EDB manufactures found an alternative use for the chemical as a pesticide. It is in this climate of mistrust between community, industry and government that current oxygenate problems exist.

2.1.1 Introduction of oxygenate additives

The origin of oxygenate additives in gasoline dates back to 1979 when MTBE was first utilised as an alternative to TEL. MTBE was introduced to the petroleum market under patent by the Atlantic Richfield Company (ARCO). The use of tertiary-alkyl ethers as oxygenate additives in gasoline was adopted as the ethers exhibited numerous benefits including increasing the octane, decreasing carbon monoxide emissions, combined with relatively low Reid vapour pressures (González et al., 2000).

As part of the Clean Air Act Amendments of 1990, a joint forum, including industry, community and government representatives, introduced the reformulated gasoline (RFG) program, which was passed into law for the reduction of ambient carbon monoxide and ozone levels. This program was implemented in two phases into the United States' most polluted

zones. The program targeted the reduction of toxic aromatics levels (benzene, toluene, ethylbenzene and xylenes, known as BTEX chemicals) in gasoline and increased the oxygen content of fuel to a minimum of 2.0 % by mass. The oxygenate requirements could be satisfied by the addition of 11 % MTBE, 12.4 % TAME or 5.7 % ethanol, by volume; thus lowering the benzene component in conventional gasoline from 5 % to 1 % by volume. Overall aromatic levels were reduced from a high of 50 % in conventional gasoline to 27 % in RFG, by volume.

In March 1991, the US EPA modified its regulations regarding oxygenate additive blending increasing the maximum allowable additive oxygen content to 2.7 % by mass. The modification used the clause "substantially similar" in describing permissible alternative oxygenates to be used in blending. This move broadened the category of oxygenates eligible for blending to include any aliphatic ethers and alcohols (except methanol). Gasoline containing up to 2.7 % by mass oxygenate is referred to as oxygenated gasoline. This increased gasoline oxygen content can be satisfied by the addition of 15.0 % MTBE, 16.7 % TAME or 4.2 % ethanol by volume to a base fuel.

Based on the fuel quality data collected in 1995 and 1996, the first phase of the RFG program exceeded all projected pollution reductions. Air toxic emissions were down by more than 22 %; volatile organic compound (VOC) emissions by 28 %; nitrogen oxide (NO*x*) emissions by approximately 2 % and benzene emissions from gasoline by 37 % (Nadim et al., 2001). Oxygenates had proved to be an extremely effective way of reducing pollution levels, maintaining octane levels while extending the output capacity of refineries given the same crude stock.

2.1.2 Lead up to MTBE phase-out

Despite the many air quality benefits borne by MTBE usage, in addition to, the health effects including comparative cancer risk reduction, detection of MTBE in vast numbers of ground and surface water reservoirs (Nadim et al., 2001), raised the issue of eliminating the oxygenate additive.

In November 1998, the United States Environmental Protection Agency (US EPA) announced the establishment of an independent panel, named the "Blue Ribbon Panel" to, inter alia,

examine the role of oxygenates in the environment. In July 1999, the panel released its recommendations stating that the use of MTBE should be reduced substantially, and that federal and state programs should be designed to regulate and/or eliminate the use of MTBE and other oxygenates that threaten water supplies (Jacobs et a.l., 2001).

At a hearing held on 6 May 1999 on Oxygenated fuels, before the Heath and Environment Subcommittee in the US House of Representatives, testimony entered into the record on behalf of the Natural Resources Defense Council (NRDC) emphasised that the current water resources dilemma required far broader scrutiny: If the solution entailed only the ban of MTBE, the associated environmental problem posed by thousands of pervasive underground storage tank leaks and gasoline spills would remain [NRDC (1999)]. Although the phasing-out of MTBE was recognised as inevitable, introduction of alternative oxygenate strategies were not advised due to the paucity of data available to assess environmental effects [US EPA (1996); Marsh et al., 1999; Nadim et al., 2001]. Table 2-1 depicts the status of health data available for oxygenate additives.

On March 26, 1999, California Governor Gray Davis instituted a 4-year phase-out plan for MTBE within the state. Federal action recommending a decrease in the use or elimination of MTBE in gasoline constitutes the most recent judgment passed on MTBE.

2.2 Alternative oxygenates for MTBE

Although several substitution strategies exist for the replacement of MTBE, ethanol is a likely substitute, with TAME arguably the most viable ether. Alternative ethers available for oxygenate use are tertiary amyl ethyl ether (TAEE), ethyl tertiary butyl ether (ETBE), di-isopropyl ether (DIPE), and di-methyl ether (DME). Possible alcohols substitutes include methanol or tertiary butyl alcohol (TBA).

Table 2-1: Availability status of health effects and exposure data for oxygenate additives and fuel products according to US EPA (1996)

	Animal								Human				Exposure		
	Pharmaco-kinetics	Muta-genicity	Sub-chronic toxicity	Chronic non-cancer	Reproduc-tive toxicity	Develop-mental toxicity	Neuro-toxicity	Onco-genicity	Acute toxicity	Chronic non-cancer	Cancer	Pharmaco-kinetics	Emissions	Transport and fate	Monitoring
Neat Additive:															
MTBE															
vapour	++	++	++	++	++	++	++	++	++	0	0	++	++	++	+
liquid	+	0	+	+	+	+	+	+	+	0	0	+	++	++	+
Ethanol															
vapour	+	0	+	0	0	0	+	0	+	0	0	0	+++	++	0
liquid	+++	+++	+++	+++	+++	+++	+++	+++	+++	+++	+++	+++	+++	++	0
TAME															
vapour	0	+	+	0	0	0	0	0	0	0	0	0	+	0	++
liquid	0	+	+	0	0	0	0	0	0	0	0	0	+	0	++
Fuel Product: Post 1990 gasoline plus:															
MTBE	0	0	0	0	0	0	0	0	++	0	0	0	++	+	+
Ethanol	0	0	0	0	0	0	0	0	0	0	0	0	++	+	+
TAME	0	0	0	0	0	0	0	0	0	0	0	0	0	0	+

Data availability key:

+++	extensive
++	moderate
+	some
0	none

Among the list of possible alcohol substitutes, methanol has been used previously as a fuel additive; however, considering this light alcohol is currently on the US EPA's Pollution Release Inventory (PRI) list as a priority chemical, it is not a viable option. The US EPA also includes MTBE on its PRI list. Tertiary butyl alcohol has been used previously as an oxygenate additive in a limited capacity.

Ethanol, has numerous benefits, but has a host of unknown health implications pertaining to inhalation; thus, it is not immediately obvious as a substitute for MTBE without further research [US EPA (1996)]. The specific oxygen content in ethanol is almost twice that of MTBE; hence, less ethanol is required by volume to meet the specified gasoline oxygen content.

Substitution of MTBE with ethanol has several drawbacks according to Nadim et al. (2001):

- Production of ethanol costs more than MTBE.
- Present production rates of ethanol may not be sufficient to replace MTBE.
- Ethanol is not produced on refinery site; hence, enhancement of infrastructure is required to bolster inadequate supply facilities.
- Ethanol is highly biodegradable and may impinge on the degradation of benzene and other hydrocarbons by soil microbes. Consequently, ethanol may extend plumes of aromatic hydrocarbons in ground water.
- Ethanol and ethanol-blended fuel conduct electricity; consequently, storage facilities will need to be modified to account for the increase in corrosiveness associated with electrically conductivity.

All the possible substitution ethers mentioned above, are expected to behave similarly to MTBE (Nadim et al., 2001); hence, the air pollution benefits associated with MTBE use are expected to extend to the other ethers. TAME is distinguished from the list of possible ethers because its benefits include the logistic advantage of being produced on site. TAME can be synthesised on the refinery from a novel feedstock of isoamylenes (tertiary C_5-olefins) providing an oxygenate, which meets octane restrictions and, subsequently, reduces the amount of olefins in gasoline (Rock, 1992).

CHAPTER 3

Environmental fate modelling and assessment

In attempts to reconcile the events, causes and effects that had borne two World Wars, the global community was left to ponder and assess the consequences of her collective decisions made over the first half of the twentieth century. This tumultuous time had heralded a period of unprecedented exponential industrial growth, in both the technology and the production sectors, leaving mankind to face the growing concern about contamination of the environment by anthropogenic chemicals.

It was soon understood that the environmental impact of some contaminants would remain a lasting legacy if not addressed. During the post-war era, man's inability to predict the fate of chemicals released into the environment was never more pronounced as even humanistic attempts made at this time to eradicate disease from the planet led to further environmental pilfering. In recognition of this phenomenon, *Silent Spring* was written by Rachel Carson and published in 1962, qualitatively raising the issue of anthropogenic contamination of the environment. Accordingly, the environmentally conscious scientist began to develop quantification methods, for the description of contaminants and contamination processes, establishing a new branch of environmental science named environmental fate modelling or chemodynamics.

The need for tools to predict the behaviour of chemicals in the environment has led to the development of numerous types of environmental models, which are designed to describe the major transport processes experienced by a chemical released into an environment. Ultimately, the models lead to the elucidation of the partitioning behaviour, or fate, of a chemical in the environment. Knowledge of the environmental fate of a substance is significant and necessary for 'green' product and process technology development. If applied during the conceptual design period of a new project, the fate predictions can be used to save money, time and safeguard the environment; Hypothetical mistakes on paper are far easier and less costly to correct than errors committed in the real world.

3.1 Hierarchy of Environmental fate modelling

According to Trapp and Matthies (1998), two different types of environmental fate models can be identified:

- The mechanistic or deductive model, which is based upon knowledge of physio-chemical and biological processes.
- The empirical or data driven model, which uses the parameterisation of monitored or measured data with significant environmental indicators.

The mechanistic model can be further sub-divided into two different model approaches:

- The hydrodynamic or flow mechanistic approach which leads to models consisting of partial differential equations (PDE's) describing dispersion, diffusion, reaction and ad/convective effects in a single medium; possibly in more than one spatial direction. Typical examples of this approach are plume or puff models simulating atmospheric transport.
- The kinetic approach which focuses on the description of phase transfer, transformation processes, as well as, bulk advective effects. This approach is built on the assumption that the environment can be seen a network of interconnected phases; each phase representing a medium in the environment. This model approach is formulated using ordinary differential equations (ODE's),. Although, explicit spatial dependency is lost upon moving from partial to ordinary differential equations implicit spatiality can be inferred by building sub-compartments within a single compartment of the multimedia model.

Both mechanistic approaches are based upon the fundamental law of conservation of mass introduced by Lavoisier, which provides the basis for all mass balance models. The empirical approach has proved useful for those processes that are too complex or too little understood to be described analytically. A typical example of such a process is the sorption of organic chemicals into humic substances.

Mackay (1991) in his multimedia approach (Mackay et al. 1979; 1981; 1982; 1992), corresponding to the Trapp and Matthies (1998) kinetic approach classification, further sub-divides multimedia models into real and evaluative models.

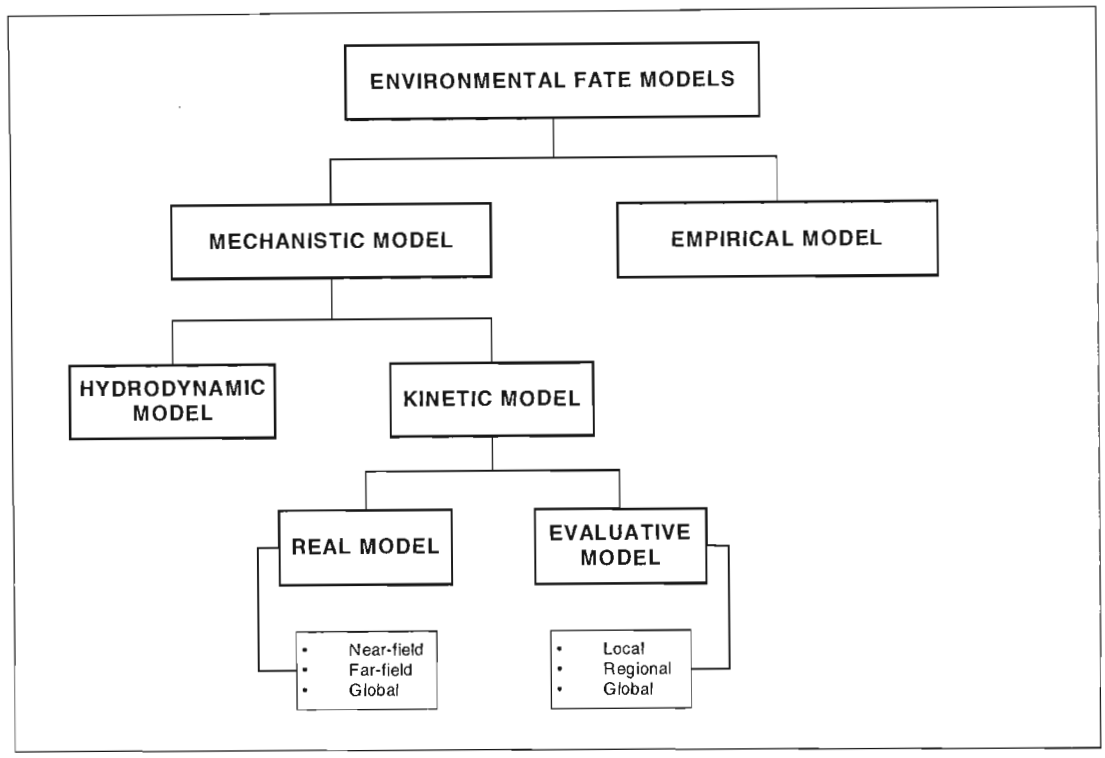

Figure 3-1: Hierarchy classification of environmental fate models

Real models are based on actual physical environments composed of field measured compartment sizes and properties. Evaluative models are user-defined to consist of selected homogenous phases of specified dimensions of constant temperature and density. This removes the complexities of real world simulation while still allowing the extraction of valuable information about how different chemicals will distribute themselves amongst various environmental compartments. Evaluative models have found application in environment impact assessments, persistence modelling and long-range transport screening. The evaluative technique was first proposed by Baughman and Lassiter (1978) enabling the environmental scientist to design a theoretical world into which new and existing chemicals can be 'released' to assess their impact. Evaluative models, thus, pose a formidable benchmarking tool, allowing comparison of the behaviour of compounds in the environment without harming the real environment.

Mackay (1991) also classifies multimedia models as being local, regional or global. A local model is constructed to simulate a specific location and surrounding region (e.g. a factory site). A regional model usually consists of a collection of localities (e.g. a city, town or country). A global model, as its name suggests, is formulated to sketch a system, which is parameterised using the dimensional properties and meteorological zones of the earth.

3.2 Current modelling practices

The estimation of environmental fate, according to Wagner and Matthies (1996), fulfils the following objectives:

- Elucidation and understanding of environmental fate processes.
- Identification of endangered ecosystems, populations or organisms.
- Determination of the present concentration and the prediction of future environmental concentrations of contaminants in abiotic and biotic environmental segments.

Additionally, Nirmalakhandan (2001) elaborates on the uses of environmental fate modelling:

- To determine short- and long-term chemical concentrations in the various compartments of the ecosphere for use in a regulatory context and in the assessment of exposures, impacts, and the risks of existing and new chemicals.
- To predict future environmental concentrations of pollutants under various loadings and/or management alternatives.
- To satisfy regulatory and statutory requirements relating to environmental emissions, discharges, transfers, and releases of pollutants.
- To implement in the design, operation, and optimisation of reactors, processes, and pollution control alternatives.
- To simulate complex systems at real, compressed, or expanded time horizons that may be too dangerous, too expensive, or too elaborate to study under real conditions.
- To use in environmental impact assessment of proposed new activities that are currently nonexistent.

3.2.1 Assumptions in environmental modelling

The assumptions made in environmental models are never trivial and are included to reduce the complexity of the model keeping in mind two main consequences:

- As complexity increases, data intensity increases, necessitating incorporation of data that may not be available.
- As complexity increases, general usage of the environmental model wanes as a complex model will only be used and understood by experts. Complexity reduces the perceived transparency of the model. The use of an environmental model by scientists, and politicians alike, dictates that transparency must be preserved for the benefit of all stakeholders.

The modeller's philosophy should be to concede each increase in complexity reluctantly, and only when necessary (Mackay, 2001). This sentiment is expressed in parallel with Ockham's razor:

Essentia non sunt multiplicanda praeter necessitatem
The essentials should not be added to unnecessarily

The quality of a model is not measured by the number of model equations or input parameters but by the gain in knowledge (Veerkamp and Wolff, 1996). Thus, environmental modellers seek to reduce the number of compartments to the minimum required to simulate the data to a satisfactory level of accuracy. Furthermore, environmental models are formulated to include only the processes considered important. Effort is usually made to keep the number of data requisites to a minimum.

In order to achieve these objectives, Trapp and Matthies (1998) proposed the following methodology as outlined in Figure 3-2 below. The methodology proposed in Figure 3-2 is a general strategy for the formulation of a completely specified environmental model. The applicability of the methodology to completely specified problems is suggested, in particular, by the inclusion of data acquisition, verification, calibration, and validation steps, which require complete data specification sets. For the purposes of this project, in which not all data are available, the methodology will be modified to an evaluative approach.

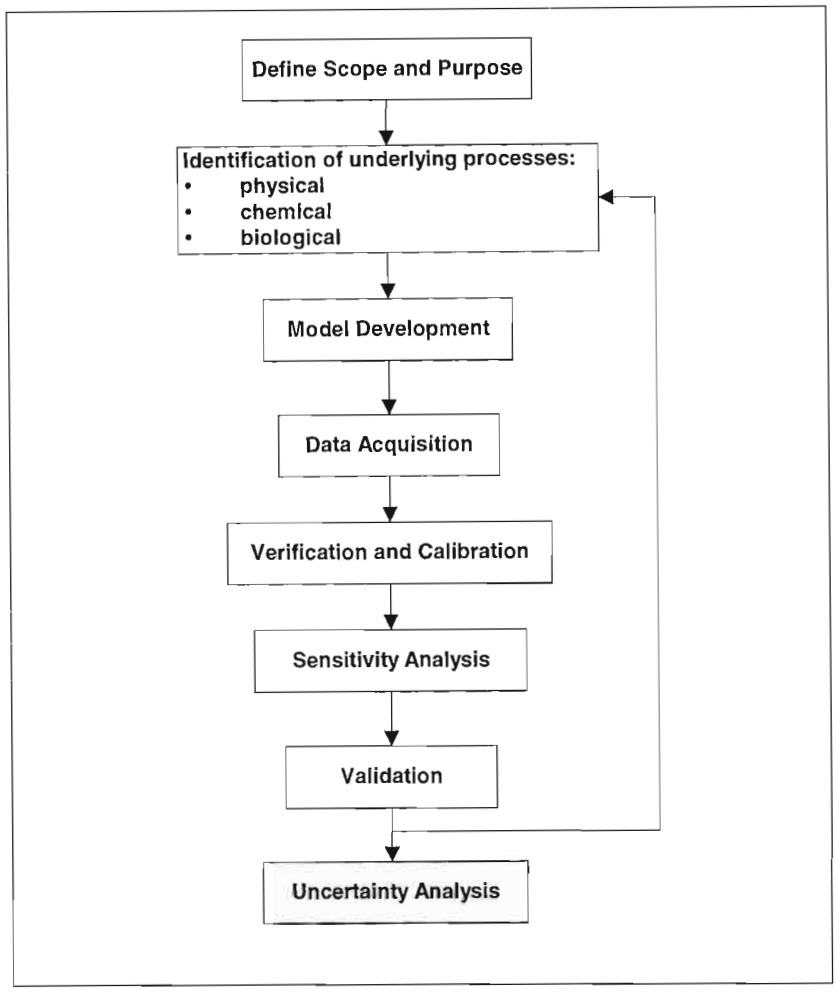

Figure 3-2: Environmental model formulation methodology according to Trapp and Matthies (1998)

The validation step, incorporated in the Trapp and Matthies (1998) methodology, is an important stage necessary for the proliferation of any new model. Validation is the comparison of independently measured concentrations with simulated model results. The successful validation of a model generates confidence in the model's ability to predict untested cases. However, environmental models, owing to the complexity of the phenomenon they describe, are difficult to validate. Accordingly, the power of environmental fate models should not be overestimated. The minimum acceptable level of the predictive capability of an environmental model is that the model correctly simulates environmental fate trends.

As the environment is a complex dynamic system with extreme spatial and dynamic variability, models of this complex system are limited by systematic errors introduced during formulation, such as simplifications and idealisations; as well as stochastic errors highlighted by the quality of the input data and its availability. Owing to the inherent errors in modelling a system as complex as the environment, the validity of the model depends strongly on its scope and purpose (Rykiel, 1996); thus, a model is unlikely to be universal in its applicability (Mackay et al., 1996). Regardless of any limitations, interpretation of the model results, and validation results, as well as complete understanding of the model formulation, are necessary to judge the limitation of a model's applicability to any given scenario.

Current literature indicates that experts are not in agreement pertaining the issue of full validation of environmental models, and it has been argued that full validation is not possible (Oreskes et al., 1994). Mackay et al. (1996) have suggested that rather than debating the meaning of validation, the labelling of "satisfactory" validation should be assigned to models which demonstrate results that are in "satisfactory" accord with field observations for a range of chemicals and environmental conditions.

3.2.2 Methodology for the assessment of the environmental fate of new and existing chemicals

In a series of papers, Mackay and co-workers (1996; 1996a; 1996b) proposed a methodology designed specifically to assess the fate of new and existing chemicals in the environment. The methodology developed by these authors was an attempt to standardise the diverse approaches and environmental conditions utilised by researchers throughout the world for fate assessment. By building a common framework, it was hoped that the burden of the environmental assessment of thousands of possible ubiquitous chemicals could be shared and communicated worldwide. The methodology proposed by Mackay et al. (1996) is illustrated in Figure 3-3.

The methodology above does not outline details regarding model formulation, as in Figure 3-2, but delineates the stages necessary for the evaluation of a chemical's general environmental fate behaviour. The assessment modelling begins in Stage 3. The methodology shows a definite order in the selection of model types used, moving from general evaluative modelling to specific near-field modelling.

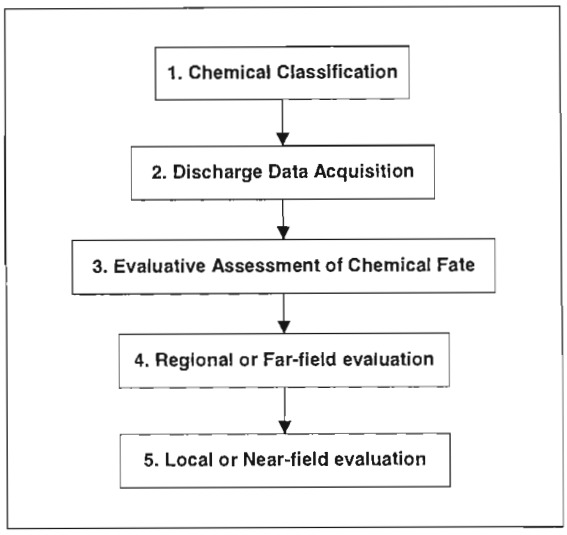

Figure 3-3: Five-stage methodology for assessing the fate of new and existing chemicals according to Mackay et al. (1996)

Stage 1 and Stage 2 outline the identification and gathering of the required data. The classification of the chemical type is important in Stage 1, as it determines what data is necessary. (Chemical classes are defined and summarised in Table 3-1 below). The acquisition of data is a crucial stage, as a well-formulated model still needs data of acceptable quality to be a useful predictive tool.

Stage 3 outlines the use of an evaluative model to establish the general behaviour characteristics of the substance in a generic environment. Within stage three, the important framework for the understanding of the chemical's environmental impact is elucidated. Omission of this stage may lead to significant large-scale multimedia processes, such as long-range transport, never being identified.

The evaluative model serves as a tool to assess the following:

- Identification of the primary environmental processes.
- Identification of the primary medium of concern.
- Identification of which medium to sample or take measurements from.
- Identification of key properties relating to a chemical's environmental fate.

To achieve the highest level of international harmonisation, agreement on dimensions and properties of a generic model environment was important. Mackay et al. (1996a) developed a generic model called the Equilibrium Criterion model (EQC model) to be used for the evaluative assessment. This multimedia evaluative model is discussed in Chapter 6 and is used as a fate assessment tool in this dissertation.

Considerable differences in national environments demand that a more specific level of investigation must be performed. Stage 4 entails the shift in focus from the understanding of the effects of the properties on determining the chemical's environmental fate to the effects of the environment on determining its fate. Consequently, a regional evaluation is performed over a fairly large homogeneous region having an area between 10000 km^2 and 1000000 km^2. This area interval, spanning two orders of magnitude, in the South African context, ranges approximately from the area of Gauteng province to the area of South Africa in its entirety. This stage entails a far-field study, which is used to identify which medium, or process, requires further scrutiny.

Stage 5 incorporates a near-field study probing the environmental fate of the chemical on a local level. For readily water-soluble oxygenates, like MTBE, the near-field study focuses on subsurface water compartments.

Table 3-1: Classification of chemical type according to Mackay et al. (1996)

Chemical Category	Classification	Example
Type 1	Partitions into all media	MTBE, TAME and Ethanol
Type 2	Partitions appreciably into the air phase	Lead
Type 3	Partitions appreciably into the water phase	Eicosane
Type 4	Partitions appreciably into the air and water phases	Polyethylene
Type 5	Speciation chemical	Mercury

3.3 Identification of priority chemicals

Most environmental jurisdictions compile a list of chemicals that are encountered in the environment. From these lists, a smaller set of priority chemicals is established isolating chemicals of environmental concern. Ultimately, these priority lists serve as a way of singling out potentially harmful chemicals that need to be controlled and regulated. In practice, chemicals, which fail to be assigned 'priority' status, are ignored and receive no priority as opposed to less priority (Mackay 2001).

Besides assessing the environmental fate of a chemical using multimedia models, identification of environmentally harmful chemical requires the evaluation of specific behavioural indicators, which have been deemed environmentally significant. These screening parameters establish the criteria according to which priority chemicals are identified.

The task of the selection of a manageable list of priority chemicals, from an initial shorthand list, has been achieved using analytical protocols, normally in the form of scoring systems or threshold comparison protocols. Scoring systems are governed by defined rules and protocols, which tally points awarded according to individual chemical property values. The total score determines what class of pollutant the chemical might be or the rank of the chemical within a list. Threshold protocols involve the simple comparison of chemical property values against threshold limits [Convention on Long Range Trans-boundary Air Pollution Persistent Organic Chemical (CLRTAP POP) Protocol; the United Nations Environment Programme (UNEP) Global Initiative; and Track 1 criteria as defined by the Canadian Toxic Substances Management Policy (TSMP), referred to by the Canadian Environmental Protection Act (CEPA 99)]. The threshold comparison protocols have found application in the screening of large chemical databases. A common thread among many of the selection processes is consideration of the following five factors: quantity, persistence, potential for long-range transport (LRT), bioaccumulation and toxicity.

3.3.1 Quantity

National environmental agencies house inventories, which track chemical releases, such as the Toxics Release Inventory (TRI) in the USA and the Canadian National Pollutant Release Inventory (NPRI). Similar programs exist in Europe, Australia and Japan.

Central to the significance of quantity as an indicator of environmental concern, is the adage stated by Paracelsus:

Dosis sola facit venenum

The dose makes the poison

However, quantity alone, as a screening parameter, does not mandate whether a chemical should be labelled a priority (Edwards et al. 1999). A corollary of this statement, that in sufficiently small doses all chemicals are safe, is the starting premise that the control and regulation of a chemical's quantity is a possible relief strategy for some pollutants.

3.3.2 Persistence

Persistence can be understood to be the amount of time a chemical remains within the confines of an environment; thus, persistence is strongly linked to the resistance of a chemical to degradation processes within an environment. Persistence has been recognised as a necessary, but not conclusive, condition for long-range transport (Gouin, 2002). Hence, the identification and regulation of persistent organic pollutants (POP's) has been the focus of considerable energy and resources (Vallack et al., 1998).

Multimedia models have been identified as useful tools in persistence screening (Gouin, 2002). The use of multimedia models ensures that properties that affect persistence are weighted according to the various environmental media in which the chemical is likely to persist. Webster et al. (1998) have highlighted that inconsistencies result when the effects of multimedia partitioning and mode entry are ignored in developing threshold screening criteria for persistence. This testifies to the limitations inherent in the simple threshold comparison protocols; several of which are outlined in Table 3-2 below regarding persistence. The comparison-approach based on individual compartment half-lives shows bias towards the persistence labelling of a chemical that does not partition appreciably into a compartment in which it is persistent. This allows the wrongful denigration of a relatively benign chemical as being an environmental concern.

Table 3-2: Threshold criteria for the assessment of the persistence of organic pollutants [Adapted from Gouin (2002)]

Factor	CLRTAP POP Protocol	UNEP Global Initiative	TSMP Track 1
Persistence	$t_{1/2,a} > 2$ days $t_{1/2,w} > 2$ months $t_{1/2,s}$ or $t_{1/2,sed} > 6$ months	$t_{1/2,a} > 2$ days $P^{sat} < 1$ kPa $t_{1/2,w} > 2$ months $t_{1/2,s}$ or $t_{1/2,sed} > 6$ months	$t_{1/2,a} > 2$ days $t_{1/2,s}$ or $t_{1/2,sed} > 12$ months $t_{1/2,w}$ or $t_{1/2,s} > 6$ months

3.3.3 Long-range transport

Long-range transport is the ability of a chemical to travel some distance from its point of discharge to a receiving environment. The potential for long-range transport is a concern for several reasons; none more pertinent than that LRT affects environments that are far removed from the source. Consequently, the occupants of the target domain are not the pollution cause but have to bear the pollution effects. Many trans-boundary air pollution cases exist in international environmental law. The following serves as an example of a documented LRT case:

- From 1896 till the 1930s, a smelter operated near Trail, British Columbia, Canada was the source of air pollution, which migrated across the border into the USA causing damage to certain areas. On behalf of local citizens, the US government, with concurrence from the Canadian government, brought the case to the International Joint Commission (IJC) who issued a judgment demonstrating an important component of modern environmental law; the acts of one state cannot be injurious to another (Olson, 1999).

Long-range transport may occur through several media: via mobile air and water phases, and through migratory biotic species (Beyer et al., 2000). The main threat is posed by the most mobile phase; consequently, the air compartment has been the focus of many investigations on long-range air transport (LRAT).

It has been recognised that persistence is a necessary condition for LRAT (Gouin, 2002). As a consequence, atmospheric residence time is accredited with being an important parameter in assessing LRAT potential (van Pul et al., 1998) with the requirement that the air residence time be sufficiently large to allow the substance opportunity to be transported (Wania and Mackay, 1996). Many volatile organic compounds (VOC's) and semi-volatile organic compounds (SVOC's) possess a ubiquitous combination of volatility and persistence, thus earmarking them as capable of LRAT.

The criteria recognised by environmental authorities, as indicative of LRT, are in line with the opinions expressed above. Volatility, indicated by vapour pressure, and persistence, represented by the air half-life, are used in threshold criteria to assess a substance's LRT potential.

3.3.4 Bioaccumulation

Bioaccumulation is also an important screening factor and is defined as the process by which a chemical becomes stored within the fatty tissues of an organism; thus achieving a concentration, which is greater inside the organism than that to which the organism is exposed.

Bioaccumulation studies have primarily focused on aquatic organisms (Mackay and Fraser, 2000). The uptake of chemical into the aquatic organism may occur through many pathways including dietary and dermal absorption, as well as, transport across the respiratory surfaces. Bioaccumulation is usually estimated using an organic phase-water partition coefficient owing to the appreciable partitioning of organic chemicals into organic media like lipid tissue.

The extent of bioaccumulation is usually expressed as a bioaccumulation factor (*BAF*), which is defined as the ratio of the chemical concentration in the organism to that which it is exposed. Pollution levels experienced by aquatic organisms are often buffered by particulate matter found in the water column (which has a high specific area capable of sorbing chemical). This reduces the fraction of chemical that is available for bioaccumulation. Dissolved organic matter can also behave like particulate matter reducing the bioavailability of chemical in the water column (Chiou et al., 1987; Resendes et al., 1992).

If the accumulation effect of a chemical propagates up a food chain, a phenomenon known as biomagnification is said to occur. The biomagnification factor (*BMF*) is defined as the ratio of the concentration of the chemical in the organism to the concentration of the chemical in the organism's diet.

A special case of bioaccumulation, usually achieved under laboratory conditions (Gobas and Morrison, 2000), is termed bioconcentration. This refers to the situation where chemical is absorbed from the water only via the dermal and respiratory surfaces.

It is clear that chemicals that bioaccumulate and, consequently, have the potential to biomagnify, can cause severe toxic effects at higher trophic levels and are, thus, important to identify. A tiered methodology, to address the large number of commercially used chemicals, has been proposed by Mackay and Fraser (2000). Threshold limit criteria are also used to assess bioaccumulation tendencies. Examples of threshold criteria protocols can be found in Table 3-3 below:

Table 3-3: Threshold criteria for the assessment of the bioaccumulation of organic pollutants [Adapted from Gouin (2002)]

Factor	CLRTAP POP Protocol	UNEP Global Initiative	TSMP track 1
Bioaccumulation	$BAF > 5000$ $BCF > 5000$ $\log K_{ow} > 5.0$	BAF (aquatic biota) > 5000 $BCF > 5000$ $4 < \log K_{ow} < 7$	$BAF > 5000$ $BCF > 5000$ $\log K_{ow} > 5.0$

3.3.5 Toxicity

For any substance to have an adverse effect on an organism, it must first enter the body of the organism. Common exposure routes for higher order vertebrae include:

- Ingestion
- Dermal contact
- Inhalation

The health effects caused by toxicity are characterised as carcinogenic and non-carcinogenic according to the duration of the exposure, which results in adversity (Jacobs et al., 2001):

- Acute: 14 days or less
- Intermediate: 15 to 365 days
- Chronic: 365 days or more

Acute toxicity is quantified by the dosage required to bring about lethal consequences for 50 % of a population (LD_{50}). Alternatively, the lethal concentration for 50 % of a population (LC_{50}) is defined. The exposure dosage or concentration required to eradicate 50% of the test population is usually defined over a given time period (usually 24-96 hours). Accordingly, the lower the lethal dosage, the greater the toxicity. In experimental determination of acute toxicity, the chemical may be administered orally or dermally to the test species.

Chronic, non-lethal, effects are more difficult to quantify and the adverse symptoms used to define the effects are numerous ranging from cessation of growth, movement, or the ability to reproduce. Genotoxicity, the ability of a toxin to affect the target's genetic material is also used as a criterion for chronic toxicity. The safety factor relating acute to chronic toxicity ranges between 10 and 100. Intermediate effects are defined as neither being acute nor chronic.

Toxicity experimentation is usually performed on animals; however, a body of data is available on plant matter (phytotoxicity). Toxicities related to specific effects, such as, genotoxicity, mutagenecity, teratogenicity and carcinogenecity are of main concern regarding humans. Although research indicates that multiple toxicants, which display similar action pathways, act additively; cases do exist where multiple toxicants have combined synergistically or antagonistically (Mackay, 2001).

Mass balance models, although outside the scope of toxicity studies, can be used to identify main exposure pathways or quantify exposure concentrations. Moreover, bioaccumulation modelling based on the fugacity concept (Mackay and Fraser, 2000) may be used to trace lethal dosage concentrations up a food chain. As LD_{50} is species-specific, a dosage that is not lethal to the producer level in a food chain, may biomagnify killing hosts higher up the food chain.

3.3.6 PBT-LRT behaviour as the defining criteria for priority assessment

Of the five criteria mentioned above: quantity, persistence, bioaccumulation, toxicity and long-range transport; the latter four are beyond the sphere of anthropogenic control as they are consequences of a chemical's properties. Consequently, the latter four criteria are used to assess a chemical's potential ability to cause environmental harm. Thus, evaluation of the persistence (P), bioaccumulation (B), toxicity (T), and long-range transport (LRT) has become a necessity for the identification of priority chemicals. Evaluative mass balance models are playing an increasingly important role in assessing the PBT-LRT potential of chemicals. If the chemical is shown to exhibit these undesirable attributes, regulatory bodies can take action, labelling these compounds as priority chemicals (Mackay, 2001).

3.4 The environment as a multi-compartment system

During the last few years, it has been increasingly recognised that to facilitate successful environmental protection protocol and policies, it is necessary for the environment to be considered in its entirety i.e. as a system consisting of interacting media (Trapp and Matthies, 1998). The recognition of the inherent multimedia nature of environmental pollution is not new (Cohen, 1986). Thus, it is a *fait accompli* that compounds released from the technosphere will enter multiple environmental media; either as the parent species, if the chemical is persistent; or as a degradation product, if the species is degradable.

3.4.1 Mathematics of compartmental systems

The environment is a spatially complex, and chaotically structured, dynamic system of biotic and abiotic components. Consequently, in order to mathematically sketch this complex system, it is useful to view the environment as consisting of a number of interconnected phases or compartments. Each defined compartment or box may be homogenous in its definition (e.g. water) or consist of a heterogeneous system of particles residing within a matrix phase (e.g. aerosol particles in the atmosphere). Accordingly, common defined environmental compartments include the atmosphere, water in the form of a lake or river, terrestrial soil, vegetation, sediment, aquatic and terrestrial biota.

The compartments are assumed homogeneously mixed, thus neglecting the detailed internal structure comprising each compartment. Mass and energy transfer can occur at the interfaces joining intimately contacted compartments. Compartments have defined geometry and, hence, defined shape and volume; thus, building on the assumption of homogeneity, compartments have defined densities and masses.

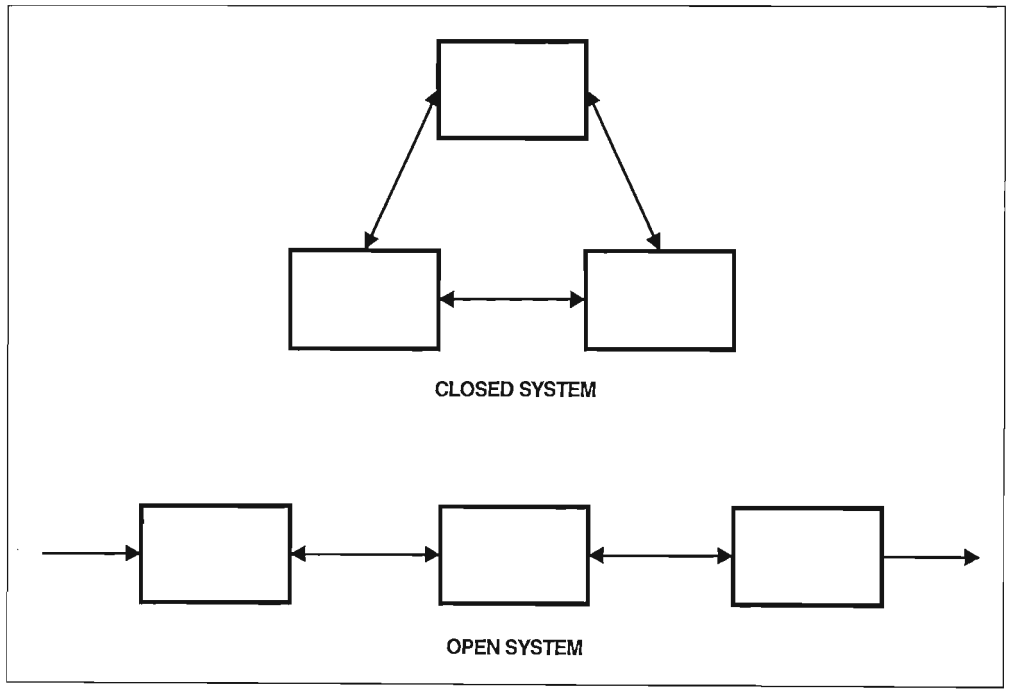

Figure 3-4: Example of an open and a closed three-box compartmental system

A system connecting several boxes representing different environmental media can be constructed, sketching a framework for the mathematical study of multimedia behaviour (Figure 3-4). Thus, each individual phase in an environmental box model can be described uniquely and set as closed or open, at steady state or unsteady state, in equilibrium or unequilibrated.

3.4.1.1 PDE formulation for single compartments

Utilising Lavoisier's principle of conservation of mass, a partial differential equation (PDE) including terms for diffusion (and/or dispersion), convective (and/or advective) flow and reaction, respectively, can be derived for a one-dimensional mass balance. The resulting

equation is a fundamental equation used for the mass balance of a compound in any defined compartment:

$$\frac{\partial C(z,t)}{\partial t} + u\frac{dC(z,t)}{dz} + r(C,T) = D(T)\frac{d^2C(z,t)}{dz^2} \tag{3-1}$$

where u is the advective velocity of the bulk compartment fluid, r is the reaction rate in the compartment and D is the diffusivity of the chemical in the compartment.

Equation (3-1) is formulated for a one-dimensional concentration profile, which can easily be generalised to a three dimensional case:

$$\frac{\partial \underline{C}}{\partial t} + \underline{u}.\nabla\underline{C} + \underline{r}(\underline{C},T) = D(T)\nabla^2\underline{C} \tag{3-2}$$

Methods for the solution of PDE's, pertaining to environmental models, are discussed in Appendix A-1.

3.4.1.2 System of ODE's for multi-compartment models

The description of the transient concentration profile of an environment consisting of n connected well-mixed compartments results in the generation of n differential equations, all first order and coupled. The system of ordinary differential equations (ODE's) generated takes the following form:

$$\begin{aligned}
\frac{dC_1(t)}{dt} &= a_{11}C_1(t) + a_{12}C_2(t) + \ldots + a_{1n}C_n(t) + b_1 \\
\frac{dC_2(t)}{dt} &= a_{21}C_1(t) + a_{22}C_2(t) + \ldots + a_{2n}C_n(t) + b_2 \\
&\vdots \\
\frac{dC_n(t)}{dt} &= a_{n1}C_1(t) + a_{n2}C_2(t) + \ldots + a_{nn}C_n(t) + b_n
\end{aligned} \tag{3-3}$$

Thus, for any compartment i:

$$\frac{dC_i(t)}{dt} = \sum_{j=1, j\neq i}^{n} a_{ij} C_{j(t)} + a_{ii} C_i(t) + b_i \qquad \textbf{(3-4)}$$

The first term on the right-hand side of Equation (3-4) is a summation of all exchange fluxes between compartment i and the other compartments. The second term on the right-hand side is a summation of all sinks out of compartment i. This includes loss by diffusion, degradation and advection: this term is subsequently negative. The last term on the right-hand side represents all external source emissions into compartment i. Equation (3-4) can be rewritten in vector format as:

$$\frac{d\underline{C}(t)}{dt} = \underline{\underline{A}}.\underline{C}(t) + \underline{B} \qquad \textbf{(3-5)}$$

where

$$\underline{C}(t) = \begin{bmatrix} C_1 \\ C_2 \\ \vdots \\ C_n \end{bmatrix} \text{ is a } (n \text{ x } 1) \text{ state vector;} \qquad \underline{B} = \begin{bmatrix} b_1 \\ b_2 \\ \vdots \\ b_n \end{bmatrix} \text{ is a } (n \text{ x } 1) \text{ control vector}$$

$$\underline{\underline{A}} = \begin{bmatrix} a_{11} & a_{12} & \cdots & a_{1n} \\ a_{21} & a_{22} & \cdots & a_{2n} \\ \vdots & \vdots & \ddots & \vdots \\ a_{n1} & a_{n2} & \cdots & a_{nn} \end{bmatrix} \text{ is a } (n \text{ x } n) \text{ state matrix}$$

Solution methods for ODE's are discussed in Appendix A-2. Included are the analytical solutions for two hypothetical, but useful, pollution case scenarios of a steady state problem and an initial value problem. Numerical solution techniques for ODE's are also discussed.

3.4.1.3 Dependent variable choice for compartmental mass balances

The ODE system resulting from the multi-compartment mass balances above can be formulated with respect to other dependent variables, besides concentration. Fugacity (Mackay, 2001) and compartment inventory [mole or mass basis] (McKone, 1993) have been used to formulate the mass balance equations. All the formulations are equivalent; consequently, all mathematical properties and trends that result are independent of the formulation (Hertwich, 2001).

Concentration and inventory

Inventory is the amount of matter present in any compartment, which is indicated by the amount of moles or mass present. The concentration (molar based unless specifically stated otherwise) and the inventory (N_i) in a compartment i are related by the following equation:

$$N_i = C_i V_i \tag{3-6}$$

Concentration and fugacity

The thermodynamic concept of fugacity was introduced by Lewis (1901) and is a measure of the tendency of a species to escape or flee a phase. Fugacity has the units of pressure and can be viewed as a thermodynamic partial pressure exerted by a chemical. A multi-phase system in equilibrium is characterised by the equality of the fugacities of a given chemical in each phase of the system. Consequently, the equivalence of fugacities is a criterion for equilibrium; similar to chemical potential [See Appendix A-3]. Mackay (1979) introduced fugacity ($\hat{f}_i$) as a variable for environmental fate modelling, defining with it the fugacity capacity factor (Z_i), a proportionality constant linking the concentration of a solute to its fugacity in the compartment. Fugacity and fugacity factors distinguish thermodynamic fate modelling from other fate model analyses.

$$C_i = Z_i\,(T, P, x_i)\,\hat{f}_i \tag{3-7}$$

The fugacity approach has several advantages:

- Fugacities of species are equal in each phase of an equilibrated multi-phase system.
- Fugacity capacities can be defined for any phase and assumes constant values under dilute conditions.
- Partition coefficients, which are defined as the ratio of equilibrium concentrations of a solute between two phases are also equal to the ratio of the fugacity capacity factors of the two phases.

CHAPTER 4

Environmental partitioning and processes

The distribution of a chemical in the environment is controlled by its rate of exchange between the various media. The transfer of a chemical across compartment boundaries can occur through equilibrium and non-equilibrium processes. Equilibrium distribution is described by partition coefficients, which represent the thermodynamic limit for exchange across a given interface. Equilibrium is a reversible but equal bi-directional process; with both phases acting as sources and sinks. Non-equilibrium processes are characterised by non-reversible, net one-directional fluxes, which convey chemical from one phase to another. This includes concentration driven mass transfer and bulk transport processes resulting from advective flows. The first half of this chapter deals with environmental partition coefficients, while the second half introduces some important environmental processes including mass transfer, sorption, settling and reaction.

4.1 Environmental partition coefficients

All transport processes from one phase to another are limited by equilibrium constraints, which are quantified by the respective partition coefficient defined for the contacted phases. This can be applied to environmental compartments pertaining to the distribution of pollutants between various environmental media.

The partition coefficient, in the context of environmental modelling, is defined as the ratio of the equilibrium concentration of a pollutant in one environmental compartment with respect to its concentration in another compartment. Hence:

$$K_{\alpha\beta,i} = \frac{C_i^{\alpha}}{C_i^{\beta}} \tag{4-1}$$

where the superscripts, α and β, represent two compartments which are intimately contacted.

Environmental partition coefficients are significant in multimedia modelling, and much time and resources are consumed in their estimation and measurement. Partition coefficients have been experimentally determined in the laboratory. Subsequent results have been analysed to generate a wealth of theoretical and empirical relations.

Several compartment partition coefficients are required when undertaking multimedia modelling. The main coefficients include:

- Air-water partitioning
- Octanol-water partitioning
- Octanol-air partitioning
- Vegetation-air partitioning
- Soil and sediment adsorption
- Bioconcentration and biomagnification
- Sorption to aerosols

Solubility, also an equilibrium process, is an important property in environmental modelling. Solubility limits represent the maximum capacity of a compartment to accumulate a solute before an additional phase is formed. A complete review of these and additional partitioning behaviour is given in Boethling and Mackay (2000).

For organic substances, the air, water and organic phases, such as lipids and other naturally occurring organic matter, pose as the most environmentally significant compartments. Partitioning to organic phases is usually quantified by the substance's tendency to distribute into 1-octanol; a solvent which has several benefits in simulating lipids owing to its lipoid structure. Consequently, the first three partition coefficients listed above (air-water, octanol-water and octanol-air coefficients) constitute the most significant coefficients. They are commonly used in the empirical prediction of other environmental partition coefficients.

The partition coefficients are best measured under dilute conditions when activity coefficients can be approximated by infinite dilution values. This is an important assumption in most of the theoretical based estimation methods.

As partition coefficients are equilibrium properties, the definition of phase equilibrium is an important pre-cursor to this topic. Equilibrium denotes a static condition in which there is the complete absence of change on a macroscopic scale. Hence, macroscopic properties like temperature and pressure in each phase of an equilibrated system are equal and constant. Phase equilibrium has been defined as the steady state condition in which the chemical potential of a given solute in each phase of the system is equal. This is known as the equilibrium criterion and leads to the synonymous statement of the equivalence of fugacity criterion [See Equation (4-2)] or the equivalence of activity criterion. The derivation of these two equivalent criteria for equilibrium can be found in Appendix A-3.

$$\hat{f}_i^{\alpha} = \hat{f}_i^{\beta} = ... = \hat{f}_i^{\Pi} \tag{4-2}$$

Hence, for equilibrium within an example environment consisting of air (*a*), aerosol particulate matter (*p*), water (*w*), soil (*s*), sediment (*sed*), suspended solids (*ss*), aquatic biota (*b*) and vegetation (*v*):

$$\hat{f}_i^{a} = \hat{f}_i^{p} = \hat{f}_i^{w} = \hat{f}_i^{s} = \hat{f}_i^{ss} = \hat{f}_i^{sed} = \hat{f}_i^{b} = \hat{f}_i^{v} \tag{4-3}$$

Using the Mackay relationship between concentration and fugacity, it can easily be shown that a partition coefficient is simply equal to the ratio of the fugacity factors of the solute in the respective compartments owing to the equilibrium criterion of equality of fugacities. Thus:

$$K_{\alpha\beta,i} = \frac{C_i^{\alpha}}{C_i^{\beta}} = \frac{Z_i^{\alpha}\hat{f}_i^{\alpha}}{Z_i^{\beta}\hat{f}_i^{\beta}} = \frac{Z_i^{\alpha}}{Z_i^{\beta}} \tag{4-4}$$

4.1.1 Air-water partition coefficients

As air and water represent two of the three primary media of accumulation in the environment, the air-water partition coefficient is a significant parameter used in the determination of all environmental air-water interactions. The fundamental thermodynamic quantity required to

characterize air-water partitioning is the limiting activity coefficient of the solute in water (Hovorka and Dohnal, 1997). Nonetheless, experimental measurement or prediction of vapour pressure and the infinite dilution activity coefficient in water, or the subsequently defined Henry's constant, can be used to generate air-water partitioning behaviour. The nature of the air-water partition coefficient, in the guise of the concentration based Henry's constant, has been reviewed by Mackay et al. (2000).

The air-water partition coefficient can easily be derived as a function of thermodynamic state variables using the ratio of respective fugacity capacity factors as indicated by Equation (4-4). The fugacity of a solute in the air phase is given by:

$$\hat{f}_i^a = x_i^a \phi_i^a P_{tot} \qquad \textbf{(4-5)}$$

where x_i^a is the mole fraction of solute in the air phase, ϕ_i^a is the fugacity coefficient of solute in the air phase and P_{tot} is the total atmospheric pressure.

Under atmospheric conditions of moderate pressure, the fugacity coefficient, which accounts for the deviation of real gas behaviour from the ideal gas law, can be assumed to be unity. Hence, any non-dissociating gas in the atmosphere will essentially behave ideally, resulting in the fugacity of the non-dissociating species being simply equal to its partial pressure (p_i^a). Hence:

$$\hat{f}_i^a = x_i^a P_{tot} = p_i^a \qquad \textbf{(4-6)}$$

Introducing the ideal gas definition for the molar concentration of a solute in a gas mixture, and combining with Equation (4-6) gives:

$$C_i^a = \frac{p_i^a}{RT} = \left(\frac{1}{RT}\right)\hat{f}_i^a \qquad \textbf{(4-7)}$$

Hence, the fugacity capacity factor for a solute in the air phase is derived to be:

$$Z_i^a = \frac{1}{RT} \qquad \textbf{(4-8)}$$

The remarkable result expressed in Equation (4-8) indicates that the fugacity capacity factor of a component behaving ideally in the air phase is independent of the type of solute, depending only on temperature. This result, however, is not mirrored by the water fugacity capacity factor. The fugacity of a solute in an aqueous phase can be expressed by:

$$\hat{f}_i^w = x_i^w \gamma_i^w P_i^{sat} \qquad \textbf{(4-9)}$$

Rewriting Equation (4-9), by replacing the mole fraction of the solute by the ratio of its aqueous concentration (C_i^w) to the total molar concentration of the aqueous phase (C_{tot}^w), yields:

$$\hat{f}_i^w = \left(\frac{C_i^w}{C_{tot}^w}\right)\gamma_i^w P_i^{sat} \qquad \textbf{(4-10)}$$

The water phase fugacity capacity factor can be generated from Equation (4-10) by rearranging C_i^w as the subject of the formula. Hence:

$$C_i^w = \left(\frac{C_{phase}^w}{\gamma_i^w P_i^{sat}} \right) \hat{f}_i^w \qquad \textbf{(4-11)}$$

As environmental contamination occur in the dilute range of parts per million (ppm), the solute can be considered to be infinitely dilute in the compartment. From a molecular viewpoint, infinite dilution has been described by Alessi et al. (1991) to represent the dilute region where around any given molecule of type (*i*), no molecules of the same type can be found to interact with it, such that the only interactions with type (*i*) that occur are with molecules of different types. Water-organic solute interactions fall under the general grouping of nonpolar-polar or polar-polar systems, which are considered, under practical conditions, to be infinitely diluted when the mole fraction of the solute is less than 10^{-4} to 10^{-5} mole fraction (Kojima et al., 1997). This reflects a solute concentration in the range of ppm's; hence, it is thermodynamically valid to assume infinitely dilute conditions in most environmental calculations.

Assuming infinite dilution enables the use of thermodynamically valid approximations for two quantities found in Equation (4-11). Firstly, as the aqueous phase is very dilute in solute, the phase is essentially comprised of water only. Consequently, the molar concentration of the aqueous phase can be approximated by the inverse of the molar volume of pure water ($\tilde{V}_w$). Secondly, and for reasons consistent with current thermodynamic practices, the limiting activity coefficient or infinite dilution activity coefficient ($\gamma_i^{w,\infty}$) can be used. Hence:

$$Z_i^w = \frac{1}{\tilde{V}_w \gamma_i^{w,\infty} P_i^{sat}} \qquad \textbf{(4-12)}$$

The triple product in the denominator of Equation (4-12), which includes P_i^{sat}, the saturated vapour pressure of the solute, is termed the concentration based Henry's constant (H_i^w). This limiting property has the SI units of mol/(m^3.Pa). The product of the infinite dilution activity

coefficient and the saturated vapour pressure is known as the mole fraction based Henry's constant ($\hat{H}_i^w$). Accordingly:

$$Z_i^w = \frac{1}{\tilde{V}_w \hat{H}_i^w} = \frac{1}{H_i^w} \tag{4-13}$$

On establishing both the air and water fugacity capacity factors, derivation of the air-water partition coefficient is complete and defined in Equation (4-14) below:

$$K_{aw,i} = \frac{C_i^a}{C_i^w} = \frac{Z_i^a}{Z_i^w} = \frac{1/RT}{1/H_i^w} = \frac{H_i^w}{RT} \tag{4-14}$$

Compounds that have a K_{aw} value greater than 0.05 at 25°C are considered to volatilise easily from water (Squillace et al., 1997).

4.1.1.1 Experimental methods for the determination of air-water partition coefficients

Accurate experimental determination of air-water partitioning is not a trivial task. Many techniques are available to measure the various properties, which span the several definitions of air-water partitioning presented above.

Experimental methods used to determine Henry's constants

Mackay et al. (1993) have reviewed current experimental methods characterising air-water partitioning using Henry's constants. These authors identified six experimental technique which are outlined in Table 4-1 below:

Table 4-1: Experimental methods for the determination of Henry's constants

Method	Reference	Note
Inert Gas Stripping (IGS)	Mackay et al. (1979)	Method ideal for relatively volatile chemicals of $K_{aw} > 10^{-4}$ (Mackay et al., 2000).
Equilibrium Partitioning In Closed Systems (EPICS)	Gosset (1987)	For highly volatile substances of $K_{aw} > 0.05$ (Mackay et al., 2000).
Wetted-wall column	Fendiger and Glotfelty (1988)	Applied to pesticides and other less volatile chemicals.
Headspace Chromatography (HSC)	Hussam and Carr (1985)	Valid for systems in which appreciable sorption occurs (Mackay et al., 2000).
Relative Gas Liquid Chromatography (RGLC)	Tse et al. (1992)	Simple and rapid method.
Direct phase analysis	Leighton and Calo (1981)	Direct sampling of both phases in a closed system.

The EPICS method used by Gosset (1987) is a static method in which equilibrium is facilitated by magnetic stirring of the water phase. A modified EPICS method has been developed by Ryu and Park (1999) using a dynamic apparatus incorporating two bubble columns. In this method, the dynamic circulation of air bubbles through the water columns was used to equilibrate the solute rapidly between the air and water phases. The modified EPICS method was demonstrated to accurately reproduce literature data for K_{aw} (Ryu and Park, 1999).

The relative gas liquid chromatography method, developed by Orbey and Sandler (1991), has been used in this study to evaluate the γ_i^{∞}'s for several organic compounds in water performed [See Appendix F]. Included amongst the list of organic compounds measured is TAME, which has no previously reported literature value.

Experimental methods used to determine limiting activity coefficients

Although the above methods were distinguished by Mackay et al. (1993) as currently employed techniques for Henry's constant measurement, any direct or indirect method for γ_i^{∞} measurement can be used to evaluate air-water partitioning. Of the methods presented in Table 4-1 above, at least three (IGS, HSC and RGLC) are considered conventional limiting activity coefficient experimental techniques. As there is a direct relationship between infinite dilution activity coefficients and Henry's constants, no differentiation between methods should be made. In light of current limiting activity coefficient experimental methods, one mitigating factor distinguishes the method as a possible technique for air-water partitioning characterisation: whether the method is versatile enough to handle water as a solvent medium as water is a relatively volatile solvent. Notwithstanding, most methods that determine γ_i^{∞} experimentally can be employed. A thorough review assessing current γ_i^{∞} experimental practices has been performed by Kojima et al. (1997). Past review papers by Eckert and Sherman (1996), and Sandler (1996) also discuss measurement techniques for limiting activity coefficients.

Despite, the γ_i^{∞} experimental techniques that overlap directly with H_i techniques described above, other experimental γ_i^{∞} techniques, which are particularly appropriate for aqueous systems include differential ebulliometry and the differential static method. The former technique is a simple and fast method for measuring γ_i^{∞} and considered suitable for γ_i^{∞} measurement of solutes in water (Bergmann and Eckert, 1991). The differential static method is also considered very suitable for γ_i^{∞} measurement of solutes in aqueous systems (Kojima et al., 1997). Pividal et al. (1992) and Wright et al. (1992) have utilised this latter method in the determination of infinite dilution activity coefficients in water for oxygenates and halogenated hydrocarbons respectively.

Extensive compilations of air-partitioning related properties are available in literature and are reported in Table 4-2 below:

Table 4-2: Extensive databases available in literature for air-water partitioning data

Reference	Quantity	Comment
Staudinger and Roberts (2001)	H_i^w	Temperature dependence for 197 organic compounds is given.
Mackay et al. (2000a)	H_i^w	Amongst many other environmental fate properties.
Kojima et al. (1997)	$\gamma_i^{w,\infty}$	Extensive list of 1469 data points ranging from 283.15 K to 373.15 K.
Mitchel and Jurs (1998)	$\gamma_i^{w,\infty}$	Compiled list containing 325 compounds at 298.15 K.
Sherman et al. (1996)	$\gamma_i^{w,\infty}$	Errors exist in this compilation, and cited references should be checked.

4.1.1.2 Predictive methods for the estimation of air-water partition coefficients

In a similar fashion to experimental determination of air-water partitioning, predictive tools estimating either Henry's constants, or limiting activity coefficients, can be used to estimate air-water partition coefficients.

Predictive methods used to estimate Henry's constants

Lyman et al. (1982) and Mackay et al. (2000) have presented a comprehensive review of Henry's constant estimation methods. Brennan et al. (1997) compared five methods for K_{aw} estimation concluding that the methods of Meylan and Howard (1991), a bond contribution method, and that of Nirmalakhandan and Speece (1988), using molecular interaction parameters, are of comparable accuracy.

The simplest method used for Henry's constant estimation is the ratio of the vapour pressure of a solute to its water solubility(Mackay, 2001). This simple approximation gleans tremendous insight into the nature of the Henry's constant. Often the misconception exists that a non-volatile species will have a low Henry's constant. This is not necessarily true as the partitioning

of a solute is dependent on its behaviour in both phases. This approximation is reported to be accurate if the water solubility of the chemical is less than 1 mol/dm^3 (Lyman et al., 1982). A thermodynamically more exact limit of application can be shown to be 0.554 mol/dm^3. This is based on the approximation that for $\gamma_i^{\infty} > 100$, the mole fraction of a solute in a phase of limited miscibility can be calculated from the inverse of the limiting activity coefficient of the solute in that phase (Eckert and Sherman, 1996).

Table 4-3: Predictive methods for the estimation of Henry's constants

Method	Description
Fragment constant method	
Hine and Mookerjee (1975)	Data base of 292 compounds correlated to bond and group contribution approaches with correction for polar interactions.
Meylan and Howard (1991)	Extended method of Hine and Mookerjee (1975) derived from a data set of 345 compounds. Generally valid for hydrocarbons, halo-hydrocarbons, esters, alcohols and phenols, (Mackay et al., 2000).
Molecular parameter method	
Nirmalakhandan and Speece (1988)	Correlation using connectivity index, polarisability and an additional hydrogen bonding indicator parameter. Generally valid for halo-alkanes and acids (Mackay et al., 2000).
Nirmalakhandan et al. (1997)	Correlation fitted to 105 chemicals including oxygen, sulphur and nitrogen containing species. This method includes a temperature dependency.
Russel et al. (1992)	Five parameter model including surface area and atomic charges correlated for 63 compounds.
Linear Solvation Energy Relationship method	
Abraham et al. (1994)	LSER method using five solvatochromic parameters for 408 chemicals.
Other	
Suzuki et al. (1992)	Combined connectivity and group contribution method for 229 mono-functional compounds from the same data set used by Hine and Mookerjee (1975).

Estimation methods for the Henry's constant are summarised in Table 4-3 above. Other estimation methods can be categorised into bond/fragment constant methods, molecular parameter methods (including connectivity indices), linear solvation energy relationship (LSER) methods or others. Bond/fragment methods are empirical techniques, which are reasonably accurate when applied to chemicals similar to the species database utilised for parameter fitting. Molecular parameter methods often exhibit inherent molecular structure information and can thus be used to estimate isomers. LSER techniques have been found to be most accurate; however, the solvatochromic parameters required are difficult to obtain.

Predictive methods used to estimate infinite dilution activity coefficients

The infinite dilution activity coefficient is also a viable parameter for air-water partitioning assessment. Hence, the wealth of established activity coefficient estimation methods available in literature can be used to predict air-water partitioning.

Among the numerous approaches that have been explored, group contribution methods have proven to be the most powerful. The UNIFAC (UNIQUAC Functional group Activity Coefficients) method and the ASOG (Analytical Solution Of Groups) method, as extended by Tochigi et al. (1990), are the most widely used. The UNIFAC method, originally developed by Fredenslund et al. (1975), has been revised and extended (Hansen et al., 1991). Additionally, it has been modified by several authors.

Voutsas and Tassios (1996) reviewed the ability of nine methods for the prediction of infinite dilution activity coefficient including the revised original UNIFAC model (Hansen et al., 1991), several modified UNIFAC approaches (Magnussen et al., 1981; Larsen et al, 1987; Bastos et al., 1988; Hooper et al., 1988; Hansen et al., 1992; Gmehling et al., 1993;) and the correlation of Pierotti, Deal and Derr [PDD] (Pierotti et al., 1959). Voutsas and Tassios (1996) drew several conclusions regarding the applicability of the different UNIFAC methods for prediction of limiting activity coefficients of various groups of solutes in aqueous mixtures. Their recommendations are presented in Table 4-4 below. Voutsas and Tassios (1996) concluded that, in general, the correlation of PDD performed the most satisfactorily; however, as the necessary parameters required for the PDD correlation are available for only a limited number of chemicals, the UNIFAC method of Magnussen et al (1981) was recommended as a

predictive tool. It was suggested that the Magnussen et al. (1981) modified method could at least provide an order of magnitude estimate in all solute-water systems except for alkane-aqueous mixtures; in which case, the method of Hooper et al. (1988) was suggested.

Table 4-4: Recommended methods for the prediction of the infinite dilution activity coefficient of various solute species in aqueous systems as suggested by Voutsas and Tassios (1996)

Aqueous mixture	Suggested method/s	Comment
n-alkanes	Hooper et al. (1988) and PDD	Hooper et al. (1988) performed satisfactorily with the PDD providing fairly good results.
cycloalkanes	Hooper et al. (1988)	Only Hooper et al. (1988) gives relatively satisfactory results.
aromatics	All except Larsen et al. (1987) and Hansen et al. (1992)	Larsen et al. (1987) becomes increasingly large with increasing carbon number.
1-alcohols	PDD	Only the PDD performs successfully even for higher carbon number 1-alcohols.
2-ketones	PDD and Magnussen et al. (1981)	PDD and Magnussen et al. (1981) predict fairly satisfactorily.
n-aldehydes	PDD and Magnussen et al. (1981)	PDD performs well with Magnussen et al. (1981) also demonstrating fair results.
n-acids	PDD	Only PDD exhibits satisfactory results.

Zhang et al. (1998) have introduced mixture-type groups to the Gmehling et al. (1993) UNIFAC method, in order to account for hydrophobic effects. Zhang et al. (1998) compared the proposed method with several UNIFAC methods (Magnussen et al., 1981; Larsen et al., 1987; Bastos et al., 1988; Hooper et al., 1988; Hansen et al., 1991; Gmehling et al., 1993; ASOG and PDD) concluding that their method showed good accuracy comparable with the PDD correlation.

Foisy et al. (1997) have proposed the modification of current UNIFAC methodology, using ABC and conjugation theory, which was developed by Mavrovouniotis and several co-workers

(Mavrovouniotis, 1990; Constantinou et al., 1993; Constantinou et al., 1994). Although not yet correlated to aqueous systems, the ABC-modified UNIFAC has demonstrated improvements on the original UNIFAC approach.

Approaches accounting for group contribution limitations

Several limitations inherent in most of the activity coefficient group contribution models discussed above include:

- Functional groups are defined empirically.
- Models cannot differentiate between isomers.
- Proximity effects of neighbouring strong functional groups are unaccounted for.

The complicated structures of many pollutant species ensure that the methods, investigated by Voutsas and Tassios (1996), have limited applicability. In recognising that most predictive techniques are limited to certain classes of compounds (Banerjee and Howard, 1988), extension of group contribution theory is necessary to ensure that the quick and easy approach of group contribution can be universally applied. Several approaches to account for the above limitations have been proposed.

Wu and Sandler (1991; 1991a) have addressed the lack of theoretical basis for functional group definition and the invalidity of previous methods for modelling multi-functional compounds. Using quantum mechanical calculations to estimate atomic charge distributions, these authors suggested that a functional group should have an approximately zero overall charge, independent of the molecule in which the group finds itself. This approach accounted for the proximity effect of strong functional groups, by recommending the definition of new larger groups containing the interacting groups.

Abildskov et al. (1996) proposed a second order group method for description of proximity effects and the differentiation of isomers as separate behavioural entities. The second order groups were defined according to the principle of conjugation and comprised of several first order groups.

Lin and Sandler (2000), in extending a group contribution solvation method applied to octanol-water partitioning (Lin and Sandler 1999), suggested that the stringent requirement of neutral overall group charge, as proposed by Wu and Sandler (1991; 1991a), was not necessary. These authors, however, promulgated the criterion that the overall group charge should remain constant, independent of the molecule in which it appeared. Subsequent definition of a reference charge distribution for each group, allowing explicit correction for deviation from the defined reference state resulting from the proximity of strong functional groups, was used to resolve all three limitations expressed above.

4.1.2 Octanol-water partition coefficients

At ambient temperature and pressure, water and 1-octanol (n-octanol or octanol) are partially miscible, forming an octanol-rich phase layer, containing 72.5 mole % octanol (Lin and Sandler, 1999), that floats on top of a water-rich layer, which is essentially water (99.99 mole % water). Several conflicting ovalues for the octanol mole fraction in the octanol-rich phase have been reported: Kuramochi et al. (1998) have reported an octanol mole fraction in the organic layer of 79.3 mole % at 298.15 K; while Arce et al. (1996) have determined the mole fraction of octanol in the organic phase to be 73.09 mole % at the same temperature. All three sources are in agreement regarding the water fraction in the aqueous phase.

By adding a small amount of solute to a two-phase mixture of octanol and water, the octanol-water partition coefficient, K_{ow}, can be defined as the equilibrium ratio of the concentration of a solute in the octanol-rich phase to its concentration in the water-rich phase:

$$K_{ow,i} = \frac{C_i^{or}}{C_i^{wr}} = \left(\frac{x_i^{or}}{x_i^{wr}}\right)\left(\frac{C_{tot}^{or}}{C_{tot}^{wr}}\right) = \left(\frac{\gamma_i^{wr}}{\gamma_i^{or}}\right)\left(\frac{C_{tot}^{or}}{C_{tot}^{wr}}\right) \qquad \textbf{(4-15)}$$

The octanol-water partition coefficient is a measure of the hydrophobicity of a solute: The greater the K_{ow}, the more hydrophobic the compound. As K_{ow}'s range in magnitude from fractions to several orders of magnitudes, this parameter is often expressed as a logarithm. This parameter has been used as a measure in quantitative structure-activity relationships (QSAR's) to embody hydrophobic interaction (Hansch et al., 1996), which are used extensively to predict the bioactivity of compounds. In 3500 QSAR studies on biological activity, 85 % are reported

to show a significant dependence on $\log K_{ow}$ (Leo, 2000). The octanol-water partition coefficient is considered one of the most important physio-chemical properties characterising soil sorption, sediment sorption and bioaccumulation; Subsequently it has been correlated empirically to describe these phenomena.

The use of octanol was popularised by Hansch and Leo (Leo et al., 1971) and it is considered a good surrogate model for lipid structures: It exhibits lipoid properties owing to its hydrophobic hydrocarbon tail, which is attached to a hydrophilic hydroxyl head. Octanol is easily available in pure form and has been shown to correlate linearly with tricaprylin, a liquid fat, (Maaßen et al. 1996) justifying its selection as a lipid model.

4.1.2.1 Experimental methods for the measurement of octanol-water partition coefficients

Several authors have reviewed experimental methods for K_{ow} measurement (Sangster, 1997; Leo, 2000). Sangster (1993) has compiled a database of more than 18000 organic compounds. The direct measurement of K_{ow} for a hydrophobic compound can be an arduous task to perform accurately owing to the dilute partitioning of hydrophobic solutes into the aqueous phase. Furthermore, the formation of micro-emulsions, or the adsorption of hydrophobic solute from the aqueous phase onto various surfaces following phase disengagement, have been reported to render unrealistic K_{ow} values (Sandler, 1996). Consequently, there is considerable uncertainty in K_{ow} data, sometimes in the range of an order of magnitude for large $\log K_{ow}$ values. Several K_{ow} experimental techniques are outlined in Table 4-5 below.

The shake flask method is the traditional measurement technique used for K_{ow} determination. As the name suggests, octanol, water and a third solute are introduced into a flask, which is shaken to ensure equilibration of the phases. Leo (2000) warns against excessive shaking and temperature control regarding this method, as most solutes are believed to equilibrate within two minutes and $\log K_{ow}$ sensitivity to temperature is less than 0.01 units/°C. Avoidance of excessive shaking is easily understandable in light of the formation of stable micelle, which may form. Constant temperature is necessary criterion for the establishment of equilibrium in the flask; hence, a critical level of temperature control is necessary. Judging from the relative insensitivity of $\log K_{ow}$ to temperature, precision in the temperature control of the flask contents

is more crucial than the accuracy of temperature measurement, as the equilibrated log K_{ow} of a solute at 25°C will be essentially the same as the equilibrated log K_{ow} at, say, 25.7°C, extrapolating from the Leo (2000) reported sensitivity.

Although slower and, perhaps more tedious, the shake flask and slow stir methods, both methods which equilibrate solute directly between the mutually miscible phases, have the greatest range of applicability (Leo, 2000). These methods are considered to produce the most reliable results (de Bruijn and Hermens, 1990).

Table 4-5: Experimental methods for the measurement of octanol-water partition coefficients [Range of applicability as established by Leo (2000)]

Method	Reference	Comment
Shake flask method	OECD (1981)	$-3.0 < \log K_{ow} < 8.0$
Slow stir method	de Bruijn et al. (1989)	$-3.0 < \log K_{ow} < 8.0$
Generator column method	Woodburn et al (1984)	No range given
Centrifugal Partition Chromatography (CPC)	El Tayar (1991)	$-3.0 < \log K_{ow} < 3.0$
Micro-Emulsion Electrokinetic Chromatography (MEEKC)	Ishihama (1994)	$-1.0 < \log K_{ow} < 4.0$
Reversed Phase High Pressure Liquid Chromatography (RP HPLC)	Veith et al. (1979)	$-3.0 < \log K_{ow} < 8.0$

In this dissertation, K_{ow}'s for various solutes, including MTBE, TAME and ethanol, have been determined using a liquid-liquid equilibrium cell [See Appendix E]. This liquid-liquid equilibrium cell accurately reproduced literature values for previously measured solutes. Hence, the reliability of direct contact equilibration techniques for K_{ow} measurement was reiterated.

Reverse Phase High Pressure Liquid Chromatography (RP HPLC), although empirical, has proven useful and sufficiently reliable as an experimental technique. This rapid technique is performed by the regression of a compound's K_{ow} against its retention time in a RP HPLC column. Although it has been established that K_{ow} temperature dependence is relatively minor compared to the temperature dependence of vapour-liquid equilibrium partitioning (Sangster, 1989), RP HPLC based methods have been used to explore the temperature dependence of octanol-water partition coefficients (Lei et al., 2000).

Composition analysis of phases in direct equilibration methods

On re-examination of the definition of K_{ow}, [Equation (4-15)] further procedural innovations can be deduced.

$$K_{ow,i} = \frac{C_i^{or}}{C_i^{wr}} = \frac{n_i^{or} / V_{tot}^{or}}{n_i^{wr} / V_{tot}^{wr}} = \left(\frac{n_i^{or}}{n_i^{wr}}\right)\left(\frac{V_{tot}^{wr}}{V_{tot}^{or}}\right) \qquad \textbf{(4-16)}$$

By adjusting the volume ratio between the two phases for each measurement, solute can be driven into the dilute phase. Although the concentration in the dilute phase will not increase as it is an intensive property, the moles in the dilute phase will increase. Consequently, especially relating to titrimetric evaluation of phases, more accurate measurement of the dilute phase is facilitated. Moreover, if only one phase is analysed, greater precision can be achieved if each phase contains a similar amount of solute (Leo, 2000).

For the aqueous phase compositional analysis of a high K_{ow} species, the method of standard addition can be used. This, however, may not remove the inherent difficulty of measuring the dilute aqueous phase as the order of uncertainty of the measurement technique may be of the same order or greater than that of the solute's actual aqueous concentration.

4.1.2.2 Prediction methods for the estimation of octanol-water partition coefficients

Current predictive techniques fall into two categories: Linear Solvation Energy Relationship (LSER) methods and fragment methods, which include group contribution methods. The prediction techniques range in their use of empiricism. A semi-empirical predictive methodology, which uses infinite dilution activity coefficients of the solute in pure water and a pure octanol phase is common.

Linear solvation energy relationship methods

Clear insights into the solvation forces evident in octanol-water partitioning have been elucidated from work performed by Kamlet, Taft and colleagues (Kamlet et al., 1988). In the LSER approaches, log K_{ow} is estimated from the sum of contributions of several interactions:

- Repulsive interactions (cavity formation)
- Non-specific attractions (polarity)
- Specific attractions (hydrogen bonding)

The repulsive contribution is assessed from the solute size, usually calculated as the solute molar volume or area. The attractive contributions can be calculated from three solvatochromic parameters defined in Kamlet et al. (1983) [Lin and Sandler, 1999]. Several researchers have replaced the solvatochromic parameters with other descriptors. With respect to hydrogen bonding, only the solute hydrogen bond acceptor strength is required for octanol-water systems, as the two solvent phases have approximately equal hydrogen bond acceptor strength. Consequently phase solute-solvent interactions are not distinguished on the basis of the solvent hydrogen bond strengths (Leo, 2000). Elsewhere, the non-specific interaction contribution, caused by molecular polarity/polarisability, has been estimated in several forms, including use of the dipole moment (Bodor and Huang, 1992) and the square of the dipole moment (Leahy, 1992), which has a theoretical basis (Leo, 2000).

Group contribution methods

Various group contribution methods, pertaining to K_{ow}, have been succinctly reviewed by Sangster (1997). Group contribution methods assume that interactions between molecules can be estimated by the sum of the contributions of the various functional groups constituting the molecules with each group contributing independently of the other groups comprising the molecule.

A refinement of this assumption is demonstrated by adding corrective terms to account for the proximity of strong functional groups. A good example of a predictive group contribution technique, which uses correction factors, is the method of Hansch and Leo (Leo, 1993; Hansch and Leo, 1995). This method has been found to successfully estimate K_{ow}; Consequently, it is considered a benchmark predictive tool. The method is empirical in nature and has very little theoretical foundation (Lin and Sandler, 1999). [Nys and Rekker (1974) were the first to publish a fragment-based method for log K_{ow}].

Kuramochi et al. (1998) used four UNIFAC group contribution methods to predict octanol-water partitioning. By modifying Equation (4-15) as below, these authors measured the total phase densities, and saturated mole fractions in the two phases and assumed that the phase concentration could be calculated from the phase densities ($\rho_{tot}^{or}, \rho_{tot}^{wr}$) and the mole fraction weighted molar masses (M_j).

$$K_{ow,i} = \frac{C_i^{or}}{C_i^{wr}} = \left(\frac{x_i^{or}}{x_i^{wr}}\right)\left(\frac{C_{tot}^{or}}{C_{tot}^{wr}}\right) \approx \left(\frac{x_i^{or}}{x_i^{wr}}\right)\left(\frac{\rho_{tot}^{or}}{\sum_j x_j^{or} M_j}\right)\left(\frac{\sum_j x_j^{wr} M_j}{\rho_{tot}^{wr}}\right) \tag{4-17}$$

Upon applying infinite dilution to the phases, and using the equi-activity criterion for liquid-liquid equilibrium [See Appendix C-4], Equation (4-17) reduces to:

$$K_{ow,i} \approx \left(\frac{\gamma_i^{wr,\infty}}{\gamma_i^{or,\infty}}\right)\left(\frac{\rho_{tot}^{or}}{x_o^{or} M_o + x_w^{or} M_w}\right)\left(\frac{x_o^{wr} M_o + x_w^{wr} M_w}{\rho_{tot}^{wr}}\right) \tag{4-18}$$

The densities reported by Kuramochi et al. (1998) for the octanol-rich and water-rich phases are 829.7 kg/m^3 and 996.7 kg/m^3 respectively. (The saturated mole fractions are reported above). Kuramochi et al. (1998) further assumed that the ratio of infinite dilution activity coefficients in the organic and aqueous phase could be approximated by their respective pure solvent values.

$$K_{ow,i} \approx \left(\frac{\gamma_i^{w,\infty}}{\gamma_i^{o,\infty}} \right) \left(\frac{\rho_{phase}^{or}}{x_o^{or} M_o + x_w^{or} M_w} \right) \left(\frac{x_o^{wr} M_o + x_w^{wr} M_w}{\rho_{phase}^{wr}} \right) \tag{4-19}$$

These authors compared K_{ow}'s calculated, using four different UNIFAC methods (Magnussen et al., 1981; Larsen et al., 1987; Hansen et al., 1991; Gmehling et al., 1993) to predict the pure solvent limiting activity coefficient ratio in Equation (4-19). The calculated values were compared with experimental K_{ow} values. The study concluded that the Larsen et al. (1987) and the Hansen et al. (1991) method produced the most acceptable estimates.

It is the assertion of this dissertation that the predictive method of Kuramochi et al. (1998) can be improved in two ways. Firstly, as the octanol-rich and water-rich phase concentrations have already been measured and reported, these can be used instead of assuming a mole fraction mixing rule for the phase molar weight. This, thus, removes an unnecessary approximation. Lin and Sandler (1999) report the phase concentrations to be 8.229 mol/L and 55.679 mol/L for the saturated octanol-rich and water-rich phase at 25°C respectively. Consequently, Equation (4-19) becomes:

$$K_{ow,i} \approx \left(\frac{\gamma_i^{w,\infty}}{\gamma_i^{o,\infty}} \right) \left(\frac{C_{tot}^{or}}{C_{tot}^{wr}} \right) \tag{4-20}$$

Secondly, following the work performed by Voutsas and Tassios (1996), the most appropriate UNIFAC method can be selected for a given solute in the hypothetical pure octanol and pure water phases. Voutsas and Tassios (1996) suggest that the Gmehling et al. (1993) UNIFAC should be applied to systems containing an organic solute in a non-aqueous polar solvent; consequently, the modified Gmehling et al. (1993) should be used for the limiting activity coefficient of a solute in pure octanol. A typical error is expected of below 10-15 % (Voutsas

and Tassios, 1996) upon using the Gmehling et al. (1993) modified UNIFAC method for this solute-solvent pair. Subsequent computation of the aqueous phase limiting activity coefficient using the most appropriate UNIFAC method as suggested by Voutsas and Tassios (1996), should improve the overall accuracy of prediction.

The approximation employed by Kuramochi et al. (1998) regarding pure phase limiting activity coefficients can be considered valid for the water-rich phase, as this phase consists of 99.99 mole % water. However, this is not a realistic assumption for the octanol-rich phase, which, although containing a majority of organic component, does not approximate pure octanol. Tse and Sandler (1994), realising this inconsistency, have fitted an empirical expression relating the ratio of the pure solvent limiting activity coefficients to their partition coefficient for 12 halogenated compounds. Lin and Sandler (1999) later revisited this expression, regressing a larger set of chemicals spanning a greater variety of organic functional groups. The empirical correlation generated by these authors is presented in Equation (4-21) below:

$$\log K_{ow,i} = (-0.68) + (0.91)\log \frac{\gamma_i^{w,\infty}}{\gamma_i^{o,\infty}} \qquad \textbf{(4-21)}$$

This two-parameter equation was fitted from a log K_{ow} database ranging from –0.34 to 5.18 and has a correlation coefficient close to unity (0.998). Although untested, it is believed that application of the improvements discussed above regarding the work of Kuramochi et al. (1998) and applying Equation (4-21) will further improve partition coefficient estimation.

For the case of hydrophobic chemicals, Lin and Sandler (1999) have reduced Equation (4-21) to a single parameter correlation [See Equation (4-22) below]. Hydrophobic solutes have large limiting activity coefficients in water but values close to unity in pure octanol. Hence, the octanol-water partition coefficient for hydrophobic solutes, which is difficult to measure, can be approximated using the most appropriate limiting activity coefficient prediction method as suggested by Voutsas and Tassios (1996), combined with Equation (4-22).

If the experimental limiting activity coefficient of the hydrophobic solute in water is available. [See Table 4-2 for a list of databases which house experimental aqueous system infinite dilution data], Equation (4-22) may be used to estimate the octanol-water partition coefficient.

$$\log K_{ow,i} = (-0.486) + (0.806)\log \gamma_i^{w,\infty} \qquad \textbf{(4-22)}$$

Wienke and Gmehling (1998) fitted new parameters to the original UNIFAC model based on a database of Henry's constants, water solubilities and octanol-water partition coefficients covering 4234 compounds. As the parameters were fitted using this wide spectrum of data, this K_{ow} predictive tool can be used to generate other environmentally relevant partition coefficients. This method, called KOW UNIFAC demonstrated a comparable accuracy to the LSER approach and the method of Hansch and Leo (Lin and Sandler, 1999). This model utilises the pure solvent phase approximation and it should, therefore, be considered semi-empirical. KOW UNIFAC did not have any parameters fitted for alkyl ethers functional groups, and as a result this method could not be used to estimate K_{ow}'s for MTBE and TAME; consequently, it is not used as a predictive tool in this dissertation.

Lin and Sandler (1999) furthering a model they developed using Group Contribution Solvation (GCS) theory, extended the technique to predict K_{ow}, calling the prediction tool GCSKOW. On analysing the interaction energies between solute and solvent obtained from computational quantum mechanical calculations, these authors realised that the interaction energies could be decomposed into contributions from functional groups. On assumption that the method developed for pure solvents, could be applied to mixtures, Lin and Sandler (1999) extended the GCS model to multi-component solvent mixtures, fitting the molecular structure and energy parameters directly to measured K_{ow} data. On comparison of GCSKOW with KOW UNIFAC, a LSER method (Kamlet et al., 1988) and the Hansch and Leo fragment method, the GCSKOW was found to be the most accurate.

Lin and Sandler (2000) have further developed GCSKOW to account for structural and proximity effects at the cost of necessitating computational chemistry calculations to determine fragment charge and dipole distributions. This additional complexity enables GCSKOW to differentiate between isomers.

Several programs based on fragment methods for the prediction of K_{ow} are available on-line. Two examples of this include the CLOGP program, which is based on the Leo (1993) fragment method and the KOWWIN program (Meylan and Howard, 1995). The website information, regarding these programs is presented in Table 4-6 below.

Table 4-6: Prediction programs for estimation of the octanol-water partition coefficient prediction available on-line on the internet/worldwide web

Method	Reference	Website
CLOGP	Leo (1993)	http://www.daylight.com/daycgi/clogp
KOWWIN	Meylan and Howard (1995)	http://esc.syrres.com/interkow/interkow.exe

K_{ow} can also be crudely estimated from the ratio of the solubility of a chemical in pure octanol to that in pure water. Specially developed group contribution methods have been established by Yalkowsky and co-workers to predict these pure phase solubilities. For octanol solubility, the OCTASOL group contribution model has been developed by Li et al. (1995); AQUAFAC, developed by Yalkowsky and Dannenfelser (1991), can be used to predict water solubility. For a solute, which is only slightly soluble in a solvent, the infinite dilution activity coefficient can be used to predict the limited solubility (Eckert and Sherman, 1996). Consequently, the appropriate UNIFAC method, depending on the solute and solvent, as recommended by Voutsas and Tassios (1996), can be used to calculate the solubility of a component, which is sparingly miscible in water or octanol.

4.1.3 Octanol-air partition coefficients

The octanol-air partition coefficient (K_{oa}) plays an important role in the study of partitioning between air and aerosols, vegetation and soil. This partition coefficient was the last of the three main partition coefficients to be defined. Its definition came as a natural consequence of the acceptance of octanol as an established model for the partitioning of a chemical into organic material. Since there was a need to quantify air-organic exchanges, it became necessary to define an octanol-air partition coefficient.

The octanol-air partition coefficient is defined, in Equation (4-23) below, as the equilibrium ratio of the concentration of a solute in liquid octanol (C_i^o) to the concentration of the solute in the air phase above the liquid (C_i^a).

$$K_{oa,i} = \frac{C_i^o}{C_i^a} \tag{4-23}$$

where the superscripts denote pure phases of octanol (o) and air (a).

The fugacity capacity factor of a solute in octanol can be derived similarly to the water capacity factor by replacement of all w super- and subscripts with o. Consequently, the fugacity capacity factor of a solute in octanol takes the form of:

$$Z_i^o = \frac{1}{\tilde{V}_0 \gamma_i^{o,\infty} P_i^{sat}} = \frac{1}{\tilde{V}_0 \hat{H}_i^o} = \frac{1}{H_i^o} \tag{4-24}$$

Combining Equation (4-24) and Equation (4-8) to form the ratio of the fugacity factors of a solute in octanol and air, an analytical form for the K_{oa} can be derived:

$$K_{oa,i} = \frac{Z_i^o}{Z_i^a} = \frac{1/H_i^o}{1/RT} = \frac{RT}{H_i^o} \tag{4-25}$$

K_{oa} can have values up to 10^{12} for substances of low volatility and becomes especially high at low temperatures (Mackay, 2001). Harner et al. (2000) have compiled K_{oa} data and report various experimental techniques.

4.1.3.1 Experimental methods for the measurement of octanol-air partition coefficients

Direct methods for K_{oa} determination include the passing of purified air over an octanol solution (Harner and Mackay, 1995; Harner and Bidleman, 1996; Harner and Bidleman, 1998). Mackay (2001) suggests the passing of air through a packed column saturated with the octanol-solute solution. Zhang et al. (1999) has proposed an interpolation method based on gas chromatographic retention times.

On examining Equation (4-25), it is clear that the infinite dilution activity coefficient of a solute in octanol or its corresponding Henry's constant can be used to indirectly determine K_{oa}. Most of the experimental γ_i^{∞} methods cited above relevant to water can theoretically be used. However, due to practical constraints, owing to the viscous nature of 1-octanol, the most viable technique is Gas-Liquid Chromatography (GLC). Tse and Sandler (1994) have used a relative gas-liquid chromatographic technique (See section 4.1.1.1 above) to determine limiting activity coefficients of volatile organic pollutants in octanol.

4.1.3.2 Predictive methods for the estimation of octanol-air partition coefficients

Often K_{oa} is not measured, but rather calculated as the quotient of the K_{ow} and K_{aw} values. Disparity between directly measured K_{oa} values and this quotient estimation exist, with the quotient calculation consistently underestimating the measured value. This is believed to be a consequence of the mutual miscibility of octanol and water. Unlike octanol-water, octanol-air and air-water represent essentially immiscible phases and thus, the quotient calculation is not a rigorous estimation technique for K_{oa}.

Synonymously to K_{aw}, K_{oa} can be estimated from the prediction of the limiting activity coefficient of the solute in octanol. The recommended group contribution technique, according to Voutsas and Tassios (1996), for a solute in a non-aqueous polar phase is the Gmehling et al. (1993) modified UNIFAC method.

4.1.4 Organic carbon-water partition coefficients

Sorption contributes significantly to the environmental fate and impact of organic compounds as this phenomenon affects several fate processes including volatilisation, bioavailability, and degradation (Doucette, 2000). Since the sorption of hydrophobic organic substances is mostly to the natural organic matter component of a particle, the standard approach is to assume that all sorption is to the organic component, and, accordingly, define a partition coefficient between the organic carbon (K_{oc}) or organic matter (K_{om}) and water (Seth et al., 1999). These two partition coefficients are directly related, as the organic carbon fraction of particulate environmental solids is approximately 50 to 60 % by mass of the organic matter present (Mackay, 2001), having an average of about 58 % by mass (Seth et al., 1999).

A review of theory, a collection of empirical correlations, and experimental K_{oc} data can be found in Doucette (2000). This reference also reports databases of experimental K_{oc} values available in literature spanning the last 20 years.

4.1.4.1 Experimental methods for the determination of organic carbon-water partition coefficients

Measurement of K_{oc} can be determined either directly [ASTM (1987)] or indirectly. Indirect measurement of the organic carbon-water partition coefficient is facilitated through measurement of the sorption coefficient (K_d). K_{oc} has been defined as the normalised sorption coefficient. In light of this, Equation (4-26) below shows the relationship between K_{oc} and K_d, which is defined as the equilibrium ratio of the concentration of the solute sorbed on an environmental solid phase (e.g. soil, sediment or suspended sediment) [C_i^s, mg solute/kg solid] to the concentration of the solute in the water solution enveloping the solid (C_i^w, mg solute/L solution). K_d and K_{oc} have the same units of L/kg.

$$K_{d,i} = \frac{C_i^s}{C_i^w} = y_{oc} K_{oc,i} \qquad \textbf{(4-26)}$$

Upon experimentally measuring K_d and knowing the mass fraction of the organic carbon component of the solid sorbent (y_{oc}), K_{oc} can be determined using Equation (4-26).

Doucette (2000) has reviewed several experimental techniques for the determination of the sorption coefficient, including batch methods [ASTM (1987a)], which are most commonly used. HPLC correlated techniques have also proved successful for the experimental determination of K_{oc} (Gawlik, 2000). Szabó et al. (1999) have reviewed the effect of different stationary phases on K_{oc} determination.

Seth et al. (1999) warns that care must be taken upon undertaking experimental measurements of sorption coefficients, as true equilibrium, which may require several months to be established, should be achieved. In many instances, an early period of rapid sorption, followed by a long slow period, is observed (Doucette, 2000). Consequently, preliminary sorption kinetics studies should be undertaken either experimentally or estimated from correlations (Seth et al., 1999) to determine the time required to attain equilibrium. Sorption kinetics for soil particles has been detailed by Schwarzenbach et al. (1993).

4.1.4.2 Predictive methods for the estimation of organic carbon-water partition coefficients

The most common predictive techniques for K_{oc} include empirical correlations; however, several more sophisticated group contribution methods do exist. The more sophisticated techniques, however, do not necessarily increase the accuracy of the prediction. Although, K_{oc} is widely used for many chemical-sorbent combinations, it is most appropriate for the prediction of the sorption of neutral hydrophobic compounds onto sorbents, which have an organic carbon content greater than 0.1 % (Doucette, 2000).

Empirical methods

Empirical predictive correlations for K_{oc} are most commonly used in environmental fate modelling. Karickhoff (1981) showed that the organic carbon-water partition coefficient is closely related to the octanol-water partition coefficient; K_{oc} has been correlated with several properties and descriptors.

Seth et al. (1999) analysed the theory underlying organic carbon-water partitioning and, on examination of a large database of K_{oc} correlations (Gawlik et al., 1997), suggested the following rule of thumb:

$$K_{oc} = 0.35\, K_{ow} \tag{4-27}$$

The organic carbon-water partition coefficient in Equation (4-27) is not dimensionless and has units of L/kg. The correlation has a variance confidence factor of 2.5 (Seth et al., 1999).

Seth et al. (1999) has suggested that ratio of the K_{oc} to K_{ow} should lie between the following range or be subject to scrutiny:

$$0.1 < \frac{K_{oc}}{K_{ow}} < 1$$

Baker et al. (2000) have recommended that care must be taken when using K_{ow} correlations to predict K_{oc} for very hydrophobic chemicals ($\log K_{ow} > 5.0$). The seemingly linear relationship between $\log K_{oc}$ and $\log K_{ow}$ appears to flatten out in the range of $\log K_{ow}$ of 6 or 7 (Baker et al., 1997). It is not known whether this observation is an actual phenomenon or a result of experimental uncertainty inherent in the measurement of K_{ow} in this hydrophobic range.

Sabljić et al. (1995) have performed a systematic study, examining an extensive database of K_{oc} data for its relationship with K_{ow}. These authors regressed measured K_{oc} and K_{ow} data determining general and chemical class-specific correlations for the prediction of K_{oc} from K_{ow}. These authors also noted the presence of large uncertainties in K_{oc}, in the range of $\log K_{ow}$ greater than 4.

Group contribution methods

Ames and Grulke (1995) used activity coefficient group contribution models (including UNIFAC) to estimate the aqueous phase and soil organic matter activity coefficients. The soil organic matter was modelled as a polymeric phase simple humic acid. The predictions were typically within an order of magnitude, and the use of an experimentally derived activity coefficient significantly improved the predictions (Doucette, 2000). This implies that the error associated with the method is more likely a result of the limitations of the predictive power of the activity coefficient model rather than a systematic error in the sorption model.

4.1.5 Bioaccumulation and biomagnification

It is widely observed that some chemicals have the ability to achieve high concentrations within an organism relative to the environmental concentration to which it is exposed. In this context, organisms include plants, invertebrate and vertebrae, such as fish, mammals, birds, and reptiles (Mackay and Fraser, 2000). The step change in concentration between environment and species (bioaccumulation or bioconcentration), and sometimes, greater concentration jump between subsequent species in a food chain (biomagnification), are important fate processes, necessary to quantify and simulate environmental fate behaviour. Several reviews pertaining to bioaccumulation have been performed including those of Gobas and Morrison (2000), and Mackay and Fraser (2000).

There are several incentives for quantifying the extent of bioaccumulation. Organisms, which are most sensitive to bioaccumulation, can be used as indicators as to the extent of pollution; Moreover, identification of organisms susceptible to bioaccumulation is important if the species forms a prey item anywhere along the human consumption food chain.

4.1.5.1 Definitions regarding the phenomenon of bioaccumulation

Several definitions are necessary for the understanding of these bio-fate processes. Consequently, bioaccumulation, bioconcentration, biomagnification and bioavailability are defined below. Often, the definitions are given in the context of aquatic biota, which is followed here.

Bioaccumulation and bioconcentration

The bioaccumulation factor of a chemical in a biota species η (BAF_η) is defined as the ratio of the concentration of a chemical inside the species (C_η) to the accessible concentration of the chemical in the organism's habitat. Thus, for aquatic biota, the habitat corresponds to the water compartment (C_w).

$$BAF_\eta = \frac{C_\eta}{C_w} \tag{4-28}$$

An aquatic organism is capable of chemical uptake through various exposure paths; through dietary absorption, through transport across respiratory or dermal surfaces (Gobas and Morrison, 2000). Bioconcentration is a special bioaccumulation case, normally achieved in the laboratory, where the only uptake mechanism is the transport of chemical across biological membranes. Accordingly, the definition of the bioconcentration factor (*BCF*) is analogous to the bioaccumulation factor but includes a specified exposure route.

Biomagnification

Biomagnification can be regarded as the special case of bioaccumulation in which the chemical concentration within an organism exceeds that in the organisms diet due to dietary absorption (Gobas and Morrison, 2000). The biomagnification factor (*BMF*) is defined as the ratio of the chemical concentration in an organism to the concentration in the organism's diet (C^η_{diet}):

$$BMF_\eta = \frac{C_\eta}{C^\eta_{diet}} \tag{4-29}$$

Biomagnification has been explained as a result of the depletion of the lipid content in the gut of successive trophic levels, which subsequently increases the chemical concentration up the food chain. This, in principle, is similar to the increase in concentration of a non-volatile solute in a volatile solvent that is evaporating (Mackay and Fraser, 2000). Biomagnification will not

manifest if metabolic transformation, elimination or growth dilution occur to a significant extent. If these phenomena are controlling, the opposite of biomagnification, trophic dilution, can occur, which also has the ability to propagate up the food chain.

Bioavailability

Not all contaminants present in an environment are in intimate contact with the biota. Some of the chemical can be sorbed to suspended particles or sediment contained within the compartment. Only a fraction of the chemical dissolved in the water is biologically available, or bioavailable, for uptake into an aquatic organism. Thus, in defining bioaccumulation and bioconcentration factors, it is important to keep in mind whether the total water concentration or the dissolved water concentration is used in the denominator of the definitions. The total concentration includes both the dissolved available component and the fraction sorbed to suspended particles or sediment.

The fraction of chemical sorbed, which is consequently not bioavailable, is considered to be controlled by partition coefficients like the organic-carbon partition coefficient [See section 4.1.4]. Although partition coefficients are often used to predict the bioavailable fraction, the complex nature of this phenomenon is beyond this simplistic approach. A phenomenon, known as "aging", has been discussed by Alexander (2000), where the bioavailability of organic compounds in soil decreases with time. Clearly this time-bound phenomenon cannot be predicted by equilibrium partition coefficients.

4.1.5.2 Bioaccumulation models

Bioaccumulation models can be divided into empirical and mechanistic approaches. The two approahces reflect different levels of data intensity and simulation realism. The lower level of complexity is represented by the empirical approach; however, many non- bioaccumulating species can be identified by this approach and it is subsequently used to set threshold limit criteria. It is accepted that bioaccumulation occurs in non-metabolising chemicals with log $K_{ow} > 5$ (Mackay and Fraser, 2000; Mackay, 2001).

Empirical models

In the empirical approach, *BCF* data is regressed against parameters like K_{ow}. The experimental determination of bioconcentration factors includes many uncontrolled factors like biological variability. Despite these problems, this approach is indicative of 'real ' conditions (Mackay and Fraser, 2000) and, thus, believed to simulate realistic values. Several empirical correlations have been collected below [See Table 4-7]:

Table 4-7: Empirical correlations for the *BCF* as a function of K_{ow}

Bioconcentration equation	Reference	Species (η)
$\log BCF_{\eta} = 0.542 \log K_{ow} + 0.124$	Neely et al. (1974)	Rainbow trout
$\log BCF_{\eta} = 0.85 \log K_{ow} - 0.70$	Veith et al. (1979)	Fathead minnows
$BCF_{\eta} = 0.048 K_{ow}$	Mackay (1982)	Fathead minnows

Neely et al. (1974) was first to report an empirical correlation relating K_{ow} to *BCF* using data measured from rainbow trout. Veith et al. (1979) extended this concept, by regressing a larger set of data obtained from fathead minnow. Mackay (1982) regressed the same data to a correlation representing the product of the K_{ow} and an effective fish lipid fraction [by volume] (L_{η}). In Table 4-7 above, L_{η} equals 0.048 in the Mackay (1982) *BCF* concentration. Meylen et al. (1999) have proposed a discrete correction factor *BCF* method, which accounts for a chemical's ability to biodegrade.

The ability of these equations to simulate bioconcentration trends can be gleaned from analysis of their mathematical form. Bioconcentration is found to increase with log K_{ow} up to a definite point (log K_{ow} = 5 or 6) after which it diminishes to zero. This is thought to occur as a result of reduction in bioavailability. Although not presented here, Meylan et al. (1999) accounts for this bi-linear behaviour by discretisation of BCF over a log K_{ow} interval. The linear nature of the three equations documented in Table 4-7 ensures that they are not valid for chemicals with log K_{ow}'s greater than 6.

The validity of the empirical correlation of bioconcentration with octanol-water partition coefficients has been contested by several researchers. Woodrow and Dorsey (1997) remonstrate the applicability of K_{ow} asserting that the free energy of solute transfer between octanol and water is dominated by entropic considerations, in contrast to water-micelle partitioning and biopartitioning, which are dominated by enthalpic terms. Consequently, Woodrow and Dorsey (1997) nominate the use of water-micelle partitioning, as determined by micro-emulsion electrokinetic studies, as being more thermodynamically relevant.

Mechanistic models

Mechanistic models entail a mass balance approach, which describes several transport processes affecting exchange of chemical into and from an organism. The processes accounted for include the passive diffusive process of respiration, dermal diffusion (which may be active in one direction owing to the transport properties of membranes), food ingestion and egestion, metabolic conversion, reproductive losses (for female organisms) and growth dilution.

The simplest approach is to treat the organism as a single compartment; however, more sophisticated models, incorporating compartmentalised connected organs or tissue groups, have been developed. Pharmacokinetic models, representing the most sophisticated mechanistic models, have been reviewed by Wen et al. (1999).

The mechanistic approach requires, amongst other properties, kinetic data to describe the transport processes. The kinetic approach can be easily formulated using the Mackay fugacity approach and numerous fugacity models have been developed (Mackay and Fraser, 2000). Typical values for kinetic data ($k_{\eta,j}$) can be found in Gobas and Morrison (2000) and Mackay and Fraser (2000).

Although generally applied to fish, mechanistic bioaccumulation models are applicable to invertebrates, mammals and birds. Amongst others, Clark et al. (1987) have examined contamination accumulation in birds and Morrison et al. (1996) have investigated the uptake of chemical into benthic invertebrates.

4.1.5.3 Food web models

The mechanistic models have been extended to simulate food chains. Examples of food web models include Gobas (1993) and Clark et al. (1990). The latter model has been extended by Campfens and Mackay (1997) to quantify trophic transfer in flexible aquatic food chains in which organisms are permitted to consume from any trophic level including their own.

Empirically based concentration relationships have also been used to simulate aquatic trophic transfer (Thomann, 1989). This type of model, unlike the mechanistic approach cannot predict the phenomenon of trophic dilution. However, in order for the phenomenon of trophic dilution to be considered as a significant amelioration process, the chemical must first be shown to be a potential bioaccumulator in, at least, the primary producer level of a food chain.

4.1.5.4 Three-tiered bioaccumulation screening method of Mackay and Fraser (2000)

Mackay and Fraser (2000), after performing an extensive review on the mechanisms and models of bioaccumulation of persistent organic chemicals, suggested a three-tiered screening process for bioaccumulation. This undesirable phenomenon forms part of the PBT-LRT profile used to classify chemicals according to their potential to cause environmental harm. Table 4-8 below summarises the three-tiered screening process, as proposed by these authors.

Each tier represents an increase in screening complexity, as previous simplifying assumptions are removed. It is believed that Tier 1 will identify chemicals, which are probable bioaccumulation species, based on partitioning properties alone. Tier 2 evaluates bioaccumulation potential taking into the account the mitigating effects of elimination processes. Tier 3 can identify possible biomagnification culprits. (Mackay and Fraser, 2000). Although the third tier is capable of divulging all relevant bioaccumulation information, it is considered superfluous to screen large sets of chemicals at the third tier when the first tier has the ability to eliminate a large portion of non-bioaccumulating chemicals.

Table 4-8: Three-tiered bioaccumulation screening process as outlined by Mackay and Fraser (2000)

Tier	Model	Assumptions	Criteria
1	Empirical: $BCF_\eta = (1 + L_\eta K_{ow})$	• Partitioning to lipids • No metabolism • No ionisation • No biomagnification • 100% bioavailability • Equilibrium applies	$BCF_\eta > 5000$ $\log K_{ow} > 5$
2	Mechanistic: $BAF_\eta = f(k_{\eta,j})$	• Steady state • No growth dilution • No ionisation	$BAF_\eta > 5000$
3	Food chain model	• Sequential food chain model	Identifies biomagnification

4.2 Environmental Processes

Many environmentally significant processes occur concurrently in several of the compartments, which comprise the environment. These processes include sorption, reaction, particle settling and mass transfer.

4.2.1 Environmental Transport Processes

Chemicals can be transported through the various environmental compartments by microscopic and/or macroscopic processes. Molecular diffusion is an important microscopic process, which is driven by concentration gradients that exist within a randomly mixed phase. At a macroscopic level, bulk fluid movement, like convection and advection, and mixing effects, due to turbulence, eddy formation and velocity gradients, facilitate transport. Transport by molecular diffusion and mixing is referred to as dispersion.

4.2.1.1 Diffusive and dispersive transport

Diffusive transport at a molecular level can take place under steady state or unsteady state conditions in homogenous or heterogeneous phases. The rate of chemical transport under steady state conditions is quantified by Fick's first law, which states that the molar diffusive transport rate of a species in a given direction (J_z) is directly proportional to the concentration gradient and the area of flow (A). The proportionality constant linking the properties is the molecular diffusivity (D).

$$J_z = -DA\left(\frac{\partial C}{\partial z}\right) \tag{4-30}$$

To account for the greater molar fluxes associated with turbulence, and eddies, a dispersion coefficient (ξ) is defined. Dispersive transport is modelled analogously to diffusive transport with the dispersion coefficient replacing the molecular diffusivity in Equation (4-30)

In diffusion of molecules through porous media, the movement of the molecules is constrained by solid phases and surfaces, which effectively slows down the transport rate. The diffusivity of the molecules is affected by the reduced area of flow and the tortuous nature of the path the molecules follow: These two factors are accounted for by multiplying the molecular diffusivity by the ratio of the voidage (or porosity) of the porous medium to the turtuousity factor, which is defined as the quotient of the actual path and the perpendicular path length. Another method accounting for the effective diffusivity through porous media uses the porosity raised to an exponent as a multiplier (Mackay, 2001). Knudsen diffusivities are used for diffusion inside pores. Diffusion through porous media is evident in the soil compartment, a heterogeneous phase consisting of solid, water and air.

4.2.1.2 Advective Transport

Advection is the general transport of the solute due to the bulk fluid movement of a medium. This mechanism allows the transport of solute across system boundaries and represents an irreversible loss of solute from the system. The molar advective rate can be calculated as the product of the concentration of a solute and the volumetric rate of the bulk fluid (G). The

volumetric rate is equivalent to the linear velocity (u) of the mobile fluid multiplied by the area of flow. Hence:

$$J_z = GC = AuC \tag{4-31}$$

In the environment, the main advective compartments are the air and water phases. The subscript z is used in Equation (4-31), as the molar advection rate is directional.

4.2.1.3 Mass transfer across an interface

Molar fluxes across an interface can be expressed using mass transfer coefficients as below [See Equation (4-32)]. Many models describing mass transfer have been formulated; the most famous of which is the Nernst (1904) stagnant film theory, the Higbie (1935) penetration theory and the Dankwerts (1951) surface renewal theory. Mass transfer is formulated similarly to Fick's first law [Equation (4-30)], in that a flux is modelled as being directly proportional to a concentration based driving force. In this case, the driving force is a concentration difference, as opposed to a concentration gradient. A mass transfer coefficient (U), thus, replaces diffusivity as the proportionality constant. Once again, the molar transfer rate is directional:

$$J_z = U A \Delta C \tag{4-32}$$

For the Nernst (1904) stagnant film theory, the mass transfer coefficient (MTC) can be shown to be the ratio of the diffusivity and the film layer thickness (Δz), which is the thickness of a stagnant layer of fluid situated adjacent to the phase boundary that controls the mass transfer rates by diffusion through the film. Hence:

$$U = \frac{D}{\Delta z} \tag{4-33}$$

For mass transfer across an interface between two phases, α and β, two-film theory can be used to quantify the exchange across the interface. The direction of mass transfer will be from the

phase of high concentration to the phase of lower concentration. Figure 4-1 illustrates two-film theory:

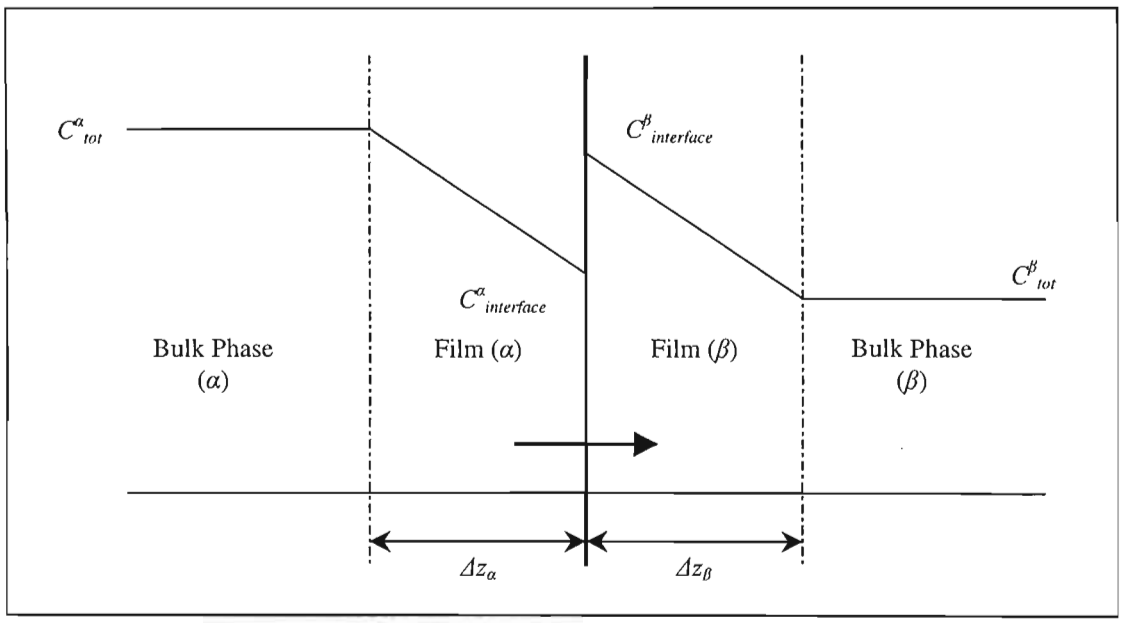

Figure 4-1: Illustration of two-film theory between the phases, α and β (The direction of mass transfer is from the α to the β phase)

Overall mass transfer coefficients ($U^{i}_{overall}$) based on either phase can be obtained by equating the two phase fluxes describing the mass transfer of solute between the bulk fluid and the phase interface. The results are expressed below as Equations (4-34) and (4-35):

$$J_{\alpha\to\beta} = U^{\alpha}_{overall} A\left(C^{\alpha}_{i} - C^{\beta}_{i}\right) \tag{4-34a}$$

where

$$U^{\alpha}_{overall} = \left(\frac{1}{U_{\beta} K_{\alpha\beta}} + \frac{1}{U_{\alpha}}\right)^{-1} \tag{4-34b}$$

or

$$J_{\alpha\to\beta} = U^{\beta}_{overall} A\left(C_i^{\alpha} - C_i^{\beta}\right)$$

(4-35a)

where

$$K_{\beta,i} = \left(\frac{1}{k_{\beta,i}} + \frac{K_{\alpha\beta,i}}{k_{\alpha,i}}\right)^{-1}$$

(4-35b)

The relationship between the mass transfer coefficient of a chemical and its diffusivity in the same phase is represented by the following relationship:

$$U \propto (D)^n$$

(4-36)

The exponent, *n*, ranges from 0 to 1, depending on which mass transfer theory is used. However a value of 0.5 is often used.

4.2.2 Environmental non-reactive processes

Non-reactive processes can cause changes in the chemical concentration of an environmental compartment without transforming the chemical. This is achieved by transference of a chemical from one phase to another or by the non-reversible transport of chemical across compartment boundaries. Sorption is an example of the former process; while settling and sedimentation is an example of the latter.

4.2.2.1 Sorption processes

Adsorption and desorption of chemicals (adsorbates) onto solid surfaces (adsorbents) is an important process in the environment. Besides affecting the bioavailability of a chemical, sorption onto particles and the subsequent settling of these particles is an important process in

environmental fate modelling. Adsorption can be divided into two types of mechanisms: chemisorption and physisorption. Absorption is distinct from adsorption and involves the diffusion of a solute from one bulk medium into another bulk medium of a different phase.

The relationship between the concentration of the sorbed species (C_i^{sorbed}) and the bulk phase concentration (C_i^{bulk}) is governed by temperature. Two common isothermal models used include the Langmuir isotherm and the Freundlich isotherm defined below:

Langmuir isotherm

$$C_i^{sorbed} = \frac{aC_i^{bulk}}{b + C_i^{bulk}} \tag{4-37}$$

Freundlich isotherm

$$C_i^{sorbed} = K_F \left(C_i^{bulk}\right)^{1/n} \tag{4-38}$$

where the constants, a and b in Equation (4-37) and K_F in Equation (4-38), depend on temperature, as well as the nature of the adsorbent and adsorbate.

The Langmuir isotherm is more prevalent in aerosol-air partitioning and the Freundlich isotherm (in linear format with $n = 1$) is found to model water-soil or sediment particle partitioning adequately.

4.2.2.2 Settling and resuspension

The fate and transport of suspended particles laden with sorbed chemicals is a significant process in environmental fate modelling. Particle sedimentation occurs in the both air and the water phases. The processes are driven by gravity, buoyancy, hydrodynamic, aerodynamic or electrostatic forces. Sedimentation involving groups of particles is far more complicated than the settling of single particles because of the interactions between particles in a group.

Resuspension is a difficult process to model. Resuspension of sediment in a water system can be caused through bioturbation of the sediment by benthic organisms. Owing to the complexity of modelling resuspension, a net settling rate can be used. If it is negative, there is a net resuspension of particles.

The theory for settling hinges upon the description of the drag forces encountered by particles experiencing relative motion between particle and fluid. The laws governing the drag coefficient (C_D) for various fluid flow regimes, is detailed by the particle Reynolds number (Re_p), defined below in Equation (4-39). Re_p is used to calculate the settling velocity of a particle in a fluid. The different laws for the various fluid flow regimes, extending from laminar to turbulent flow, can be found in Table 4-9:

Table 4-9: Drag coefficient correlations for various fluid flow regimes extending from laminar to turbulent flow

Region	Drag Coefficient (C_D)	Settling law
$Re_p < 0.2$	$C_D = \frac{24}{Re_p}$	Stokes
$0.2 < Re_p < 1000$	$C_D = \frac{24}{Re_p}\left[1 + 0.15 Re_p^{0.687}\right]$	Allen
$1000 < Re_p < 2x10^5$	$C_D = 0.44$ (constant)	Newton
$Re_p > 2x10^5$	$C_D = 0.10 \rightarrow 0.20$	None

where

$$Re_p = \frac{u_p d_p \rho}{\mu} \qquad \textbf{(4-39)}$$

To ascertain the terminal velocity of a particle, and hence, its settling velocity, Equation (4-39) and Equation (4-40) together with the corresponding drag coefficient law, must be combined to

solve for u_p. Analytical solutions exist for the Stokes' and Newton's law regimes, as well as for high Re_p values; however, an iterative solution is required solve for the Allen's law regime.

$$C_D \, \mathrm{Re}_p^2 = \frac{4}{3}\left(\frac{d_p^3 \rho (\rho_p - \rho) g}{\mu^2} \right) \tag{4-40}$$

The term on the right-hand side of Equation (4-40) is known as the Archimedes number.

4.2.3 Environmental reactive processes

Reactive processes cause the change in the chemical concentration of an environmental compartment by transforming the chemical into other compounds. Reactions can occur in a single step or through multiple mechanisms, in serial, in parallel or in cycles. Examples of environmental reactions, which occur naturally, include biodegradation, oxidation, hydrolysis, photolysis, and reduction amongst others. Mackay (2001) briefly reviews these reaction types. A more detailed review is outlined in Boethling and Mackay (2000).

Determination of the rates of these reactions is extremely important, especially regarding the persistence of a compound in the environment. Howard (1991) has compiled a handbook of environmental degradation rates. Degradation rates for MTBE and ethanol can be found in this reference. Gouin (2002), in Appendix B, reviews several estimation methods for degradation half-lives.

4.2.3.1 First order reactions

Although biological reactions, and numerous other reactions occurring in the environment, are complicated and almost certainly not first order, it is commonly assumed that the reaction can be described as pseudo-first order (Mackay, 2001). The rate or kinetics of a reaction is quantified using the law of mass action.

For a first order reaction, the rate of reaction is directly proportional to the chemical concentration. Hence:

$$\frac{dC_i}{dt} = -k_i C_i \tag{4-41}$$

Solving Equation (4-41) for the time required for half the initial concentration of chemical to be depleted ($t_{1/2,i}$) yields:

$$t_{1/2,i} = \frac{\ln 2}{k_i} \tag{4-42}$$

Degradation data for organic compounds is normally given in the form of the half-life and can be converted to a pseudo-first order reaction constant using Equation (4-42) above.

4.2.3.2 Biological reactions

Biological reactions, which are facilitated by enzyme controlled microbial activity, are commonly described using the Michaelis-Menten model (Mackay, 2001). This model is derived from a two-step reaction sequence, where a substrate is converted to product in the presence of an enzyme. The resulting model is a two-parameter equation:

$$rate = \mu_{MM} \frac{[P][S]}{K_{MM} + [S]} \tag{4-43}$$

where $[P]$ and $[S]$ are the product and substrate concentrations respectively, and μ_{MM} and K_{MM} are fitted constants which depend on temperature, as well as the nature of the substrate and enzyme. However, extensive data on the biological degradation of consumer products has shown that biodegradation kinetics can be adequately described by pseudo-first order reactions (Larson and Cowan, 1995).

CHAPTER 5

The nature of environmental media

The environment consists of numerous naturally defined compartments, all interconnected and dynamic; consequently, the environment can be viewed as a series of sources and sinks for the movement and accumulation of energy and matter. In order to model the fate of chemicals within its boundaries, physical understanding of the environment and its compartments must precede it.

The environment of significance to the fate modelling of organic chemicals may be broken up into four main compartments:

- The atmosphere
- The hydrosphere
- The geosphere
- The biosphere

5.1 The atmosphere

The atmosphere consists of a thin layer of mixed gases covering the earth's surface; this blanket of gases is held to the earth by gravity. Excluding atmospheric water vapour, which varies with temperature and proximity to water sources, air consists (by volume) of the following according to Manahan (2000):

- 78.1 % nitrogen (N_2)
- 21.0 % oxygen (O_2)
- 0.9 % argon (Ar)
- 0.03 % carbon dioxide (CO_2)

The atmosphere may contain anywhere between 0.1 and 5 % (by volume) water vapour, with a normal range of 1–3 %. However, a global average of 1 % is commonly assumed (Manahan, 1990). In addition, air contains a large variety of trace level gases at levels below 0.002 by volume percent, including neon, helium, methane, krypton, NO_x, hydrogen, xenon, sulphur dioxide, ozone, ammonia and carbon monoxide.

The atmosphere serves as a protective blanket, which nurtures life on the earth and protects her from the hostile environment of outer space. Furthermore, the atmosphere is the source of carbon dioxide for plant photosynthesis and oxygen for respiration. It also provides the nitrogen utilised by nitrogen-fixing bacteria. As part of the hydrologic cycle, the atmosphere permits the transport of water from the oceans to land; thus, acting as a condenser in a vast solar-powered still. Unfortunately, the atmosphere has been used as a sink for many pollutants, due to its vast volume and effective dilution powers.

In its essential role as a protective shield, the atmosphere absorbs most of the cosmic rays protecting terrestrial organisms from their damaging effects. It also absorbs most of the electromagnetic radiation from the sun, allowing transmission of radiation only in the regions of 300-2500 nm (near-ultraviolet, visible, and near-infrared radiation) and 0.01-40 m (radio waves) [Manahan, 1990]. By absorbing electromagnetic radiation below 300 nm, the atmosphere acts as a filter of ultraviolet radiation that would otherwise be very harmful. Furthermore, as it emits infrared radiation into space, after absorbing energy released by the earth, the atmosphere moderates the planet's temperature (Manahan, 1990).

Carbon dioxide is an important re-absorbing specimen. As studies show that its concentration is increasing by 1 ppm (on a volume basis) per annum (Manahan, 2000), concerns about the extent of this disturbance on the earth's energy balance has lead to the development of "greenhouse effect" theory. The photochemical reactions involved in absorbing energy constitute the majority of chemistry that exists in the atmosphere.

5.1.1 Stratification of the Atmosphere

The atmosphere is stratified into four layers based on temperature/density relationships, resulting from interactions between physical and photochemical processes in the air compartment.

Table 5-1: Temperature and altitudes intervals of the stratified atmosphere

Layer	Altitude [km]	Temperature [°C]
Troposphere	10-16	15 to –56
Stratosphere	50	-56 to -2
Mesosphere	85	-2 to -92
Thermosphere	500	-92 to >200

The troposphere is the lowest layer of the atmosphere extending from sea level to an altitude of 10-16 km, and is characterised by a generally homogeneous composition of gases (Manahan, 2000). It has a decreasing temperature profile with increasing altitude resulting from the heat-radiating earth. The upper limit of the troposphere, which has a temperature minimum of about -56°C, varies in altitude by a kilometre or more with underlying terrestrial surface conditions. The homogeneous composition of the troposphere results from constant mixing facilitated by circulating air masses (Mackay, 2001). The water vapour content of the troposphere is, however, extremely variable because of cloud formation, precipitation, and evaporation of water from terrestrial sources.

The cryogenic temperature of the upper level of the troposphere forms a layer called the tropopause, which acts as a barrier to water loss. The cold temperature causes water vapour to condense, not allowing water to transmit to higher altitudes. If this barrier did not exist than water would undergo photolysis at higher altitudes, and be lost from the earth's atmosphere as hydrogen.

The atmospheric layer directly above the troposphere is the stratosphere, in which the temperature rises to a maximum of about -2°C. The reason for this increase is the absorption of ultraviolet solar energy by ozone (O_3), which may reach a concentration of around 10 ppm by volume in the mid-range of the stratum (Manahan, 2000). Wavelengths ranging between 220 nm and 330nm are absorbed by ozone.

The absence of high levels of radiation-absorbing species in the mesosphere, immediately above the stratosphere, results in a further temperature decrease to about –92°C at an altitude around 85 km. The upper regions of the mesosphere and higher define a region called the exosphere from which molecules, and ions, can completely escape the atmosphere.

The outermost layer of the atmosphere is the thermosphere, in which highly rarefied gases are present. This stratum reaches a temperature as high as 1200°C owing to the absorption of high frequency radiation.

The lower region of the atmosphere (up to approximately 50 km) is relatively homogenous in composition (Manahan, 1990); consequently, both the troposphere and stratosphere are grouped together and called the homosphere. Conversely, the upper region, including the meso-and thermosphere, is termed the heterosphere, due to its great variability in composition.

5.1.2 Pressure-altitude relationship

Atmospheric pressure decreases exponentially with increasing altitude. The pressure profile largely determines the characteristics of the atmosphere. The pressure-altitude profile may be derived from a force balance for a differential box of air and the assumption of an ideal gas [See Appendix A-4]

$$P(z) = P_0 \exp\left[\left(\frac{Mg}{RT}\right)z\right] \tag{5-1}$$

5.1.3 Movement of air masses

Movement of air occurs both laterally and vertically. Lateral movement is known as advection or wind, while vertical movement is known as convection. Both air movements play a role in the formation of weather and climate. According to Manahan (2000), weather is the result of the interaction of the following three effects:

- Redistribution of solar energy.
- Horizontal and vertical movement of air masses with varying moisture contents.
- Evaporation and condensation of water accompanied by the uptake and release of heat.

On a global scale, weather becomes known as climate. As solar energy is absorbed by a body of water, some of the surface water will evaporate. The water vapour, and the accompanying latent heat, humidifies the air adjacent to the water source. The warm, moist mass of air, thus produced, moves from a region of high pressure to a region of low pressure, cooling by expansion as it rises through the convection column. As the air mass cools, water condenses from it and latent energy is released; this forms a major pathway by which energy is transferred from the geosphere to the atmosphere. Wind or advection currents arise due to the laws governing fluid mechanics, and consequently, movement is from a high pressure to a lower pressure.

5.1.4 Particulate matter

Particulate matter found in the atmosphere range from aggregates of a few micrometers to pieces of dust visible to the naked eye. Some of these atmospheric particles, such as sea salt formed by the evaporation of water from sea spray droplets, are natural and even beneficial to atmospheric constituents. Particulate matter, especially very small particles serve as important seeding agents called condensation nuclei allowing water vapour to condense in the formation of raindrops. Colloidal-sized particles in the atmosphere are called aerosols. Aerosols formed from the grinding up of bulk matter are known as dispersion aerosols. Most aerosols of natural origin have a diameter of less than 0.2 micrometers (Manahan, 1990). These particles are called Aitken particles.

Aerosols in ambient air may be classified into three types according to size:

- Nucleation (< 0.1 μm)
- Accumulation (0.1 to 1 μm)
- Sedimentation (> 1 μm)

Nucleation aerosols coagulate, forming the accumulation type particles, which have a large residence time, residing for more than a week in the atmospheric mixing layer. Thus, they can form and be transported thousands of kilometres carrying sorbed chemical species on their extensive internal surface areas. Larger particles will fall more quickly due to sedimentation, and, are, thus, not transported large lateral distances.

For the most part, aerosols consist of carbonaceous material, metal oxides and glasses, dissolved electrolytes, and ionic solids. The predominant constituents are carbonaceous material, water, sulphates, nitrates, ammonium salts, nitrogen and silicon. The carbon or organic content of aerosols and the high specific area of these particles result in their affinity for the sorption of organic chemicals from the air compartment. The composition of aerosol particles varies significantly with size.

Airborne particles undergo a variety of processes in the atmosphere. Small colloidal particles are subject to diffusion. Particles may react with atmospheric gases and species. Smaller particles may coagulate together to form larger particles. Coagulated particles, and other particulate matter of sufficient size, may undergo sedimentation or dry deposition. A major process effecting atmospheric particles is wet deposition or the scavenging of particulate matter by raindrops and other forms of precipitation. Wet deposition rates are determined by rainfall intensity, while dry deposition is primarily a function of particle size.

It is significant to note that besides diffusive interaction between air and other terrestrial surface compartments, deposition, both dry and wet, is an important non-diffusive process linking the contents of the air compartment, non-diffusively, to the other surface compartments like lakes, rivers and soil. Thus, deposition processes rely on particulate matter as a medium of transportation.

5.2 Modelling the air compartment

The air compartment is usually modelled containing two phases: an air phase and an aerosol phase. Although the aerosol phase comprises a minute component of the overall atmospheric volume, it plays a significant role in the fate of organic chemicals (Scheringer, 1997).

5.2.1 Atmosphere

Although the atmosphere extends through four strata, the stratum, which is in most intimate contact with the earth, is of greatest significance regarding environmental modelling. The tropopause behaves as an effective barrier slowing exchange of matter between the troposphere and the stratosphere and it is rare, unless of particular interest for chemicals like freon, to model beyond the troposphere (Mackay, 2001). Furthermore, approximately 85% of the mass of the atmosphere resides in the troposphere directly into which most air borne discharges occur; thus, this region of the atmosphere is of particular importance.

To negate the modelling complexity as a result of the changing pressure-altitude profile, the troposphere can equivalently be represented by a homogeneous compartment, 6 km in height (Mackay, 2001) behaving like an ideal mixture with a pressure of 1 atm, a temperature of 25°C and a density of 1.19 kg/m^3. [See Appendix A-5 for derivation].

If the environment of concern is localised, it is highly unlikely that pollutants will manage to penetrate to an altitude of 6 km; Hence, according to Mackay (2001), an air compartment height of between 500 and 2000 m is more reasonable to use for modelling purposes, depending on airflow patterns. Mackay et al. (1996a) and Beyer et al. (2000) have used an atmospheric height of 1000 m; McKone (1993) has used an atmospheric height of 800 m in the CalTOX model. Hertwich and McKone (2001) have used a chemical dependent characteristic atmospheric height, called the atmospheric scale height, which is defined as the height of atmosphere required to contain the pollutant if the entire atmosphere exhibits the ground concentration. Subsequently, the atmospheric scale height ranged from essentially ground level to 3900 m for the 288 organic pollutants investigated by Hertwich and McKone (2001).

5.2.2 Aerosols

Aerosols vary extensively in size, distribution, and in their atmospheric concentration, and consequently, it is difficult to assign values to them. However, as they may play an important role in the fate of a chemical, ranges or estimated values are assigned to them.

According to Mackay (2001), aerosols have the following properties:

- Typical aerosol diameters are of a few micrometers (μm).
- Concentrations of particulate matter or total suspended particulates (*TSP*) in the atmosphere range from 5 μg/m^3, in a rural area, to 100 μg/m^3, in an urban polluted area. A typical value of 30 μg/m^3 is suggested with a confidence factor of five.
- The density of the aerosol particles is approximately 1.5 g/cm^3.
- The fraction of organic matter of the aerosol is typically 0.2 (by mass).
- Particulate matter volume fraction (v_p^a) in the air compartment is about 2 x 10^{-11}.

The generalised aerosol properties, recommended by Mackay (2001) concur with average properties reported by Whitby (1978), presented in Bidleman and Harner (2000), for aerosols ranging in size from 0.1 to 1 μm. Table 5-2 outlines measured aerosol properties of different air types. Included in this table is the surface area per unit volume (θ, cm^2 aerosol/cm^3 air) of the aerosols, which is an important parameter for aerosol-air partitioning. A typical background value measured in the USA is 1.5 x 10^{-6} cm^2 aerosol/cm^3 air (Bidleman, 1988). Various assumed aerosol particle densities have been used in literature. The density is necessary to convert *TSP*'s into aerosol volumetric fractions and vice versa. Table 5-2 below indicates *TSP*'s calculated using three different literature sources for particle density.

Shah et al., (1986) have reported *TSP*s corresponding to 30 and 80 μg/m^3 for 20 rural locations and 46 U.S. cities, respectively. Eisenberg et al. (1998) have used a *TSP* value of 50 μg/m^3 to represent a global average ranging between 20 to 100 μg/m^3.

Table 5-2: Aerosol properties for several air types [adapted from Bidleman and Harner (2000)]

Air Type	θ [cm^2 aerosol/cm^3 air]	v_p^a [-]	$TSP^{\dagger}$ [µg/m^3]		
			Manahan (2000)	Mackay (2001)	Corn et al. (1971)
Clean	0.4×10^{-6}	6.5×10^{-12}	6.5	10	13
Background	1.5×10^{-6}	30×10^{-12}	30	45	60
Local	3.5×10^{-6}	43×10^{-12}	43	65	86
Urban	11×10^{-6}	70×10^{-12}	70	105	140

Note: †TSP calculated, assuming a particle density of:
Manahan (2000): 1 g/cm^3
Mackay (2001): 1.5 g/cm^3
Corn et al. (1971): 2 g/cm^3

Another aerosol property relevant to aerosol sorption is the organic carbon content of the particle. Shah et al. (1986) have reported the organic carbon content of airborne particles to be 0.084. Cotham and Bidleman (1995) have reported an organic matter carbon content of 0.23 for aerosol matter in Chicago, Illinois.

5.2.3 Environmental processes in the air compartment

Environmental processes occurring in the atmosphere that are significant in environmental fate modelling include:

- Advection
- Deposition, both wet and dry processes
- Aerosol sorption
- Atmospheric reaction
- Diffusion and dispersion

5.2.3.1 Advection

According to Atkinson (2000), vertical mixing in the free troposphere is fairly rapid, with residence times of the order of 1 to 30 days. Within a hemisphere, horizontal mixing is also fairly rapid with residence times ranging from a few hours for local transport (<100 km), a few hours to a few days for transport over regional zones (100 to 1000 km), and greater than 10 days for transport over global distances of a few thousand kilometres (Atkinson, 2000). The timescale for transport between northern and southern hemispheres is approximately a year.

Air residence times will depend on location, topography, meteorological conditions and many other factors. Surveying several publications, regional air residence times lie between 0.168 to 5 days. Mackay et al. (1996a), in their evaluative model, have used an air compartment residence time of 100 hours (~4 days).

5.2.3.2 Aerosol sorption

Aerosol particles have a high surface area, which can subsequently serve as an interface for organic chemical sorption. Aerosol sorption is usually quantified as the fraction of sorbed species associated with the aerosol. The fraction sorbed is important to quantify for reasons beyond quantification of deposition effects: Studies have shown that the sorbed chemical species is shielded from atmospheric reaction degradation, which can significantly alter calculated persistence and spatial range (Scheringer, 1997).

Aerosol sorption is modelled using both adsorption and absorption theory. Adsorption models are based on Langmuir adsorption; Absorption models are built on the assumption that the aerosol behaves as if it consisted of particles surrounded by a liquid-like organic film, normalised to the organic content of the aerosol.

The fraction of chemical sorbed (ϕ) is related to the particle-gas partition coefficient (K_p), which has units of $m^3/\mu g$. The relationship, in terms of the total suspended particulates (TSP), is defined below:

$$\phi = \frac{(TSP)K_p}{1+(TSP)K_p} \tag{5-2}$$

Several models exist for the prediction of the particle-gas partition coefficient and are presented below. These include the simple methods of Junge (1977), Mackay et al. (1986) and Bidleman and Harner (2000), and the more sophisticated methods of Strommen and Kamens (1997) and Jang et al. (1997). Most methods are simplifications of the following two expressions indicating the two types of sorption mechanisms [Equations (5-3) and (5-5) below]:

Adsorption (Junge, 1977):

$$K_p = \frac{1}{P^{sat}}\left(\frac{c\theta}{TSP}\right) \tag{5-3}$$

where

$$c = 10^6 RTN_s \exp\left[\frac{\Delta H_d - \Delta H_v}{RT}\right] \tag{5-4}$$

Absorption (Pankow, 1994; 1994a):

$$K_p = \frac{RT y_{om}}{10^6 M_{om}\gamma_{om}^p} \tag{5-5}$$

In Equation (5-4), N_s is the number of moles of sorption sites, ΔH_d and ΔH_v are the heats of desorption and vaporisation respectively. In Equation (5-5), M_{om} is the molecular mass of the

organic matter, y_{om} is the organic matter mass fraction of the aerosol particles and γ_{om}^{p} is the activity coefficient of the organic matter liquid film which coats the particles.

The Jung adsorption model

This Langmuir-adsorption type equation was first proposed by Junge (1977). Combining Equations (5-3) and (5-4), Junge (1977) described the fraction of chemical adsorbed onto the aerosol particles by the following equation:

$$\phi = \frac{c\theta}{P^{sat} + c\theta} \tag{5-6}$$

The parameter, *c*, is defined in Equation (5-4) above. Several values for c have been proposed: Junge (1977) suggested a value of 17.2 Pa.cm while Pankow (1987), more recently, has suggested a value of 13 Pa.cm at 298 K.

Most experimental data relating to aerosol sorption has been correlated satisfactorily to K_p. This partition coefficient has been linearly correlated with saturated liquid vapour pressure. Bidleman and Harner (2000) report parameters (m_1 and m_2) for the linear relationship represented by Equation (5-7) below, fitted for a series of 21 compounds:

$$\log K_p = m_1 \log P^{sat} + m_2 \tag{5-7}$$

The Mackay adsorption model

Mackay et al. (1986) have defined a dimensionless particle-air partition coefficient (K_{pa}), correlating it to saturated vapour pressure:

$$K_{pa} = \frac{C_p}{C_a} = \frac{6x10^6}{P^{sat}} \tag{5-8}$$

Using the aerosol particle density (ρ_p) in kg/m^3, the dimensionless particle-air partition coefficient can be converted to K_p:

$$K_{pa} = K_p \cdot \frac{v_p^a}{TSP} = 10^9 K_p \rho_p \qquad \textbf{(5-9)}$$

Octanol-air partition coefficient model (absorption model)

Finizio et al. (1997), extending absorption work performed by Pankow (1994; 1994a), suggested that the octanol-air partition coefficient could replace the vapour pressure as a dependent description variable for aerosol sorption. Upon the assumption of equivalence of solute activity coefficients between a species in octanol and the organic matter of an aerosol particle, and a typical organic matter content of 20 %, Bidleman and Harner (2000), derived a simplified expression for K_p as a function of the octanol-air partition coefficient:

$$\log K_p = \log K_{oa} - 12.61 \qquad \textbf{(5-10)}$$

Other aerosol absorption models

A model available for the prediction of aerosol sorption based on absorption theory is a duel impedance model developed by Strommen and Kamens (1997). By describing the aerosol as an inner layer of discrete solids surrounded by an outer layer consisting primarily of liquid-like organics, a superior fit to experimental data was obtained when compared to single layer models. This study found that single layer absorption models are limited by mass transfer effects.

A technique, using activity coefficient estimation group contribution methods, was explicated by Jang et al. (1997). These researchers used the UNIFAC model (Hansen et al., 1991), and a group contribution method based on cohesive energies and solubility parameters formulated by

Hansen and Beerbower in Barton (1991) to evaluate the activity coefficient in the liquid-like organic phase. This method was reported to have improved results.

Comparison of the Junge adsorption model, the Mackay adsorption model and the K_{oa} model for the prediction of the sorbed aerosol fraction in urban air shows reasonable agreement. Of the three correlations the K_{oa} model sets the lower estimation boundary and the Mackay model sets the upper boundary (Bidleman and Harner, 2000).

5.2.3.3 Deposition

Atmospheric deposition of contaminants has been determined to be a prominent source of pollutants for various ecosystems (Dickhut and Gustafson, 1995). As mentioned previously, deposition can be divided into dry and wet processes.

Dry deposition

Dry deposition can be divided into particle and gas deposition. The latter deposition process is a diffusive process. The dry gas deposition velocity ($u_{d,g}$) can be evaluated from Equation (5-11), as suggested by Thompson (1983):

$$u_{d,g} = u_{d,g}(ref)\sqrt{\frac{M(ref)}{M}} \qquad \textbf{(5-11)}$$

where

$u_{d,g}(ref)$ = 5 mm/s $\qquad$ $M(ref)$ = 300 g/mol

Dry particle deposition is the gravity induced sedimentation of particles, or coagulated aggregates of sufficient diameter, to the geosphere. This phenomenon is fundamentally a function of particle size and is usually of the order of a few mm/s (Bidleman, 1988) [See Table 5-3], typically 3 mm/s (Mackay, 2001). This typical value can be calculated from Stoke's

law using a particle diameter of 7 μm under environmental parameters evaluated at standard conditions of pressure and temperature. McMahon and Denison (1979), Voldner et al. (1986) and Nicholson (1988) have reviewed numerous studies on the theory and measurements of dry particle deposition.

Table 5-3: Dry particle depositions according to various studies

Study	$u_{d,p}$ [mm/s]	Reference
POP's	1 to 5	Eisenreich et al. (1981)
PAH's	1.3 to 11	McVeety and Hites (1988)
POP's	1.6	Swackhamer et al. (1988)
PCB's	3.8 to 5.1	Holsen et al. (1991)
POP's	2	Hoff et al. (1996)

Note: POP's – Persistent organic pollutants
PAH's – Polyaromatic hydrocarbons
PCB's – Polychlorinated biphenyls

Close to urban areas, coarse particles have been found to dominate dry deposition fluxes (Holsen et al, 1991, 1993; Pirrone, 1995) and much higher deposition velocities of 50 mm/s may be applicable (Wania et al, 1998). For a more detailed assessment of the dry particle deposition, the relevant fluid regime law can be obtained from Table 4-9 and used to calculate the settling velocity (i.e. $u_p = u_{d,p}$).

The overall dry deposition velocity (u_d), composed of a particle and gas component, is the summation of the sorbed aerosol fraction weighting of the two dry deposition processes:

$$u_d = (1-\phi)u_{d,g} + \phi u_{d,p} \tag{5-12}$$

Temperature changes will have an influence on the overall dry deposition velocity, as the amount of chemical sorbed onto the particulate matter is dependent on temperature; increasing with decreasing temperature. POP concentrations on particles tend to be higher at lower temperatures (Wania et al, 1998).

Wet deposition

Wet deposition refers to the removal of the chemical from the bulk atmosphere, and that bound to particulate matter, by precipitation. The overall efficiency of this process, the atmospheric washout ratio (W), is said to be of the order of 10^5 (Atkinson, 2000). The atmospheric washout ratio is composed of two types of wet processes: the scavenging of atmospheric chemical species (wet gas deposition) and the collection of aerosol particles into falling precipitation (wet particle deposition):

The wet gas washout (W_g) is usually calculated as the equilibrium solubility of the species in water. Thus:

$$W_g = \frac{C_w}{C_a} = \frac{1}{K_{aw}} \qquad \textbf{(5-13)}$$

The wet particle washout (W_p) is in the range of 10^5 to 10^6 (Eisenreich et al., 1981) and is usually given the value of 2×10^5 (Mackay et al. 1991, 1996a; Scheringer, 1996; Bennett et al., 1999; Mackay, 2001); although Wania et al. (2000) have used a value of 0.68×10^5.

The overall washout ratio is defined as the sorbed aerosol fraction weighted summation of the two wet processes. Consequently:

$$W = (1-\phi)W_g + \phi W_p \qquad \textbf{(5-14)}$$

Particle washout ratios have been found to increase with increasing precipitation rate indicating an increase in efficiency of particle scavenging as precipitation increases (Dickhut and Gustafson, 1995). The wet deposition velocity is related to the overall washout ratio and is proportional to rainfall intensity.

Using the precipitation rate (P) and the atmospheric washout ratio, the wet deposition velocity (u_w) is defined as follows:

$$W = \frac{u_w}{P} \tag{5-15}$$

where P is normally given in mm/a; u_w will have the same units as P.

5.2.3.4 Atmospheric reactions

Organic gas phase compounds may undergo a variety of chemical transformation paths in the troposphere including photolysis, ozonolysis, reaction with hydroxyl (OH) radicals and reaction with nitrate (NO_3) radicals; However for the majority of gas-phase organic chemicals in the troposphere, reaction with the OH radical is the predominant loss mechanism (Atkinson, 1995).

All organic chemicals, except for chlorofluorocarbons and certain saturated halocarbons, react with the hydroxyl radical, resulting in the splitting of the parent species. Hydroxyl radicals are formed from the decomposition of atmospheric water molecules by electronically excited oxygen atoms originating from photolytically decomposed ozone. As the hydroxyl radical is formed from photolysis products, its concentration in the atmosphere exhibits a marked diurnal profile. Maximum hydroxyl radical concentrations at ground level typically range from 3×10^6 to 1×10^7 molecules/cm^3 (Atkinson, 2000). A 24-hour average OH radical concentration was obtained by Prinn et al. (1995) of 9.7×10^5 molecules/cm^3. Trapp and Matthies (1998) suggest an average concentration of 5×10^5 molecules/cm^3.

Reaction with hydroxyl radicals

The reaction between a hydroxyl radical and a substrate molecule is bimolecular; first order with respect to the hydroxyl radical, and first order with respect to the substrate. Thus, a pseudo-first order rate constant for the bimolecular reaction can be obtained if the second order rate constant and the hydroxyl radical concentration are known. As the concentration of ambient hydroxyl radicals varies and therefore, no single value can be expected to reflect this, use of a pseudo-first order rate constant will introduce uncertainty into a fate assessment. However, utilisation of a pseudo-first order rate constant allows the linear nature of a multimedia model to

be preserved, which has several benefits when solving the model. Consequently, the pseudo-first order rate constant can be obtained as follows:

$$k_{OH} = k'_{OH} C^{a}_{OH} = \left(9.7\ x\ 10^{5}\right) k'_{OH}$$

(5-16)

where k'_{OH} is a second order rate constant ($cm^3/s/molecules$) and k_{OH} is a pseudo-first order rate constant (s^{-1})

Reaction with nitrate radicals

Nitrate (NO_3) radical reactions are potentially important loss processes for unsaturated hydrocarbons, phenolics and certain nitrogen containing compounds (Atkinson, 1991). As NO_3 radicals undergo photolysis readily, radical concentrations are low during daylight and elevated at night. A 12-hour nighttime average concentration of approximately 5 x 10^8 molecules/cm^3, has been proposed with an uncertainty factor of about 10 (Atkinson, 1991).

Reaction with ozone

The extent of ozone (O_3) reactions with gas-phase organic compounds is only significant for unsaturated carbon-carbon compounds and certain nitrogen containing compounds (Atkinson, 1997). Photolysis of organic compounds may occur directly, but is dependent on the nature of the compounds themselves.

Overall air compartment reaction rate constant

Generally, the overall first order reaction rate constant in the atmosphere, which is the sum of the individual first, or pseudo-first, order rate constants, is dominated by the hydroxyl reaction rate:

$$k_a = k_{OH} + k_{NO_3} + k_{O_3} + k_{photo} \approx k_{OH} = k'_{OH} C^{a}_{OH}$$

(5-17)

Formidable literature exists covering gas-phase kinetics of organic compounds; however, not all chemicals have been measured. Furthermore, transformation products generated from the above processes are generated in situ in the atmosphere increasing the number of compounds to study. Thus, the need for reliable prediction techniques is necessary. Atkinson (2000) provides an overview of predictive techniques available for atmospheric oxidation losses.

5.2.3.5 Diffusion and dispersion

In the atmosphere, dispersion dominates over molecular diffusion. A vertical dispersion coefficient of 0.5 m^2/s has been used by Hertwich and McKone (2001). Scheringer (1996) has used a horizontal dispersion coefficient of 2×10^{-6} m^2/s.

Air compartment-surface diffusive processes are usually modelled using mass transfer coefficients. Soil-air interactions are normally quantified by the use of an assumed typical value for the overall mass transfer coefficient of 6.7×10^{-3} m/h. Wania et al. (2000) and Diamond et al. (2001) have used an overall vegetation-air mass transfer coefficient of 15.4 and 23 m/h respectively. Numerous correlations for the air-film over water mass transfer coefficients exist in literature and have been reviewed by Schwarzenbach et al. (1993). The correlation of Mackay and Yuen (1983) is recommended as it is sensitive to changing surface conditions regimes and it predicts a non-zero still air value. Air-film, and water-film mass transfer coefficients are normally correlated with wind speed. The wind speed used in the correlations is usually the wind speed at a reference height of 10 m above the air-water interface. If the given wind speed is at another height, it can be converted to the wind speed at 10 m assuming a logarithmic wind profile (Trapp and Matthies, 1998).

5.3 The hydrosphere

Throughout history, the quantity and quality of water has been a vital feature in determining the well being of a civilisation or the continuation of a species. All available water on the face of the planet can be collectively grouped as the hydrosphere. The hydrosphere, thus, includes rivers, lakes, estuaries, oceans, groundwater and soil water. Seventy percent of the earth's surface is covered by water; most of this fraction contributed by the ocean. The various water bodies range widely in their properties and chemistry. Even within the boundaries of a single

water reserve, the chemistry and processes between the surface and bottom waters vary greatly. Water serves its most important environmental purpose in the hydrological cycle. This dynamic cycle links the geosphere and the atmosphere through evaporation, transpiration and precipitation.

Human activities are primarily concerned with fresh surface water and groundwater. Surface water in lakes or reservoirs usually contains essential mineral nutrients providing an environment conducive for biota. Surface water with high levels of biodegradable organic material may support a large population of bacteria. These factors, consequently, have a significant effect upon the quality of the water body. Groundwater can dissolve minerals from the rock formations through which it percolates; its subsequent chemistry and properties change as it filters through the rock bed. This salt chemistry has profound impact on groundwater's ability to support biota as the mineral content may cause an undesirably high salinity.

5.3.1 Characteristics of water bodies

Surface water occurs primarily in streams, lakes and reservoirs. Lakes can be classified as oligotrophic, eutrophic or dystrophic. Oligotrophic refers to deep lakes, which are generally clear, deficient in nutrients and without much biological activity. Eutrophic lakes have more nutrients, support more life and are consequently more turbid as a result of the products produced from the aquatic biota. Dystrophic lakes are shallow and clogged with flora. This type of lake normally contains coloured water of low pH. Reservoirs are man-made water bodies, which may be constructed to be similar to lakes; however they may also differ great from their natural storage counterparts.

Estuaries constitute another type of body of water. Estuaries act as an intersection point for streams flowing into the ocean. The mixing of fresh and saltwater gives estuaries unique chemical and biological properties.

5.3.1.1 Stratification of non-flowing water bodies

Non-flowing bodies of water like lakes and reservoirs with large volumes relative to their in- and outflows can be stratified into two thermal layers. The surface layer, known as the epilimnion, is heated by solar radiation, and because of its lower density (water's maximum density is at 4°C), floats upon the bottom layer, or the hypolimnion. When an appreciable temperature difference exists between the two layers, they will not mix and may consequently have very different biological and chemical properties.

The epilimnion, which is exposed to light, may support photosynthesising organisms or producers like algae. Moreover, as it is the surface layer, it is in contact with the atmosphere and, thus, gaseous exchange can occur between their mutual interface. The epilimnion thus has high levels of dissolved oxygen and, generally, is aerobic. In the hypolimnion, bacterial action on biodegradable organic material causes the layer to be anaerobic. As a direct consequence of microbial activity, chemical species found in the hypolimnion tend to exist in a reduced oxidation state. The plane formed between the two layers is called the thermocline.

The chemistry and biology of the ocean is very different from that of freshwater owing to its high salt content and great depth amongst other factors. Wania et al. (1998) have reviewed the air-sea exchange of POP's stating that more data measurements as a function of salinity are required. This highlights that most of the data currently gathered regarding the hydrosphere pertains to freshwater, as opposed to seawater.

5.4 Modelling the water compartment

Numerous difficulties are encountered in attempting to model the water compartment, as each body of water is unique. The general classification of the water body or bodies must be stipulated before the water compartment can be modelled. Generally, all aquatic systems modelled employ the assumption that the water body consists of pure water. A pseudo-first order overall reaction rate is used in this medium to account for transformation losses.

5.4.1 The water compartment

The assumed water fraction of the total surface area and the water compartment depths used in literature vary depending on the purpose of the model. Intervals, as gathered from literature, are reported below. Although 70 % of the earth's surface is covered with water, lower surface area fractions have been used in multimedia models. Evaluative models have used a 10 % water cover (Mackay et al., 1996a; Beyer et al., 2000) unless simulating global conditions (Scheringer, 1996). Kawamoto et al. (2001) used a fraction of 0.0082 in their regional model of Japan. South Africa's water fraction is of the same low magnitude as that of Japan. Water compartment depths of 0.38 (Diamond et al., 2001) to 50 m (Mackay and Paterson, 1991) have been used in literature.

5.4.2 Particulate matter

Particulate matter in the form of sediment and suspended sediment play a role in influencing the aquatic concentration of chemicals. Oligotrophic water bodies, which have clear water, may have a concentration of suspended particles as low as 1 mg/L (Mackay, 2001). Very turbid water as found in eutrophic or dystrophic water bodies may have concentrations over 100 mg/L; however, in most cases the concentration ranges from 5 to 20 mg/L (Mackay, 2001). A particulate matter density of 1.5 g/mL and a concentration of 7.5 mg/L corresponds to a volumetric fraction of suspended solids of 5×10^{-6}. This value has been used by several authors to represent the suspended sediment fraction in the water compartment (Mackay et al., 1996a).

5.4.3 Aquatic biota

Aquatic biota is normally assumed to occupy 1×10^{-6} volume fraction of the total water compartment. This figure is high, as it does not just represent fish (which are most visibly observed) but all aquatic organisms that inhabit the water compartment (Mackay and Paterson, 1991).

5.4.4 Environmental processes in the water compartment

Environmental processes occurring in the water compartment of significance to environmental fate are:

- Advection
- Sorption to particulate matter
- Deposition of particulate matter
- Mass transfer

5.4.4.1 Advection

Advection rates through the water compartment vary, and residence times from a few days (Diamond et al., 2001; Kawamoto et al., 2001) to about 40 days (Mackay et al., 1996a) have been used. The upper limit is the advective residence time of water through a large regional model with a surface area of the order of 10^5 km^2; the lower limit is for a smaller local model having a surface area of the order of 10^3 km^2.

5.4.4.2 Sorption to suspended sediment

Some of the chemicals found in the water compartment are sequestered in sorbed form on the organic component of suspended sediment. Thus, suspended sediment controls the bioavailability of chemical in the water compartment. The K_d is used to describe the partitioning of solute between the suspended sediment and the bulk water compartment. A typical organic content of suspended sediment particles is 0.2 (Mackay, 2001).

5.4.4.3 Deposition of particulate matter

Particulate matter, like aerosols in the atmosphere, serves as a medium for the transport of bulk chemical to the bottom of a compartment. A typical deposition velocity for particulate matter in water is of the order of 4.6×10^{-8} m/h (Mackay, 2001).

5.4.4.4 Mass transfer

Diffusion in the water compartment occurs across the air-water interface, between sediment and water, and between aquatic biota and water. Sediment-water interactions are normally quantified by the use of an assumed mass transfer coefficient of the order of 1×10^{-4} m/h (Mackay et al., 1996a). Numerous correlations are available for prediction of the air-water exchange water-film mass transfer coefficient. Schwarzenbach et al. (1993) have reviewed several correlations. The correlation of Mackay and Yuen (1983) is recommended, as it is sensitive to changing surface conditions regimes and predicts a non-zero still air value. This correlation is a function of the wind speed at a height of 10 m above the air-water interface. Wind speeds at heights other than 10 m can be converted to this reference height by assuming a logarithmic wind profile.

5.5 The geosphere

The geosphere, or solid earth, is composed of the lithosphere (upper crust) and pedosphere (soil) amongst other systems. The primary areas of concern for environmental models regarding the geosphere are the soil and sediment compartments. The status of soil as an environmental medium worth protecting was recognised later than the other media (Trapp and Matthies, 1998). Soil was once thought to have unlimited capacity to buffer anthropogenic activity. In contrast to air and water, soil is a heterogeneous system representing a four-dimensional intersection of ecosystems where the lithosphere, the hydrosphere, the atmosphere and the biosphere overlap. Sediment serves as an intersection point for the lithosphere, the hydrosphere and the biosphere.

5.5.1 Soil

Soil is a complex matrix consisting of air, water, mineral and organic matter. The mineral portion is formed from the weathering of parent rocks; the organic portion consists of plant biomass. Populations of biota are also found in soil.

Typical soils exhibit the formation of distinct layers called horizons. The top layer, typically several inches in thickness, is known as topsoil or A horizon. This is the layer of maximum biological activity and contains most of the soil organic matter (Manahan, 1990). The next layer

is called B horizon, or the subsoil, which receives organic matter, salts and mineral particles that have leached from the topsoil. The C horizon is composed of weathered parent rocks from whence the soil originated. The three horizons rest on a layer of bedrock.

The organic matter content of a typically productive soil is approximately 5 % (by mass) with the remainder representing the mineral content (Manahan, 1990). Other soils may contain as little as 1 % (by mass) organic matter while peat and forest soils may have much higher organic matter contents. The organic carbon content of a typical soil is about 2 % by mass (Mackay, 2001). Of the organic components in soil, humus is by far the most significant. Humus is composed of base-soluble fractions of humic and fulvic acids and an insoluble fraction called humin, which is a residue left over from microbial degradation of plant biomass. The most common inorganic component found in soil is silica. Clay is also found frequently and is considered chemically significant (Manahan, 1990).

Water and air form part of the three-phase, solid-liquid-gas system comprising soil. The water is used as a basic transportation medium carrying essential nutrients from the soil to vegetation. Aeration and mixing of soil is facilitated through burrowing organisms. A typical soil consists of 50 % solid matter, 20 % air and 30 % water (Mackay, 2001).

5.5.2 Sediment

Lake bottoms are lined with a nepheloid layer, which forms at the water-sediment interface. This region, known as the benthic region, is composed of deposited sediment, faecal matter and other organic matter from the water column. This layer typically consists of 95 % water and 5 % particles and is highly organic in nature compared with soil (Mackay, 2001). The top few centimetres of the interface between sediment and water house a unique ecosystem of burrowing organisms, which bioturbate the nepheloid layer, mixing it. Typically the top 5 cm contain the most activity in the sediment; however, it is misleading to assume that sediment deeper than this is inaccessible (Mackay, 2001). Depending on the condition and depth of the water column, the sediment layer may be oxygenated or anaerobic. Moving through the nepheloid layer into the waterbed, the sediment becomes more consolidated containing up to about 50 % solids (Mackay, 2001). Fast flowing river systems produce sufficient turbulence to ensure that bottom sediment is not accumulated. Hence, riverbeds of fast flowing systems are

normally rock or mineral based. Slow moving rivers, however, will accumulate sediment, which will line the riverbed.

5.6 Modelling the soil and sediment compartment

On modelling the soil and sediment compartments, the assumption of well-mixed compartments is applied. This assumption is not realistic; however, it is a starting point for model formulation. Pseudo-first order overall reaction rates are used in these media.

5.6.1 The soil compartment

The soil compartment model most extensively used in literature is the model of Jury et al. (1983). Soil is considered to be a mixture of four phases: air, water, organic matter and inorganic matter where the organic matter is assumed to be 56 % (by mass) organic carbon (Mackay, 2001). The most abundantly used organic carbon content is 0.02. Assumed densities for the air, water, organic and inorganic matter are 1.19, 1000, 1000, 2500 kg/m^3, respectively (Mackay, 2001) enabling the volume fractions and bulk soil density to be calculated. It is necessary for both the soil depth and area to be specified. The area fraction of the total surface area ranges depending on the purpose of the model. A review of current multimedia models indicates that the assumed soil depth is usually between 0.05 and 0.2 m. The Jury et al. (1983) volumetric fractions of air, water and solids of 0.2, 0.3 and 0.5, respectively, are commonly employed although slight variations have been used (Eisenberg et al., 1998; Wania et al., 2000). The typical groundwater leaching rate, as used in multimedia models is of 3.9×10^{-5} m/h (Mackay and Paterson, 1991; Mackay, 2001). Jury et al. (1983) suggest a typical mass transfer coefficient between air and soil of 3.77 m/h. Alternatively, an overall mass transfer coefficient can be calculated using effective diffusivities in the parallel soil air and water phases with a film thickness of 5 cm (Mackay, 2001), in series with the air-film mass transfer coefficient of the soil-air interface. Assumed runoff rates for soil solids and soil water into the water compartment, which serves as a catchment, are of the order of 3.9×10^{-5} and 2.3×10^{-8} m/h respectively (Mackay, 2001).

5.6.2 The sediment compartment

Sediment has been modelled as consisting of 80 % water and 20 % solid particles. The organic carbon content of the sediment is higher than that of soil, and in multimedia models literature it ranges between 0.03 and 0.05. Current literature indicates that the assumed active sediment depth lies between 0.01 and 0.05 m with a typical sediment diffusion film thickness of 0.005 m (Mackay, 2001). Resuspension and burial rates of sediment, according to Mackay (2001), are of the order of 1.1×10^{-8} and 3.4×10^{-8} m/h respectively.

5.7 The biosphere

The term biosphere refers to all living organisms; thus included are aquatic and terrestrial biota as well as terrestrial vegetation. Aquatic biota have already been briefly discussed in section 5.4.3 above. Terrestrial biota, although not often modelled, are dealt with similarly to aquatic biota. A large proportion of the earth's surface area is covered with vegetation, with the subsequent implication being that vegetation may be an important sink for organic pollutants (McLachlan and Hortsmann, 1998). The potential photodegradation capabilities of vegetation, owing to its high foliage surface area, may lead to the partial amelioration of air pollution.

5.8 Modelling the biosphere

Both biota and vegetation, as a consequence of their complexity, are modelled using empirical correlations. The starting premise in the empirical models is the assumption that partitioning to octanol adequately simulates the partitioning of a chemical into the lipid and organic components found in biota and vegetation respectively.

5.8.1 Biota

Modelling interactions between different biota have already been discussed in section 4.1.5 regarding the phenomena of bioaccumulation and biomagnification in food chain models. On modelling individual species, the biota-water partition coefficient is employed, which is the product of the volume based lipid fraction of the biota and the octanol-water partition coefficient (Mackay, 1991; Sandler and Orbey, 1993) [See Equation (5-18) below]. A lipid

volume fraction of 0.05 is typically used for aquatic biota (Mackay, 2001). Campfens and Mackay (1997) have reported lipid fractions for several aquatic species in their food web model. DeVito (2000) has reviewed adsorption of chemicals through cellular membranes.

$$K_{bw} = L_{\eta} K_{ow} \tag{5-18}$$

5.8.2 The vegetation compartment

The complexities of the mechanisms involved in the uptake and metabolism of chemicals in vegetation lends itself to empirical model types. McLachlan (2000) has reviewed several empirical models for the estimation of vegetation-air or plant-air partitioning (K_{va}). The subsurface component of the plant is not included in this coefficient. This distinction is believed to be sensible as the aerial and subsurface parts reside in different media (McLachlan, 2000). This coefficient has been correlated with octanol-water and air-water partition coefficients, as wells as the volume fractions of air, water and lipid comprising the vegetation. Diamond et al. (2001) have modelled vegetation as consisting of 0.18, 0.80 and 0.02 for air, water and lipid, by volume fraction respectively.

Severinsen and Jager (1998) have developed a terrestrial vegetation sub-model for use in Mackay-type multimedia models. Cousins and Mackay (2001) have also suggested several approaches for the inclusion of vegetation in multimedia models. These include the segmentation of the vegetation compartment into different sections, such as roots, stems, foliage and fruit or the differentiation between different species of vegetation, separating each species into a compartment representing each type. Hung and Mackay (1997) developed a segmented vegetation model segmenting the vegetation into leaf, stem, root, xylem and phloem sap. The water partitioning with the latter two sap segments was assumed to be one. Vegetation-water partition coefficients have been simply modelled, synonymously to soil-water adsorption, using the organic carbon-water partition coefficients and a mass based organic carbon content (Mackay, 1991; Sandler and Orbey, 1993).

It has been noted that due to lack of data availability, inclusion of vegetation compartments may not enhance the accuracy of multimedia fate prediction (Gouin, 2002). Several authors have reiterated the need for more data relevant to the vegetation compartment (Bennett et al., 1998; Cousin and Mackay, 2001). Gouin (2002) reports that, in lieu of vegetation reaction rate data, the assumption of equivalency between air compartment degradation rates and vegetation rates has been previously used.

CHAPTER 6

Multimedia models

Multimedia models are mass balance models that focus on the partitioning of chemicals between various environmental compartments. The discovery of the ubiquitous occurrence of xenobiotics in several environmental compartments motivated the development of multimedia models, which have been found to adequately describe the fate of a chemical in the environment (Trapp and Matthies, 1998).

Multimedia models are built on the following assumptions:

- The environment can be broken up into compartments consisting of phases or mixtures of phases.
- Each compartment is well mixed.
- Single compounds are considered independently of other components in a mixture of pollutants; thus, interactions between components of a mixture are not described.
- Equilibrium conditions are usually assumed within each compartment, but not necessarily between compartments.

The models used in this dissertation are based on the fugacity concept, which is reviewed below. Mackay and various co-workers (1979; 1981; 1982, 1985) published a series of papers adapting the concept of fugacity introducing it as a feasible variable for multimedia environmental model formulation. For a comprehensive review of fate modelling based on the fugacity approach refer to Mackay (2001).

In Mackay's fugacity approach, the molar rate of chemical transport and transformation is described through the use of transfer coefficients (D), such that:

$$\frac{dN}{dT} = D\,\hat{f} \qquad \textbf{(6-1)}$$

The Mackay transport coefficients, or D values, are typically expressed in units of mol/(Pa.h). This notation can be used to represent a variety of processes including reaction, diffusive exchange, advection and other bulk transport processes.

Mackay has defined levels of model calculation complexity ranging from Level I to IV. The levels are summarised in Table 6-1 below. The simplest level, Level I, describes equilibrium partitioning in a closed system comprised of well-mixed compartments.

$$N_{tot} = \sum_i N_i = \sum_i C_i V_i = \hat{f} \sum_i Z_i V_i \qquad \textbf{(6-2)}$$

Level II calculations build on the system boundaries of the Level I model: Level II models are steady state equilibrium distribution models with open system boundaries. Level II models incorporate degradation and advection losses represented by D_i values, the sum of which is equal to the sum of the emissions (E_i) into the system. Thus:

$$E_{tot} = \sum_i E_i = \hat{f} \sum_i D_i \qquad \textbf{(6-3)}$$

Level III models describe non-equilibrium conditions between environmental compartments, although the overall system remains at steady state with the total emission rate balancing the removal rate. The non-equilibrium condition increases the system degree of freedom, dictating that a mass balance must be performed over each system compartment for solution. A steady state mass balance over each compartment yields:

$$E_i + \sum_j D_{ji} \hat{f}_j - \hat{f}_i \sum_j D_{ij} = 0 \qquad \textbf{(6-4)}$$

Finally, an unsteady state, non-equilibrium model tracking the time course of fugacities is defined as a Level IV calculation. A general mass balance, at this level, over each compartment yields:

$$\frac{dN_i}{dt} = \frac{d\left(Z_i \hat{f}_i V_i\right)}{dt} = E_i + \sum_j D_{ji} \hat{f}_j - \hat{f}_i \sum_j D_{ij} \qquad (6\text{-}5)$$

Table 6-1: Multimedia model levels as defined by Mackay and Paterson (1979)

Level	Description
I	Closed system, steady state, equilibrium
II	Open system, steady state, equilibrium
III	Open system, steady state, non-equilibrium
IV	Open system, unsteady state, non-equilibrium

6.1 Number and types of compartments

Multimedia models show variation in the number and types of compartments described. The three primary compartments in the environment are air, water and solid media including soils, sediment and biota. The minimum segmentation is thus into these three media. Upon assumption of the applicability of octanol to model an organic compartment, these basic media can be represented by air, water and octanol respectively. Gouin et al. (2000) have used these three phases in an evaluative persistence model. Several authors have used air, water and soil compartments to represent the environment (Scheringer, 1996; Müller-Herold, 1996; Wania, 1998; Bennett et al. 1999; Fenner et al., 2000); however, a more commonly accepted segmentation is that of a four-compartment model consisting of air, water soil and sediment (Mackay et al., 1996a; Webster et al., 1998;Beyer et al., 2000).

Several other compartments types, or combinations of segmented compartments, have been previously incorporated into multimedia models. McKone (1993), inter alia (Wania and Mackay, 1993; Bennett et al., 1998; Diamond et al., 2001) have included a vegetation

compartment. Soil has been segmented into different horizons (McKone, 1993; Bennett et al., 1998) or different zones depending on use (van de Meent, 1993; Brandes et al., 1996; Wania et al., 2000). The atmosphere has been sub-compartmentalised into several layers and the water medium has been segmented into fresh-and saltwater compartments (MacLeod et al, 2001; Woodfine et al., 2001). Diamond et al. (2001) have included an impervious organic film, as a separate compartment, in their evaluative urban city model. Simple inclusion of biota, usually as a sub-compartment is common. Notwithstanding the numerous permutations of sub-compartments and possible compartment additions, there is a general consensus that four compartment systems are adequate for screening purposes.

6.2 Conditional equivalence of models of various levels

Steady state modelling is currently a favoured environmental modelling practise. However, it is the assertion of this dissertation, that significant environmental outputs, which can only be obtained from transient models, shed additional insight into chemical fate behaviour.

Equivalence has been shown to exist between environmental parameters evaluated from both Level IV (dynamic) and Level III (steady state) models by several researchers (Heijungs, 1995; Fenner et al., 2000; Hertwich, 2001; Hertwich and McKone, 2001). Equivalence between models of varying spatial complexity has also been shown. In an extension of the work performed by Scheringer (1996; 1997), Held (2001) formulated a model to account for the two-dimensional dispersion of a chemical on the spherical surface of the earth. These calculations demonstrated that Scheringer's one-dimensional approach [See Figure 6-6 below] did not introduce significant differences. In fact, Held (2001) illustrated a one-to-one relationship between the two-dimensional spherical model and the one-dimensional ring model (Hertwich and McKone, 2001).

Müller-Herold (1996) and Bennett et al. (1999) have performed studies on persistence relating to the applicability of simple models as a substitute for more complicated models. Müller-Herold (1996) demonstrated that in the advent of high inter-compartmental transport rates relative to degradation rates, the system persistence approaches the equilibrium result. This intuitive observation suggests that a substance existing in a mobile phase in which its transport rate is far greater than its reactive loss, is essentially exhibiting equilibrium behaviour.

Bennett et al. (1999) graphically demonstrated the conclusion deduced by Müller-Herold (1996) relating to model equivalence. Furthermore, Bennett et al. (1999) showed that transport rate dominated systems (with respect to reaction) did not only show equilibrium results that approached steady state results; but that these results were similar to the dynamic response. Additionally, this study concluded that it was appropriate to use a steady state model, in lieu of a dynamic model, to simulate an environment disturbed by a series of pulse releases, if the time between each release was less than time it took for the dynamically modelled system to reach steady state.

The time taken for a compartmental system output, namely fugacity, to reach a steady state has been defined as the settling time by Bru et al. (1998) and Paraiba et al. (1999). The fugacity settling time is a unique property of a dynamic system, which cannot be gleamed from steady state modelling. Conceptually, the fugacity settling time can be conceived as the time required for a system to attenuate a pollutant loading and return to a steady state value. If a pulse emission is modelled, the fugacity settling time can be viewed as a measure of the compartment-specific persistence. The fugacity settling time quantifies the extent of the disturbance affected on a compartment as a result of an emission loading.

6.3 Applications of multimedia models

Multimedia models of the Mackay type have been extended to numerous applications. In response to the need for quantitative methods in exposure analysis, multimedia models are used for legislative purposes to set clean-up standards [DTSC (1992)] and to assess the risk and environmental fate of new and existing chemicals [EU (1996)]. Multimedia models have also found application in lifecycle assessment (Guinée, 1996). Multimedia models are used in the evaluation of persistence and long-range transport (Scheringer, 1996; Bennett et al., 1998) and in the assessment of toxicity ranking (Edwards et al., 1999).

6.4 Review of various multimedia models

As indicated in Chapter 3, environmental models are categorised into various model types. The model types discussed below include evaluative, regional and global models. Models may also

be categorised according to their purpose. Accordingly, models (predominantly evaluative in nature), which determine persistence and long-range transport, are reviewed below in sections 6.4.4 and 6.4.5 respectively.

6.4.1 Evaluative models

Evaluative models are often formulated as single unit world or closed box models and are used to characterise the general fate behaviour of a chemical within an environment comprised of several compartments. The most widely accepted model of this type is the equilibrium criterion or EQC model of Mackay et al (1996a). Evaluative models have the capacity to determine the persistence and the long-range transport of organic pollutants, although the models reviewed in this section were not designed specifically with this intention. The evaluative models discussed below are presented in Table 6-2.

Table 6-2: Several evaluative multimedia models used for environmental fate assessment

Model	Reference	Description
EQC	Mackay et al. (1996a)	Definitive evaluative model
		Level I, II and III four-compartment models
-	Bru et al. (1998)	Introduces fugacity settling time
		Level IV three-compartment model
-	Edwards et al. (1999)	Used for toxicity ranking
		Level III three-compartment model

6.4.1.1 The EQC model of Mackay et al. (1996a)

The EQC model (Mackay et al., 1996a) is a regional evaluative model consisting of four bulk environmental compartments including air, soil, water, and bottom sediment. The bulk air compartment is comprised of an air and an aerosol phase. The bulk water compartment is composed of water, aquatic biota and suspended sediment. Soil is segmented into air, water and solids while the bulk sediment compartment consists of solids and water. The EQC model has a fixed area of 100000 km^2, which is regarded as being typical of an ecologically homogeneous region. As in other multimedia models, the EQC assumes that equilibrium exists within the four bulk compartments.

This model was designed with the intention of creating a standardised forum for chemical fate comparison. A Windows based EQC program is available at www.trentu.ca/envmodel/EQC. This program allows the user to run through the Mackay calculation levels I, II and III. Details regarding a Matlab program written to simulate the Level III version of the EQC model can be found in Appendix B-1, B-2 and B-6.

This model has become the definitive evaluative regional model and consequently has been applied and extended to numerous studies. Examples of its application include a study on chlorobenzenes by MacLeod and Mackay (1999), as well as a study performed by Booty and Wong (1996), in the same region, investigating polychlorinated biphenyls, mirex, dieldrin and hexachlorobenzene.

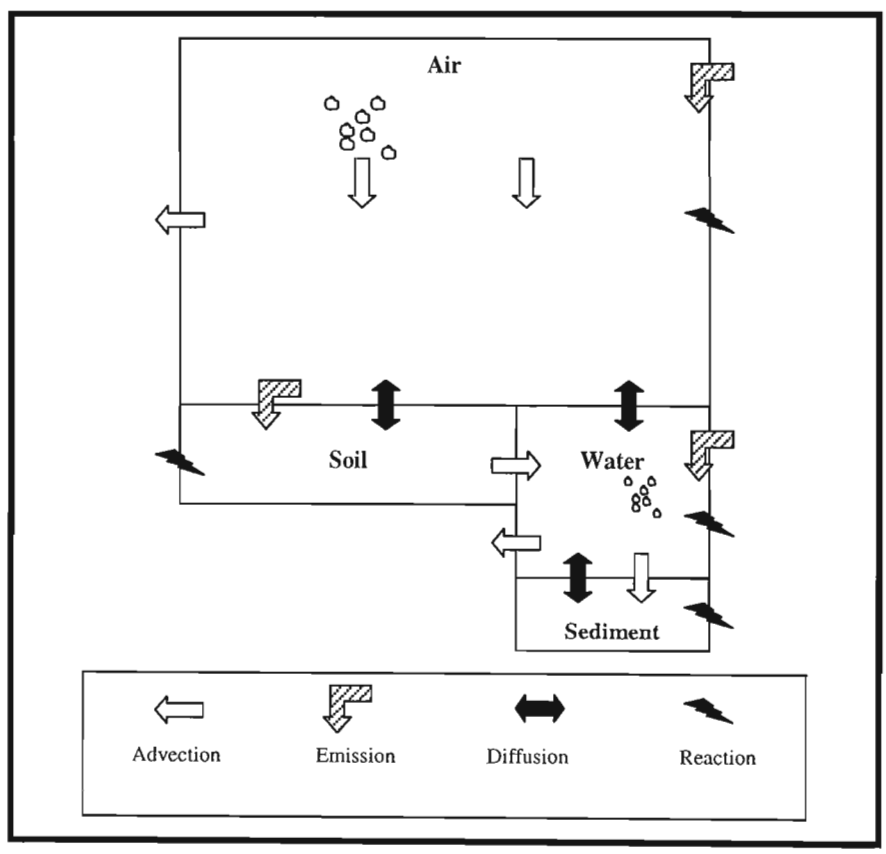

Figure 6-1: Four-compartment model environment of the Equilibrium Criterion (EQC) model of Mackay et al. (1996a)

6.4.1.2 Evaluative model of Bru et al. (1998)

A dynamic three-compartment fugacity model has been developed by Bru et al. (1998) and used to illustrate a numerical solution, using discretisation, to solve the resulting ODE system. The three compartments included in this model are air, water and sediment. The main intention of this paper was to examine the mathematical stability and positivity properties of the proposed numerical solution; however, a fugacity model was fortuitously selected, as it is an example of a first order continuous time dynamic system.

Bru and co-workers published a second paper illustrating the numerical solution algorithm using an unsteady state evaluative multimedia model (Paraiba et al., 1999). These authors have suggested an algorithm for the evaluation of fugacity settling time.

6.4.1.3 Evaluative model of Edwards et al. (1999)

Edwards et al. (1999) used a three-compartment Level III fugacity model, incorporating it into an existing methodology for chemical toxicity ranking. Edwards and co-workers, on considering a review of 51 different toxicity risk scoring and ranking systems, realised that none of the systems utilised multimedia modelling to determine exposure concentrations. Since the effects of toxicity are a function of exposure and concentration, Edwards et al. (1999) suggested the inclusion of multimedia model predicted exposure concentrations to improve risk assessment. Edwards et al. (1999) combined the estimated exposure concentrations from the fugacity model into the ranking algorithms. The study showed that the order of chemicals changed on inclusion of the chemical's fate in the ranking methodology. The inclusion of fate modelling into the ranking system was found to weight the compartmental exposures into which the chemical was most likely to distribute; thus, establishing a realistic indication of the chemical's ranking.

6.4.2 Regional multimedia models

Regional models have been established to predict the distribution of a chemical in a real environment. Examples of this type are reviewed below and can be found in Table 6-3.

Table 6-3: Several regional multimedia models used in environmental fate assessment

Model	Reference	Description
CalTOX	McKone (1993)	Regional human health assessment model Dynamic, seven-compartment model
MUM	Diamond et al. (2001)	Regional urban model Level III four-compartment model
CoZMo-POP	Wania et al. (2000)	Regional water drainage model Level IV eight-compartment model
BETR-North America	MacLeod et al. (2001) Woodfine et al. (2001)	Regionally segmented seven-compartment model
ChemCAN	Mackay et al. (1991)	EQC based Level III regional model Parameterised for Canada
ChemFRANCE	Devillers et al. (1995)	EQC based Level III regional model Parameterised for France
SimpleBOX1.1	van de Meent (1993)	Used in EUSES† risk assessment software Regional eight-compartment model
SimpleBOX2.1	Brandes et al. (1996)	Used in EUSES† risk assessment software Regional-global eight-compartment model

Note: † EUSES - European Union System for the Evaluation of Substances

6.4.2.1 The CalTOX model of McKone (1993)

The California toxicity, or CalTOX, model (McKone, 1993) is a regional seven-compartment multimedia model, which was developed to assist the California Environmental Protection Agency in assessing human health by examining the impact of exposure factors on both the ultimate route and quantity of contact with humans.

The seven compartments included in the CalTOX model are: air, surface water, vegetation, sediment, surface soil, root-zone soil and vadose-zone soil. The assumption of equilibrium between phases within a compartment is made.

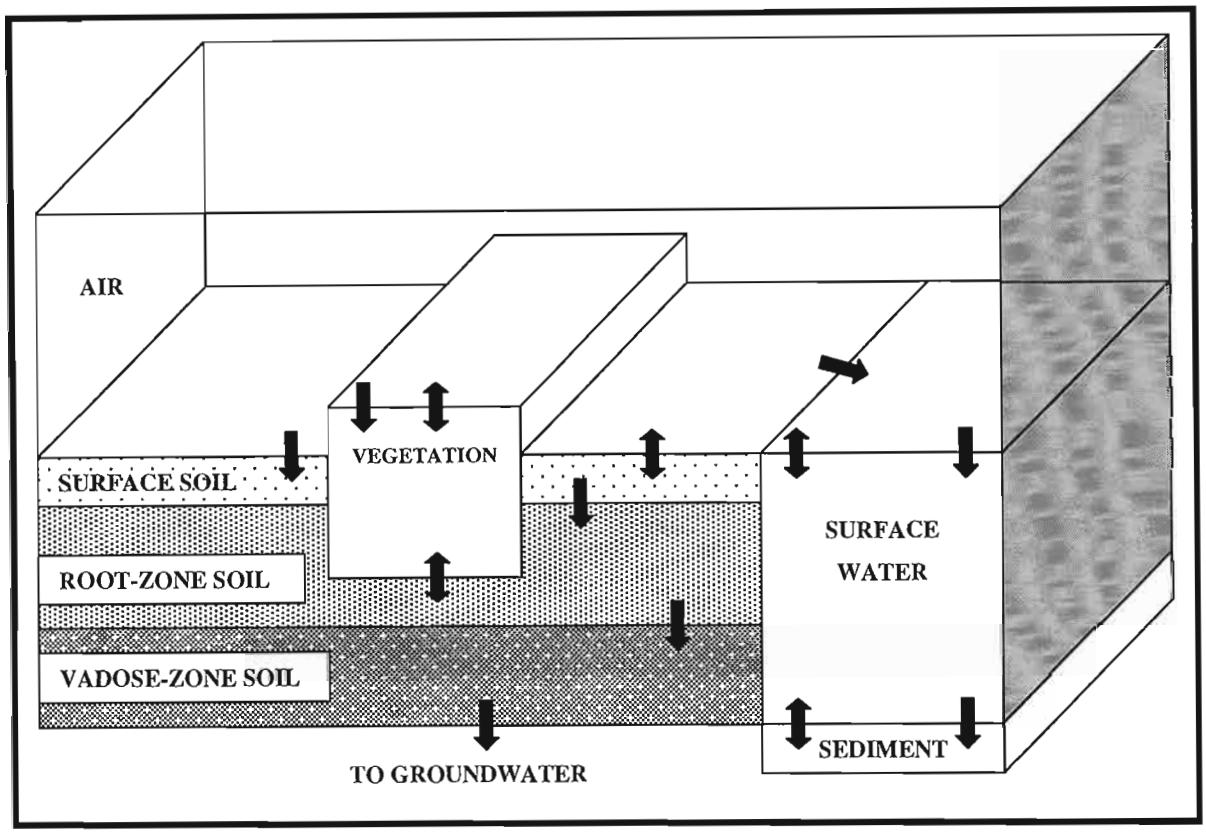

Figure 6-2: Seven-compartment model environment of the CalTOX model of McKone (1993)

This model can be used to assess time-varying concentrations of contaminants introduced into the soil horizons or released continuously into the air, surface soil, root soil, or water compartments. The exposure model encompasses twenty-three exposure pathways.

CalTOX differs from most other multimedia models in that it is a semi-transient model. It models the root and vadose soil zones using a dynamic Level IV approach and then assumes a steady state relationship between the other compartments and the soil zones. This increase in complexity, as a result of hybridisation of a Level IV and Level III model, is believed necessary to more accurately quantify the behaviour of soil-bound contaminants and their subsequent uptake by vegetation (McKone, 1993).

6.4.2.2 The Multimedia Urban Model (MUM) of Diamond et al. (2001)

The Multimedia Urban Model is a Level III fugacity model developed to account for the movement of semi-volatiles in the urban environment. It has been parameterised to simulate the summer conditions of downtown Toronto (Canada). The model includes all major media, namely: air, surface water, sediment, soil, vegetation and introduces an organic film compartment describing an organic layer coating impervious surfaces. MUM employs standard inter-compartmental transfer coefficients between the four typical compartments of air, water, soil, sediment and vegetation; while introducing new transport coefficients to describe the mass transfer to and from the organic film compartment.

Diamond et al. (2001) found that the organic film reflected more volatile chemicals into the air compartment and facilitated greater wash-off of chemical to surface waters. It also provided an additional surface for photolytic degradation. This film coating was modelled as being 30 to 250 nm thick. The bulk film comprised a wide range of organic compounds, inorganic species and particles. The film was modelled as 30% by mass organics, with the remainder composed of particulates. The organic carbon content of the organic component was set at 0.74.

6.4.2.3 The CoZMo-POP model of Wania et al. (2000)

The Coastal Zone Model for Persistent Organic Pollutants model (known as CoZMo-POP) is an unsteady state multimedia model consisting of eight-compartments designed to simulate the long-term fate of POP's in a coastal environment or the drainage basin of a large lake (Wania et al., 2000). The model landscape is composed of an air compartment, a forest canopy, forest soil, agricultural soil, freshwater, coastal water, freshwater sediment and coastal water sediment. The forest canopy can be divided into coniferous and deciduous tree types.

The system boundaries of CoZMo-POP deviates from most previous large water body models, which have tended to be restricted to the aquatic environment only. Previously aquatic model system boundaries were bordered by the air-water interface: CoZMo-POP is comprised of a large water body, and its entire drainage system, including the troposphere above it. Thus, parameters, which are input parameters in other aquatic models, are simulation outputs in CoZMo-POP.

This model has been designed, in particular, to examine the seasonal effects in the trajectory and distribution of organic pollutants in a coastal environment. Consequently, the model has the capacity to include time-varying parameters. Temperature can change with time, as well as the foliage volume of the tree canopy, as it responds to diurnal and seasonal changes. This model represents one of the most sophisticated single unit world regional models currently available. However, as it is input data intensive, it is not appealing to be used as a screening tool.

6.4.2.4 The BETR North America model of MacLeod et al. & Woodfine et al. (2001)

The Berkeley-Trent North American model (BETR North America) is a regionally segmented multimedia contaminant fate model based on the fugacity concept (MacLeod et al., 2001; Woodfine et al., 2001). This linearly connected unit-world model is built on a framework that links contaminant fate models of individual regions. It consists of 24 regions that are characteristic of distinct ecological zones in North America, with each zone comprised of seven discrete homogeneous compartments including a vertically bi-segmented atmosphere, freshwater, freshwater sediment, soil, coastal water and vegetation.

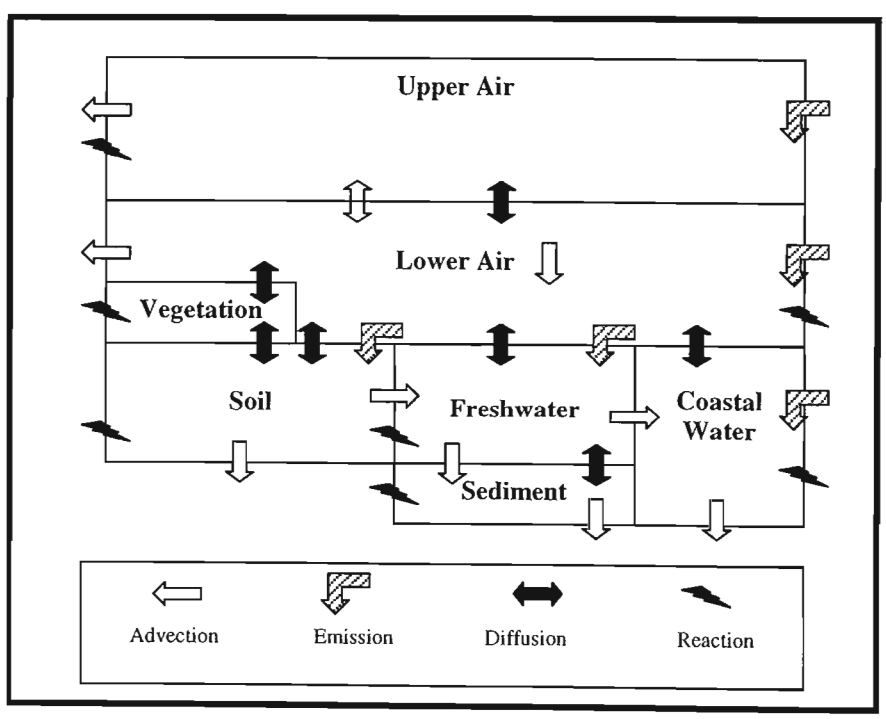

Figure 6-3: Seven-compartment model environment of the BETR-North America model of MacLeod et al. (2001) and Woodfine et al. (2001)

The 168 resulting mass balance equations include a number of diffusive and advective transport processes, which can be solved for either steady state or transient behaviour. The BETR North American model has a built-in temperature dependency for parameters like the Henry's constant and the octanol-water partition coefficient. Consequently, the investigation of temperature driven effects are within the models simulation capability.

6.4.2.5 The ChemCAN model of Mackay et al. (1991)

ChemCAN (Mackay et al., 1991) is a Level III multimedia model regionally parameterised for Canada. The ChemCAN model is based on the EQC model and is available online at www.trentu.ca/envmodel/ChemCAN. The online version is a Windows based program incorporating an existing database of chemicals. This Mackay model has been applied to various countries including Germany (Berding et al., 2000), France (Devillers et al., 1995) and Japan (Kawomoto et al., 2001).

6.4.2.6 The ChemFRANCE model of Devillers et al. (1995)

This model (Devillers et al., 1995) describes a Level III fugacity model, which has been used to assess the fate of organic chemicals in France. Within the model structure, France is divided into twelve regions, where its environment is represented by six bulk compartments including air, surface water, soil, bottom sediment, groundwater and coastal water. The first four compartments are considered as a combination of sub-compartments with equilibrium assumed within each compartment. Expressions for emissions, advective flows, degrading reactions, interphase transport by diffusive and non-diffusive processes are included. The model has been employed to model the fate of the persistent chemicals lindane and atrazine in France (Bintein and Devillers, 1996; 1996a respectively).

6.4.2.7 The SimpleBOX 1.1 model of van de Meent (1993)

The SimpleBOX 1.1 (van de Meent, 1993) is a regional scale model, developed for the Netherlands at the Institute of Public Health and Environment. It is a steady state Level III, eight-compartment model comprised of three types of soil compartments, surface water, biota,

sediment, aerosol and air. Unlike other Level III models, SimpleBOX 1.1 treats sediment, aerosols and biota as separate compartments, not employing the assumption that these compartments are in equilibrium with their respective bulk compartments. By providing the model user the capability of adjusting several types of input parameters, including the selection of soil types, the program allows substantial customisation of the model environment; thus, facilitating the creation of a regionally specific model. Consequently, SimpleBOX 1.1 has been incorporated into the European Union System for the Evaluation of Substances (EUSES) [RIVM (1996)].

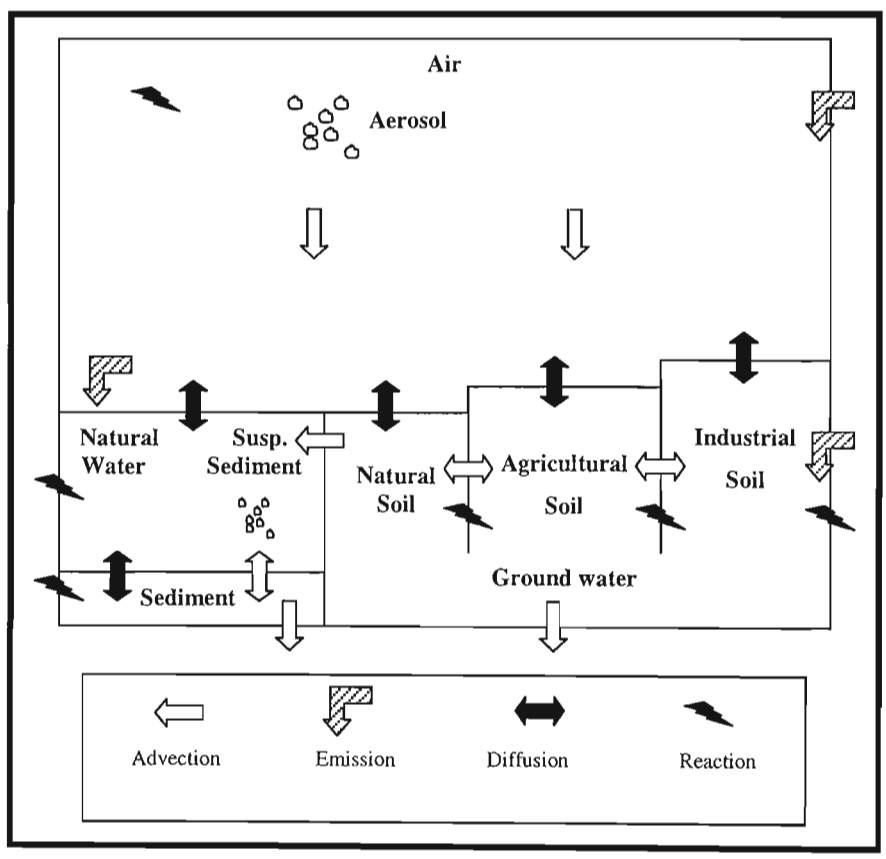

Figure 6-4: Eight-compartment model environment of the SimpleBOX1.1 model of van de Meent (1993)

6.4.2.8 The SimpleBOX 2.1 model of Brandes et al. (1996)

The SimpleBOX 2.1 model (Brandes et al., 1996) is a nested box approach consisting of a regional scale, a continental scale and a global scale model that is comprised of three parts: an arctic, temperate and tropic climate zone. The regional scale environment is contained within a

continental scale environment, which is in turn, contained within a global scale environment. The model can be executed in either a steady state or dynamic mode.

SimpleBOX 2.1 exhibits several extensions from the SimpleBOX 1.1 described above. SimpleBOX 2.1 includes two additional vegetation compartments and a second water compartment. However, classification of aerosol, suspended sediment and biota as separate bulk phases has been relinquished and these phases are treated as being in equilibrium with their respective air and water bulk phases.

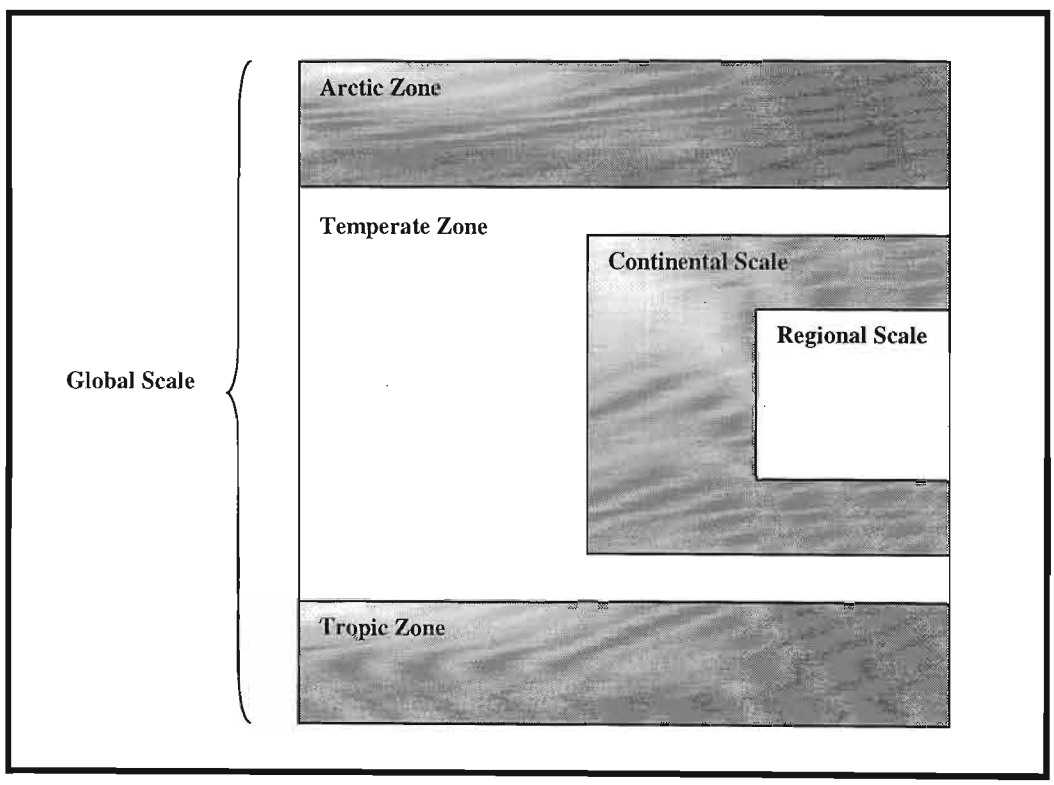

Figure 6-5: Eight-compartment model environment of the SimpleBOX2.1 model of Brandes et al (1993)

Combined with the SimpleBOX 1.1 model, the regional and continental spatial scales of SimpleBOX 2.1 are incorporated in the EUSES risk assessment software [RIVM (1996)]. However, several of the modifications included in SimpleBOX 2.1 are not used by EUSES: These include the variable soil depth calculation, the vegetation compartment and the temperature dependence of several parameters. Omission of these modifications within the EUSES framework is possibly in recognition of the uncertainty and increased level of complexity related to their inclusion.

6.4.3 Global multimedia models

Global models, owing to their large scale, can be used as persistence models. Although intuitive, this will become particularly more evident upon the definition and discussion of persistence below in section 6.4.4. The two global models discussed are presented in Table 6-4:

Table 6-4: Several global multimedia models used in environmental fate assessment

Model	Reference	Description
-	Wania (1998)	Level III three-compartment model
GloboPOP	Wania and Mackay (1993) Wania and Mackay (1995) Wania et al. (1999) Wania and Mackay (1999)	Dynamic six-compartment model consisting of nine climatic zones

6.4.3.1 The global model of Wania (1998)

A three-compartment Level III model describing chemical partitioning behaviour between air, water and soil has been developed by Wania (1998) and is used to estimate the overall persistence of an organic chemical in the global environment. The increase in level from a regional scale to a global scale is based on the axiom that only substances that are truly recalcitrant will be persistent enough to migrate on a global scale. Wania (1998) simplified the global environment by regarding air, water and soil as being the three major storage and degradation compartments. The model accounted for many permanent irreversible loss mechanisms of chemical from the biosphere including losses to the stratosphere, losses to deep ocean and permanent burial. Wania (1998) recognised that such losses would ultimately contribute to the removal of long-lived chemicals in the environment and consequently, reduce the unrealistic persistence, which would have been otherwise generated.

The development of global evaluative models serves as an orchestrated attempt to harmonise the persistence assessment process. On a global level, regional prejudices cannot exert any control over the model results. This integrated, broad approach has many appealing applications especially as world focus shifts to sustainable development.

6.4.3.2 The GloboPOP model of Wania and Mackay

The Global distribution model for persistent organic pollutants (GloboPOP) is the result of a series of publications (Wania and Mackay, 1993; Wania and Mackay, 1995; Wania et al., 1999; Wania and Mackay, 1999) developing a dynamic, multi-compartment, linearly connected mass balance model, which describes the global migration of organic pollutants. As the key focus of the development of the model was to identify the factors responsible for global fractionation, spatial and temporal temperature dependency was explicitly built into the model since temperature is believed to be a controlling influence.

On a global scale, persistent organic pollutants undergo a cycle of distillation and fractionation in which they are vaporised into the atmosphere in warmer regions of the earth, and condensed and deposited in the colder regions. The theory of this phenomenon holds that the distribution of such pollutants is governed by their physicochemical properties and the temperature conditions to which they are exposed. As a result, the persistent pollutants of highest volatility are distilled into the polar regions; those of intermediate volatility deposit at the mid latitude region; and the least volatile persistent organic pollutants are deposited near their sources. This phenomenon has clear and important implications regarding the accumulation of POP's in the environmentally fragile polar region, far from their industrial sources.

The model includes nine distinct climatic zones, each comprised of six environmental compartments (air, freshwater, freshwater sediment, ocean water and two soil compartments). The compartments are linked by numerous diffusive and advective processes, which are significant in simulating realistic global transport. Hertwich and McKone (2001) have expounded on the importance of including both dispersion and advective effects. Dispersion dominates longitudinal (north-south) transport while advection contributes significantly to latitudinal (east-west) transport.

Wania and Mackay (1995), using the GloboPOP model were able to demonstrate that temperature is indeed a key parameter in global fractionation; however, several other variables including organic carbon content of soils, soil depth and vegetation were found to be important factors controlling air-surface interactions.

Wania and Mackay (1999) and Wania et al. (1999) demonstrated the accuracy of the GloboPOP model to predict the global distribution of α-hexachlorocyclohexane to within one order of magnitude: The averaging of environmental inputs according to climatic zone is believed to be the limiting factor regarding the model accuracy.

6.4.4 Persistence models

Persistence is defined by Pennington (2001) as a measure of the tendency of a substance to remain in the environment unless removed by irreversible degradation. In the definitions of persistence found in literature, interchange of the terms overall system reaction half-life and overall persistence is common. However, as persistence has been mathematically defined, these two properties are not mathematically equivalent although they are directly proportional [See Equation (6-10)].

Persistence is an overall system property and is sometimes referred to as characteristic time (Bennett et al., 1999). Several definitions for persistence exist in literature. Equivalence of the various definitions is conditional; occurring only when the multimedia model used to assess the environmental distribution does not contain advection losses in the model formulation.

The original definition for the overall persistence was based on a transient model developed by Scheringer (1996):

$$\tau = \frac{\sum_i \int_0^\infty N_i(t)dt}{\sum_i N_i(0)} \qquad \textbf{(6-6)}$$

The time-integrated solution of an initial value problem corresponds directly to the steady state formulation if the steady state source emission vector ($\underline{E}$) replaces the initial molar inventory vector [$\underline{N}(0)$] (Hertwich and McKone, 2001). Hence, the overall persistence as evaluated from

the Scheringer (1996) definition in Equation (6-6) above may be equivalently generated from a steady state solution to the same model system using:

$$\tau = \frac{\sum_i N_i^{ss}}{\sum_i E_i}$$

(6-7)

Equation (6-7) has been derived by Hertwich and McKone, (2001). Under the condition of exclusion of advection in the model formulation, Equation (6-7) can be expressed equivalently by a definition suggested by Wania and Mackay (2000):

$$\tau = \frac{\text{Inventory holdup}}{\text{reaction rate loss}} = \frac{\sum_i \hat{f}_i^{ss} Z_i V_i}{\sum_i D_{r,i} \hat{f}_i^{ss}}$$

(6-8)

Wania and Mackay (2000) have also defined a fourth equivalent definition for persistence stating that persistence is equal to the inverse of the overall system reaction rate constant, ($k_{overall}$), defined as follows:

$$k_{overall} = \frac{1}{\tau} = \frac{\sum_i N_i^{ss} k_i}{\sum_i N_i^{ss}} = \sum_i \frac{N_i}{N_{tot}} k_i = \sum_i Y_i^{ss} k_i$$

(6-9)

where Y_i^{ss} is the mole fraction of chemical in compartment i at steady state. Equation (6-9) alludes to the directly proportional relationship between overall system half-life and persistence as mentioned above:

$$\tau = \frac{1}{k_{overall}} = \frac{t_{1/2,overall}}{\ln 2}$$

(6-10)

Persistence is modelled using both box compartments and connected unit worlds (also known as nested box models). Nested box models consist of a system of linked unit world boxes, either in series or parallel, extended in one or two dimensions. The introduction of a series of unit worlds adds an implicit spatial variability to the nested box model. As compared with single unit worlds, the linearly connected unit worlds are typically more complex, requiring more environmental and chemical specific data.

Despite models specifically developed for persistence, any unit world may be modified to evaluate persistence. This is facilitated by the removal of advective losses from the defining model equations. Advection poses an irreversible loss to a chemical in a defined control volume; hence, if included, it will serve to extraneously reduce the persistence of the chemical. In a worst-case scenario, a recalcitrant pollutant can appear not persistent if it is volatile enough to distribute itself mainly into the most mobile compartment, the air phase, swiftly being conveyed from the system. A Level III transport and persistence model (TaPL3), developed by Webster et al. (1998), and extended by Beyer et al. (2000) is considered to be the definitive persistence model. It is based on the EQC model but has been modified by removal of advection terms from the EQC model formulation.

Persistence is currently an evaluative property as it is calculated from evaluative models. In the extension of persistence to simulate real world conditions, it could be argued that loss processes other than degradation that lead to permanent and irreversible removal of chemical from the system should be included in the estimation of overall persistence to avoid unrealistic persistence values (Wania, 1998). Current persistence evaluation models, although not simulating real world conditions, do simulate observed persistence trends. Consequently, evaluative persistence studies have been used to calibrate threshold intervals from the simulation of chemicals whose persistence classifications are known from real world observations.

By expanding the principle that persistence models should not include advection terms, multimedia models, which are dominated by reactive losses with respect to advection losses, may be used to evaluate persistence. Global and some nested box, regional models span large volumes and are essentially closed systems; consequently, these models satisfy the above criterion. Thus, models of this type, although designed as fate models, may be used to calculate persistence.

The following table summarises models designed for persistence assessment:

Table 6-5: Models available for the assessment of persistence

Model	Reference	Description
Limiting law	Müller-Herold (1996) Müller-Herold et al. (1997)	Equilibrium based persistence assessment using a three-compartment model.
-	Gouin et al. (2000)	Equilibrium based persistence assessment using a three-compartment model identifying key half-lives.
-	Pennington (2001)	Heuristic approach to determine significant contributing half-lives to persistence.
TaPL3	Webster et al. (1998) Beyer et al. (2000)	Level III, four-compartment transport and persistence model (EQC based).
-	Pennington and Ralston (1999)	Level III, four-compartment model (EQC based) with no advection.
-	Bennett et al. (1999)	Three compartment multimedia model evaluating characteristic time.
-	Scheringer (1996) Scheringer (1997)	Three-compartment circular world model evaluating persistence and spatial range.
-	Fenner et al. (2000)	Level IV three-compartment model evaluating joint persistence of parent and transformation products.
CART	Bennett et al. (2000)	Persistence evaluation using a logical tree algorithm.
EPIWIN	Meylan (1999)	Persistence evaluation using software estimated inputs into Level III four-compartment model.

Simple persistence models

Several simple models for persistence evaluation exist including equilibrium approaches and recommended guideline methodology. Equilibrium based persistence is calculated by using the steady state distribution evaluated at equilibrium conditions.

6.4.4.1 Persistence calculation approach of Müller-Herold (1996)

One of the first multimedia models to directly address persistence was the so-called limiting law model of Müller-Herold (1996). Utilising a three-compartment environment consisting of air, water and soil, Müller-Herold (1996) demonstrated that the persistence of a substance approaches a limiting value (the equilibrium calculated value) if inter-compartmental transport processes are much faster than degradation processes. Furthermore, Müller-Herold (1996) illustrated that the overall half-life was bound between the equilibrium weighted half-life and the maximum compartment half-life:

$$\frac{1}{\sum_i \left(\frac{Y_i^{eq}}{t_{1/2,i}} \right)} < \tau \ln 2 < \max\left(t_{1/2,i}\right) \qquad \textbf{(6-11)}$$

The approach of Müller-Herold (1996) exhibits several advantages for persistence screening purposes. It is not data intensive: In fact, the limiting law requires only a minimal set of data inputs including environmental degradation half-lives, the air-water partition and the octanol-water partition coefficients. Furthermore, the calculated persistence is independent of the emission source mode of entry. The validity of the limiting law was demonstrated by Müller-Herold et al. (1997) in a subsequent paper applying the methodology to 29 chemicals.

6.4.4.2 Persistence calculation approach of Gouin et al. (1996)

Gouin et al. (2000), recognising the merit in the minimalist data requisite of the Müller-Herold (1996) approach, proposed the use of an equilibrium, steady state or Mackay Level II model as a screening method for persistence. Gouin et al. (2000) assumed that the environment

could be categorised by compartments of air, water and octanol; the octanol compartment representing the organic carbon content in both soil and sediment.

Gouin et al. (2000) employed the assumption that the half-life of a species in soil is equivalent to its half-life in octanol. The assumption was deemed reasonable as 97.8 % of the equivalent octanol volume used to represent soil and sediment, was derived from the soil compartment alone, with the remaining overall equivalent octanol volume contributed by the sediment compartment. Gouin et al. (2000) used the volume ratios 650000, 1300 and 1 for air, water, and octanol respectively. These volume ratios were based on the relative volumes used in the EQC model (Mackay et al., 1996a). The overall half-life was thus defined as the equilibrium distribution weighted summation of the three compartment half-lives. Hence, on combining the air-water partition coefficient and the octanol-water partition coefficient with compound half-lives in air, water and soil, the overall equilibrium half-life could be calculated as follows:

$$\frac{1}{t_{1/2,eq}} = \sum_i \frac{Y_i^{eq}}{t_{1/2,i}} \qquad \textbf{(6-12a)}$$

where

$$Y_i^{eq} = \frac{V_i K_{iw}}{V_w + V_a K_{aw} + V_o K_{ow}} \qquad \textbf{(6-12b)}$$

Based on the equations above, it is clear that the volume ratios will influence the mole fraction distribution and hence, the overall equilibrium persistence. Gouin et al. (2000) suggested that if a substance is found to have an equilibrium calculated mole fraction in a particular compartment of greater than 99%, then it is unlikely that the half-lives in the other compartments are of any significance in the determination of overall persistence. In the study, a novel graphical technique was used to identify dominant half-lives. Lines of constant mole fraction were plotted on a graph of $\log K_{aw}$ verse $\log K_{ow}$, allowing regions of significant degradation half-lives to be identified. Gouin et al. (2000) proposed this procedure as a first tier in a multi-tiered approach for identification of persistent chemicals.

6.4.4.3 Persistence guidelines of Pennington (2001)

A heuristic approach developed by Pennington (2001) proposes a set of guidelines for the Henry's constant and the octanol-water partition coefficient in order to determine which compartment half-lives contribute significantly to overall persistence. This method is similar to the method of Gouin et al. (2000). In this study an attempt was made to maintain the minimal data requisites used in simple screening techniques.

The guidelines were developed using a sequential trial algorithm based on 318 chemicals in which their overall persistence, in the absence of "unimportant" half-life data, was estimated and plotted against the Henry's constant and K_{ow}. The accumulated error distribution was used to deduce which values of the Henry's constant and K_{ow} corresponded to acceptable estimation of the overall half-life. The following guidelines were obtained:

Table 6-6: Significance of compartment half-life on overall persistence according to Pennington (2001)

Condition	Conclusion
$\hat{H}_i^w > 0.01$ Pa.m^3/mol	Air compartment half-life is significant.
$\hat{H}_i^w < 1$ Pa.m^3/mol	Water compartment half-life is significant.
log $K_{ow} > 3$	Soil compartment half-life is significant.
log $K_{ow} > 5$	Sediment compartment half-life is significant.

Generally, the equilibrium approaches proposed by Müller-Herold (1996), Gouin et al. (2000) and Pennington (2001) are simple to understand and do not require an overwhelming amount of input data. Thus, these approaches can be applied to exclude many distinctly non-persistent chemicals from the list of thousands of chemicals commercially distributed. However, equilibrium approaches leave several unresolved issues since factors, like mode of entry, have no influence on equilibrium distribution, but still play an important role in the persistence of a compound (Webster et al., 1998). Moreover, a limitation inherent to equilibrium based persistence assessments is that they may underestimate persistence by assuming the chemical partitions into a phase of high degradation which it cannot reach, owing to significant inter-media transfer resistances (Wania, 1998).

Non-equilibrium based persistence models

Several non-equilibrium persistence models have been formulated, with the TaPL3 model perceived as being the best suited for the persistence assessment of organic substances in a regulatory context (Gouin, 2002). Although the EQC model violates the advection free formulation principle, the EQC model yields an overall persistence, which is composed of separable advection and reaction components [See Appendix B-2, Equation (B-4)]. Consequently, the EQC model can report a separate reaction persistence. Even though the reaction persistence is evaluated with respect to degradation losses only, the fugacity used in evaluating the reaction persistence originates from a model formulation, which includes advection. Hence, it could be argued that the reaction persistence calculated from the EQC model elicits a more realistic value for persistence, as the calculated persistence is based on reaction data, which is tempered by an advection component.

Based on Level III models used for persistence evaluation, the following input parameters have been identified as critical for persistence modelling:

- Inter-media partition coefficients describing the equilibrium distribution of chemical between air-water and soil/sediment-water phases, typically defined by Henry's constants and K_{ow}.
- First order or pseudo-first order reaction rate constants or corresponding medium half-lives in air, water, soil and sediment.
- Stipulation of emission scenario.

6.4.4.4 Persistence using the TaPL3 model

Given the limitations encountered in equilibrium persistence approaches, Webster et al. (1998) have suggested a Level III model formulation, modifying the EQC Level III model by the exclusion of advective losses. Additionally, Webster et al. (1998) have investigated the importance of mode of entry on persistence, showing that both persistence and LRAT are clearly dependent on the system emission profile. This dependency has been reiterated by Pennington (2001) who has suggested that overall persistence can vary by more than two orders of magnitude depending on the medium of release.

The TaPL3 model is an evaluative model, which contains the same four bulk compartments as used in the EQC model. It has a 10 % water surface cover with the remainder surface area attributed to soil. The atmosphere scale height is 1000 m high, the water depth is 20 m and the soil and sediment depth is 20 and 5 cm respectively. The model results are entirely complimentary to those evaluated using the EQC model with no advection losses by air, water or sediment burial. A wind velocity of 4 m/s has been adopted from Bennett et al. (1998) and a water velocity of 1 m/s representing a typical river current is used (Beyer et al., 2000).

6.4.4.5 Persistence calculation approach of Pennington and Ralston (1999)

Pennington and Ralston (1999) developed a Level II multimedia fate model, which is utilised by the US EPA Waste Minimization Prioritisation Tool (WMPT) in screening thousands of chemicals for persistence, toxicity and the tendency to bioaccumulate. The model has the same form as the EQC model (Mackay et al., 1996a) but excludes all advection terms. It is comprised of a four environmental compartment unit world (air, water soil and sediment). The model is formulated with respect to concentration, as opposed to the Mackay fugacity approach: This difference is merely superficial and is equivalent, yielding the same results.

6.4.4.6 Persistence calculation approach of Bennett et al. (1999)

Previously, Bennett and co-workers illustrated an informative methodology in the determination of characteristic travel distance, a quantity linked to long-range transport (Bennett et al., 1998). Bennett et al. (1998) defined an overall or effective decay rate, relating it to the characteristic travel distance, which was later used by Bennett et al. (1999) to define characteristic time.

In the study performed by Bennett et al. (1999), a comparison was made using various calculation complexity assumptions (Level I to Level IV) in the evaluation of persistence. This study extended work performed by Müller-Herold (1996) regarding the influence of inter-compartment transport and reactive loss rate on the selection of which model level to use to calculate persistence.

6.4.4.7 Persistence calculation approach of Scheringer (1996)

Scheringer (1996) developed a three-compartment, linearly connected, circular model that was used to calculate both the persistence and the spatial range of organic chemicals. Scheringer (1996) mathematically defined spatial range, and proposed that it be viewed as a counterpart to persistence. Scheringer (1996) illustrated that both persistence and spatial range served as proxy measures reflecting the influence of several transport and degradation mechanisms.

This model consisted of air, oceanic surface water, and soil compartments contained within a "tube" having a perimeter of 40000 km to represent the circumference of the earth. Persistence and spatial range were defined relative to a particular discharge event, which occurred at a fixed point in the spherical model environment. The "tube" was divided into *n* cells, each containing an air, water, and soil compartment, with transport mechanisms governed by the assumptions that only long-range transport described by atmospheric and oceanic eddy diffusion were important and that one-dimensional transport was representative of global circulation. The latter assumption has been validated by Held (2001). Inter-media exchange and loss processes, such as wet and dry deposition and degradation, were considered.

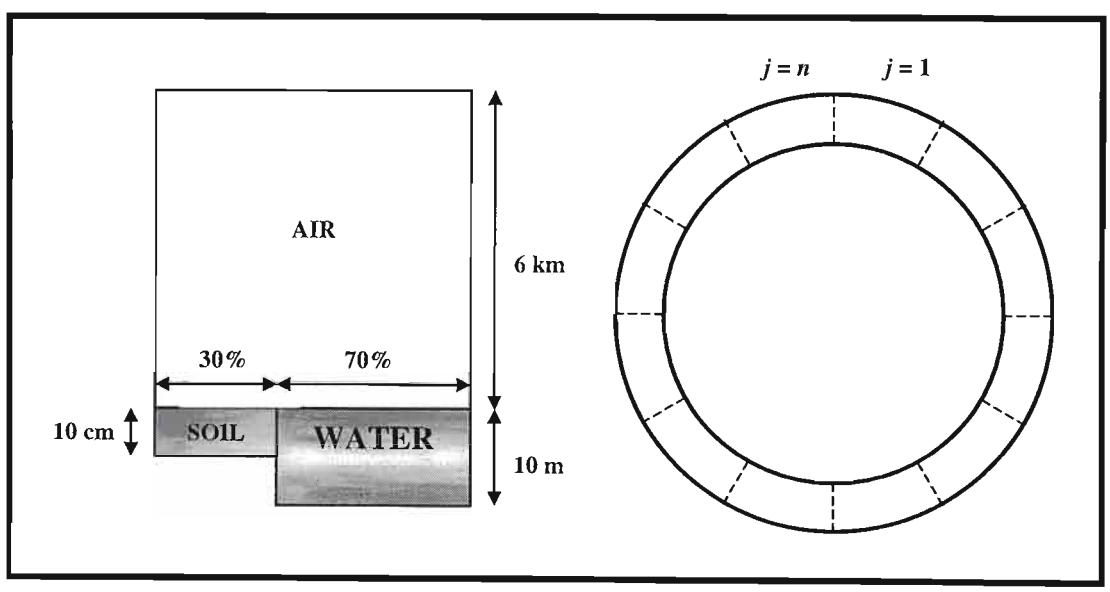

Figure 6-6: Three-compartment spherical ring model environment of the persistence and spatial range model of Scheringer (1996)

Although the persistence defined by Scheringer (1996) was an overall persistence, the spatial range, on the other hand, could be calculated for the three individual phases or as an overall spatial range. Scheringer (1997), employing the model formulated in his earlier work, evaluated 32 organic chemicals for persistence and spatial range.

6.4.4.8 Persistence calculation approach of Fenner et al. (2000)

This model explicated the concept of joint persistence, extending persistence to include both a parent and its transformation compounds. Fenner et al. (2000) used a closed three-compartment model consisting of air, water and soil in order to calculate the dynamic formation of parent pollutant and transformation products. The several transformation products were accounted for by including their rate of formation, and subsequent fraction of formation, in the total inventory of recalcitrant species within the model boundaries. In this way, analogous to the typical steady state Level II persistence, joint persistence is calculated as the ratio of the mass of the parent compound and all persistent transformation products in the steady state to the total emission of the parent compound into the model environment. This model is particularly useful for non-persistent species that degrade into persistent by-products. The normal definition of persistence would not identify such species as being a source of environmental concern.

6.4.4.9 Persistence designation according to Bennett et al. (2000)

Bennett et al. (2000) addressed chemical persistence utilising a non-equilibrium, steady state unit world model coupled to a classification and regression tree. The Classification and Regression Tree approach, or CART, is a non-analytic, computationally intensive, statistical algorithm that classifies data by producing a binary logic tree (Bennett et al., 2000). The CART tree was produced by evaluating 10000 hypothetical chemicals, spanning a broad spectrum of physio-chemical properties, in the multimedia model and identifying the ranges of property values that result in a residence time corresponding to a "non-persistent" classification.

The chemicals were binary passed through the decision tree, which assessed their physical-chemical properties at various nodes. The chemical would propagate through the tree, being split at each node, according to a logical objective function, until a terminal node was encountered. For each input, CART would try to maximise the difference in the output between

each specific split. Splitting would continue until a stopping rule was reached. At the terminal node, the chemical would be classified as "persistent" or "non-persistent". CART was programmed to only assign a classification of "non-persistent" when 95% of the chemicals in that parameter grouping were found to be non-persistent. Furthermore, the system was constructed to behave conservatively, thus allowing false positives through the screen. Consequently, on analysis of CART classified persistent chemicals at higher evaluation levels, a superfluous number will be rejected for being wrongfully labelled.

The physical-chemicals properties required for CART analysis include:

- Reactivity data in air, water, soil and sediment.
- Air-water and octanol-water partition coefficients.

6.4.4.10 Persistence according to the EPIWIN software of Meylan (1999)

Meylan (1999) has developed EPIWIN or Estimation Program Interface for Windows software. This Windows based software is available from the Syracuse Research Corporation (SRC). This program interfaces with other Windows based SRC property estimation packages, using them to estimate input parameters for a Level III fugacity model. As the SRC property estimation software is driven by the structural inputs of SMILES code (a special molecular structure description code), EPIWIN can be used to estimate the environmental persistence of unmeasured or even hypothetical compounds. This technology heralds an age of designer compounds where the structure of the compound will be back calculated from desirable properties.

The property estimation software packages used by EPIWIN include: AOPWIN (atmospheric oxidation rates), BCFWIN (*BCF*), BIOWIN (biodegradation rates), HENRYWIN (Henry's constants), HYDROWIN (hydrolysis rates), KOWWIN (K_{ow}), MPBPVPWIN (melting points; boiling points; vapour pressures), PCKOCWIN (K_{oc}) and WSKOWWIN (water solubility).

6.4.5 Long-range transport models

Multimedia model based assessment of the potential of a chemical to undergo long-range transport (LRT) usually use spatial range (Scheringer, 1996; Hertwich and McKone, 2001) or characteristic travel distance (Bennett et al., 1998; Beyer et al, 2000) as indicators of long-range transport. A chemical with a high spatial range or characteristic travel distance has a high LRT potential. It is important to note that a high LRT potential does not indicate a certain environmental threat, but merely the capacity for a threat (Beyer et al., 2000). As mentioned previously, LRT is associated with high residence time in the air compartment suggesting that atmospheric reaction (Pennington, 2001a) and air convection rates (Bennett et al., 1998) are significant variables.

The spatial range may be of concern for several reasons: A high spatial range may lead to a chemical becoming too dispersed to be identified as the cause of adverse health effects. On the other hand, a low spatial range may be of concern owing to the fact that the corresponding exposure is more concentrated and, thus, more likely to exceed toxicity thresholds (Hertwich and McKone 2001).

Hertwich and McKone (2001) highlight that existing multimedia models used for LRT evaluation differ in several ways:

- Whether they account for advective or dispersive transport
- Whether transport occurs in one or multiple compartments
- Whether and how the curvature of the earth's surface is accounted for

Many of the models that expound spatial range or characteristic travel distance, have already been introduced while discussing persistence. (This serves to emphasise the strong connection between the two parameters). Several new models are assessed, and those related above in the context of persistence, are re-explored from a LRT perspective.

Table 6-7: Models available for the assessment of long-range transport

Name	Reference	Description
-	Scheringer (1996) Scheringer (1997)	Three-compartment circular world model evaluating persistence and spatial range.
-	Bennett et al. (1998)	Four-compartment model evaluating characteristic travel distance.
-	van Pul et al. (1998)	Single-compartment model evaluating characteristic half-distance.
TaPL3	Beyer et al. (2000)	Level III, four-compartment transport and persistence model (EQC based).
-	Pennington (2001a)	Heuristic approach to determine significant contributing half-lives to LRT.
-	Hertwich and McKone (2001)	Most general definition of spatial range. Defines mobility, the relationship between spatial range and persistence.

6.4.5.1 The spatial range model of Scheringer (1996)

The concept of horizontal spatial range was first introduced by Scheringer (1996) and has been described, by Hertwich and McKone (2001), as a generic indicator for how far a pollutant is likely to travel. In the Scheringer (1996) model, based on a ring of adjacent boxes, spatial range was defined as the distance occupied by the 95th percentile of a chemical's accumulative exposure distribution about the point of discharge into the circular model environment.

The calculation of the spatial range in the Scheringer (1996) model was based on large-scale turbulent diffusion in the water and air compartments. This is unrealistic for short-lived chemicals because such chemicals are predominantly lost through degradation before being distributed by large-scale circulation. Therefore, the spatial ranges calculated by the model for short-lived compounds are systematically too high (Scheringer, 1996).

The spatial range, as defined by Scheringer (1996), could be evaluated with respect to a compartment or the overall system. Scheringer (1996) concluded several results based on the influence of compartment-specific spatial ranges regarding the mode of entry of the emission source. These results are summarised in Table 6-8 below. Scheringer (1996) further disclosed that the spatial range in air is nearly independent of the discharge scenario.

In a subsequent case study performed by Scheringer (1997), it was concluded that spatial ranges calculated from the model had to exceed 10 % of the earth's circumference in order to have any validity. Any spatial range calculated at less than this critical distance was considered to be dominated by short-range transport mechanisms, which were not accounted for in the model derivation. Furthermore, the critical distance for spatial range indicating potential long-range transport was determined to be 20 % of the earth's circumference. These threshold values were ascertained from case study results, reconciling the model simulations with field observations of the 32 chemicals investigated in the study.

Table 6-8: Influence of mode of entry on spatial range according to Scheringer (1996)

Discharge scenario	Compartment-specific spatial ranges (R_j)	Description
Soil	$R_s < R_w \leq R_a$	Phase transfer from soil to air and soil to water must occur before the chemical becomes mobile.
Water	$R_w \leq R_s \approx R_a$	Chemical reaches the water only via volatilisation and deposition from air.
Air	$R_w \approx R_s \approx R_a$	Both soil and water are exposed through the deposition from air.

6.4.5.2 The characteristic travel distance model of Bennett et al. (1998)

Bennett et al. (1998) constructed a four-compartment model defining the characteristic travel distance (CTD). These authors used a Lagrangian model consisting of four compartments including three immobile phases (surface soil-zone, soil root-zone and vegetation), and a mobile air phase.

Initially utilising a two-compartment model, Bennett et al. (1998) tracked a Lagrangian cell of air passing over soil to introduce the concept of the characteristic travel distance. This was defined as the distance required from the emission point for the concentration in the Lagrangian air cell to be reduced to 1/e (or 63 %) of its initial concentration. As the study only dealt with a single mobile phase, that of air, the definition was not valid for several moving phases. This study investigated the effect of vegetation on the characteristic travel distance, highlighting the possible importance of including a vegetation compartment when modelling persistence and LRT. However, the lack of the data required for the general inclusion of vegetation compartments in multimedia models was noted.

6.4.5.3 The half-distance model of van Pul et al. (1998)

Similar work performed by van Pul et al. (1998) suggested that the calculation of a spatial range in air could be achieved by developing a one-compartmental approach for the atmosphere. To avoid the need for the description of surface compartments, van Pul et al. (1998) employed a net deposition flux for transport of material from the mobile air compartment to the surface. A characteristic distance, called the half distance, in this study was defined as the distance taken to reduce the initial concentration by 50 % as opposed to 63 % used by Bennett et al. (1998).

6.4.5.4 The characteristic travel distance of Beyer et al. (2000)

Beyer et al. (2000) generalised the approach of Bennett et al. (1998) and van Pul et al. (1998) to other moving compartments. Thus, the characteristic travel distance was extended to apply separately to several mobile phases. Beyer et al. (2000) also introduced the effective travel distance (ETD), which was applicable to non-mobile species, which did not distribute appreciably into the mobile phase to be calculated using the Bennett et al. (1998) definition of

characteristic travel distance. Beyer et al. (2000) also introduced the concept of "stickiness", which described the fraction of substance that partitions into and remains in a non-mobile medium.

Beyer et al. (2000) showed that existing multimedia unit world models could be used to estimate CTD and that a simple relationship between CTD for a mobile phase and the overall persistence existed:

$$\mathrm{CTD}_i = u_i \tau Y_i \qquad \textbf{(6-13)}$$

Beyer et al. (2000) advocated the use of the TaPL3 model due to its conceptual development as a persistence and long-range transport model. The TaPL3 model has already been described above in section 6.4.4.4 regarding persistence. A water velocity of 1 m/s representing a typical river or current velocity is used; consequently, the CTD, calculated with respect to water as the mobile phase, does not depict LRT potential in oceanic waters.

Performing a case study on 18 chemicals, Beyer et al. (2000) defined threshold intervals for the classifications of a substance's potential for LRT from comparison of field observations with simulation results. The classifications are based on the air characteristic travel distance (CTD_a) and apply to simulations performed in the TaPL3 model for an atmospheric scale height of 1000 m at 25°C for a wind speed of 4 m/s (Table 6-9):

Table 6-9: Classification intervals depicting long-range transport potential according to Beyer et al. (2000)

Classification	CTD_a	Description
Class 1	$CTD_a > 2000$ km	High LRT potential
Class 2	700 km $< CTD_a <$ 2000 km	Possible LRT potential
Class 3	$CTD_a < 700$ km	Minimal LRT potential

6.4.5.5 Long-range transport guidelines of Pennington (2001a)

Pennington, (2001a), analogously to his study on persistence discussed above, defined guidelines to assist in the pre-determination of which degradation rates are pertinent to LRT potential. Of the threshold criteria used in LRT screening, an atmospheric degradation half-life of two days is commonly used (Rodan et al., 1999). Webster et al. (1998) has warned as to the disparities and inconsistencies, which result from threshold comparison approaches. Accordingly, Pennington (2001a) has emphasised that the critical values chosen for the proposed guidelines reflect a trade-off between data acquisition requirements and uncertainty. Consequently, Pennington (2001a) proposes the guidelines as a first tier approach in a multi-tiered screening procedure.

Table 6-10: Significance of compartment half-life to long-range transport potential according to Pennington (2001a)

Condition	Conclusion
$\hat{H}_i^w > 1 \times 10^{-5}$ Pa.m^3/mol and log $K_{oa} > 8.4$	Air compartment half-life is significant.
$\hat{H}_i^w < 1 \times 10^{-5}$ Pa.m^3/mol	Water compartment half-life is significant.
log $K_{oa} > 8.4$	Soil compartment half-life is significant.
log $K_{oa} > 10.4$	Sediment compartment half-life is significant.

6.4.5.6 The spatial range of Hertwich and McKone (2001)

Hertwich and McKone (2001) established a definition for spatial range, which could account for several mobile phases. Included in their derivation was the formulation of the direct relationship between persistence and long-range transport, alluded to by Scheringer (1996) and Beyer et al. (2000). Upon surveying the literature pertaining to long-range transport, Hertwich and McKone (2001) suggested that the common basis for all approaches lay in their accounting

of both persistence and mobility. Hertwich and McKone (2001) defined the mobility of a pollutant released to compartment j, (m_j), as:

$$m_j = \frac{\int_0^\infty \sum_i N_i(t)\, u_i\, dt}{\int_0^\infty \sum_i N_i(t)\, dt} = \frac{\sum_i N_i^{ss} u_i}{\sum_i N_i^{ss}} \qquad \textbf{(6-14)}$$

The spatial range was built on the definition of mobility formulating the relationship between mobility, persistence and spatial range.

$$R_j = m_j \tau = \frac{\int_0^\infty \sum_i N_i(t)\, u_i\, dt}{\sum_i N_i(0)} = \frac{\sum_i u_i N_i^{ss}}{\sum_i E_i} \qquad \textbf{(6-15)}$$

Hertwich and McKone (2001) also introduced a quantity called the atmospheric scale height, defined as the height of atmosphere required to contain all the pollutant, if the entire atmosphere had a uniform concentration taking into account deposition and degradation processes. Atmospheric scale height was correlated to spatial range, as both are dependent on persistence.

6.5 Validation of multimedia models

Several examples of multimedia models validated to observed concentrations exist in literature: Level III models used by various authors (Mackay and Paterson, 1991; Bennett et al., 1998; Kawamoto et al., 2001) have demonstrated simulation results, which agree with measured data to within an order of magnitude. Wania and Mackay (1999) and Wania et al. (1999) have used a global distribution model predicting the fate of α-hexachlorocyclohexane to within one order of magnitude. In particular, the ratios of compartment concentrations have been found to be considerably accurate (Sandler, 1996).

A study by Kawamoto et al. (2001), utilising both a modified EUSES and ChemCAN model exhibited excellent correlation between predicted and experimental values. Where disparities lay, the assumptions made in the model, like background air devoid of pollutant, were identified as the main source of error. The order of magnitude accuracy of this study was found to be particularly satisfactory, considering that the range of observed environmental concentrations spanned 24 orders of magnitude. Furthermore, an order of magnitude accuracy can be considered satisfactory for most real multimedia models, taking into account that discharge data, a fundamental input parameter, is believed to have an uncertainty of approximately an order of magnitude (Mackay and Paterson, 1991).

6.5.1 Fundamental similarity between more sophisticated multimedia models

Excellent agreement has been reported between various models. Maddalena et al. (1995) has compared the CalTOX model to a model formulated by Mackay and Paterson (1991) concluding that the results were in good agreement. Excellent agreement has also been achieved between ChemCAN, SimpleBOX and other models for two representative chemicals by the harmonisation of several input parameters describing environmental properties and kinetic processes (Kawamoto et al., 2001). The Kawamoto et al. (2001) study compared the EUSES and ChemCAN models showing a linear correlation index between the two models of 0.97. Hence, the choice of model used to assess a given scenario does not impact significantly on the results if the correct type of model is chosen.

6.6 Uncertainty propagation in multimedia models

The uncertainty inherent in environmental models has been highlighted by Ragas et al. (1999). Consequently, uncertainty analysis is considered an integral process in the development of environmental models (Mackay et al., 1996b). MacLeod (2002) has recently suggested a method for evaluating the uncertainty in chemical fate models, focussing on the accurate parameterisation of input uncertainties and their contributions to overall model uncertainty. This method includes sensitivity and uncertainty propagation analyses.

The uncertainty analysis methodology described by MacLeod (2002) has been shown to be consistent with Monte Carlo analysis, which is considered the technique of choice for

uncertainty quantification. However, as Monte Carlo analyses tend to be computationally intensive, the methodology of MacLeod (2002) offers a simpler analytical alternative.

6.6.1 Uncertainty analysis of MacLeod (2002)

It is important to note that most of the models described in this section require a large number of physical-chemical and environmental input parameters. MacLeod (2002) suggests that since many of these parameters are subject to uncertainty and variability, it is crucial that key input parameters be identified. Key input parameters are defined as those parameters, to which the system outputs are most sensitive. Key parameters are identified by the execution of a sensitivity and uncertainty analysis. The MacLeod (2002) methodology represents an approximate analytical technique based on a Taylor expansion of the function relating input variables to outputs.

In conventional sensitivity analysis, the sensitivity (S) of an output with respect to an input variable is defined as the partial derivative of the logarithm of the output variable (O) with respect to the logarithm of the input variable (I):

$$S = \frac{\partial \ln O}{\partial \ln I} \tag{6-16}$$

Numerically, Equation (6-16) can be approximated by modifying each input variable by a small change (1 %), and monitoring the corresponding change in the output parameters. Sensitivity can thus be approximated by:

$$S \approx \frac{\Delta O / O}{\Delta I / I} \tag{6-17}$$

Upon assigning a lognormal distribution to the input and output variables, the numerator and denominator of Equation (6-17) correspond to measures of the standard deviations of the output and input variables respectively. The validity of the assignment of lognormality, as opposed to a symmetric normal distribution, has been investigated and confirmed by Juan et al. (2002).

Slob (1994) has concluded that it is a good strategy to choose a lognormal distribution for nonnegative physical data. The standard deviations for lognormally distributed inputs and outputs can thus be represented as:

$$\sigma_O \propto \Delta O/O \tag{6-18}$$

$$\sigma_I \propto \Delta I/I \tag{6-19}$$

The relationship between the confidence factor (*Cf*) of a variable and its standard deviation for a lognormal distribution is:

$$\sigma = \frac{1}{2}\ln Cf \tag{6-20}$$

Consequently, combining the results of Equations (6-18) and (6-19) with Equations (6-20), and substituting into Equation (6-17) yields:

$$|S| = \frac{\sigma_O}{\sigma_I} = \frac{\ln Cf_O}{\ln Cf_I} \tag{6-21}$$

Equation (6-21) is rigorously valid upon assumption that the transformation function mapping inputs to outputs is linear. Input parameters do not have identical errors or confidence intervals. For example, reaction rates are usually more variable and uncertain than other data (Scheringer, 1997). For each input variable a confidence factor can be selected quantifying the range about which the parameter's true value is expected to lie to within a confidence level of 95 %.

The output variance (σ_O^2) can be expressed as the weighted sum of the variance in the uncertainty of the individual input parameters. Assuming n input variables, the output variance is:

$$\sigma_O^2 = \frac{\sum_{k=1}^{n}\left[I_k^2\sigma_{I,k}^2\left(\frac{\partial O}{\partial I_k}\right)^2\right]}{O^2} = \sum_{k=1}^{n}\sigma_{I,k}^2 S_{I,k}^2$$

(6-22)

where I_k is the k^{th} input variable, $\sigma_{I,k}$ is the variance of the k^{th} input variable and $S_{I,k}$ is the sensitivity of the output variable to the k^{th} input variable.

Converting from variance to confidence factors yields:

$$Cf_O = \exp\left[S_{I,1}^2(\ln Cf_{I,1})^2 + S_{I,2}^2(\ln Cf_{I,2})^2 + \ldots + S_{I,n}^2(\ln Cf_{I,n})^2\right]^{1/2}$$

(6-23)

The contribution of an individual input variable to the variance in an output variable can then be calculated as:

$$\frac{\sigma_{I,j}^2 S_{I,j}^2}{\sigma_O^2} = \frac{\sigma_{I,j}^2 S_{I,j}^2}{\sum_{k=1}^{n}\sigma_{I,k}^2 S_{I,k}^2} = \frac{(\ln Cf_{I,j})^2 S_{I,j}^2}{\sum_{k=1}^{n}(\ln Cf_{I,k})^2 S_{I,k}^2}$$

(6-24)

6.7 Use of chemical independent values in multimedia models

The use of chemical independent parameters or typical values, especially regarding transport parameters, is a common practice in multimedia modelling. The typical values selected are usually average values, chosen to indicate the correct order of magnitude for a parameter. Typical values are only assigned to parameters which show little variability over a range of

chemicals and can thus be averaged; or for parameters, which do not contribute significantly to model output variance.

Typical values for transport parameters like diffusivities, mass transfer coefficients and deposition velocities have been employed extensively in multimedia models. According to Mackay and Paterson (1991), transport coefficients have a variability of approximately a factor of four. Deposition velocities may vary by a factor of three (Eisenberg et al., 1998).

CHAPTER 7

Properties of MTBE, TAME and ethanol

Although physio-chemical properties do not describe the complete fate of a compound, they do convey important insights into the chemical's behaviour. The properties of a molecule are a result of its structure. The structural formulae of the three oxygenates are shown in Table 7-1 below. Despite the similar structures between MTBE and TAME, their property values can vary substantially.

Table 7-1: Structure and general information regarding the three oxygenates: MTBE, TAME and ethanol

Chemical	Molecular Formula	Structure	Synonyms
MTBE	$C_5H_{12}O$	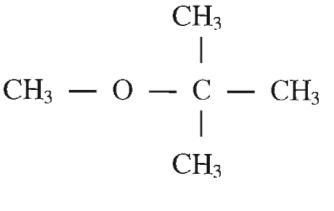	Methyl tertiary-butyl ether Methyl tert-butyl ether Methyl t-butyl ether 2-Methoxy-2-methylpropane
TAME	$C_6H_{14}O$	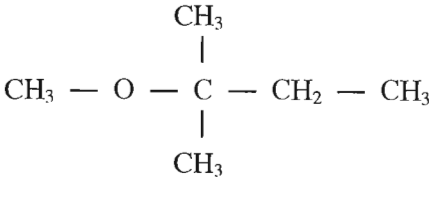	Tertiary-amyl methyl ether tert-Pentyl methyl ether 2-Methoxy-2-methylbutane
Ethanol	C_2H_5OH		Ethyl alcohol Anhydrol Alcohol Grain alcohol

7.1 Physio-chemical properties of MTBE, TAME, and ethanol

A collection of all the physio-chemical properties required for the fate analysis of MTBE, TAME and ethanol has been compiled and is presented in Table 7-4 below.

7.1.1 Structure

MTBE and TAME are both ethers having the structural form of R_1-O-R_2, where R_1 and R_2 represent aliphatic branches attached to an oxygen ether linkage. The molecular formula for MTBE is $C_5H_{12}O$; while that of TAME is $C_6H_{14}O$; TAME is one methylene-group (CH_2) heavier than MTBE. In both MTBE and TAME, the ether linkage is attached on one side by the tertiary carbon of an aliphatic branch and, on the other side by a methyl group. They differ only in the length of the aliphatic branch; TAME has the bulkier side branch one-methylene group longer. The oxygen linkage can act as a hydrogen bond acceptor, endowing ethers with polar behaviour. Ethanol is a light alcohol (R-OH), second in the homologous series of alcohols. Alcohols are defined by the presence of a hydroxyl functional group attached to a hydrocarbon chain. A direct consequence of the hydroxyl group is the polar nature of alcohols. The extent of the polar nature is reduced by the length of the hydrocarbon chain. As ethanol is the second lightest alcohol, it is extremely polar in nature. At standard temperature and pressure (STP), all three oxygenates are colourless liquids.

7.1.2 Boiling points at STP

MTBE is more volatile than TAME boiling at 55.2°C approximately 33°C lower than TAME (86.3°C). Even though, ethanol is the lightest of the three oxygenates compared in this investigation, it does not have the lowest boiling point (78.5°C). This is evidence of the strong polar intermolecular forces experienced by its molecules.

7.1.3 Aqueous and organic solubility

Both ethers are partially soluble in water; with MTBE having the greater affinity for the aqueous phase. The presence of the oxygen atom in the ether structures provides a site for hydrogen bonding between water and ether. Although the strength of the hydrogen bonds are relatively weak, it is this interaction that accounts for the high water solubility of MTBE and

TAME, when compared with other hydrocarbons of similar weight and size. MTBE (42 g/L) has a water solubility approximately four-fold that of TAME (11 g/L). This can be explained as a consequence of its smaller molecular size and apparent stronger hydrogen bonds. The heavier alkyl branch of TAME causes a greater inductive effect on the ether linkage, decreasing the polarity of this species relative to MTBE. Hence, MTBE will pack more efficiently, and consequently have a smaller excess volume when combined with water. This can be extended to the behaviour of the ethers in any polar solvent. However, this inductive effect, which enhances n-π interactions in the ethers, will result in the better packing of TAME when combined with non-polar compounds, like organic solvents. Consequently, TAME will have a smaller excess volume on being mixed with non-polar compounds relative to MTBE (Domańska and Łachwa, 2000). The inductive effect is more apparent in aqueous mixtures. Both ethers are completely soluble in organic solvents.

Ethanol's highly polar nature ensures that it is completely miscible in water. Unlike the ethers, ethanol can act as a donor and receptor of hydrogen bonding, ensuring that it is extremely miscible in water and other polar solvents. It is also soluble in organic solvents because of its non-polar two-carbon alkyl branch.

7.1.4 Octanol-water and organic carbon-water partition coefficients

The octanol-water partition coefficients of the ethers reiterate their water/organic solubility behaviour as discussed above. As TAME and MTBE share similar lipophilic tendencies, but TAME's water solubility is lower than MTBE's, TAME has a higher octanol-water partition coefficient. Ethanol partitions more predominantly into the aqueous phase than into the organic octanol phase. Consequently, it has a very low octanol-water partition coefficient.

The octanol-water partition coefficients for MTBE (Fujiwara et al., 1984) and ethanol (Hansch and Leo, 1985) in Table 7-4 are values recommended by the Syracuse Research Center. The K_{ow} value used for TAME ($\log K_{ow} = 1.57$) was measured in this study [See Appendix E]. This is comparable to the value ($\log K_{ow} = 1.55$) measured by Huttunen et al. (1997). The organic carbon-partition coefficients tabulated below are computed from the correlation proposed by Seth et al. (1997) [See Equation (4-27)].

7.1.5 Vapour pressure

MTBE is the most volatile of the three oxygenates, with TAME being marginally more volatile than ethanol at room temperature. It must be noted that ethanol is a lower boiler than TAME; hence, although less volatile at room temperature ethanol's vapour pressure increases faster than TAME's as a function of temperature. The vapour pressure parameters that are reported in Table 7-2 are used in the Reid et al. (1987) vapour pressure equation below:

$$\ln\left(\frac{P^{sat}}{P_c}\right) = (1-x)^{-1}\left[VP_1 x + VP_2 x^{1.5} + VP_3 x^3 + VP_4 x^6\right] \tag{7.1}$$

where

$$x = 1 - \frac{T}{T_c}$$

The four vapour pressure parameters for MTBE and ethanol are reported in Reid et al. (1987). The parameters for TAME were fitted to Equation (7.1) from experimental vapour pressure data collected in this study [See Appendix D].

Table 7-2: Data required for Reid et al. (1987) type vapour pressure prediction correlation using Equation (7-1)

	MTBE	TAME	Ethanol
Critical Pressure, P_c [bar]	33.7	31.9	61.6
Critical Temperature, T_c [K]	496.4	536.2	513.9
VP_1	-7.82516	-7.8714	-8.51838
VP_2	2.95493	2.4416	0.34163
VP_3	-6.94079	-5.1738	-5.573683
VP_4	12.17416	2.9644	8.32581
Reference	Reid et al. (1987)	This Study	Reid et al. (1987)

Three-parameter Antoine equation constants can be found in the Dortmund Database (DDB, 1999), which has compiled constants for all three oxygenates. Several other authors have

reported Antoine equation constants for MTBE (Huey et al., 1991; Wisniak et al., 1997; Hiaki et al., 1999) and TAME (Boublik et al., 1984; Antosik and Sandler, 1994; Delcros et al., 1995).

7.1.6 Density

The densities of all three oxygenates are all relatively similar. Most significantly, though, they are all less than the density of water; consequently, all three oxygenates will float on top of water as a separate phase if their solubility in the aqueous phase is exceeded.

7.1.7 Henry's constants

The Henry's constants decrease in the following order: TAME > MTBE > ethanol. This is an inverse relationship to that exhibited by the water solubility of the three oxygenates. Regarding TAME, Huttunen et al. (1997) have reported an estimated Henry's constant of 90 Pa.m^3/mol, using the simple vapour pressure/water solubility ratio estimation method. The value reported for TAME in Table 7-4 has been calculated from the infinite dilution activity coefficient of TAME in water measured in this study [See Appendix F]. The Henry's constants used for MTBE and ethanol are the Syracuse Research Center recommended values, which are very similar to those calculated from infinite dilution activity coefficients and from the vapour pressure/solubility ratios. The bolded values in Table 7-3 below have been used in this study.

Table 7-3: Henry's constants for MTBE, TAME and ethanol at 25°C using various predictive techniques

Property	MTBE	TAME	Ethanol
		H_i^w [Pa.m^3/mol]	
$\gamma_i^{w,\infty}$ data-based	67.8	**81.2**	0.534
P^{sat}/C_{sat}^w data-based	70.0	93.4	-
Literature	**59.5**[†]	90[‡]	**0.527**[§]

References:

† Hine and Mookerjee (1975)

‡ Huttunen et al. (1997)

§ Snider and Dawson (1985)

Some environmental models do not use the Henry's constant as an input but estimate it from the vapour pressure/solubility ratio. Accordingly, a hypothetical water solubility for ethanol [691.5 g/L] can be back calculated from the Henry's constant, using the vapour pressure/water solubility ratio to input into such models.

7.1.8 Odour and taste thresholds

The odour thresholds mirror the Henry's constant trend as vapour must volatilise from a water sample in order to stimulate the olfactory senses. The taste threshold in water of TAME is approximately 4 times greater than MTBE. This mirrors the water solubility of the two ethers. The low occurrence of reported toxic effects in humans, who have consumed MTBE contaminated water, is thought to be a result of the minimised consumption owing to MTBE's low taste and odour threshold. The drinking water standard for MTBE in California is 13 parts per billion (ppb) [Jacobs et al., 2001]. This is just below the taste threshold. Using the Henry's constant for MTBE, at this drinking standard limit, the equilibrium air concentration calculated is approximately 0.3 ppm, which is above the odour threshold. Consequently, water contaminated with MTBE will be detected by smell first, before it is tasted.

7.1.9 Degradation half-lives

The degradation half-lives for MTBE and ethanol were obtained from Howard et al. (1991). It was assumed that sediment degradation was equal to the anaerobic degradation of the compound. The geometric means of the half-lives were calculated from the high and low values as indicated by Howard et al. (1991). Each half-life reported in Table 7-4 has an associated confidence factor reported with it in brackets; the product and quotient of the geometric mean and the confidence factor will respectively regenerate the high and low values reported in Howard et al. (1991).

TAME and MTBE have been shown to have similar aerobic (Kharoune et al., 2001) and anaerobic (Mormile et al., 1994) biodegradation rates. As biodegradation processes dominate the overall half-life estimates from Howard et al. (1991) for soil, groundwater and surface water media, it was assumed that the degradation half-lives of TAME in these media are equal to those of MTBE. The same assumption was made regarding the sediment degradation rate for TAME. With respect to the air compartment, where hydroxyl reaction dominates

(Atkinson, 1995), the ratio of TAME to MTBE hydroxyl reaction half-lives was used to estimate the overall air half-life of TAME from the value reported for MTBE in Howard et al. (1991). Atkinson (1989) measured the atmospheric hydroxyl reaction half-lives for MTBE, TAME and ethanol to be 5.7, 2 and 4.9 days respectively.

Ethers are generally resistant to biodegradation (Howard, 2000). In particular, TAME and MTBE are non-biodegradable as the oxygen atom is shielded from attack by the tertiary carbon structure directly adjacent to it. A significant consequence of their lack of biodegradability is that natural attenuation as a remediation option is generally not feasible. The stability of the tertiary carbon-structure, predicted by Markovnikov's rule, ensures that these ethers are resistant to both biodegradation and chemical oxidation. The stability of the tertiary carbo-cation is reiterated as the tertiary structure prevails often in the degradation product. Ethanol is extremely biodegradable, and consequently is easily degraded by microbes in soil, sediment and water. This is reflected in its substantially lower half-lives in these media when compared to the ethers. Generally, alcohols are more degradable than ethers (Howard, 2000).

7.1.10 Toxicity

Aquatic and oral rat toxicities are displayed in Table 7-4. The trend for both aquatic biota and small mammals holds the same: TAME is marginally more toxic than MTBE, with ethanol the least toxic. It appears that mammals are more susceptible to the toxic affects of ethanol than fish. Mackay (2001) reports a correlation of fish toxicity by Konemann (1981), which can be used to estimate aquatic toxicity. These estimates are tabulated with the literature fish toxicity LC_{50} values in Table 7-4 below.

$$\log\left(\frac{1}{LC_{50}}\right) = 0.87\log K_{ow} - 4.87 \qquad \textbf{(7-2)}$$

The LC_{50} calculated from Equation (7-2) is a molar-based toxic concentration in μmol/L. This was converted to a mass-based concentration (mg/L) using the chemical's molar mass. Although no absolute value for the oral rat LD_{50} is reported in literature, Rock (1992) states that the toxicity of TAME is approximately 25 % more toxic than MTBE. This was used to estimate an oral rat toxicity for TAME.

Table 7-4: Compilation of general physio-chemical properties and environmental fate properties of MTBE, TAME and ethanol

Property	MTBE	TAME	Ethanol
CAS number	1634-04-4	994-0508	64-17-5
Molar mass [g/mol] ‡‡	88.150	102.177	46.069
Boiling point [°C] ‡‡	55.0	86.3	78.2
Octane number§§§	110	105	115
Taste threshold [ppb] §§§	20 to 40	128	N/A
Odour threshold [ppm] §§§	0.053	0.027	49
Water solubility [g/L]	42‡	11‡	Miscible
Density @ 25°C [g/cm^3]§§	0.73540	0.76587	0.78524
Critical pressure [bar]	33.7‡‡	31.9†	61.6‡‡
Critical temperature [K]	496.4‡‡	536.2†	513.9‡‡
Critical molar volume [cm^3/mol]	326.5‡‡	377.0†	167.1‡‡
Acentric factor	0.269‡‡	0.347†	0.644‡‡
Vapour pressure @ 25°C from Equation (7-1) [bar]	0.3336	0.1006	0.0791
Partitioning data			
H_i^w [Pa.m^3/mol]	59.5††	81.2	0.527§
log K_{ow}	1.24*	1.57	-0.31**
K_{oc} from Equation (4-27) [L/kg]	6.1	13	0.17
Degradation data			
Air half-life [h]	74 (4)†††	~26 (4)	39 (3)†††
Surface water half-life [h]†††	1700 (3)	1700 (3)	13 (2)
Groundwater half-life [h]†††	3410 (3)	3410 (3)	26 (2)
Soil half-life [h]†††	1270 (2)	1270 (2)	8 (3)
Sediment half-life [h]†††	6815 (3)	6815 (3)	52 (2)
Toxicity data			
96 h Aquatic toxicity LC_{50} [mg/L]	>100‡	>100‡	13480‡‡‡
Predicted aquatic toxicity from Equation (7-2) [mg/L]	545	326	6355
Oral rat LD_{50} [mL/kg]	5.4***	~4	13.7‡‡‡

References:

† Tsonopoulos and Dymond (1997) †† Hine and Mookerjee (1975) ††† Howard et al. (1991)

‡ Huttunen et al. (1997) ‡‡ Reid et al. (1987) ‡‡‡ Verschuren (1983)

§ Snider and Dawson (1985) §§ Tamura et al. (2000) §§§ Blue Ribbon Report (1999)

* Fujiwara et al. (1984) ** Hansch and Leo (1985) *** Jacobs et al. (2001)

7.2 The Fate of MTBE in the environment

As MTBE is a well-documented chemical, it was selected as the benchmark species in this investigation. Accordingly, a review of the fate literature pertaining to this oxygenate was performed, which provides material for the qualitative validation of the assessment studies to follow.

The primary sources of MTBE to subsurface soil and groundwater are underground storage tanks, pipelines and refuelling stations. If migrating subsurface plumes enter any drinking water sources, the resulting remediation process will entail complete shutdown of the water well at high cleanup costs. MTBE is not expected to accumulate in plants and animals [US EPA (1994)].

7.2.1 Transport and fate of MTBE in the atmosphere

The occurrence of MTBE in the atmosphere is a result of evaporative processes and incomplete combustion. (Squillace et al., 1997). The environmental transport of MTBE in the atmosphere is controlled by wind speed and air temperature, which increase its mass transfer rates. MTBE is removed from the atmosphere primarily through chemical degradation and precipitation (Squillace et al., 1997). Due to incomplete combustion, MTBE has been found to increase the atmospheric levels of formaldehyde, while TAME and ethanol are believed to increase acetaldehyde levels. Ethanol may also produce formaldehyde and peroxyacetylnitrate as incomplete combustion products [NRDC (1999)].

Fate of atmospheric MTBE

Owing to MTBE's relatively high vapour pressure and Henry's constant, the compound will partition to the atmosphere. However, MTBE will not remain in this compartment for excessive periods, as degradation in the air compartment will reduce the pollution burden. Precipitation scavenging of this water-soluble additive serves as a non-reactive loss process, which merely transfers MTBE from the air phase to surface compartments. Pankow et al. (1997) attributes the air compartment as a non-point source for MTBE infiltration of groundwater primarily due to wet deposition of the chemical.

A major controlling process which governs the fate of fuel oxygenates in the atmosphere is the reaction with hydroxyl radicals (Wallington et al., 1988). Predicted atmospheric half-lives of OOD radical reaction with MTBE range from 4 to 5.7 days, depending on the concentration of the radicals assumed (Atkinson, 1989; Smith et al., 1991). Estimates of the overall half-life of MTBE in a regional air-shed are as short as 3 days; however, MTBE will have a higher half-life in areas where the concentrations of the radical are relatively low, such as, metropolitan areas (Squillace et al., 1997).

Degradation

The degradation products formed from the reaction of MTBE with hydroxyl radicals include tertiary butyl formate (TBF), tertiary butyl alcohol (TBA), acetic acid, acetone and formaldehyde. The first two transformation products listed retain the tertiary carbon structure. TBF is a potential groundwater contaminant as it resists further photoxidation and its chemical structure suggests that it will resist biodegradation (Jacobs et al., 2001).

7.2.2 Transport and Fate of MTBE in surface waters

MTBE has been detected in surface water in the US with concentrations as high as 12 mg/L in recreational areas where motorised boats are operated (Jacobs et al., 2001). Gasoline usage represents the greatest point source emission of MTBE into surface water; the transport of which is controlled by several factors including atmospheric conditions, water velocity, water depth, and temperature. MTBE concentrations in storm water runoff samples of 2 mg/L have been reported in California (Jacobs et al., 2001).

MTBE volatilisation from surface water increases with increasing temperature and water velocity and decreases with increasing water depth (Pankow et al., 1996). If the surface water body is a deep, slow moving lake, volatilisation rates become equilibrium controlled and MTBE volatilises at rates similar to BTEX compounds (Squillace et al., 1997). For shallow, fast moving flows, MTBE volatilises at rates that are significantly slower than BTEX compounds (Pankow et al., 1996). This holds for urban runoff channels and fast flowing rivers. MTBE has been reported to have a volatilisation half-life of approximately 9 hours in surface water

(Pankow et al., 1996); however, this can range upto between 4 weeks and 6 months depending on the water source (Howard et al., 1991).

7.2.3 Transport and fate of MTBE in groundwater

Primary sources of MTBE in groundwater include recurrent leaks in underground tanks and/or their associated pipe network. To a lesser extent, wet atmospheric deposition and surface runoff may contribute to groundwater infiltration. MTBE is susceptible to groundwater pollution owing to its persistence in both water and soil, in conjunction with its mobility in groundwater plumes.

MTBE is not retarded during its percolation through the soil matrix. Its relatively low octanol-water partition coefficient underlies its weak adsorption to the organic component of soil particles. Consequently, being readily soluble in water, it will move into this phase from the vapour fraction within the soil, and propagate with the groundwater through the soil column. Furthermore, as MTBE does not degrade biologically, or abiotically, this persistent chemical can contaminate large areas through distribution via the subsurface water system. Squillace et al. (1997) suggests that MTBE will propagate at close to the groundwater velocity. Groundwater velocities are extremely variable, depending on several soil characteristics including permeability, porosity and the hydraulic gradient, and may range from a few millimetres per day to a meter per day (Squillace et al., 1997).

No natural attenuation of MTBE occurs in groundwater. Recent research investigating bacterial strains isolated from biotreated sludge have demonstrated that MTBE can be metabolised as a carbon source (Salanitro et al., 1994). This holds promise for use of MTBE-acclimated microbes in the remediation of contaminated subsurface sites. MTBE does not undergo chemical transformation via hydrolysis or through hydroxyl reaction in water (Jacobs et al., 2001). Furthermore, MTBE has been reported as recalcitrant, resisting both aerobic (Yeh and Novak, 1995) and anoxic biodegradation (Suflita and Mormile, 1993; Mormile et al., 1994). Anaerobic degradation has been reported by Yeh and Novak (1994); however, this has occurred only under controlled conditions (Squillace et al., 1997).

The possible inhibitory effects of MTBE on BTEX hydrocarbons have been investigated with varying results (Squillace et al., 1997). Corseuil et al. (1998) have reported that ethanol inhibits the degradation of BTEX chemicals; the extent of which is determined by the amount of ethanol present.

CHAPTER 8

Environmental fate characteristics of MTBE, TAME and ethanol

This chapter presents three techniques for the investigation of the environmental fate characteristics of the oxygenates studied. Firstly, the three oxygenates are modelled using the EQC model (Mackay et al., 1996a) which is an evaluative, steady state, non-equilibrium simulation. This provides a generic evaluation of the environmental behaviour of the additives. Secondly, the EQC environmental landscape is customised to South African conditions (called ChemSA) in order to assess the influence of local conditions on the environmental behaviour of the oxygenates. Lastly, the South African model is evaluated at an unsteady state level (Mackay Level IV) in order to assess the transient behaviour of the chemicals resulting from a change in the emission loading.

8.1 Model description

All three models calculations are based on the same multimedia model framework composed of four bulk compartments:

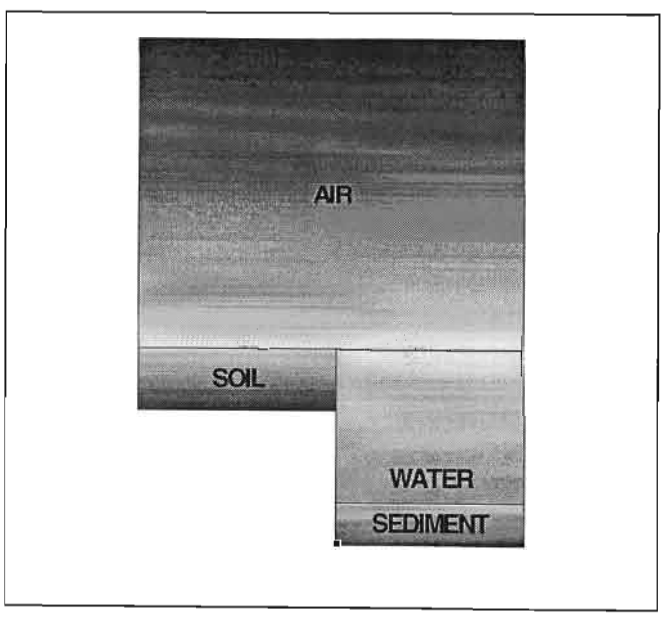

Figure 8-1: Four bulk compartments of the EQC and ChemSA models consisting of air, water, soil and sediment

The four bulk compartments include air (*a* or 1), water (*w* or 2), soil (*s* or 3) and sediment (*sed* or 4). The water phase contains both suspended sediment (*ss* or 5) and aquatic biota (*b* or 6), namely fish. The bulk air compartment incorporates an aerosol or particulate matter phase (*p* or 7). The bulk soil compartment is composed of soil particles, air and water. The sediment compartment is composed of water and sediment particles. The environmental dimensions, phase and landscape parameters for EQC and ChemSA are listed in Table 8-1 below:

Table 8-1: Model environment dimensions and landscape properties for the EQC and ChemSA models

Compartment	Characteristic	EQC	ChemSA
General features	Area [km^2]	100 000	1 267 676[†]
	Annual rainfall [mm/yr]	876	462[†]
Air	Height [m]	1000	1500[‡]
	Residence time [h]	100	56[*]
	Volume fraction of particles	2×10^{-11}	2×10^{-11}
Water	Fraction of surface area	0.1	0.0023[*]
	Average depth [m]	20	9
	Residence time [h]	100	100
	Fraction of biota in water	1×10^{-6}	1×10^{-6}
	Volume fraction of suspended sediment	5×10^{-6}	5×10^{-6}
	Suspended solid organic carbon content	0.2	0.2
Soil	Volume fraction water	0.3	0.3
	Volume fraction air	0.2	0.2
	Organic carbon fraction (m/m)	0.02	0.02
	Active layer depth [cm]	20	10[*]
Sediment	Volume fraction solids	0.2	0.2
	Organic carbon fraction (m/m)	0.2	0.2
	Active layer depth [cm]	5	5
	Residence time [h]	50 000	50 000

Note: [*] Appendix B-5

[†] Appendix B-5 and Schulze et al. (1997)

[‡] Piketh et al. (1999)

Six EQC landscape parameters were customised to South African conditions in order to develop ChemSA. These parameters include: model surface area, atmospheric height, water depth, soil depth, air advection residence time and rainfall rate. The first four parameters were identified as significant contributors to the variance in the EQC model outputs obtained from a sensitivity/uncertainty analysis of the model performed according to the method proposed by Macleod (2002). Although the rainfall rate was not found to contribute significantly to the various outputs evaluated, it was included in the customisation as rainfall data is easily available. The full uncertainty analyses performed for both the EQC and ChemSA models can be found in Appendix B-4. A discussion of the methods used in the parameterisation of the ChemSA model can be found in Appendix B-5.

8.1.1 Model formulation

The models were formulated upon the following assumptions:

- Equilibrium exists between sub-compartments within a bulk phase; but not between bulk compartments.
- The advective currents of mobile phases flowing into the model boundaries were clear of contamination i.e. there is no background contamination.

The variation of the fugacity with respect to time, for each bulk compartment is described by the following system of ordinary differential equations generated by a mass balance over the bulk compartments:

$$V_i Z_i \frac{d\hat{f}_i}{dt} = E_i + \sum_{j \varepsilon J_i} D_{ji} \hat{f}_j - \left(D_{r,i} + D_{ad,i} + \sum_{j \varepsilon J_i} D_{ij} \right) \hat{f}_i \qquad \textbf{(8-1)}$$

where $J_i = \{j \varepsilon N$: the set of indices $i \neq j$ of compartments where there is direct interfacial area between compartment i and compartment $j\}$.

$$D_{r,i} = k_i V_i Z_i \qquad \text{and} \qquad D_{ad,i} = G_i Z_i \qquad \textbf{(8-2)}$$

The other D values (subscripts ij or ji) are inter-media transfer coefficients relating fugacity to the molar transfer rate.

The EQC and ChemSA describe the following environmental processes between bulk compartments:

Table 8-2: Inter-media transport processes accounted for in the EQC and ChemSA models

Environmental Media		Process
From	**To**	
Air	Water	Absorption Rain dissolution Dry and wet aerosol deposition
Water	Air	Volatilisation
Air	Soil	Absorption Rain dissolution Dry and wet aerosol deposition
Soil	Air	Volatilisation
Water	Sediment	Diffusion Deposition
Sediment	Water	Diffusion Resuspension
Soil	Water	Soil water run-off Soil Solids run-off

8.1.2 Level III investigation of the EQC and ChemSA models

The EQC model was used to evaluate the steady state distribution of the oxygenates corresponding to a simultaneous emission loading of 1000 kg/h into each of the bulk air, water and soil compartments. The temperature of the model environment was fixed at 25°C. Similarly, the discharge profile of the oxygenates into the ChemSA environment, also fixed at 25°C, included emission into the air, water and soil compartments; however, the emission rates inputted into ChemSA were adjusted to facilitate the same source concentrations in both models. This distinction was necessary, as the same emission rates into both models would result in drastic differences in the respective environmental loading owing to their large difference in model dimensions. This, unaccounted for, would remove similitude between the models. The emissions into the ChemSA model were 19015.1 kg/h, 131.2 kg/h and 7026.4 kg/h into air, water and soil respectively. Model details can be found in Appendix B. The Level III model equations are in Appendix B-2.

The Level III study provided information on steady state compartmental fugacities and concentrations, as well as persistence values. As the model included advection terms, persistence was broken up into advection persistence, reaction persistence and overall persistence. All three persistence types are defined in Appendix B-2.

8.1.3 Level IV investigation of the ChemSA model

An unsteady state evaluation of the oxygenates behaviour was performed within the ChemSA environment. The initial conditions of the transient study corresponded to the steady state solutions from the Level III study. This represented a situation where a chemical was injected into the ChemSA environment and allowed to reach steady state. At time zero, the emission sources were "switched off" and the dynamic response was tracked. Solution of the transient response to this defined emission profile was calculated using the Runge-Kutta integration technique (in the ODE suit of Matlab 5.3). As there is no background contamination of the model environment, the new steady state solution reached was that of a pristine environment. General model details can be found in Appendix B. The Level IV model equations can be found in Appendix B-3.

The Level IV study allowed the evaluation of the fugacity settling time (Bru et al., 1998; Paraiba et al., 1999). This gives an indication as to the extent of the disturbance on an environmental compartment caused by a contamination loading.

8.2 Model results

Tables 8-3 through 8-7 contain results obtained from the Level III simulations of the EQC and ChemSA models. Table 8-8 and Figures 8-1 through 8-4 exhibit the results computed from the Level IV simulation of the ChemSA model.

Table 8-3: Compartmental fugacities for the Level III EQC and ChemSA simulations

	EQC			ChemSA		
	MTBE	**TAME**	**Ethanol**	**MTBE**	**TAME**	**Ethanol**
Fugacity [mPa]						
Air	0.0350	0.0160	0.0187	0.0139	0.00740	0.0150
Water	1.17	1.28	0.0108	3.66	3.23	0.00214
Soil	12.8	11.3	0.0242	6.68	5.92	0.0239
Sediment	1.12	1.23	0.00017	3.50	3.09	0.00034

Table 8.4: Compartmental concentrations for the Level III EQC and ChemSA simulations

	EQC			ChemSA		
	MTBE	**TAME**	**Ethanol**	**MTBE**	**TAME**	**Ethanol**
Concentration [ppb]						
Air	1.10	0.57	0.29	0.42	0.26	0.24
Output *Cf*	(1.393)	(1.820)	(1.370)	(1.258)	(1.548)	(1.281)
Water	1.70	1.60	0.09	5.40	4.10	0.19
Output *Cf*	(1.157)	(1.386)	(1.373)	(2.342)	(2.320)	(1.888)
Soil	3.60	3.70	0.27	1.90	1.90	0.26
Output *Cf*	(1.624)	(3.011)	(2.123)	(2.058)	(2.058)	(2.090)
Sediment	0.63	0.63	0.01	2.00	1.70	0.01
Output *Cf*	(1.244)	(1.623)	(2.859)	(2.558)	(2.574)	(3.938)

Note: ppb - parts per billion by mass [µg/kg]

Table 8-5: Compartmental mass distributions for the Level III EQC and ChemSA simulations

	EQC			ChemSA		
	MTBE	**TAME**	**Ethanol**	**MTBE**	**TAME**	**Ethanol**
Mass distribution [%]						
Air	20.0	12.2	53.3	57.1	45.6	86.2
Water	55.4	58.7	29.0	8.6	8.4	0.8
Soil	24.5	29.0	17.7	34.2	46.0	13.0
Sediment	0.1	0.1	~0	0.1	~0	~0

Table 8-6: Advection, reaction and overall persistence for the Level III EQC and ChemSA simulations

	EQC			ChemSA		
	MTBE	**TAME**	**Ethanol**	**MTBE**	**TAME**	**Ethanol**
Persistence [h]						
Advection	392.4	553.0	177.9	97.2	121.7	65.0
Output *Cf*	(1.184)	(1.307)	(1.131)	(1.174)	(1.412)	(1.088)
% of total persistence	53.4	33.1	12.2	64.9	39.8	36.3
Reaction	448.8	273.7	24.8	179.5	80.5	37.0
Output *Cf*	(1.445)	(1.272)	(1.156)	(2.108)	(1.851)	(1.371)
% of total persistence	46.6	46.9	87.8	35.1	60.2	63.7
Total	209.3	183.1	21.8	63.1	48.4	23.6
Output *Cf*	(1.092)	(1.127)	(1.115)	(1.152)	(1.305)	(1.145)

Table 8-7: Combined output percentage variance for selected Level III model inputs

Input variable	EQC			ChemSA		
	MTBE	**TAME**	**Ethanol**	**MTBE**	**TAME**	**Ethanol**
Atmospheric height	3.5	1.9	3.4	5.0	2.6	4.6
Water depth	4.5	4.1	4.7	0.2	0.2	2.6
Air residence time	3.1	1.6	7.1	7.2	2.7	14.9
Half-life in air	27.9	27.5	33.8	25.0	28.8	34.2
Half-life in surface water	2.7	2.1	19.6	0.1	0.1	7.6
Half-life in soil	0.1	0.1	17.8	0	0	19.1
Soil particle-air MTC	20.6	20.6	0	34.0	32.0	0
Soil water run-off rate	0.7	0.4	0	11.1	10.4	4.7

Level IV results

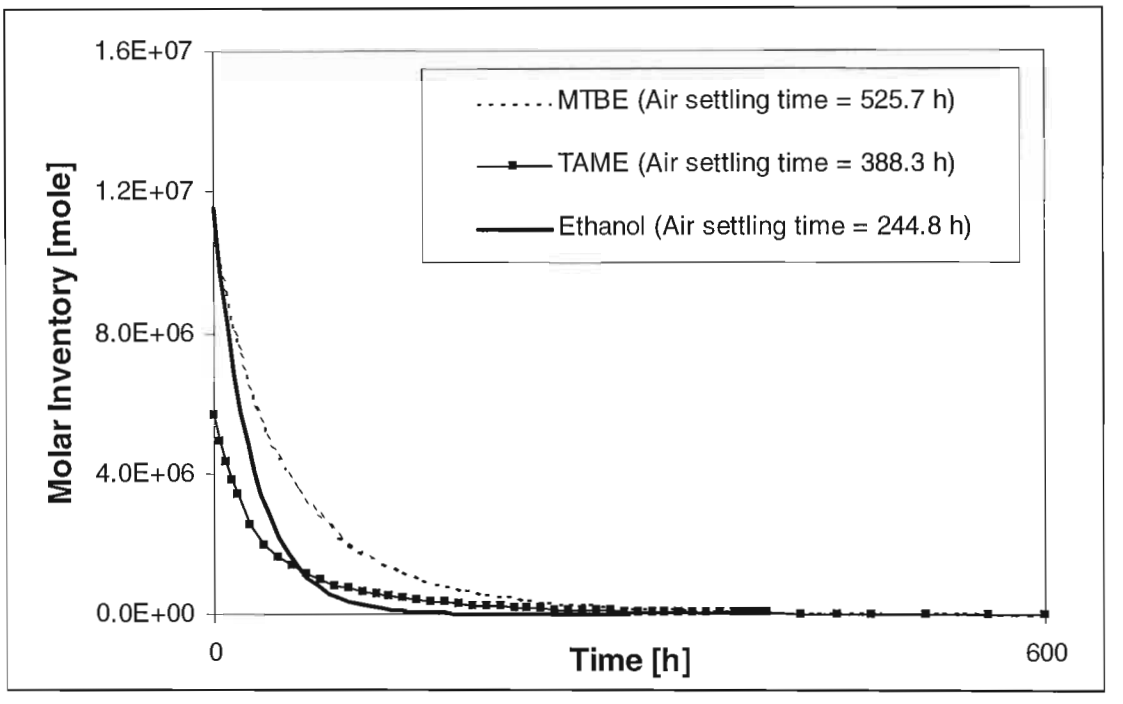

Figure 8-2: Dynamic response of MTBE, TAME and ethanol in the air compartment of the ChemSA model to the abatement of the emission source

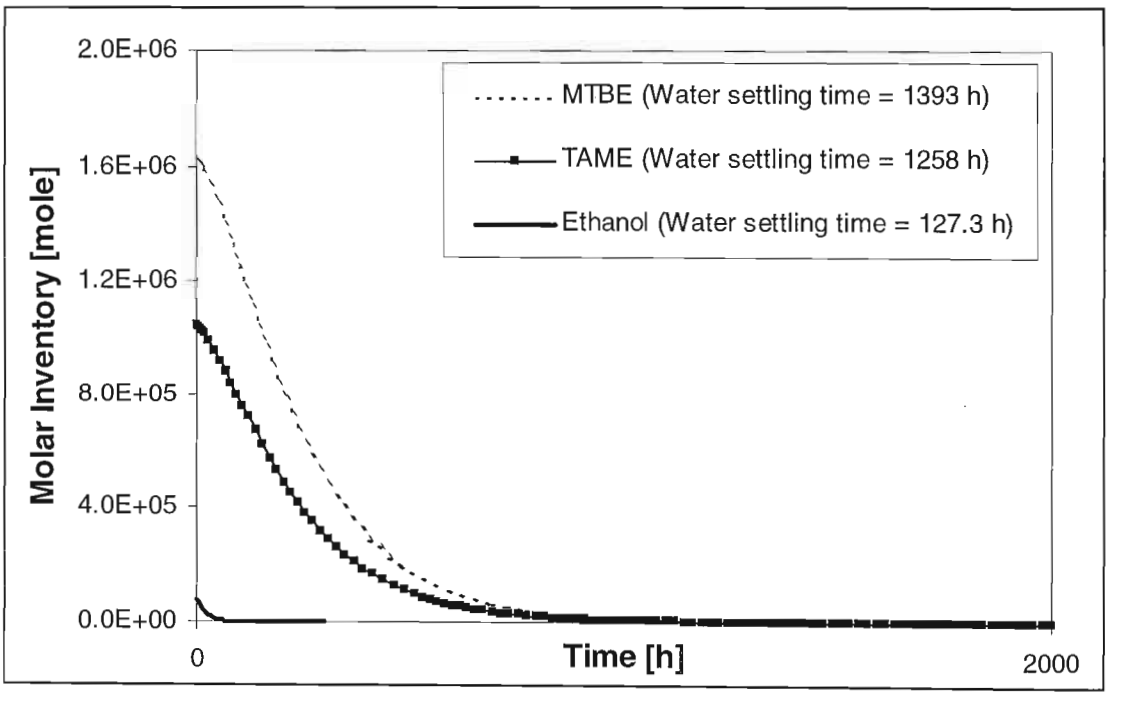

Figure 8-3: Dynamic response of MTBE, TAME and ethanol in the water compartment of the ChemSA model to the abatement of the emission source

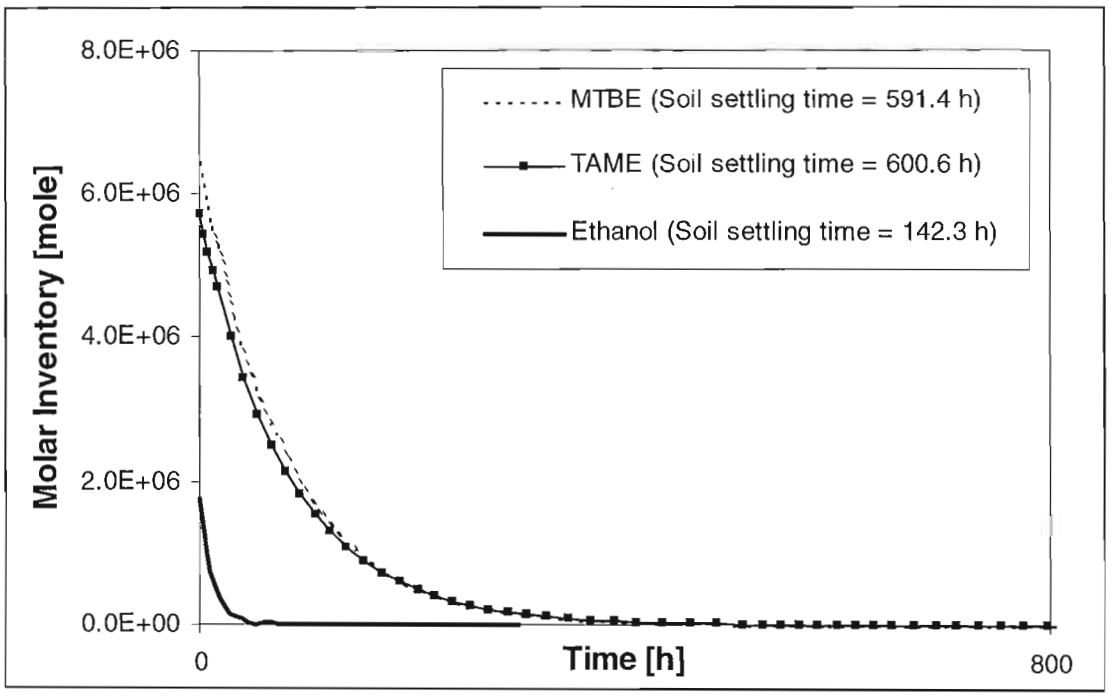

Figure 8-4: Dynamic response of MTBE, TAME and ethanol in the soil compartment of the ChemSA model to the abatement of the emission source

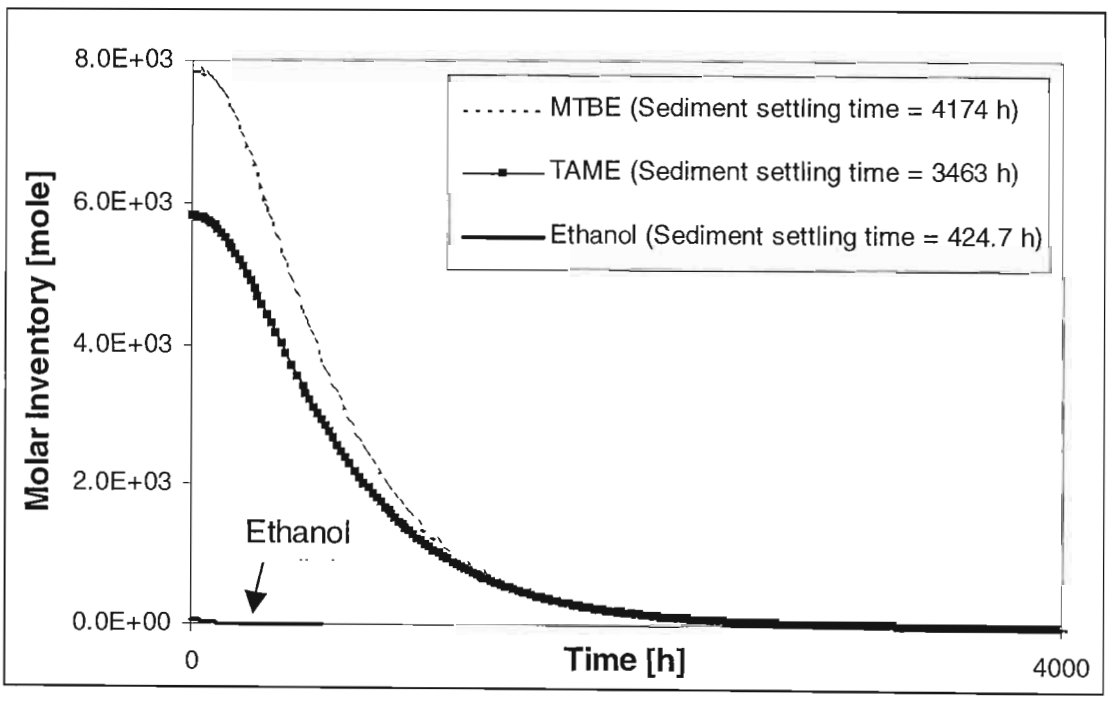

Figure 8-5: Dynamic response of MTBE, TAME and ethanol in the sediment compartment of the ChemSA model to the abatement of the emission source

Table 8-8: Fugacity settling time computed from the ChemSA model for the four bulk compartments

Bulk compartment	Fugacity settling time [h]		
	MTBE	TAME	Ethanol
Air	525.7	388.3	244.8
Water	1393	1258	127.3
Soil	591.4	600.6	142.3
Sediment	4174	3463	424.7

8.3 Discussion

Both the EQC and ChemSA models are evaluative in nature, as hypothetical emission profiles have been used. Consequently, the values obtained from the models are for characterisation of the general fate behaviour and not real scenario simulation. Subsequent use of the ChemSA as a real model could be achieved upon the inputting of field collected emission data. Identical emission loadings for each oxygenate, on a mass basis, were used in the simulations.

An advantage of the formulation of multimedia models with respect to fugacity is immediately evident in Table 8-3, as the direct identification of compartments that can be considered in equilibrium is facilitated. Table 8-3 indicates that for MTBE and TAME, the fugacities computed for the bulk water and sediment compartment are approximately equal in both models. This demonstrates that conditions close to equilibrium will prevail between these two intimately contacted phases for the ether oxygenates. This cannot be directly deduced from the concentration data presented in Table 8-4. The necessity for the unsteady state level of modelling can be understood from this same example. Knowing that the sediment and water phase may be in equilibrium, the Level III model does not explicate the time required to reach this steady state. The transient behaviour gleamed from the Level IV study indicates that the sediment compartment will take about thrice as long as the water phase to reach a steady value; at least in the direction of natural amelioration of oxygenate.

The EQC model simulation shows that MTBE exhibits a great affinity for the water compartment: a tendency, which is mirrored by TAME. This model also shows that ethanol is

air phase accumulating. These results are apparently undermined by the ChemSA model, which computes much larger mass distributions of the oxygenates in air. In order to understand this apparent disparity, it is necessary to analyse the effect of the differing emission profiles used in the two models on the simulation results.

The emission profiles represent the initial contamination of the system compartments. A consequence of fixing the emission concentrations, by varying the emission rates for the two dimensionally different models, is the similar order of magnitude solutions generated from the simulations; however, by holding the respective compartment emission concentrations constant, bias in the initial compartment inventory distribution is created. It can be seen that the ratio of the air emission rate to the water emission rate in the EQC simulation is one (1000 / 1000); however, in the ChemSA simulation, it is approximately 144 (19015.1 / 131.2). Hence, the contamination in the ChemSA model, although having the same initial concentrations, is heavily slanted towards the air compartment in terms of inventory. The ChemSA model shows air to water steady state inventory ratios of approximately 6.6, 5.4 and 108 for MTBE, TAME and ethanol respectively. This demonstrates how the relative contamination between air and water of the three oxygenates is ameliorated, substantially for MTBE and TAME, from the emission ratio of 144. Using a similar comparison process to analyse the contamination ratios between water and air, and the ratios from the ChemSA mass distribution solutions, it can be shown that the steady state inventory ratios of the ChemSA water compartment relative to the air compartment are approximately 21.6, 26.5 and 1.3 times greater than the emission ratios, for MTBE, TAME and ethanol respectively. This demonstrates MTBE and TAME's ability to be drawn into the water compartment and ethanol's ability to remain accumulated in the air compartment.

The increase in the simulated soil distribution loading from the EQC to the ChemSA model is surmised to be a result of the increase of the soil area fraction. As all three oxygenates are water-soluble and volatile enough to exist in the air compartment, the increase is attributed to wet deposition of the chemicals. Moreover, the increase in the variance of the soil-air mass transfer coefficient from the EQC to ChemSA model illustrates that mass transfer-driven volatilisation of chemical from soil to air is a limiting process. Thus, a uni-directional process in the opposite direction, namely precipitation scavenging, is a major transference mechanism from air to surface soil. This is supported by the lower air compartment concentrations in the ChemSA model.

All the processes in Table 8-2 above represent transference of chemical from one compartment to another. The only chemical losses occurring in the models are through advection or reaction. Consequently, advection persistence and reaction persistence can be defined separately. Their definitions can be found in Appendix B-2. The advection loss dominates the MTBE overall persistence as calculated by the EQC and ChemSA models; however, for TAME and ethanol, the reaction loss dominates the overall persistence.

Table 8-7 lists the main variables contributing to the combined output variance [See Appendix B-4 for details]. The air half-life was found to be a significant contributor to the variance of model outputs. Bennett et al. (1999) have also found this compartment half-life to contribute significantly to environmental fate analysis. The soil water run-off rate contribution to variance in model outputs increased significantly from the EQC to the ChemSA model. This notable difference is a consequence of the increase of the soil fraction of the total surface area moving from the EQC model to the ChemSA model.

The higher output confidence factors associated with the ChemSA outputs are a result of inflated input confidence factors assumed for several variables. If no reference could be found for a particular input variable during the parameterisation of the EQC model to South African conditions, typical parameter values as suggested by Mackay (2001) were used as defaults, but the respective input confidence factors were increased to acknowledge the greater uncertainty.

The fugacity settling times gleamed from the Level IV study quantify the extent of the disturbance that the oxygenates affect on a particular compartment. Although ethanol was found to be much less persistent than MTBE and TAME, its fugacity settling time in the air compartment is of the same order; thus, indicating that its disturbance on the air compartment is similar to more persistent species. The Level IV results indicate that both MTBE and TAME disturb the water and sediment compartments considerably. The ethers decay slowly in these media in response to an abatement of the emission sources. In the soil compartment both ethers decay at similar rates, substantially slower than ethanol. The sediment compartment is exposed to the greatest disturbance, with all three oxygenates exhibiting their highest fugacity settling times in this medium.

It is the assertion of this dissertation that fugacity settling time is a measure of compartmental persistence. The concept of a compartment specific persistence has been introduced by Scheringer (1996) but has not been developed further. The definition proposed by Scheringer (1996) is limited, owing to a mass hold-up term in the denominator of the definition that will tend to zero as the compartment becomes depleted of chemical. By making the assumption that the compartment properties exhibits first order decay, the time taken to settle to steady state within a compartment is approximately equal to five times the compartment time constant. Mathematically, five time constants correspond to a period of time in which the system attains 99.3 % of its ultimate steady state value. As the time constant for a first-order system is the inverse of its overall decay rate constant, the fugacity settling time is directly related to the compartment's persistence through the time constant, and is thus, a measure of compartment specific persistence.

8.4 Conclusions

- MTBE and TAME were demonstrated to have similar water accumulation tendencies. The simulation results indicated that these two ethers approximately equilibrate between the sediment and water compartments. TAME showed a greater affinity for the soil compartment, relative to MTBE.
- Ethanol was shown to be generally non-persistent. However, it was found to have an affinity for the air compartment.
- The half-life in air was shown to be an important input variable contributing significantly to model output variance.
- Fugacity settling time was introduced as a measure of compartment specific persistence.

CHAPTER 9

Persistence and long-range transport of MTBE, TAME and ethanol

The evaluation of the persistence and the long-range transport potential of MTBE, TAME and ethanol was performed using a multimedia model to evaluate environmental distribution. The equivalent definitions for persistence of Beyer et al. (2000) and, Hertwich and McKone (2001), were used in this evaluation. Regarding long-range transport, Beyer et al. (2000) have defined characteristic travel distance (CTD), which is a compartment specific LRT measure; Hertwich and McKone (2001) have defined and used spatial range. Both LRT parameters are assessed in this evaluation. The persistence of the three oxygenates was scrutinised using the CLRTAP POP protocol criteria, the UNEP global initiative criteria and the TSMP Track 1 criteria, as summarised in Chapter 3. The long-range transport potential of the three species was classified according to the intervals defined by Beyer et al. (2000).

9.1 Model selection

The multimedia model chosen to evaluate persistence and long-range transport in this work is the TaPL3 model developed by Webster et al. (1998) and extended by Beyer et al. (2000). This model is available online at www.trentu.ca/cemc/TaPL3. A Matlab program simulating the TaPL3 model has been compiled and can be found in Appendix C-1. The TaPL3 model was selected for the following reasons:

- The TaPL3 model is based on the Mackay fugacity approach and is similar, in its formulation, to the EQC and ChemSA models.
- The TaPL3 model has been calibrated relating simulation results to field observations. Consequently, this evaluative model can be used to classify real long-range transport potential.
- It allows the parallel computation of persistence and long-range transport.

9.2 Model description

TaPL3 is a Level III fugacity model based on the EQC model, differing only regarding its exclusion of advective losses by bulk air transport, bulk water transport and sediment burial. It is composed of the same environment dimensions as the EQC model having a 1000 m high atmospheric compartment, a 20 m deep water compartment, an active soil depth of 20 cm and a sediment depth of 5 cm. Additionally, TaPL3 has two declared mobile phase velocities. A wind velocity of 4 m/s (14.4 km/h), adopted from Bennett et al. (1998), is used in the model. TaPL3 uses a water velocity of 1 m/s (3.6 km/h), which was selected to represent a typical river velocity (Beyer et al., 2000).

The TaPL3 model available on-line treats two source mode entry scenarios: computing an air emission scenario consisting of a release of 1000 kg/h exclusively to the air compartment, and a separate single emission scenario of 1000 kg/h into water. The two-emission scenario methodology has been incorporated in this investigation as Webster et al. (1998) has shown that persistence and long-range transport depend on mode of entry.

Hertwich and McKone (2001) have explicated the relationship between persistence and long-range transport through the definition of mobility. This relationship has been alluded to by Scheringer (1996) and Beyer et al. (2000). The Hertwich and McKone (2001) definition of spatial range, unlike the CTD of Beyer et al. (2000), allows for determination of LRT in an environment composed of multiple mobile media. The Hertwich and McKone (2001) definitions can be computed from the TaPL3 model distribution outputs and mobile phase velocities.

The reader is referred to Appendix B-2 to view the model equations for TaPL3. The mathematical form of TaPL3 is equivalent to the EQC and ChemSA model with advection losses set to zero. The Matlab program simulation, outlined in Appendix C-1, has been compared to the TaPL3 program available on-line and was found to produce equivalent results.

9.3 Model results

Table 9-1: Persistence and long-range transport of MTBE, TAME and ethanol as computed by the TaPL3 model environment using the definitions proposed by Beyer et al. (2000) and Hertwich and McKone (2001)

	Air emission scenario			Water emission scenario		
	MTBE	**TAME**	**Ethanol**	**MTBE**	**TAME**	**Ethanol**
Beyer et al. (2000)						
CTD_a [km]	1533	539.7	766.4	1256	447.4	0.75
CTD_w [km]	22.6	6.1	1.94	1615	1515	67.4
ΣCTD_i [km]	1556	545.8	768.3	2871	1963	68.2
Persistence [h]	113.1	39.3	54.1	537.2	453.2	18.8
Hertwich and McKone (2001)						
Spatial range [km]	1556	545.8	768.3	2871	1963	68.2
Persistence [h]	113.1	39.3	54.1	537.2	453.2	18.8
Mobility [km/h]	13.8	13.9	14.2	5.3	4.3	3.6

Table 9-2: Classification of the persistence of MTBE, TAME and ethanol according to three threshold limit protocols

Criterion	**MTBE**	**TAME**	**Ethanol**
CLRTAP POP Protocol	Persistent	Persistent	Not Persistent
UNEP Global Initiative	Persistent	Persistent	Not Persistent
TSMP Track 1	Persistent	Not Persistent	Not Persistent

Table 9-3: Classification of long-range transport potential according to the characteristic travel distance in air intervals as defined by Beyer et al. (2000)

Emission scenario	**MTBE**	**TAME**	**Ethanol**
Air emission	Class 2 Possible LRT potential	Class 3 Minimal LRT Potential	Class 2 Possible LRT potential
Water emission	Class 2 Possible LRT potential	Class 3 Minimal LRT Potential	Class 3 Minimal LRT Potential

9.4 Discussion

According to the threshold comparison criteria, two unanimous results are presented above in Table 9-2. MTBE is classified as persistent and ethanol is categorised as non-persistent according to all three protocols. TAME, however, is classified as persistent by the CLRTAP POP protocol and the UNEP Global Initiative threshold criteria, but as not persistent by the TSMP Track 1 criteria. In order to distinguish the true classification of TAME's persistence; it is necessary to look at the TaPL3 model results. The model results reiterate the mixed classification showing that the nature of TAME's persistence depends on the emission scenario. In the air emission scenario, TAME is computed to be the least persistent of the three oxygenates; even less persistent than ethanol, which is clearly not a persistence threat according to the threshold protocols. Conversely, in the water emission scenario, TAME exhibits similar persistent behaviour compared to MTBE, which is unanimously classified as persistent by the threshold criteria. This remarkable difference in the persistence behaviour of TAME can be explained in terms of the general fate characteristics of TAME as evaluated in Chapter 8.

TAME can partition appreciably into the air compartment. The extent of its distribution into the air compartment was shown to increase, as the air component of the emission profile is increased. This is evident on moving from the EQC model to the ChemSA. In the TaPL3 simulation of an air emission, an appreciable amount of TAME is released into the air compartment where it degrades rapidly owing to the ether's high reaction rate in this compartment. Consequently, when released into the atmosphere TAME is not particularly persistent. However, when released into the water compartment, TAME, having a great affinity for this medium will not distribute appreciably into the other media. Thus, its strong affinity for the water compartment and its low degradation rate in this medium underlies its persistence upon release to this medium.

On comparison of the above persistence values with those evaluated from the EQC model in Chapter 8, it can be seen that the relative difference between the ethers is starker in the TaPL3 simulation. The reason for this difference is the dependency of the oxygenates' total persistence on advective losses. As pointed out in Chapter 8, the total persistence of MTBE is dominated by advection; thus the contribution of advection to MTBE's total persistence in the EQC model is significant. As a result, the persistence of this recalcitrant ether is inadvertently lowered. The exclusion of the advection terms in the TaPL3 model ensures that the system losses are only as a result of the chemical's innate ability to degrade.

According to the Beyer et al. (2000) LRT classification criteria, TAME is considered to have a minimal LRT potential and MTBE is categorised as a possible LRT candidate. The LRT classification of ethanol depends on the emission scenario. The aqueous compartment affinity of the water-soluble alcohol facilitates its lower characteristic travel distance in air, which occurs in the water discharge scenario. As ethanol is a marginally categorised Class 2 chemical for an air emission, but a definite Class 3 chemical for a water emission, it is most likely that ethanol is not a LRT threat. As no literature source documents MTBE as exhibiting LRT behaviour, it is reasonable to deduce that this possible LRT threat, as classified by Beyer et al. (2000), does not manifest itself as a LRT threat. The strong dependency of persistence and LRT, as suggested by van Pul et al. (1998), is demonstrated by MTBE.

Although not highlighted by Hertwich and McKone (2001) in their derivation of spatial range, the relationship between characteristic travel distance and spatial range as indicated above in Table 9-1 is:

$$\text{Spatial range} = \sum_i \text{CTD}_i \qquad \textbf{(9-1)}$$

9.5 Conclusions

- TAME was shown to be less persistent than MTBE. However, the classification of TAME's persistence depended on the emission scenario. If released into water, it was persistent owing to its strong affinity for this medium. If released into the air compartment, it was found to be non-persistent. In all emission scenarios, MTBE was found to be persistent while ethanol was found to be non-persistent independent of the emission profile.
- TAME was shown to have a low probability of long-range transport. The long-range transport potential of ethanol was shown to increase in probability from a Class 3 designation to a Class 2 designation on moving from a water to an air emission scenario. However, it is not believed that ethanol is a likely long-range transport candidate. MTBE was elucidated to be a possible long-range transport threat; however, the lack of LRT reports, regarding this abundantly used, well-documented chemical, indicates that it is probably not a long-range transport candidate.

CHAPTER 10

Toxicity of MTBE, TAME and ethanol

This chapter qualitatively reviews toxicity information available for the three oxygenates. MTBE has been thoroughly investigated regarding toxicity data relevant to possible additive exposure routes. Literature sources that contain a comprehensive review of oxygenate toxicity data, especially pertaining to MTBE, include US EPA (1996) and the Blue Ribbon Report (1999). Ethanol has also been investigated extensively regarding its toxicity; however, its toxicity database is found lacking in inhalation exposure data [US EPA (1996)]. By comparison with the toxicity data available on MTBE, great data gaps exist in other oxygenates, particularly with respect to TAME (Rock, 1992).

None of the three oxygenates investigated in this work are considered lethal; especially in comparison to the associated components found combined with these additives in gasoline proper. LC_{50} and LD_{50} have already been presented in this dissertation (in Table 7-4) but are reproduced below for the convenience of the reader:

Table 10-1: Toxicity data for MTBE, TAME and ethanol

Toxicity data	MTBE	TAME	Ethanol
96 h Aquatic toxicity LC_{50} [mg/L]	>100[‡]	>100[‡]	13480[‡‡‡]
Predicted aquatic toxicity from Equation (7-2) [mg/L]	545	326	6355
Oral rat LD_{50} [mL/kg]	5.4[‡‡]	~4	13.7[‡‡‡]

References:

‡ Huttunen et al. (1997)

‡‡ Jacobs et al. (2001)

‡‡‡ Verschuren (1983)

10.1 Toxicity of MTBE

As MTBE is primarily found in groundwater, human exposure to this ether is most probable through drinking water or the consumption of affected animals. Dermal contact with

contaminated water can occur possibly through bathing and washing. Inhalation of fumes will most likely occur at petrol stations for time periods of a few minutes. Humans may also be exposed through inhalation during showering as MTBE may volatilise from the shower water due to the increased mass transfer facilitated by the rapid spray.

Although MTBE has been found to induce cancer in rats and mice through several exposure routes [US EPA (1996); Blue Ribbon Report, 1999], no rigorous studies exist indicating MTBE exposure to be a human cancer risk, especially in light of the likely exposure concentrations (Jacobs et al., 2001). Thus, current carcinogenic studies available for MTBE cancer bioassays leave some uncertainty about the efficacy and potency of MTBE to induce cancer. Nonetheless, the US EPA cautiously considers MTBE a weak inhalation carcinogen classifying it as a Group C chemical (i.e. a possible human carcinogen). In terms of the US EPA's inhalation cancer risk index, MTBE is 55 times less potent than benzene.

No deaths relating to humans or laboratory mammals have been reported as a result of inhalation or dermal exposure to MTBE. Jacobs et al. (20001) reports that MTBE inhalation studies have determined the no-observed-adverse-effects level (NOAEL) in humans to be 1.5 ppm, which is approximately 30 times the odour threshold. A 6-hour dermal exposure to rats at a concentration of 400 mg/kg body mass/d was found to cause no fatalities (Jacobs et al., 2001). Regarding dermal contact in humans, an exposure study has demonstrated MTBE to be "moderately" irritating to skin (Blue Ribbon Report, 1999).

An LD_{50} for rats of about 4000 mg/kg body mass has been observed and, consequently, MTBE is considered to have a low ingestion toxicity (Jacobs et al., 2001). For rats, the NOAEL through ingestion is reported to be about 70 mg/kg body mass/d; with the lowest-observed-adverse-effects level (LOAEL) being about 100 mg/kg body mass/d. Although no experimental studies have been performed pertaining to human ingestion, it is highly unlikely that accidental ingestion or inhalation of MTBE will occur owing to the low odour and taste threshold of this oxygenate.

10.2 Toxicity of TAME

Although TAME toxicology studies trail MTBE, Rock (1992) states that the effects of TAME are similar to and only slightly more severe than exposures at the same levels to MTBE. Rock (1992) reports inhalation studies performed on rats showing significant central nervous system depression at exposure levels between 2000 to 4000 ppm. A NOAEL of 500 ppm has been reported. Extrapolation of this data to humans at significantly lower concentrations associated with environmental exposure levels, suggests that the inhalation toxicity of TAME is minor.

The oral ingestion toxicity of TAME is considered to be approximately 25% more potent than MTBE based on a rat study (Rock, 1992). This information was used to approximate the rat oral LD_{50} for TAME in Table 10-1. TAME has been tested for genotoxicity showing that it is neither mutagenic, nor clastogenic (Rock, 1992).

10.3 Toxicity of ethanol

Toxicity testing indicates that ethanol is not a potent toxicant (Rock, 1992). Although a large body of literature exist on the health effects of ingested ethanol, no research has been devoted to inhalation effects at environmentally relevant concentrations [US EPA (1996)].

The handbook of Verschuren (1983) contains toxicity data for ethanol reporting that the alcohol is not carcinogenic. Verschuren (1983) contains human inhalation data from Patty (1967), which was performed at concentrations far in excess of likely environmental exposure levels. Verschuren (1983) reports oral LD_{50} for both rats and rabbits, which are of similar magnitude for these small mammals. Inhalation studies on guinea pigs and rats also exhibit results of similar magnitude. Extrapolation of the small mammal inhalation results to humans indicates that ethanol does not pose a likely inhalation risk.

CHAPTER 11

Bioaccumulation potential of MTBE, TAME and ethanol

The evaluation of the bioaccumulation potential of the oxygenates is considered a mere formality: None of these chemicals are expected to bioaccumulate or biomagnify owing to their relatively low K_{ow} values. However, illustration of this phenomenon will be demonstrated in order to facilitate a complete fate assessment of the additives. The first tier of the three-tiered methodology proposed by Mackay and Fraser (2000), combined with the threshold protocols introduced in Chapter 3, are used to evaluate the bioaccumulation tendencies of the oxygenates. The behaviour of the additives in an aquatic food chain is explored using a model developed by Thomann (1989). The food chain model derivation is expounded upon in Appendix A-6.

11.1 Food chain model description

A four-tiered food web consisting of a producer species (tier 1, e.g. phytoplankton), a primary consumer (tier 2, e.g. zooplankton), a secondary producer (tier 3, e.g. a small fish species), and a tertiary consumer (tier 4, e.g. a large fish species) is used in the Thomann (1989) model. A food assimilation coefficient (δ_η) correlation and corresponding parameters fitted by Thomann (1989) can be found below:

$$\delta_\eta = \frac{a_\eta}{b_\eta + \frac{c_\eta}{K_{ow}}} \qquad \textbf{(11-1)}$$

Table 11-1: Correlation parameters for the food assimilation coefficient fitted by Thomann (1989)

Food chain tier	Example	a_η	b_η	c_η
2	Zooplankton	0.18	0.04	2×10^5
3	Small fish	0.024	0.0046	9×10^3
4	Large fish	0.012	0.0025	2.5×10^3

The Thomann (1989) food chain model is built on a steady state mass balance for each of the four species (η) in the food chain. By assuming equilibrium conditions for the uptake of chemical from water, and excretion and decomposition rates, based on the large surface area of biological tissue membranes, it can be shown that the producer species has a *BMF* of one. By restricting the feeding pattern of each tier to that of the tier below it, a baseline biomagnification factor (θ_η) can be defined as in Equation (11-2) below:

$$\theta_\eta = \frac{C_\eta}{C_1} \tag{11-2}$$

The baseline biomagnification factor is the ratio of the concentration of chemical in food chain species η (C_η) to that in the primary producer (C_1). Consequently, the concentration of any tier or the BMF of any tier can be calculated respectively from Equation (11-3) and Equation (11-4) below:

$$C_\eta = C_1\left(1 + \delta_\eta \theta_{\eta-1}\right) \tag{11-3}$$

$$BMF_\eta = \frac{\theta_\eta}{\theta_{\eta-1}} \tag{11-4}$$

Using the water compartment concentrations computed in the ChemSA model (See Chapter 8), the concentrations up the four-tiered food chain can be calculated using Equation (11-3). For simplification purposes, the density for each tier was assumed to be the same and equal to that of water. Moreover, the fractional lipid content of each species was assumed to be 0.05 (Mackay, 1991). [In the more complicated food web model of Campfens and Mackay (1997), eight species lipid contents ranging from 0.015 to 0.16, having an average lipid content of 0.05, have been used]. The Matlab program written to perform the food chain simulation can be found in Appendix C-2.

11.2 Results

Table 11-2 contains the results for the first tier of the Mackay and Fraser (2000) approach, as well as bioaccumulation classification of the oxygenates according to the CLRTAP POP protocol, the UNEP Global Initiative and the TSMP Track 1 threshold criteria. Table 11-3 contains the results from the Thomann (1989) food chain model for MTBE, TAME and ethanol. Figures 11-1 and 11-2 reiterate the prevalence of the bioaccumulation threshold of log $K_{ow} > 5$. These figures were generated from the Thomann (1989) model.

Table 11-2: Classification of bioaccumulation potential of MTBE, TAME and ethanol according to the Mackay and Fraser (2000) first tier approach and three threshold criteria protocols

Criterion	MTBE	TAME	Ethanol
BCF*	1.87	2.86	1.02
Mackay and Fraser (2000)	No potential	No potential	No potential
CLRTAP POP Protocol	No potential	No potential	No potential
UNEP Global Initiative	No potential	No potential	No potential
TSMP Track 1	No potential	No potential	No potential

Note: * $BCF_i = (1 + LK_{ow,i})$ [Mackay and Fraser (2000) tier 1 equation from Table 4-8]

Table 11-3: Food chain bioconcentration for MTBE, TAME and ethanol as evaluated by the Thomann (1989) four-tiered food web model

Food chain tier	Concentration [ppb]*		
	MTBE	TAME	Ethanol
1	0.0834	0.1783	0.0024
2	0.0834	0.1783	0.0024
3	0.0834	0.1783	0.0024
4	0.0834	0.1783	0.0024
Biomagnification	None	None	None

Note: * ppb – parts per billion by mass

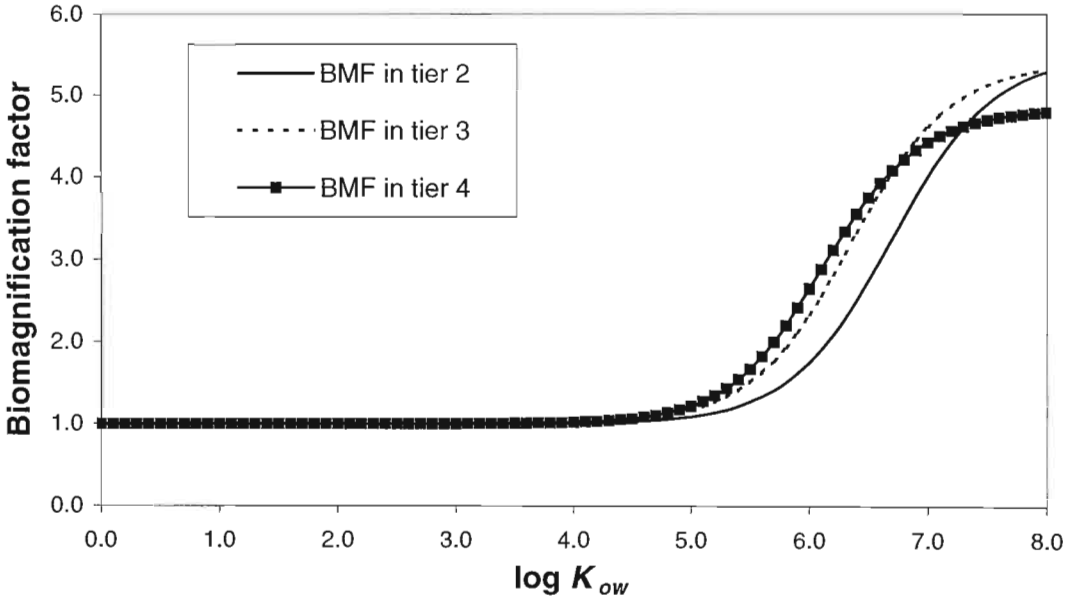

Figure 11-1: **Graph illustrating the dependency of the BMF on the octanol-water partition coefficient in the Thomann (1989) food chain model**

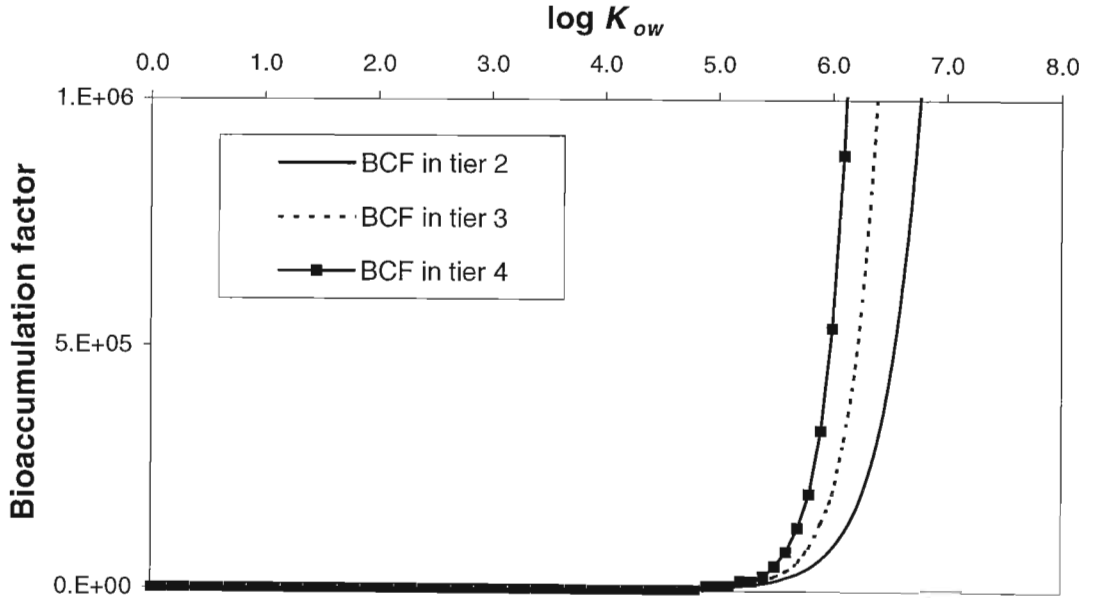

Figure 11-2: **Graph illustrating the dependency of the BAF on the octanol-water partition coefficient in the Thomann (1989) food chain model**

11.3 Discussion

As presumed, the oxygenates showed no tendencies to bioaccumulate or biomagnify and were established as having no potential to bioaccumulate by all screening methods employed in this study. The results of the Thomann (1989) model indicated that chemical compounds exhibiting a $\log K_{ow} > 5$ are particularly susceptible to bioaccumulation and biomagnification. This threshold limit is consistent with the threshold limits as employed by the first tier of the Mackay and Fraser (2000) approach and the three threshold comparison protocols.

11.4 Conclusions

- MTBE, TAME and ethanol are not expected to bioaccumulate or biomagnify in the environment.
- The threshold limit of $\log K_{ow} > 5$ as a criterion for bioaccumulation, as used in the CLRTAP POP protocol criteria, the UNEP global initiative criteria and the TSMP Track 1 threshold criteria, as well as the Mackay and Fraser (2000) approach, is supported by the simulation results of a four-tiered food chain model developed by Thomann (1989).

CHAPTER 12

Aqueous behaviour of MTBE, TAME and ethanol

The water compartment is historically the main medium associated with MTBE pollution; consequently, on performing an environmental analysis of water-soluble oxygenates, the water medium necessitates further scrutiny. Moreover, the need for additional investigation of the water medium is justified from the results gleamed in previous chapters, regarding the general fate characteristics, persistence and long-range transport of the oxygenates. In this chapter, an equilibrium water mobility study is undertaken to estimate the speed at which a plume of oxygenate will travel with respect to groundwater flow. Secondly, the thermodynamics of liquid-liquid equilibria involving an oxygenate, water and a pseudo-fuel chemical is investigated.

12.1 Equilibrium groundwater model

MTBE has been scorned for its high water mobility; Combined with its persistent nature, it is cause for great environmental concern in the aqueous environment. Comparatively, TAME has a low degradation rate in groundwater; however, its mobility is not known. Owing to its high water solubility, ethanol is expected to be extremely mobile in groundwater; but as it has a high degradation rate in this medium, it is not persistent and, thus, not of environmental concern. Consequently, less emphasis is placed on ethanol in this groundwater study and the model focus falls upon TAME and MTBE.

Based on the work of Müller-Herold (1996) and Bennett et al. (1999), equilibrium models have been demonstrated to approximate steady state models when transport rates exceed reaction rates. This approximation is valid for TAME and MTBE in groundwater; Accordingly, a simple equilibrium "vignette" model has been derived. The equilibrium model can be used to simulate results for ethanol; however, the results of the ethanol simulation must be interpreted in light of its low persistence in this medium and the subsequent lack of full applicability of the equilibrium model to this chemical.

12.1.1 Groundwater model formulation

The total phase concentration of a chemical in a heterogeneous soil phase (C^s_{tot}) is the summation of the bulk concentrations of the chemical in the water phase (C^s_w), the air phase (C^s_a) and the concentration of chemical sorbed to the solid particles (C^s_{solids}) within the bulk soil matrix. Hence:

$$C^s_{phase} = C^s_w + C^s_a + C^s_{solids} \tag{12-1}$$

The bulk phase concentrations are related to their sub-compartment concentrations by the volumetric fractions of the phases (ε_i) in the bulk soil:

$$C^s_w = \varepsilon_w C_w \qquad C^s_a = \varepsilon_a C_a \qquad C^s_{solids} = (1-\varepsilon_w-\varepsilon_a)C_{solids} \tag{12-2}$$

As there are three phases present in soil, only two equilibrium partition coefficients are independent. On selecting the partition coefficients, which describe the distribution of chemical between a non-aqueous phase and the water phase, the air-water and solids-water partition coefficients can be used to relate the non-aqueous soil sub-compartment concentrations to the aqueous sub-compartment concentration:

$$K_{aw} = \frac{C_a}{C_w} \qquad K_{solids,w} = \frac{K_p \rho_s}{1000} = \frac{y_{oc} K_{oc} \rho_s}{1000} \tag{12-3}$$

Substituting the results of Equations (12-2) and (12-3) above into Equation (12-1) yields:

$$C^s_{tot} = C_w \left(\varepsilon_w + \varepsilon_a K_{aw} + (1-\varepsilon_w-\varepsilon_a)\frac{y_{oc} K_{oc} \rho_s}{1000} \right) \tag{12-4}$$

Thus, the fraction of chemical in the water phase of the bulk soil is:

$$Y_w = \frac{C_w^s}{C_{tot}^s} = \frac{\varepsilon_w}{\left(\varepsilon_w + \varepsilon_a K_{aw} + (1-\varepsilon_w - \varepsilon_a)\frac{y_{oc} K_{oc} \rho_s}{1000}\right)} \qquad \textbf{(12-5)}$$

By the continuity equation:

$$Au_w C_w^s = AuC_{tot}^s \qquad \text{or} \qquad \frac{C_w^s}{C_{tot}^s} = \frac{u}{u_w} \qquad \textbf{(12-6)}$$

Consequently, by combining Equations (12-5) and (12-6), the mobility of a chemical in groundwater can be defined as the velocity of the chemical (u) relative to the velocity of the groundwater flow (u_w). Hence:

$$\frac{u}{u_w} = \frac{\varepsilon_w}{\left(\varepsilon_w + \varepsilon_a K_{aw} + (1-\varepsilon_w - \varepsilon_a)\frac{y_{oc} K_{oc} \rho_s}{1000}\right)} \qquad \textbf{(12-7)}$$

The parameter values used in the groundwater model for the volumetric fraction of water in soil, the volumetric fraction of air in soil, the organic carbon content of the soil and the bulk soil density, are the same as those used in the EQC and ChemSA models. A Matlab program was compiled to simulate the above model and can be found in Appendix C-3. As large variances exist in real soil landscape parameters, an uncertainty analysis was performed to distinguish significant inputs.

12.1.2 Model results

Table 12-1 contains the results for the groundwater mobility simulation. The mobilities of TAME and ethanol relative to MTBE are presented; thus, benchmarking the groundwater mobility of these oxygenates with respect to MTBE. Table 12-2 includes the percentage contribution of several input variables to the variance in the predicted mobility.

Table 12-1: Results of the equilibrium groundwater vignette model for MTBE, TAME and ethanol

	MTBE	TAME	Ethanol
Mobility relative to groundwater flow	0.757	0.598	0.991
Output confidence factor	1.153	1.493	1.002
Mobility relative to MTBE	1	0.790	1.310

Table 12-2: Contribution of selected input variables to the variance in the groundwater mobility as simulated using a equilibrium groundwater model for MTBE, TAME and ethanol

Input variable	Contribution to output variance [%]		
	MTBE	TAME	Ethanol
Organic carbon-water partition coefficient	31.4	31.5	31.6
Organic carbon content of soil	45.1	45.2	45.4
Volumetric fraction of water in soil	16.6	16.4	15.9
Density of bulk soil	6.1	6.2	6.2

12.1.3 Discussion

The groundwater model results indicated that TAME is 79 % as mobile as MTBE in groundwater. Huttunen et al. (1997) report TAME to have a relative groundwater mobility of 69 % compared with MTBE. Their groundwater mobility assessment was calculated using a simplified soil model based on the more complex model of Jury et al. (1983). Ethanol was shown to be extremely mobile in groundwater, moving at essentially the same velocity as the groundwater. The uncertainty analysis revealed that the organic carbon content of the soil, which has extensive spatial variation, contributes significantly to the predicted mobility of a substance in soil.

The model omits reactive loss of chemical; consequently, the applicability of the model to ethanol is low, as ethanol degrades readily in groundwater having a half-life of 26 h in this medium (Howard et al., 1991). Thus, the equilibrium model indicates that undegraded ethanol

will possibly be transported with groundwater flow. TAME has an assumed groundwater half-life of 3410 h, equivalent to that of MTBE; consequently, the ethers are slow to degrade in this medium and will be transported in a groundwater plume. The applicability of the equilibrium model to the ethers is valid owing to their low degradation rates relative to their transport rates.

12.2 Liquid-liquid equilibrium behaviour of oxygenates with pseudo-fuel chemicals in an aqueous environment

The review of thermodynamic liquid-liquid equilibrium (LLE) data involving an oxygenate, water and a fuel substitution chemical demonstrates an increase in complexity of the environmental assessment. Although equilibrium conditions are investigated, this thermodynamic assessment includes the effect of a secondary reagent on the oxygenates' environmental activity; a factor not accounted for in most environmental models, including the vignette model above. The nature of this interaction is assessed using the selectivity factor, which is a thermodynamic indicator used in chemical engineering for solvent selection in liquid-liquid extraction processes. The selectivity factor shows the equilibrium partitioning of a solute between two phases. (It is consequently a partition coefficient). Additionally, ternary liquid-liquid equilibrium systems containing an oxygenate, a pseudo-fuel and water are analysed to assess the co-solvency tendencies of the oxygenates.

12.2.1 Selection of fuel substitution chemicals for gasoline phase simulation

Gasoline is a complex mixture containing hundreds of organic components. Consequently, when simulating this multi-component mixture, it is often simplified and represented by a selection of fuel substitution chemicals or by a single pseudo-fuel chemical. Gasoline can be broken up into three chemical group fractions:

- Aromatics
- Paraffins (saturated components, including both iso-and normal structures)
- Olefins (unsaturated aliphatic components)

Peng et al. (1996), investigating the water solubility of gasoline and oxygenates, analysed a high-aromatic gasoline. From an ASTM D2892-73 distillation, it was established that the

gasoline consisted of 33.8 vol% aromatics, 61.8 vol% paraffins and 4.4 vol% olefins. In a study on the densities and excess molar volumes of MTBE and ETBE with hydrocarbons and hydrocarbon mixtures, Jangkamolkulchal et al. (1991) performed a compositional analysis on a gasoline sample and found it to contain 34.9 wt% aromatics, 56.1 wt% paraffins and 9.0 wt% olefins.

The fuel substitution chemicals selected for this dissertation are:

- Toluene
- TMP (i-octane or 2,2,4-trimethylpentane)
- Heptane (n-heptane)

These chemicals were identified after a literature survey reviewing recent gasoline studies and their selection of representative fuel substitution chemicals [See Table 12-3 below].

Table 12-3: Fuel substitution chemicals used in literature to simulate gasoline

Reference	Study	Gasoline Substitution Chemical			Description
		TMP	Toluene	Heptane	
Jangkamolkulchal et al. (1991)	LLE	Yes	Yes	-	2 components
Huey et al. (1991)	VLE	Yes	Yes	Yes	4 components including methylcyclohexane
Bennett et al. (1993)	VLE	Yes	Yes	-	4 components including methyl-cyclohexane and 1-heptene
Antosik and Sandler (1994)	VLE	Yes	Yes	-	4 components including methyl-cyclohexane and 1-heptene
Peng et al. (1996)	LLE	Yes	-	-	3 components including p-xylene and iso-hexene
Chamorro et al. (1999)	VLE	-	-	Yes	4 components including 1-hexene and benzene
Alkandary et al. (2001)	LLE	Yes	-	-	3 components including o-xylene and cyclohexane

Toluene and TMP are demonstrated to be favoured fuel substitution chemicals. Heptane, although not as commonly employed as the other two chemicals, is included in this work as a gasoline substitution chemical, as it forms an integral part of the definition of an extremely important gasoline property, namely the octane number. The octane number is defined as the percentage by volume TMP added to n-heptane in order to establish the same knock characteristics as the petrol when compared in a standard motor engine.

Regarding the number of components required to represent the fuel phase, only binary mixtures are used in this dissertation, i.e. an oxygenate in toluene, TMP and heptane separately. Justification of this simplification is evident by a study rendered by Alkandary et al. (2001), who used a three-component simulation fuel. These authors concluded that the results obtained agreed closely with results published by Peschke and Sandler (1995), who used toluene and TMP separately to examine ternary LLE for oxygenates, water and a gasoline substitution chemical.

12.2.2 Selectivity factor of oxygenates with respect to an aqueous phase and a pseudo-fuel phase

The selectivity factor ($\beta_{I,II}$) is defined as the ratio of the mole fraction of solute in one liquid phase of a binary liquid phase (I) to the mole fraction in another liquid phase (II). The selectivity factor is usually evaluated under infinite dilute conditions and is defined as the ratio of the limiting activity coefficients of a solute in the two liquid phases [See Equation (12-6) below and Appendix C-4 for derivation of this relationship]

$$\beta_{I,II}^{\infty} = \frac{\gamma_i^{II,\infty}}{\gamma_i^{I,\infty}} \qquad \textbf{(12-8)}$$

The selectivity factor is a thermodynamic indicator used in chemical engineering for solvent selection in liquid-liquid extraction processes. A high selectivity factor indicates that the solute has a high partitioning tendency into liquid phase *I*.

In this work, the selectivity factor is used to assess the distribution of an oxygenate between an aqueous phase and a fuel phase. Rewriting Equation (12-8) for the specific case of an oxygenate solute in water and a fuel phase yields:

$$\beta^{\infty}_{w,fuel} = \frac{\gamma^{fuel,\infty}_{oxy}}{\gamma^{w,\infty}_{oxy}} \qquad (12\text{-}9)$$

A high selectivity factor is indicative of a high partitioning tendency of the oxygenate into the aqueous phase. The selectivity factors were evaluated from binary limiting activity coefficients for the oxygenates in water, toluene, TMP and heptane at 25°C and are presented in Table 12-5 below. Various methods were used in compiling the γ_i^{∞} data presented below: Limiting activity coefficients for the oxygenates in the respective solvents were either measured directly [See Appendix F], regressed from isothermal P-x-y data [See Appendix G-1] or interpolated from infinite dilution activity coefficients [See Appendix G-2].

Table 12-4: Infinite dilution activity coefficients for MTBE, TAME and ethanol in water, toluene, TMP and heptane respectively at 25°C

Solvent	Infinite dilution activity coefficient of oxygenate solutes at 25°C		
	MTBE	**TAME**	**Ethanol**
Water	112.5 (Kojima et al., 1997)	447 (Appendix F)	3.74 (Kojima et al., 1997)
Toluene	1.47 (Appendix G-2)	1.18 (Appendix G-1)	47.3 (Appendix G-2)
TMP	1.21 (Appendix G-2)	1.14 (Appendix G-2)	16.6 (Appendix G-2)
Heptane	1.43 (Appendix G-1)	1.14 (Appendix G-2)	40.0 (Appendix G-2)

Table 12-5: Selectivity factors of MTBE, TAME and ethanol between an aqueous and pseudo-fuel phase of toluene, TMP and heptane respectively at 25°C

Solvent	Selectivity factor of oxygenate solutes at 25°C		
	MTBE	TAME	Ethanol
Water(I)-Toluene(II)	0.0131	0.00264	12.6
Water(I)-TMP(II)	0.0108	0.00255	4.44
Water(I)-Heptane(II)	0.0127	0.00255	10.7

12.2.3 Ternary liquid-liquid equilibria for oxygenates, water and a gasoline substitution chemicals

Various authors have analysed ternary LLE of oxygenate-water-fuel substitution chemicals (Peng et al., 1996; Alkandary et al., 2001). Quaternary systems for ethanol including fuel and aqueous phases have also been investigated (Tamura et al., 2000). Presented below are ternary systems for MTBE, TAME and ethanol in water and in toluene or TMP as measured by Peschke and Sandler (1995) at 25°C. Wagner and Sandler (1995) measured the same systems at two other temperatures of 5 and 40°C. Only the 25°C LLE data are shown below, as there is no substantial qualitative change in the LLE behaviour over the temperature range investigated by Sandler and co-workers. The ternary LLE data elucidates any co-solvency characteristics exhibited by the oxygenates. All ternary phase diagram are expressed in terms of species mole fractions.

Temperature-mutual solubility data for binary systems of water and oxygenate can be found in Zikmundová et al. (1990) [MTBE-water] and Domańska et al. (1999) [TAME-water]. Ethanol is completely miscible in water.

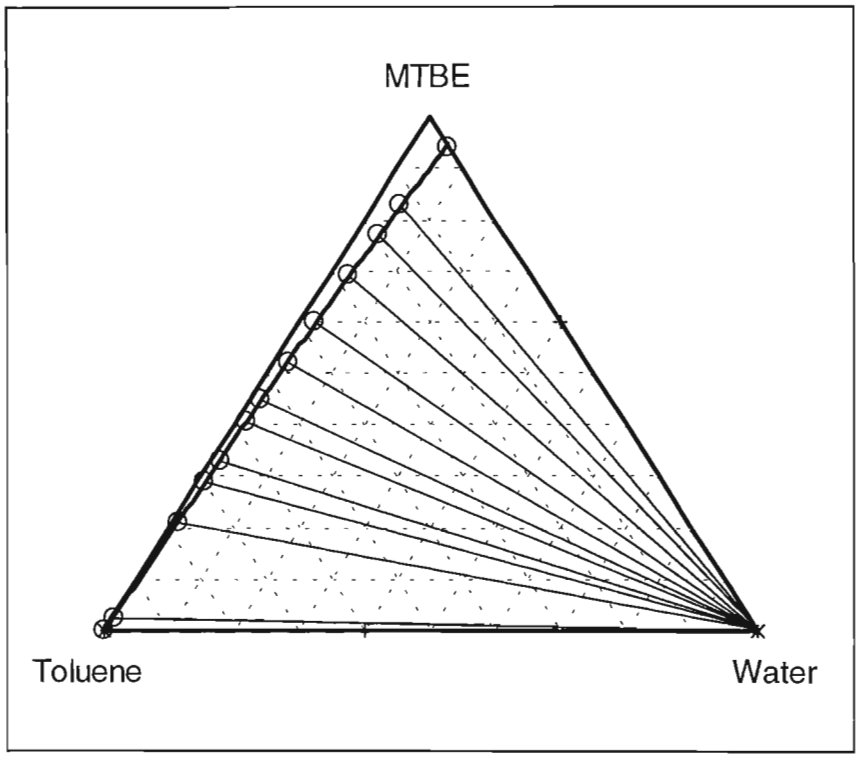

Figure 12-1: Ternary liquid-liquid equilibrium phase diagram for mixture mole fractions of MTBE-water-toluene at 25°C

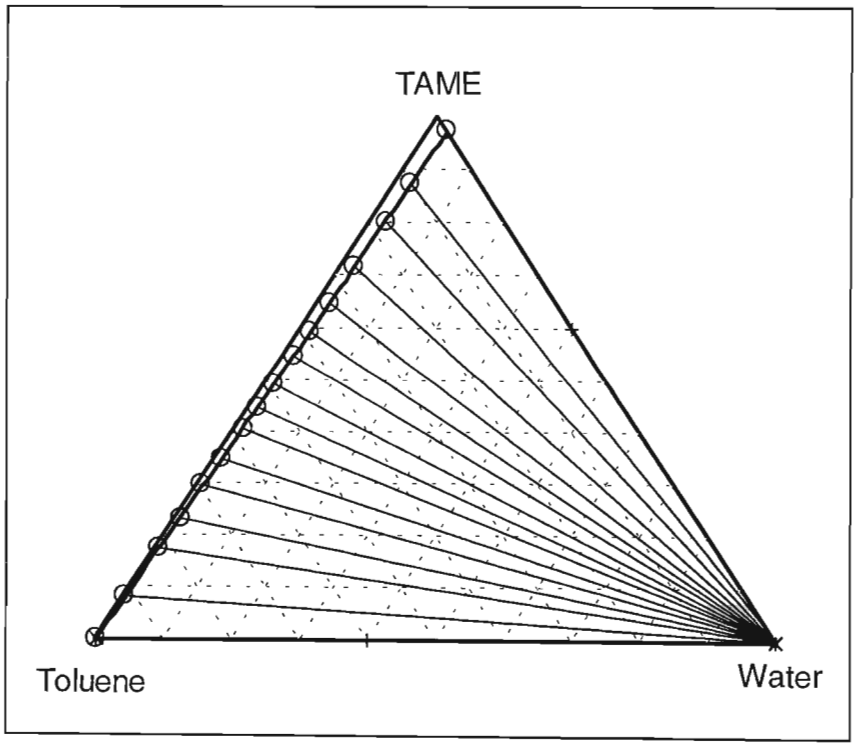

Figure 12-2: Ternary liquid-liquid equilibrium phase diagram for mixture mole fractions of TAME-water-toluene at 25°C

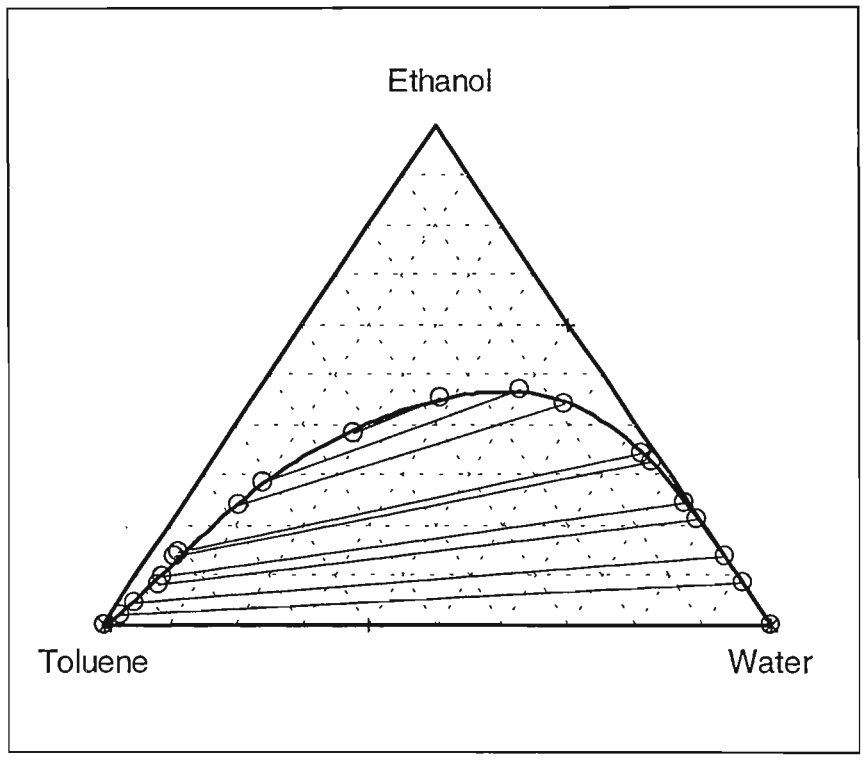

Figure 12-3: Ternary liquid-liquid equilibrium phase diagram for mixture mole fractions of ethanol-water-toluene at 25°C

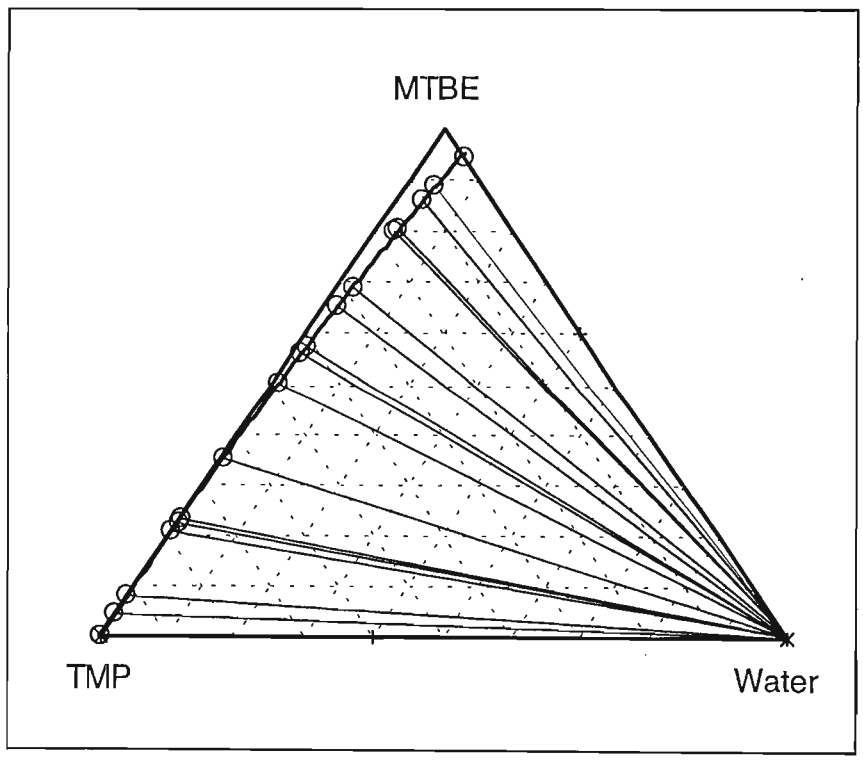

Figure 12-4: Ternary liquid-liquid equilibrium phase diagram for mixture mole fractions of MTBE-water-TMP at 25°C

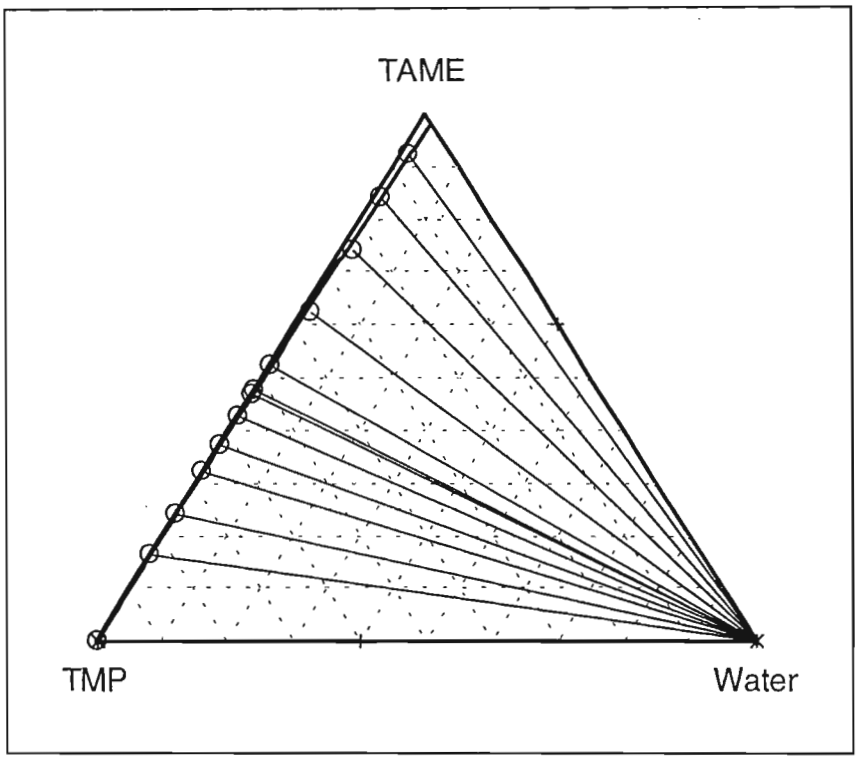

Figure 12-5: Ternary liquid-liquid equilibrium phase diagram for mixture mole fractions of TAME-water-TMP at 25°C

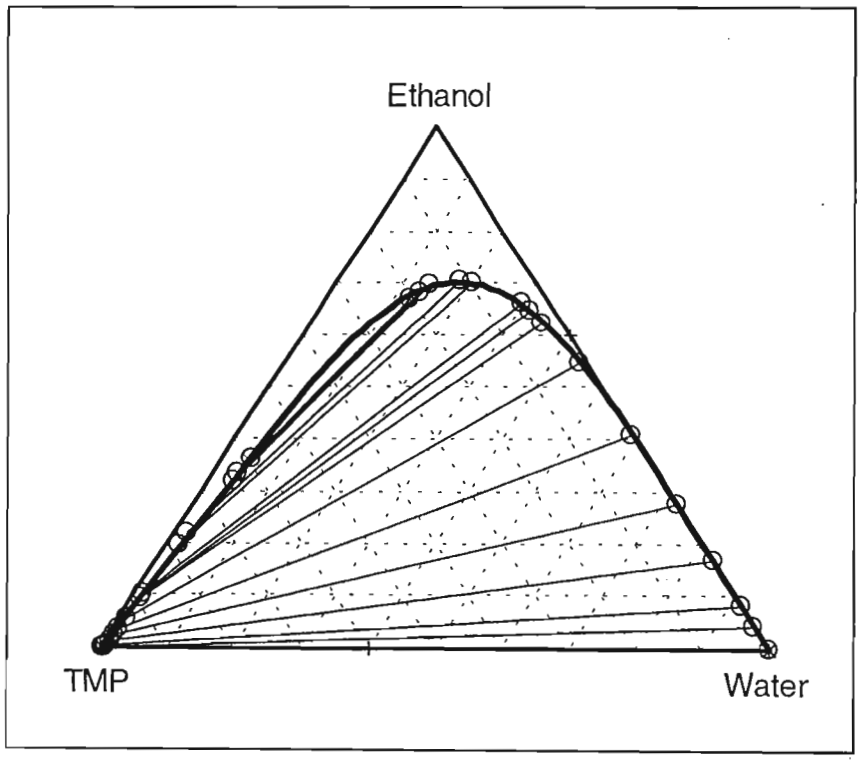

Figure 12-6: Ternary liquid-liquid equilibrium phase diagram for mixture mole fractions of ethanol-water-TMP at 25°C

12.2.4 Discussion

The selectivity factors for ethanol indicate that the alcohol will partition predominantly into the aqueous phase from a fuel phase; whereas MTBE and TAME will remain in the fuel phase, partitioning sparingly into an adjacent water phase. TAME has the lowest selectivity factor, an order of magnitude lower than MTBE, and several orders of magnitude lower than ethanol. This indicates that TAME has the lowest tendency to partition into the aqueous phase from a fuel phase. Moreover, TAME has the least water tolerance of the three oxygenates, followed closely by MTBE. This means that the addition of TAME to gasoline will lower its water solubility compared to gasoline blended with MTBE or ethanol. Environmentally, this translates to TAME blended gasoline being less bioavailable to microbial activity, which requires water.

The ternary phase diagrams indicate that MTBE and TAME in water and gasoline substitution chemical systems form a type 2 phase diagram. (The phase diagram type is defined as the number of immiscible pairs formed in the ternary system). Conversely, ethanol forms a type 1 liquid-liquid phase diagram with water and a pseudo-fuel chemical. The steep tie-lines in the MTBE and TAME ternary systems above, anchored on one side in the vicinity of the water apex of the triangular diagrams indicate the low co-solvency tendencies of MTBE and TAME. However, the shifting tie lines in the ethanol type 1 diagrams indicate that ethanol acts as a co-solvent of gasoline substitution chemicals.

12.3 Conclusions

- TAME was found to be 79 % as mobile as MTBE in groundwater.
- Ethanol was found to be extremely mobile in groundwater; however, owing to its high degradation rate in this medium, it is not considered an environmental concern.
- The selectivity factors indicate that TAME will partition sparingly into water from a fuel phase. The same result was found for MTBE. However, ethanol partitions substantially into an aqueous phase from a fuel phase.
- The ternary diagrams indicate that ethanol does not only partition appreciably into water but that it acts as a co-solvent drawing other hydrocarbons into the water phase. Combined with its high mobility in water, the fraction of ethanol not degraded will draw gasoline substitution chemicals into groundwater increasing their apparent mobility.

CHAPTER 13

Conclusions and recommendations

13.1 Environmental fate assessment of MTBE

MTBE has been confirmed as a priority chemical. The environmental assessment performed in this work has shown MTBE to have a distinct affinity for the water compartment. This is consistent with the environmental fate literature reviewed regarding MTBE in Chapter 7, and with field observations. This ether was shown to be persistent independent of the emission profile. Furthermore, MTBE was found to have the potential for long-range transport. However, the lack of literature supporting this conclusion, removes MTBE as a likely suspect for long-range transport. The toxicity data gathered for MTBE showed that it was not considered particularly toxic; notwithstanding, MTBE is currently classed by the US EPA as a possible carcinogen. MTBE was shown to have a high groundwater mobility, moving at approximately 76 % of the groundwater velocity. The banned additive was not found to partition appreciably from a fuel phase into an associated water phase. Moreover, MTBE was shown to not exhibit the undesirable property of co-solvency and therefore, will not draw fuel chemicals from an organic phase into an associated aqueous phase.

13.2 Environmental fate assessment of TAME

TAME was shown to be less of an environmental burden compared to MTBE, generally behaving differently to MTBE in the environment; however, with respect to the water compartment their behaviour seemed to converge. The general fate assessment of TAME revealed that it had an affinity for the water compartment. TAME's classification as a non-persistent species was found to rely upon the discharge scenario. This ether was found to be substantially less persistent than MTBE when discharged to air; however, upon release into water, the behaviour of TAME tended to that of MTBE. This serves to emphasise TAME's pre-disposition for the water compartment. TAME was shown to be an unlikely long-range transport candidate, although its susceptibility to long-range transport was seen to increase upon emission into the water compartment. The groundwater simulation revealed that TAME was 21 % less mobile than MTBE in groundwater. This is possibly attributed to TAME's greater

affinity for the soil phase. The relative groundwater mobility evaluated in this study is similar to that reported by Huttunen et al. (1997). TAME was shown to partition the least into water from a fuel phase, showing no co-solvency characteristics. TAME was found to be the most toxic of the three oxygenates investigated; however, it is not classified as a lethal agent.

13.3 Environmental fate assessment of ethanol

Although ethanol was demonstrated to be environmentally benign, its fate assessment indicates that this alcohol has an affinity for the air compartment. The extent of the disturbance of ethanol on the air compartment was classified in a Level IV study demonstrating that ethanol's fugacity settling time approached that of the more persistent ethers. Besides the air compartment disposition, ethanol was shown to be non-persistent, posing an unlikely long-range transport threat. The alcohol additive was found to have the least toxic nature of the oxygenates studied. The groundwater model showed that ethanol is highly mobile in groundwater; however, it was noted that the model had limited applicability to ethanol owing to its readily degradable structure. The environmental concern associated with ethanol is not its behaviour in the aqueous phase, but the extent of its influence on neighbouring solutes. Ethanol was shown to partition appreciably into an aqueous compartment from an associated fuel phase. Moreover, it was determined that ethanol acts as a co-solvent drawing fuel chemicals into the water phase. Ethanol has also been reported to inhibit degradation of BTEX chemicals (Corseuil et al., 1998).

13.4 Recommendations

Three recommendations follow from the work performed in this project:

- This project has shown significant variation in the environmental behaviour of TAME and MTBE converse to the accepted precept that these ethers will behave the same in the environment: TAME has been shown to be less persistent, less of a LRT candidate and less groundwater mobile than MTBE. Thus, it is evident that TAME does behave differently to MTBE in the environment and is, subsequently less of an environmental burden than MTBE. However, as MTBE is a significant problem chemical associated with the water compartment, and TAME has been found to share a similar water

affinity, it is cautiously recommended that the assumption regarding similarity between the environmental behaviour of TAME and MTBE be discarded, except for the water compartment. Furthermore, it is recommended that field studies be performed to further differentiate the behavioural tendencies of these two ether additives.

- It is recommended that modelling emphasis be placed on ethanol in the air compartment in light of its affinity for this medium. Furthermore, the extent of its co-solvency and degradation inhibiting effects on particular secondary solutes in gasoline blends should be investigated prior to the future adoption of this alcohol as a fuel oxygenate.

- The parameterisation of the EQC multimedia model to South African conditions has been used to evaluate the environmental fate of possible oxygenate additives pertaining to the petroleum industry. It is recommended that the ChemSA multimedia model be extended in a similarly fashion to the work performed by Mackay et al. (1991) in Canada, Devillers et al. (1995) in France, Berding et al. (2000) in Germany, and Kawamoto et al. (2001) in Japan. These multimedia models, based on the same formulation as the ChemSA model, have been used effectively in the national screening and environmental assessment of priority chemicals.

References

Abildskov, J., L. Constantinou, and R. Gani; Towards the Development of a Second-Order Approximation in Activity Coefficient Models based on Group Contributions, *Fluid Phase Equilibria*, 118, 1-12 (1996)

Abraham, M.H., J. Andonian-Haftvan, G.S. Whiting, A. Leo, and S. Taft; Hydrogen Bonding 34: The Factors that Influence the Solubility of Gases and Vapors in Water at 298 K, and a New Method for its Determination, *J. Chem. Soc. Perkin. Trans.*, 2, 1777-1791 (1994)

Abrams, D.S., and J.M. Prausnitz; Statistical Thermodynamics of Liquid Mixtures: A New Expression for the Excess Gibbs Energy of Partly or Completely Miscible Systems, *AIChE J.*, 21, 116-128 (1975)

Alessi, P., M. Fermeglia, and I. Kikic; Significance of Dilute Regions, *Fluid Phase Equilibria*, 70, 239-249 (1991)

Alexander, M.; Aging, Bioavailability, and Overestimation of Risk from Environmental Pollutants, *Environ. Sci. Technol.*, 34, 4259-4265 (2000)

Alkandary, J.A., A.S. Aljimaz, M.S. Fandary, and M.A. Fahim; Liquid-Liquid Equilibria of Water + MTBE + Reformate, *Fluid Phase Equilibria*, 187-188, 131-138 (2001)

Ames, T.T., and E.A. Grulke; Group Contribution Method for Predicting Equilibria of nonionic Organic Compounds between Soil Organic Matter and Water, *Environ. Sci. Technol.*, 29, 2273-2279 (1995)

Antosik, M., and S.I. Sandler; Vapor-Liquid Equilibria of Hydrocarbons and tert-Amyl Methyl Ether, *J. Chem. Eng. Data*, 39, 584-587 (1994)

Arce, A., M. Blanco, A. Soto, and I. Vidal; Extraction Equilibria of the Type 2: Ternary Liquid Mixture {x1 tert-butyl methyl ether + x2 water + (1-x1-x2) 1-octanol} at 298.15 K and 308.15 K, *J. Chem. Thermo.*, 28, 3-6 (1996)

ASTM (1987); *Standard test for determining a sorption constant (k_{oc}) for an organic chemical in soil and sediments*, ASTM, D 1195-87, American Society for Testing and Materials, Philadelphia, PA, pp731-737

ASTM (1987a); *Standard test method for 24-h batch-type measurement of containment sorption by soils and sediments*, ASTM, D 4646, American Society for Testing and Materials, Philadelphia, PA, pp120-123

Atkinson, R.; Kinetics and Mechanisms of the Gas-phase Reactions of the Hydroxyl Radical with Organic Compounds, *J. Phys. Chem. Ref. Data*, Monograph 1 (1989)

Atkinson, R.; Kinetics and Mechanisms of the Gas-phase Reactions of the NO_3 Radical with Organic Compounds, *J. Phys. Chem. Ref. Data*, 20, 459-507 (1991)

Atkinson, R.; Gas Phase Tropospheric Chemistry of Organic Compounds, in *Issues in Environmental Science and Technology*, Issue No. 4, R.E. Hester and R.M. Harrison, The Royal Society of Chemistry, Cambridge, UK (1995)

Atkinson, R.; Gas-phase Tropospheric Chemistry of Volatile Organic Compounds. 1. Alkanes and Alkenes, *J. Phys. Chem. Ref. Data*, 26, 215-290 (1997)

Atkinson, R.; Chapter 14: Atmospheric Oxidation, in *Handbook of Property Estimation Methods for Chemicals-Environmental and Health Sciences*, Boethling, R.S., and D. Mackay, CRC Press, Boca Raton, Florida, (2000)

Baker, J.R., J.R. Mihelcic, D.C. Luehrs, and J.P. Hickey; Evolution of Estimation Methods for Organic Carbon Normalized Sorption Coefficients, *Water Environ. Res.*, 69, 136-145 (1997)

Baker, J.R., J.R. Mihelcic, and E. Shea; Estimating K_{oc} for Persistent Organic Pollutants: Limitations of Correlation with K_{ow}, *Chemosphere*, 41, 813-817 (2000)

Banerjee, S., and P.H. Howard; Improved Estimation of Solubility and Partitioning through Correction of UNIFAC-Derived Activity Coefficients, *Environ. Sci. Technol.*, 22, 839-848 (1988)

Bastos, J.C., M.E. Soares, and A.G. Medina; Infinite Dilution activity Coefficients Predicted by UNIFAC Group Contribution, *Ind. Eng. Chem. Res.*, 27, 1269-1277 (1988)

Barton, A.F.M.; *Handbook of Solubility Parameters and Other Cohesion Parameters*, 2nd edition, CRC Press, Boston, 1991.

Baughman, G. and R. Lassiter; *Prediction of Environmental Pollutant Concentrations*, ASTM STP 657, Philadelphia, PA (1978)

Bennett, A., S. Lamm, H. Orbey, and S.I. Sandler, Vapor-Liquid Equilibria of Hydrocarbons and Fuel Oxygenates. 2., *J. Chem. Eng. Data*, 38, 263-269 (1993)

Bennett, D.H., T.E. McKone, M. Matthies, and W.E. Kastenberg; General Formulation of the Characteristic Travel Distance for Semivolatile Organic Chemicals in a Multimedia Environment, *Environ. Sci. Technol.*, 32, 4023-4030 (1998)

Bennett, D.H, W.E. Kastenberg, and T.E. McKone; General Formulation of Characteristic Time for Persistent Chemicals in a Multimedia Environment, *Environ. Sci. Technol.*, 33, 503-509 (1999)

Bennett, D.H., T.E. McKone, and W.E. Kastenberg; Evaluating Multimedia Chemical Persistence: Classification and Regression Tree Analysis, *Environ. Toxicol. Chem.*, 19, 810-819 (2000)

Berding, V., S. Schwartz, and M. Matthies; Scenario Analysis of a Level III Multimedia Model using Generic and Regional Data, *Environ. Sci. Pollut. Res.*, 7, 147-158 (2000)

Bergmann, D.L., and C.A. Eckert; Measurement of Limiting Activity Coefficients for Aqueous Systems by Differential Ebulliometry, *Fluid Phase Equilibria,* 63, 141 (1991)

Beyer, A., D. Mackay, M. Matthies, F. Wania, and E. Webster; Assessing Long-Range Transport Potential of Persistent Organic Pollutants, *Environ. Sci. Technol.*, 34, 699-703 (2000)

Bidleman, T.F.; Atmospheric Processes, *Environ. Sci. Technol.*, 22, 361-367 (1988)

Bidleman, T.F., and T. Harner; Chapter 10: Sorption to Aerosols, in *Handbook of Property Estimation Methods for Chemicals-Environmental and Health Sciences*, Boethling, R.S., and D. Mackay, CRC Press, Boca Raton, Florida, (2000)

Bintein, S., and J. Devillers; Evaluating the Environmental Fate of Lindane in France, *Chemosphere*, 32(12), 2427-2440 (1996)

Bintein, S., and J. Devillers; Evaluating the Environmental Fate of Atrazine in France, *Chemosphere*, 32(12), 2441-2456 (1996a)

Blue Ribbon Report; Achieving Clean Air and Clean Water: *The Report of the Blue Ribbon Panel on Oxygenates in Gasoline*, Various Authors, Available on-line at: http://www.epa.gov, Document No. B-0031 (1999)

Bodor, N., and M.-J. Huang; An Extended Version of a Novel Method for the Estimation of Partition Coefficients, *J. Pharm. Sci.*, 81, 272-281 (1992)

Boethling, R.S., and D. Mackay; *Handbook of Property Estimation Methods for Chemicals-Environmental and Health Sciences*, CRC Press, Boca Raton, Florida, (2000)

Booty, W.G., and I.W.S. Wong; Application of a Fugacity Model for Assessing Chemical in Ecodistricts of Southern Ontario, *Ecol. Modeling*, 84, 245-263 (1996)

Boublik, T., V. Fried, and E. Hala; *The Vapor Pressures of Pure Substances*, 2nd edition, Elsevier, Amsterdam (1984)

Brandani, S., V. Brandani, G. Del Re, and G. Di Giacomo; Activity Coefficients from a Virial Expansion about their Infinite Dilution Values, *Chem. Eng. J.*, 46, 35-42 (1991)

Brandes, L.J., H. den Hollander, and D. van de Meent; *SimpleBox 2.0: A Nested Multimedia Fate Model for Evaluating the Environmental Fate of Chemicals*, RIVM Report 719101029, Bilthoven, The Netherlands (1996)

Brennan, R.A., N. Nirmalakhandan, and R.E. Speece; Comparison of predictive methods for Henry's Law Constants of Organic Chemicals, *Water Res.*, 32, 1901-1911 (1997)

Bru, R., J.M. Carrasco, and L.C. Paraiba; Unsteady State fugacity Model by a Dynamic Control System, *Appl. Math. Modelling*, 22, 485-494 (1998)

Campfens, J., and D. Mackay; Fugacity-based Model of PCB Bioaccumulation in Complex Aquatic Food Webs, *Environ. Sci. Technol.*, 31, 577-583 (1997)

Carson, R.; *Silent Spring*, Houghton Mifflin, Boston, MA (1962)

Chamorro, C.R., J.J. Segovia, M.C. Martin, E.A. Montero, and M.A. Villamanan; Phase Equilibrium Properties of Binary and Ternary Systems containing tert-Amyl Methyl Ether (TAME) as Oxygenate Additive and Gasoline Substitution Hydrocarbons at 313.15 K, *Fluid Phase Equilibria*, 156, 73-87 (1999)

Chiou, C.T., D.E. Kile, T.I. Brinton, R.L. Malcolme, J.A. Leenheer, and P. MacCarthy; A Comparison of Water Solubility Enhancements of Organic Solutes by Aquatic Humic Materials and Commercial Humic Acids, *Environ. Sci. Technol.*, 21, 1231-1234 (1987)

Clark, T.P., R.J. Norstrom, G.A. Fox, and H.T. Won; Dynamics of Organochlorine Compounds in Herring Gulls (*Larus argentatus*): II. A Two Compartment Model and Data for Ten Compounds, *Environ. Toxicol. Chem.*, 6, 547-559 (1987)

Clark, K.E., F.A.P.C. Gobas, and D. Mackay; Model of Organic Chemical Uptake and Clearance by Fish from Food and Water, *Environ. Sci. Technol.*, 24, 1203-1213 (1990)

Cohen, Y.; *Intermedia Transport Modeling in Multimedia Systems of Pollutants in a Multimedia Environment*, Cohen, Y. (Editor), Plenum Press (1986)

Constantinou, L., S.E. Prickett, and M.L. Mavrovouniotis; Estimation of Thermodynamic and Physical Properties of Acyclic Hydrocarbons using the ABC Approach and Conjugation Operators. *Ind. Eng. Chem. Res.*, 32, 1734-1746 (1993)

Constantinou, L., S.E. Prickett, and M.L. Mavrovouniotis; Estimation of Properties of Acyclic Organic Compounds using Conjugation Operators, *Ind. Eng. Chem. Res.*, 33, 395-402 (1994)

Corn, M., T.L. Montgomery, and N.A. Esman; Suspended Particular Matter: Seasonal Variation in Specific Surface Areas and Densities, *Environ. Sci. Technol.*, 5, 155-158 (1971)

Corseuil, H., C. Hunt, R. Santos Ferreira, and P. Alvarez; The influence of Gasoline Oxygenate Ethanol on Aerobic and Anaerobic BTEX degradation, *Water Res.*, 32, 2065-2072 (1998)

Cotham, W.E., and T.F. Bidleman; Polycyclic Aromatic Hydrocarbons and Polychlorinated Biphenyls in Air at an Urban and Rural Site near Lake Michigan, *Environ. Sci. Technol.*, 29. 2782-2789 (1995)

Cousins, I.T., and D. Mackay; Strategies for including Vegetation Compartments in Multimedia Models, *Chemosphere*, 44, 643-654 (2001)

Danckwerts, P.V.; *Ind. Eng. Chem.*, 43, 1460-1467 (1951); Referenced in Seader and Henley (1998)

Danner, R.P, and M.A. Gess; A Data Base Standard for the Evaluation of Vapor-Liquid-Equilibrium Models, *Fluid Phase Equilibria*, 56, 285-301 (1990)

DDB Software, *Pure Component Properties*, Dos Version (1999)

DDB Software, *Vapour-Liquid Equilibrium Data*, Dos Version (1999a)

de Bruijn, J., F. Busser, W. Seinen, and J. Hermens; Determination of Octanol/Water Partition Coefficients for Hydrophobic Organic Chemicals with the "Slow-Stirring" Method, *Environ. Toxicol. Chem.*, 8, 499-512 (1989)

de Bruijn, J., and J. Hermens; Relation between Octanol/Water Partition Coefficients and Total Molecular Surface Area and Total Molecular Volume of Hydrophobic Organic Chemicals, *Quant. Struct.-Act. Relat.*, 9, 11-21 (1990)

Delcros, S., J.-P.E. Grolier, V. Dohnal, and D. Fenclova; Infinite-dilution Activity Coefficients by Comparative Ebulliometry: Measurements and Group Contribution Calculations for some binary mixtures Ether + n-Alkane and Ether + Alcohol, *Chem. Eng. Sci.*, 50(18), 2957-2962 (1995)

Devillers, J., S. Bintein, and W. Karcher; ChemFRANCE: A Regional Level III Fugacity Model applied to France, *Chemosphere*, 30, 457-476 (1995)

DeVito, S.C.; Chapter 11: Absorption through Cellular Membranes, in *Handbook of Property Estimation Methods for Chemicals-Environmental and Health Sciences*, Boethling, R.S., and D. Mackay, CRC Press, Boca Raton, Florida, (2000)

Diamond, M.L., D.A. Priemer, and N.L. Law; Developing a Multimedia Model of Chemical Dynamics in an Urban Area, *Chemosphere*, 44, 1655-1667 (2001)

Dickhut, R.M., and K.E. Gustafson; Atmospheric Washout of Polycyclic Aromatic Hydrocarbons in the Southern Chesapeake Bay Region, *Environ. Sci. Technol.*, 29, 1518-1525 (1995)

DTSC (1992); *Guidance for Site Characterization and Multimedia Risk Assessment for Hazardous Substances Release Sites*, UCRL-CR-103462, Department of Toxic Substances Control, State of California and Lawrence Livermore National Laboratory, Livermore, CA

Domańska, U., J. Łachwa, P. Morawski, and S.K. Malanowski; Phase Equilibria and Volumetric Properties in Binary Mixtures containing Branched Chain Ethers (Methyl 1,1-Dimethylethyl Ether or Ethyl 1,1-Dimethylethyl Ether or Methyl 1,1-Dimethylpropyl Ether or Ethyl 1,1-Dimethylpropyl Ether), *J. Chem. Eng. Data*, 44, 974-984 (1999)

Domańska, U., and J. Łachwa; Excess Molar Volumes of (Hydrocarbon + Ethyl 1,1-dimethylpropyl ether) at T = (298.15 and 308.15) K, *J. Chem. Thermo.*, 32, 857-875 (2000)

Doucette, W.J.; Chapter 8: Soil and Sediment Sorption Coefficients, in *Handbook of Property Estimation Methods for Chemicals-Environmental and Health Sciences*, Boethling, R.S., and D. Mackay, CRC Press, Boca Raton, Florida, (2000)

Eckert, C.A., and S.R. Sherman; Measurement and Prediction of Limiting Activity Coefficients, *Fluid Phase Equilibria*, 116, 333-342 (1996)

Edwards, F.G., E. Egemen, R. Brennan, and N. Nirmalakhandan; Ranking of Toxics Release Inventory Chemicals using a Level III Fugacity Model and Toxicity, *Water Sci. Tech.*, 39, 83-90 (1999)

Eisenberg, J.S., D. Bennett, and T.E. McKone; Chemical Dynamics of Persistent Organic Pollutants: A Sensitivity Analysis Relating Soil Concentration Levels to Atmospheric Emissions, *Environ. Sci. Technol.*, 32, 115-123 (1998)

Eisenreich, S.J., B.B. Looney, and J.D. Thornton; Airborne Organic Contaminants in the Great Lakes Ecosystem, *Environ. Sci. Technol.*, 15, 30-38 (1981)

Ellis, S.R.M., and D.A. Jonah; Prediction of Activity Coefficients at Infinite Dilution, *Chem. Eng. Sci.*, 17, 971-976 (1962)

El Tayar, N., R.-S. Tsai, P. Vallat, C. Altomare, and B. Testa; Measurement of Partition Coefficients by various Centrifuge Partition Chromatographic Techniques: A Comparative Evaluation, *J. Chromatog.*, 556, 181-194 (1991)

EU (1996); Technical Guidance Documents in Support of The Commission Directive 93/67/EEC on Risk Assessment For New Notified Substances and the Commission Regulation (EC) 1488/94 on Risk Assessment for Existing Substances, ECB, Ispra, Italia, advanced pre-print version

Fendinger, N.J., and D.E. Glotfelty; A Laboratory Method for the Experimental Determination of Air-Water Henry's Law Constants for Several Pesticides, *Environ. Sci. Technol.*, 22, 1289-1293 (1988)

Fenner, K., M. Scheringer, and K. Hungerbuhler; Persistence of Parent Compounds and Transformation Products in a Level IV Multimedia Model, *Environ. Sci. Technol.*, 34, 3809-3817 (2000)

Finizio, A., D. Mackay, T.F. Bidleman, and T. Harner; Octanol-Air Partition Coefficient as a Predictor of Trace Organic Pollutants, *Environ. Sci. Technol.*, 31, 2289-2296 (1997)

Foisy, M., D. Takamoto, M.L. Mavrovouniotis; A Conjugation-Based Version of the UNIFAC Method, *Fluid Phase Equilibria*, 137, 111-119 (1997)

Fredenslund, A., R.L. Jones, and J.M. Prausnitz; Group-Contribution Estimation of Activity Coefficients in Nonideal Liquid Mixtures, *AIChE J.*, 21, 1086-1099 (1975)

Fujiwara, Y., T. Kinoshita, H. Sato, and I. Kojima, Biodegradation and Bioconcentration of Alkyl Ethers, *Yukagaku.*, 33, 111-114 (1984)

Gautreaux, M.F., and J. Coates; Activity Coefficients at Infinite Dilution, *AIChE J.*, 1, 496-500 (1955)

Gawlik, B.M., N. Sotiriou, E.A. Feicht, S. Schulte-Hostede, and A. Kettrup; Alternatives for the Determination of the soil Adsorption Coefficient, K_{oc}, of non-ionic organic compounds – A Review, *Chemosphere*, 34, 2525-2551 (1997)

Gawlik, B.M., A. Kettrup, and H. Muntau; Estimation of soil Adsorption Coefficients of Organic Compounds by HPLC screening using the Second Generation of European Reference Soil Set, *Chemosphere*, 41, 1337-1347 (2000)

Gmehling, J., J. Li, and M. Schiller; A Modified UNIFAC: 2. Present Parameter Matrix and Results for Different Thermodynamic Properties, *Ind. Eng. Chem. Res.*, 32, 178-193 (1993)

Gobas, F.A.P.C.; A Model for Predicting the Bioaccumulation of Hydrophobic Organic Chemicals in Aquatic Food-Webs: Application to Lake Ontario, *Ecol. Modelling*, 69, 1-17 (1993)

Gobas, F.A.P.C., and H.A. Morrison; Chapter 9: Bioconcentration and Biomagnification in the Aquatic Environment, in *Handbook of Property Estimation Methods for Chemicals-Environmental and Health Sciences*, Boethling, R.S., and D. Mackay, CRC Press, Boca Raton, Florida, (2000)

González, J.A., F.J. Carmona, N. Riesco, I.G. de la Fuente, and J.C. Cobos; Part I. DISQUAC Characterization of Systems of MTBE, TAME or ETBE with n-Alkanes, Cyclohexane, Benzene, Alkan-1-ols, or Alkan-2-ols. Comparison with Dortmund UNIFAC Results, *Phys. Chem. Chem. Phys.*, 2, 2587-2596 (2000)

Gosset, R.; Measurement of Henry's Law Constants for C_1 and C_2 Chlorinated Hydrocarbons, *Environ. Sci. Technol.*, 21, 202-208 (1987)

Gouin, T., D. Mackay, E. Webster, F. Wania; Screening Chemicals for Persistence in the Environment, *Environ. Sci. Technol.*, 34, 881-884 (2000)

Gouin, T.; Long-range Transport of Organic Contaminants: The Role of Air-Surface Exchange, MSc Thesis, Trent University, Canada (2002)

Guinée, B.J., R. Heijungs, L.F.C.M. van Oers, A. Sleeswijk, D. van de Meent, T. Vermeire, and M. Rikken; Inclusion of Fate in LCA Characterization of Toxic Releases Applying USES 1.0., *Int. J. LCA*, 1, 118-133 (1996)

Hansch, C., and A.J. Leo; *MEDCHEM Project*, Pomona College, Claremont, CA, Issue No. 26 (1985)

Hansch, C., and A.J. Leo; Exploring *QSAR: Fundamentals and Applications in Chemistry and Biology*, American Chemical Society, Washington, DC (1995)

Hansch, C., D. Hoekman, and H., Gao; Comparative QSAR: Toward a Deeper Understanding of Chemicobiological Interactions, *Chem. Rev.*, 96, 1045-1075 (1996)

Hansen, H.K., P. Rasmussen, A. Fredenslund, M. Schiller, and J. Gmehling; Vapor-Liquid Equilibria by UNIFAC Group Contribution. 5. Revision and Extension, *Ind. Eng. Chem. Res.*, 30, 2352-2358 (1991)

Hansen, H.K., B. Coto, and B. Kuhlmann; *UNIFAC with Linearly Temperature-dependent Group-interaction Parameters*, SEP 9212, Institute for Kemiteknik, DTH, Lyngby (1992)

Harner, T., and D. Mackay; Measurement of Octanol-Air Partition Coefficients for Chlorobenzenes, PCBs, and DDT, *Environ. Sci. Technol.*, 29, 1599-1606 (1995)

Harner,T., and T.F. Bidleman; Measurement of Octanol-Air Partition Coefficients for Polychlorinated Biphenyls, *J. Chem. Eng. Data*, 41, 895-899 (1996)

Harner, T., and T.F. Bidleman; Measurement of Octanol-Air Partition Coefficients for Polycyclic Aromatic Hydrocarbons (PAHs) and Polychlorinated Naphthalenes (PCNs), *J. Chem. Eng. Data*, 43, 40-46 (1998)

Harner, T., N.J.L. Green, and K.C. Jones; Measurements of Octanol-Air Partition Coefficients for PCDD/Fs: A Tool in Assessing Air-Soil Equilibrium Status, *Environ. Sci. Technol.*, 29, 1200-1209 (2000)

Heijungs, R.; Harmonization of Methods for Impact Assessment, *Environ. Sci. Pollut. Res.*, 2, 217-224 (1995)

Held, H.; Spherical Spatial Ranges of Non-polar Chemicals for Reaction-Diffusion Type Dynamics, *Appl. Math. Comp.*, 124, 29-43 (2001)

Hertwich, E.G.; Fugacity Superposition: A New Approach to Dynamic Multimedia Fate Modeling, *Chemosphere*, 44, 843-853 (2001)

Hertwich, E.G., and T.E. McKone; Pollutant-Specific Scale of Multimedia Models and its Implications for the Potential Dose, *Environ. Sci. Technol.*, 35, 142-148 (2001)

Hiaki, T., K. Tatsuhana, T. Tsuji, and M. Hongo; Isobaric Vapor-Liquid Equilibria for 2-Methoxy-2-methylpropane + Ethanol + Octane and Constituent Binary Systems at 101.3 kPa, *J. Chem. Eng. Data*, 44, 323-327 (1999)

Higbie, R.; *Trans. AIChE*, 31, 365-389 (1935); Referenced in Seader and Henley (1998)

Hine, J., and P.K. Mookerjee; The Intrinsic Hydrophilic Character of Organic Compounds. Correlations in terms of Structural Contributions, *J. Org. Chem.*, 40, 292-298 (1975)

Hoff, J.T., W.M.J. Strachan, C.W. Sweet, C.H. Chan, M. Shackleton, T.F. Bidleman, K.A. Brice, D.A. Burniston, S. Cussion, D.F. Gatz, K. Harlin, and W.H. Schroeder; Atmospheric Deposition of Toxic Chemicals to the Great Lakes: A Review of Data Through 1994, *Atmos. Environ.*, 30, 3505-3527 (1996)

Holsen, T.M., K.E. Noll, S.P. Liu, and W.J. Lee; Dry Deposition of Polychlorinated Biphenyls in Urban Areas, *Environ. Sci. Technol.*, 25, 1075-1081 (1991)

Holsen, T.M., K.E. Noll, G.-C. Fang, W.J. Lee, and J.-M. Lin; Dry Deposition and Particle Size Distributions Measured during the Lake Michigan Urban Air Toxics Study, *Environ. Sci. Technol.*, 27, 1327-1333 (1993)

Hooper, H.H., S. Michel, and J.M. Prausnitz; Correlation of Liquid-Liquid Equilibria for some Water-Organic Liquid Systems in the region 20-250°C, *Ind. Eng. Chem. Res.*, 27, 2182-2187 (1988)

Hovorka, Š., and V. Dohnal; Determination of Air-Water Partitioning of Volatile Halogenated Hydrocarbons by the Inert Gas Stripping Method, *J. Chem. Eng. Data*, 42, 624-933 (1997)

Howard, P.H., R.S. Boethling, W.F. Jarvis, W.M. Meylan, and E.M. Michalenko; *Handbook of Environmental Degradation Rates*, Lewis Publishers, Chelsea, Michigan (1991)

Howard, P.H.; Chapter 12: Biodegradation, in *Handbook of Property Estimation Methods for Chemicals-Environmental and Health Sciences*, Boethling, R.S., and D. Mackay, CRC Press, Boca Raton, Florida, (2000)

Hung, H., and D. Mackay; A Novel and Simple Model of the Uptake of Organic Chemicals by Vegetation from Air and Soil, *Chemosphere*, 35, 959-977 (1997)

Huey, S.W., K.A. Pividal, and S.I. Sandler; Vapour-Liquid Equilibria of hydrocarbons and fuel oxygenates, *J. Chem. Eng. Data*, 36, 418-421 (1991)

Hussam, A., and P.W. Carr; Rapid and Precise Method for the Measurement of Vapor/Liquid Equilibria by Headspace Gas Chromatography, *Anal. Chem.*, 57, 793-801 (1985)

Huttunen, H., L.E. Wyness, and P. Kalliokoski; Identification of Environmental Hazards of Gasoline Oxygenate Tert-Amyl Methyl Ether (TAME), *Chemosphere*, 35, 1199-1214 (1997)

Ishihama, Y. Y. Oda, K. Uchikawa, and N. Asakawa; Correlation of Octanol/Water Partition Coefficients with Capacity Factors by Micellar Electrokinetic Chromatography, *Chem. Pharm. Bull.*, 42, 1525-1527 (1994)

Jacobs, J., J. Guertin, and C. Heron; *MTBE: Effects on Soil and Groundwater Resources*, CRC Press, Boca Raton, Florida, (2001)

Jang., M., R.M. Kamens, K.B. Leach, and M.R. Strommen; A Thermodynamic Approach Using Group Contribution Methods to Model the Partitioning of Semivolatile Organic Compounds on Atmospheric Particulate Matter, *Environ. Sci. Technol.*, 31, 2805-2811 (1997)

Jangkamolkulchal, A., G.C. Alfred, and W.E. Parrish, Densities and Excess Molar Volumes of Methyl tert-Butyl Ether and Ethyl tert-Butyl Ether with Hydrocarbons from 255.4 to 333.2 K, *J. Chem. Eng. Data.*, 36, 481-484 (1991)

Joseph, M.A., J.D. Raal, and D. Ramjugernath; Phase Equilibrium Properties of Binary Systems with Diacetyl from a Computer Controlled Vapour-Liquid Equilibrium Still, *Fluid Phase Equilibria*, 182, 157-176 (2001)

Juan, C.-Y., M. Green, and G.O. Thomas; The Statistical Merits of Various Methods of Calculating Transfer Coefficients between Environmental Media- Development of the Ideal Formula for Data-sets with a Log-normal Distribution, *Chemosphere*, 46, 1091-1097 (2002)

Junge, C.E.; Basic Considerations about Trace Constituents in the Atmosphere as related to the Fate of Global Pollutants, in Fate of Pollutants in the Air and Water Environments, in *Adv. in Environ. Sci. Technol. Ser.*, Volume 8, Part I, Wiley-Interscience, NY (1977)

Jury, W.A., W.F. Spencer, and W.J. Farmer; Behavior Assessment Model for Trace Organics in Soil I. Model Description, *J. Environ. Qual.*, 12, 558-564 (1983)

Kamlet, M.J., J.-L.M. Abboud, M.H. Abraham, and R.W. Taft; Linear Solvation Energy Relationships. 23. A Comprehensive Collection of the Solvatochromic Parameters, π^*, α, β, and Some Methods for simplifying the Generalized Solvatochromic Equation, *J. Org. Chem.*, 48, 2877 (1983)

Kamlet, M.J., R.M. Doherty, M.H. Abraham, and R.W. Taft; Linear Solvation Energy Relationships. 46. An Improved Equation for Correlation and Prediction of Octanol/Water Partition Coefficients of Organic Non-electrolytes. (Including Strong Hydrogen Bond Donor Solutes), *J. Phys. Chem.*, 92, 5244-5255 (1988)

Karickhoff, S.W.; Semi-empirical Estimation of Sorption of Hydrophobic Pollutants on Natural Sediments and Soils, Chemosphere, 10, 833-849 (1981)

Kawamoto, K., M. MacLeod, and D. Mackay; Evaluation and Comparison of Multimedia Mass Balance Models of Chemical Fate: Application of EUSES and ChemCAN to 68 Chemicals in Japan, *Chemosphere*, 44, 599-612 (2001)

Kharoune, M., A. Pauss, and J.M. Lebeault; Aerobic Biodegradation of an Oxygenates Mixture: ETBE, MTBE and TAME in an Upflow Fixed-bed Reactor, *Water Res.*, 35, 1665-1674 (2001)

Kojima, K., S. Zhang, and T. Hiaki; Measuring Methods of Infinite Dilution Activity Coefficients and a Database of Systems including Water, *Fluid Phase Equilibria*, 131, 145-179 (1997)

Konemann, H.; Quantitative Structure-Activity Relationship in Fish Toxicity Studies. Part I. Relationship for 50 Industrial Pollutants, *Toxicology*, 11, 495-496 (1981)

Korte, F.; *Lehrbruch der ökologischen Chemie: Grundlagen und Konzepte für die ökologische Beurteilung von Chemikalien*, 3rd edition, Thieme, Stuttgart, Germany (1992)

Kuramochi, H., H. Noritomi, D. Hoshino, S. Kato, and K. Nagahama; Application of UNIFAC Models to Partition Coefficients of Biochemicals between Water and n-Octanol or n-Butanol, *Fluid Phase Equilibria*, 144, 87-95 (1998)

Larsen, B.L., P. Rasmussen, and A. Fredenslund; A Modified UNIFAC Group Contribution Model for the Prediction of Phase Equilibria and Heats of Mixing, *Ind. Eng. Chem. Res.*, 26, 2274-2286 (1987)

Larson, R.J., and C.E. Cowan, Quantitative Application of Biodegradation Data to Environmental Risk and Exposure Assessments, *Environ. Toxicol. Chem.*, 14, 1433-1442 (1995)

Leahy, D., J.J. Morris, and P.J. Taylor; Model Solvent Systems for QSAR. Part 3. An LSER Analysis of the "Critical Quartet": New Light on Hydrogen Bond Strength and Directionality, *J. Chem. Soc. Perkin Trans.*, 2, 705-731 (1992)

Lei, Y.D., F. Wania, W.Y. Shiu, and D.G.B. Boocock; HPLC-Based Method for Estimating the Temperature Dependence of n-Octanol-Water Partition Coefficients, *J. Chem. Eng. Data*, 45, 738-742 (2000)

Leighton, D.T., and J.M. Calo; Distribution Coefficients of Chlorinated Hydrocarbons in Dilute Air-Water Systems for Groundwater Contamination Applications, *J. Chem. Eng. Data*, 26, 381-385 (1981)

Leo, A.J., C. Hansch, and D. Elkins; Partition Coefficients and their Uses, *Chem. Rev.*, 71, 525-616 (1971)

Leo, A.J., P.Y.C. Jow, C. Silipo, and C. Hansch; Calculation of hydrophobic constant (Log P) from * and f constants, *J. Med. Chem.*, 18, 865-868 (1975)

Leo, A.J.; Calculating log P_{oct} from Structures, *Chem. Rev.*, 93, 1281-1306 (1993)

Leo, A.J.; Chapter 5: Octanol/Water Partition Coefficients, in *Handbook of Property Estimation Methods for Chemicals-Environmental and Health Sciences*, Boethling, R.S., and D. Mackay, CRC Press, Boca Raton, Florida, (2000)

Lewis, G.N.; The Law of Physico-chemical Change, *Proc. Am. Acad. Sci.*, 34, 49 (1901), As referenced in Bru et al. (1998)

Li, A., S. Pinsuwan, and S.H. Yalkowsky; Estimation of Solubility of Organic Compounds in 1-Octanol, *Ind. Eng. Chem. Res.*, 34, 915-920 (1995)

Lin, S.-T., and S.I. Sandler; Prediction of Octanol-Water Partition Coefficients Using a Group Contribution Solvation Model, *Ind. Eng. Chem. Res.*, 38, 4081-4091 (1999)

Lin, S.-T., and S.I. Sandler; Multipole Corrections to Account for Structure and Proximity Effects in Group Contribution Methods: Octanol-Water Partition Coefficients, *J. Phys. Chem. A*, 104, 7099-7105 (2000)

Lincoln, K.J.; *The Secret History of Lead: Special Report*, The Nation March, 11-45 (2000)

Lyman, W.J., W.F. Reehl, and D.H. Rosenblatt; *Handbook of Chemical Property Estimation Methods*, McGraw-Hill, New York, NY (1982)

Maaßen, S., H. Knapp, and W. Arlt; Determination and Correlation of Henry's Law Coefficients, Activity Coefficients and Distribution Coefficients for Environmental Use, *Fluid Phase Equilibria*, 116, 354-360 (1996)

MacLeod M., and D. Mackay; An Assessment of the Environmental Fate and Exposure of Benzene and the Chlorobenzenes in Canada, *Chemosphere*, 38, 1777-1796 (1999)

MacLeod, M., D. Woodfine, D. Mackay, T.E. McKone, D. Bennett, and R. Maddalena; BETR North America: A Regionally Segmented Multimedia Contaminant Fate Model for North America, *Environ. Sci. Pollut. Res.*, 8, 156-163 (2001)

MacLeod, M.; *Contamination Fate Models to Support the Sustainable Use of Chemicals in North America*, PhD Thesis, Trent University, Canada (2002)

Mackay, D.; Finding Fugacity Feasible, *Environ. Sci. Technol.*, 13, 1218-1223 (1979)

Mackay, D., W.Y. Shiu, and R.P. Sutherland; Determination of Air-Water Henry's Law Constants for Hydrophobic Pollutants, *Environ. Sci. Technol.*, 13, 333-337 (1979)

Mackay, D., and S. Paterson; Calculating Fugacity, *Environ. Sci. Technol.*, 15, 1006-1014 (1981)

Mackay, D.; Correlation of Bioconcentration Factors, *Environ. Sci. Technol.*, 16, 274-278 (1982)

Mackay, D., and S. Paterson; Fugacity Revisited, *Environ. Sci. Technol.*, 16, 654-660 (1982)

Mackay, D., and A.T.K. Yuen; Mass Transfer Coefficient Correlations for Volatilization of Organic Solutes from Water, *Environ. Sci. Technol.*, 17, 211-216 (1983)

Mackay, D., S. Paterson, B. Cheung, and W. Nealy; Evaluation of the Environmental Behavior of Chemicals with a Level III Fugacity Model, *Chemosphere*, 14, 335-375 (1985)

Mackay, D., S. Paterson, and W.H. Shroeder; Model Describing the Rates of Transfer Processes of Organic Chemicals between Atmosphere and Water, *Environ. Sci. Technol.*, 20, 810-816 (1986)

Mackay, D.; *Multimedia Environmental Models*, Lewis Pub Inc, Chelsea, MI, (1991)

Mackay, D., and S. Paterson; Evaluating the Multimedia Fate of Organic Chemicals: A Level III Fugacity Model, *Environ. Sci. Technol.*, 25, 427-436 (1991)

Mackay, D., S. Paterson, and D.D. Tam; *Assessment of Chemical Fate in Canada: Continued Development of a Fugacity Model*, Health Canada, Bureau of Chemical Hazards, Ottawa, ON, Canada (1991)

Mackay, D., S. Paterson, and W.Y. Shiu; Generic Models for Evaluating the Regional Fate of Chemicals, *Chemosphere*, 24, 695-717 (1992)

Mackay, D., W.Y. Shiu, and K.C. Ma; *Illustrated Handbook of Physical-Chemical Properties and Environmental Fate for Organic Chemicals. Vol. III Volatile Organic Chemicals*, Lewis Publishers, CRC Press, Boca Raton, Florida (1993)

Mackay, D., A. Di Guardo, S. Paterson, G. Kicsi, and C.E. Cowan; Assessing the Fate of New and Existing Chemicals: A Five-stage Process, *Environ. Toxicol. Chem.*, 15, 1618-1626 (1996)

Mackay, D., A. Di Guardo, S. Paterson, and C.E. Cowan; Evaluating the Environmental Fate of a Variety of Types of Chemicals using the EQC Model, *Environ. Toxicol. Chem.*, 15, 1627-1637 (1996a)

Mackay, D., A. Di Guardo, S. Paterson, G. Kicsi, C.E. Cowan and D.M. Kane; Assessment of chemical Fate in the Environment using Evaluative, Regional and Local-scale Models: Illustrative Application to Chlorobenzene and Linear Alkylbenzene Sulfonate, *Environ. Toxicol. Chem.*, 15, 1638-1648 (1996b)

Mackay, D., and A. Fraser; Bioaccumulation of Persistent Organic Chemicals: Mechanisms and Models, *Environ. Pollut.*, 110, 375-391 (2000)

Mackay, D., W.Y. Shiu, and K.C. Ma; Chapter 4: Henry's Law Constant, in *Handbook of Property Estimation Methods for Chemicals-Environmental and Health Sciences*, Boethling, R.S., and D. Mackay, CRC Press, Boca Raton, Florida, (2000)

Mackay, D., W.-Y. Shiu, and K.-C. Ma; *Physical-Chemical Properties and Environmental Fate Handbook*, Chapman & Hall/CRCnetBASE, Boca Raton, Florida (2000a)

Mackay, D.; *Multimedia Environmental Models: The Fugacity Approach*, 2nd edition, CRC Press, Boca Raton, Florida, (2001)

Maddalena, R.L., T.E. McKone, D.W. Layton, and D.P.H. Hsieh; Comparison of Multi-Media Transport and Transformation Models: Regional Fugacity Model vs. CalTox, *Chemosphere*, 30, 869-889 (1995)

Maher, P.J., and B.D. Smith, Infinite Dilution Activity Coefficient Values from Total Pressure Vapor-Liquid Equilibrium Data. Effect of Equation of State Used, *Ind. Eng. Chem. Fundam.*, 18, 354-357 (1979)

Magnussen, T., P. Rasmussen, A. Fredenslund; UNIFAC Parameter Table for Prediction of Liquid-Liquid Equilibria, *Ind. Eng. Chem. Process Des. Dev.*, 20, 331-339 (1981)

Manahan, S. E.; *Environmental Chemistry*, 4th edition, Chapter 1, 10 and 11, CRC Press, Boca Raton, Florida, (1990)

Manahan, S. E.; *Environmental Chemistry*, 7th edition, Chapters 9, 10, 12, 15 and 16, CRC Press, Boca Raton, Florida, (2000)

Marquadt, D.W.; An Algorithm for Least-squares Estimation of Non-linear Parameters, *J. Soc. Indus. App, Math.*, 11, 431-441 (1963)

Marsh, K.N., P. Niamskul, J. Gmehling, and R. Bölts; Review of Thermophysical Property Measurements on Mixtures containing MTBE, TAME, and Other Ethers with Non-polar Solvents, *Fluid Phase Equilibria*, 156, 207-227 (1999)

Mavrovouniotis, M.L.; Estimation of Properties from Conjugate Forms of Molecular Structures: The ABC Approach, *Ind. Eng. Chem. Res.*, 29, 1943-1953 (1990)

McMahon, T.A., and P.J. Denison; Empirical Atmospheric Deposition Parameters-A Survey, *Atmos. Environ.*, 13, 571-585 (1979)

McKone, T.E.; *CalTOX: A Multimedia Total Exposure Model for Hazardous-Waste Sites*, UCRL-CR-111456PtI-IV, Lawrence Livermore National Laboratory, Livermore, CA; Available on http://www.cwo.com/herd1/caltox.htm (1993)

McLachlan, M.S, and M. Horstmann; Forests as Filters of Airborne Organic Pollutants: A Model, *Environ. Sci. Technol.*, 32, 413-420 (1998)

McLachlan, M.S; Chapter 6: Vegetation/Air Partition Coefficient, in *Handbook of Property Estimation Methods for Chemicals-Environmental and Health Sciences*, Boethling, R.S., and D. Mackay, CRC Press, Boca Raton, Florida, (2000)

McVeety, B.D., and R.A. Hites; Atmospheric Deposition of Polycyclic Aromatic Hydrocarbons to Water Surfaces: A Mass Balance Approach, *Atmos. Environ.*, 22, 511-536 (1988)

Meylan, W.M., and P.H. Howard; Bond contribution Method for Estimating Henry's Law Constants, *Environ. Toxicol. Chem.*, 10, 1283-1293 (1991)

Meylan, W.M., and P.H. Howard; Atom/Fragment Group Contribution method for Estimating Octanol-Water Partition Coefficients, *J. Pharm. Sci.*, 84, 83-92 (1995)

Meylan, W.M.; *EPIWIN version 3.04*, Syracuse Research Corporation, Computer program (1999)

Meylan, W.M., P.H. Howard, R.S. Boethling, D. Aronson, H. Printup, and S. Gouchie; Improved Method for Estimating Bioconcentration/Bioaccumulation Factor from Octanol/Water Partition Coefficient, *Environ. Toxicol. Chem.*, 18, 664-672 (1999)

Midgley, D.C., W.V. Pitman, and B.J. Middleton, *Surface Water Resources of South Africa (1990)*, Vol. 1 to 6, 1st edition, Water Res. Commission Report, No. 298/21/94 (1994)

Mitchel, B.E., and P.C. Jurs; Prediction of Infinite Dilution Activity Coefficients of Organic Compounds in Aqueous Solution from Molecular Structure, *J. Chem. Inf. Comput. Sci.*, 38, 200-209 (1998)

Moessner, F., B. Coto, C. Pando, J.A.R. Renuncio; *Ber. Bunsen-Ges. Phys. Chem.*, 101, 1146 (1997); Referenced in DDB (1999a)

Mormile, M.R., S. Liu, and J.M. Suflita, Anaerobic Biodegradation of Gasoline Oxygenates: Extrapolation of Information to Multiple Sites and Redox Conditions, *Environ. Sci. Technol.*, 28, 1727-1732 (1994)

Morrison, H.A., F.A.P.C. Gobas, R. Lazar, and G.D. Haffner; Development and Verification of a Bioaccumulation Model for Organic Contaminants in Benthic Invertebrates, *Environ. Sci. Technol.*, 30, 3377-3384 (1996)

Müller-Herold, U.; A Simple General Limiting Law for Overall Decay of Organic Compounds with Global Pollution Potential, *Environ. Sci. Technol.*, 30, 586-591 (1996)

Müller-Herold, U., D. Caderas, and P. Funck; Validity of Global Lifetime Estimates by a Simple General Limiting Law for the Decay of Organic Compounds with Long-range Pollution Potential, *Environ. Sci. Technol.*, 31, 3511-3515 (1997)

Nadim, F., P. Zack, G.E. Hoag, and S. Liu; Unites States Experience with Gasoline Additives, *Energy Policy*, 29, 1-5 (2001)

Neely, B.W., D.R. Branson, and G.E. Blau; Partition Coefficients to Measure Bioconcentration Potential of Organic Chemicals in Fish, *Environ. Sci. Technol.*, 8, 1113-1115 (1974)

Nernst, W.; *Phys. Chem.*, 47, 52 (1904); Referenced in Seader and Henley (1998)

Nicholson, K.W.; The Dry Deposition of Small Particles: A Review of Experimental Measurements, *Environ. Atmos.*, 22, 2653-2666 (1988)

Nirmalakhandan, N.N., and R.E. Speece; QSAR Model for Predicting Henry's Law Constant, *Environ. Sci. Technol.*, 22, 1349-1357 (1988)

Nirmalakhandan, N.N., R.A. Brennan and R.E. Speece; Predicting Henry's Law Constant and the Effect of Temperature on Henry's Law Constant, *Water Res.*, 31, 1471-1481 (1997)

Nirmalakhandan, N.N.; *Modeling Tools for Environmental Engineers and Scientists*, Chapter 1, CRC Press, Boca Raton, Florida, (2001)

NRDC (1999); *Hearing on Oxygenated Fuels before The Health and Environmental Subcommittee US House of Representatives*, May, Testimony of J. Hathaway and D. Hawkins on behalf of the Natural Resources Defense Council, available on www.epa/gov/otaq/consumer/fuel/oxypanel

Nys, G., and R. Rekker; Concept of Hydrophobic Fragment Constant (f-value) II, *Eur. J. Med. Chem.*, 9, 361-375 (1974)

OECD (1981); *Guideline for Testing of Chemicals*, Guideline for Testing of Chemicals, 107, 1-9, adapted 12 May 1981

Olson, S.S.; *International Environmental Standards Handbook,* Chapter 5, Lewis Pub Inc, Chelsea, MI, (1999)

Orbey, H., and S. I. Sandler; Relative Measurement of Activity Coefficients at Infinite Dilution by Gas Chromatography, *Ind. Eng. Chem. Res.*, 30, 2006-2011 (1991)

Oreskes, N., K. Shrader-Frechette and K. Belitz; Verification, Validation, and Confirmation of Numerical Models in the Earth Sciences, *Science*, 263, 641-646 (1994)

Pankow, J.F.; Review and Comparative Analysis of the Theories on Partitioning between the Gas and Aerosol Particulate Phases in the Atmosphere, *Atmos. Environ.*, 21, 2275-2283 (1987)

Pankow, J.F., An Absorption Model of Gas-Particle Partitioning in the Atmosphere, *Atmos. Environ.*, 28, 185-188 (1994)

Pankow, J.F., An Absorption Model of Gas-Aerosol Partitioning involved in the Formation of Secondary Organic Aerosol, *Atmos. Environ.*, 28, 189-193 (1994a)

Pankow, J.F., R.E. Rathburn, and J.S. Zogorski, Calculated Volatilization Rates of Fuel Oxygenate Compounds and other Gasoline-Related Compounds from Rivers and Streams, *Chemosphere*, 33, 921-937 (1996)

Pankow, J.F., N.R. Thomson, R.L. Johnson, A.L. Baehr, and J.S. Zogorski; The Urban Atmosphere as a Non-point Source for the Transport of MTBE and other Volatile Organic Compounds (VOCs) to Shallow Groundwater, *Environ. Sci. Technol.*, 31, 2821-2828 (1997)

Paraiba, L.C., J.M. Carrasco, and R. Bru; Level IV Fugacity Model by a Continuous Time Control System, *Chemosphere*, 38, 1763-1775 (1999)

Patty, F.A.; *Industrial Hygiene and Toxicology*, Vol. 2, Interscience Publishers (1967)

Peng, C., K.C. Lewis, and F.P. Stein; Water Solubilities in Blends of Gasoline and Oxygenates, *Fluid Phase Equilibria*, 116, 437-444 (1996)

Pennington, D.W., and M. Ralston; *Multimedia Persistence and the EPA's Waste Minimization Prioritizing Tool (WMPT)*, SETAC News, 19, 20 (1999)

Pennington, D.W.; An Evaluation of Chemical Persistence Screening Approaches, *Chemosphere*, 44, 1589-1601 (2001)

Pennington, D.W.; Relationship of Approaches and a Tiered Methodology for Screening Chemicals in the Context of Long-range Transport, *Chemosphere*, 44, 1617-1631 (2001a)

Peschke, N., and S.I. Sandler; Liquid-Liquid Equilibria of Fuel Oxygenate + Water + Hydrocarbon Mixtures. 1., *J. Chem. Eng. Data*, 40, 315-320 (1995)

Pierotti, G.J., C.H. Deal, and E.L. Derr; Activity Coefficients and Molecular Structure, *Ind. Eng. Chem.*, 51, 95-102 (1959)

Piketh, S.J., R.J. Swap, C.A. Anderson, M.T. Freiman, M. Zunckel, and G. Held; The Ben Macdhui High Altitude Trace Gas and Aerosol Transport Experiment, *South African. J. Sci*, 95, January (1999)

Pirrone, N., G.J. Keeler, and T.M. Holsen; Dry Deposition of Semivolatile Organic Compounds to Lake Michigan, *Environ. Sci. Technol.*, 29, 2123-2132 (1995)

Pividal, K.A., A. Birtigh, and S.I. Sandler; Infinite Dilution Activity Coefficients for Oxygenate Systems Determined Using a Differential Static Cell, *J. Chem. Eng. Data*, 37, 484-487 (1992)

Pividal, K.A., C. Sterner, S.I. Sandler, and H. Orbey; Vapor-Liquid Equilibrium from Infinite Dilution Activity Coefficients: Measurements and Prediction of Oxygenated Fuel Additives with Alkanes, *Fluid Phase Equilibria*, 72, 227-249 (1992a)

Plura, J., J. Matous, J.P. Novak, J. Sobr; *Collect. Czech. Chem. Commun.*, 44, 3627 (1979); Referenced in DDB (1999a)

POC; *Properties of Organic Compounds*, Web Version 6.0, Copyright 1982-2002, Chapman & Hall/CRCPRESS, www.chemnetbase.com/Scripts/pocweb.exe (2002)

Prinn, R.G., R.F. Weiss, B.R. Miller, J. Huang, F.N. Alyea, D.N. Cunnold, P.J. Fraser, D.E. Hartley, and P.G. Simmonds; Atmospheric Trends and Lifetime of CH_3CCl_3 and Global OH Concentrations, *Science*, 269, 187-192 (1995)

Raal, J.D., and A.L. Mühlbauer; *Phase Equilibria: Measurement and Computation*, Chapters 2,3 and 4, Taylor & Francis Publishers, Washington, D.C., (1998)

Rackett, H.G., Equations of State for Saturated Liquids, *J. Chem. Eng. Data*, 15, 514-517 (1970)

Ragas, A.M.J., R.S. Etienne, F.H. Willemsen, and D. van de Meent; Assessing Model Uncertainty for Environmental Decision Making: A Case Study of the Coherence of Independently Derived Environmental Quality Objectives for Air and Water, *Environ. Toxicol. Chem.*, 18, 1856-1867 (1999)

Reid, R.C., J.M. Prausnitz, and B.E. Poling; *The Properties of Gases and Liquids*, 4th edition, Appendix A, McGraw-Hill, New York (1987)

Renon, H., and J.M. Prausnitz; Local Compositions in Thermodynamic Excess Functions for Liquid Mixtures, *AIChE J.*, 14, 135-144 (1968)

Resendes, J.W., Y. Shiu, and D. Mackay; Sensing the Fugacity of Hydrophobic Organic Chemicals in Aqueous Systems, *Environ. Sci. Technol.*, 26, 2381-2387 (1992)

Rice, R.G., and D.D. Do; *Applied Mathematics and Modelling for Chemical Engineers*, 1st edition, John Wiley and Sons, New York (1994)

RIVM (1996); Institute of Public Health and the Environment, The Netherlands, *EUSES – The European Union System for the Evaluation of Substances*, Available from the European Chemicals Bureau, Ispra, Italy

Rock, K.; TAME: Technology Merits, *Hydrocarbon Processing*, May, 86-88 (1992)

Rodan, B.D., N. Eckley, D.W. Pennington, and R.S. Boethling; Screening Persistent Organic Pollutants: Techniques to provide a Scientific Basis for POPs Criteria in International Negotiations, *Environ. Sci. Technol.*, 33, 3482-3488 (1999)

Russel, C.J., S. Dixon, and P.Jurs; Computer-assisted Study of the Relationship between Molecular Structure and Henry's Law Constant, *Anal. Chem.*, 64, 1350-1355 (1992)

Rykiel, E.J.; Testing Ecological Models: The Meaning of Validation, *Ecological Modelling*, 90, 229-244 (1996)

Ryu, S.-A., and S.–J. Park; A Rapid Determination Method of the Air/Water Partition Coefficient and its Application, *Fluid Phase Equilibria*, 161, 295-304 (1999)

Sabljić, A., H. Güsten, H. Verhaar, and J. Hermens; QSAR Modelling of Soil Sorption. Improvements and Systematics of log K_{oc} vs log K_{ow} Correlations, *Chemosphere*, 31, 4489-4514 (1995)

Salanitro, J.P., L.A. Daiz, M.P. Williams, and H.L. Wisniewski; Isolation of Bacterial culture that Degrades Methyl t-Butyl Ether, Appl. *Environ. Microbiol.*, 60, 2593-2596 (1994)

Sandler, S.I., and H. Orbey; The Thermodynamics of Long-lived Organic Pollutants, *Fluid Phase Equilibria*, 82, 63-69, (1993)

Sandler, S.I.; Infinite Dilution Activity Coefficients in Chemical, Environmental and Biochemical Engineering, *Fluid Phase Equilibria*, 116, 343-353 (1996)

Sangster, J.; Octanol-Water Partition Coefficients of Simple Organic Compounds, *J. Phy. Chem. Ref. Data*, 18, 1211-1229 (1989)

Sangster, J.; *LOGKOW – A Databank of Evaluated Octanol-Water Partition Coefficients*, Sangster Research Laboratories, Montreal (1993)

Sangster, J.; *Octanol-Water Partition Coefficient: Fundamentals and Physical Chemistry*, John Wiley and Sons, New York (1997)

Scheringer, M.; Persistence and Spatial Range as Endpoints of an Exposure-based Assessment of Organic Chemicals, *Environ. Sci. Technol.*, 30, 1652-1659 (1996)

Scheringer, M.; Characterization of the Environmental Distribution Behavior of Organic Chemicals by Means of Persistence and Spatial range, *Environ. Sci. Technol.*, 31, 2891-2897 (1997)

Schulze, R.E., M. Maharaj, S.D. Lynch, B.J. Howe, B. Melvil-Thomson; *South African Atlas of Agrohydrology and Climatology*, Dept. of Agricultural Engineering, UNP, SA, Water Res. Commission Report, No. TT82-96 (1997)

Schwarzenbach, R.P., P.M. Gschwend, and D.M. Imboden; *Environmental Organic Chemistry*, Wiley-Interscience, New York (1993)

Seader, J.D., and E.J. Henley; *Separation Process Principles*, 1st edition, John Wiley & Sons, New York (1998)

Seth, R., D. Mackay, and J. Muncke; Estimating the Organic Carbon Partition Coefficient and its Variability for Hydrophobic Chemicals, *Environ. Sci. Technol.*, 33, 2390-2394 (1999)

Severinsen, M., and T. Jager; Modelling the Influence of terrestrial Vegetation on the Environmental fate of Xenobiotics, *Chemosphere*, 37, 41-62 (1998)

Shah, J.J., R.L. Johnson, E.K. Heyerdahl, and J.J. Huntzicker; Carbonaceous Aerosol at Urban and Rural Sites in the United States, *J. Air Pollut. Cont. Assoc.*, 36, 254-257 (1986)

Shampine, L.F.; *Numerical Solution of Ordinary Differential Equations,* Chapman & Hall, New York (1994)

Sherman, S.R., D.B. Trampe, D.M. Bush, M. Schiller, C.A. Eckert, A.J. Dallas, L. Li, and P.W. Carr; Compilation and Correlation of Limiting Activity Coefficients of Nonelectrolytes in Water, *Ind. Eng. Chem. Res.*, 35, 1044-1058 (1996)

Slob, W.; Uncertainty Analysis in Multiplicative Models, *Risk Analysis*, 14, 571-576 (1994)

Smith, F.B.; The Significance of Wet and Dry Synoptic Regions on Long-range Transport of Pollution and its Deposition, *Atmos. Environ.*, 15, 863-873 (1981)

Smith, D.F., T.E. Kleindienst, E.E. Hudgens, C.D. Melver, J.J. Buffalini, The Photo-oxidation of Methyl Tertiary-Butyl Ether, *Int. J. Chem. Kinetics*, 23, 907-924 (1991)

Snider, J.R., and G.A. Dawson; Tropopsheric Light Alcohols, Carbonyls, and Acetonitrile Concentrations in the Southwestern Unites States and Henry's Law Data, *J. Geophys. Res. D.: Atmos.*, 90, 3797-3805 (1985)

Somlyody, L., M. Henze, L. Koncsos, W. Rauch, P. Reichert, P. Shanahan, and P. Vanrolleghem; River Water Quality Modelling. III. Future of the Art, *Water Res.*, 38, 253-260 (1998)

Squillace, P.J., J.F. Pankow, N.E. Korte, and J.S. Zogorski; Review of the Environmental Behavior and Fate of Methyl tert-Butyl Ether, *Environ. Toxicol. Chem.*, 16, 1836-1844 (1997)

Staudinger, J., and P.V. Roberts; A Critical Compilation of Henry's Law Constant Temperature Dependence Relations for Organic Compounds in Dilute Aqueous Solutions, *Chemosphere*, 44, 561-576 (2001)

Strommen, M.R., and R.M. Kamens; Development and Application of a Dual-Impedance Radial Diffusion Model to Simulate the Partitioning of Semivolatile Organic Compounds in Combustion Aerosols, *Environ. Sci. Technol.*, 31, 2983-2990 (1997)

Suflita, J.M., and M.R. Mormile; Anaerobic biodegradation of known and potential gasoline oxygenates in the terrestrial subsurface, *Environ. Sci. Technol.*, 27, 976-978 (1993)

Suzuki, T., K. Ohtaguchi, and K. Koide; Application of Principal Components Analysis to Calculated Henry's Constant from Molecular Structure, *Comput. Chem.*, 16, 41-52 (1992)

Swackhamer, D.L., B.D. McVeety, and R.A. Hites; Deposition and Evaporation of Polychlorinated Cogeners to and from Siskiwit Lake, Isle Royale, Lake Superior, *Environ. Sci. Technol.*, 22, 664-672 (1988)

Szabó, G., J. Guczi, W. Kördel, A. Zsolnay, V. Major, and P. Keresztes; Comparison of Different HPLC Stationary Phases for Determination of Soil-Water Distribution Coefficient, K_{oc}, Values of Organic Chemicals in RP-HPLC System, *Chemosphere*, 39, 431-442 (1999)

Tamura, K, Y. Chen, K. Tada, and T. Yamada, Liquid-liquid Equilibria for Quaternary Mixtures of Water, Ethanol and 2,2,4-Trimethylpentane with Fuel additives, *Fluid Phase. Equilibria*, 171, 115-126 (2000)

Thomann, R.V.; Bioaccumulation Model of Organic Chemicals in Aquatic Food-Webs, *Environ. Sci. Technol*, 23, 699-707 (1989)

Thomann, R.V.; The Future "Golden Age" of Predictive Models for Surface Water Quality and Ecosystem Management, *J. Environ. Eng.*, ASCE, 124, 94-103 (1998)

Thomas, E.R., B.A. Newman, T.C. Long, D.A. Wood, and C.A. Eckert; Limiting Activity Coefficients of Nonpolar and Polar Solutes in Both Volatile and nonvolatile Solvents by Gas Chromatography, *J. Chem. Eng. Data*, 27, 399-405 (1982)

Thomas, V.M.; *The Elimination of Lead in Gasoline*, Annual Review of Energy and Environment, 20, 301-324 (1995)

Thompson, N.; Diffusion and Uptake of Chemical Vapour Volatilising from a Sprayed Target Area, *Pestic. Sci.*, 14, 33-39 (1983)

Tochigi, K., D. Tiegs, J. Gmehling, and K. Kojima; Determination of new ASOG parameters, *J. Chem. Eng. Jpn.*, 23, 453-463 (1990)

Trapp, S., and M. Matthies; *Chemodynamics and Environmental Modeling: An Introduction*, Springer Verlag, Heidelberg, Germany, (1998)

Tse, G., H. Orbey, and S.I. Sandler; Infinite Dilution Activity Coefficients and Henry's Law Coefficients of Some Priority Water Pollutants Determined by a Relative Gas Chromatographic Method, *Environ. Sci. Technol.*, 26, 2017-2022, (1992)

Tse, G., and S.I. Sandler; Determination of the Infinite Dilution Activity Coefficients and 1-Octanol/Water Partition Coefficients of Volatile Organic Pollutants, *J. Chem. Eng. Data*, 39, 354-357 (1994)

Tsonopoulos, C., and J.H. Dymond; Second Virial Coefficients of Normal Alkanes, Linear 1-Alknaols (and Water), Alkyl Ethers, and their Mixtures, *Fluid Phase Equilibria*, 133, 11-34 (1997)

US EPA (1994); *Chemicals in the Environment: Methyl-tert-Butyl Ether*, United States Environmental Protection Agency: Office of Pollution Prevention and Toxics, Report No. EPA.749/F/94/017, August, Washington, DC

US EPA (1996); *Oxyfuels Information Needs*, United States Environmental Protection Agency: Office of Research and Development, Report No. EPA.600/R/96/069, May, Research Triangle Park and Washington, DC

Vallack, H.W., D.J. Bakker, I. Brandt, E. Bromström-Lundén, A. Bouwer, K.R. Bull, C. Gough, R. Guardans, I. Holoubek, B. Jansson, R. Koch, J. Kuylenstierna, A. Lecloux, D. Mackay, P. McCutcheon, P. Mocarelli, and R.D.F. Taalman; Controlling Persistent Organic Chemicals – What Next?, *Environ. Toxicol. Pharmacol.*, 6, 143-175 (1998)

van de Meent, D.; *SimpleBOX: A Generic Fate Evaluation Model*, RIVM Report No. 67272001, RIVM (National Institute of Public Health and the Environment) Bilthoven, Netherlands (1993)

van Ness, H.C., M. Byers, and R.E. Gibbs; Vapor-Liquid Equilibrium: Part I. An Appraisal of Data Reduction Methods, *AIChE J.*, 19, 238-251 (1973)

van Pul, W.A.J., F.A.A.M. de Leeuw, J.A. van Jaarsveld, M.A. van der Gaag, and C.J. Sliggers; The Potential for Long-range Transboundary Atmospheric Transport, *Chemosphere*, 37, 113-141 (1998)

Veerkamp, W., and C. Wolff, Developments and Validation Criteria, *Environ. Sci. Pollut. Res.*, 3, 91-95 (1996)

Veith, G.D., N.M. Austin, and R.T. Morris; A Rapid Method for Estimating log P for Organic Chemicals, *Water Res.*, 13, 43-47 (1979)

Veith, G.D., D.L. Defoe, and B.V. Bergstedt; Measuring and Estimating the Bioconcentration Factor of Chemicals in Fish, *J. Fisheries Res. Board of Canada*, 36, 1040-1048 (1979)

Verschuren, K.; *Handbook of Environmental Data on Organic Chemicals*; Chapman & Hall, New York, NY (1983)

Voldner, E.C., L.A. Barrie, and A. Sirois; A Literature Review of Dry Deposition of Oxides of Sulphur and Nitrogen with emphasis on Long-Range Transport Modelling in North America, *Atmos. Environ.*, 20, 2101-2123 (1986)

Voutsas, E.C., and D.P. Tassios; Prediction of Infinite Dilution activity Coefficients in Binary Mixtures with UNIFAC. A Critical Evaluation, *Ind. Eng. Chem. Res.*, 35, 1438-1445 (1996)

Wagner, J.-O., and M. Matthies; Guidelines for Selection and Application of Fate and Exposure Models, *Environ. Sci. Pollut. Res.*, 3, 47-51 (1996)

Wagner, G., and S.I. Sandler; Liquid-liquid Equilibria of Fuel Oxygenate + Water + Hydrocarbon Mixtures. 3. Effect of Temperature, *J. Chem. Eng. Data*, 40, 1119-1123 (1995)

Wallington, T.J., P. Dagaut, R. Liu, and M.J. Kurylo; Gas-phase Reactions of Hydroxyl Radicals with the Fuel Additives Methyl tert-Butyl Ether and tert-Butyl Alcohol over the Temperature Range 240-440 K, *Environ. Sci. Technol.*, 22, 842-844 (1988)

Wania, F., and D. Mackay; An Approach to Modelling the Global Distribution of Toxaphene: A Discussion of Feasibility and Desirability, *Chemosphere*, 27, 2079-2094 (1993)

Wania, F., and D. Mackay; A Global Distribution Model for Persistent Organic Chemicals, *Sci. Total Environ.*, 160/161, 211-232 (1995)

Wania, F., and D. Mackay; Tracking the Distribution of Persistent Organic Chemicals, *Environ. Sci. Technol.*, 30, 390-396 (1996)

Wania, F.; *An Integrated Criterion for the Persistence of Organic Chemicals based on Model Calculations*, WECC-Report 1/1998, July, 31 pages (1998)

Wania, F., J. Axelman, and D. Broman; A Review of Processes involved in the Exchange of Persistent Organic Pollutants across the Air-Sea Interface, *Environ. Pollut.*, 102, 3-23 (1998)

Wania, F., D. Mackay, Y.-F. Li, T.F. Bidleman, and A. Strand; Global Chemical Fate of α-Hexachlorocyclohexane. 1. Evaluation of a Global Distribution Model, *Environ. Toxicol. Chem.*, 18, 1390-1399 (1999)

Wania, F., and D. Mackay; Global Chemical Fate of α-Hexachlorocyclohexane. 2. Use of a Global Distribution Model for Mass Balancing Source Apportionment, and Trend Predictions, *Environ. Toxicol. Chem.*, 18, 1400-1407 (1999)

Wania, F., J. Persson, A. Di Guardo, and M.S. McLachlan; *A Fugacity-based Multi-compartmental Mass Balance Model of the Fate of Persistent Organic Pollutants in the Coastal Zone*, WECC-Report 1/2000, April, 27 pages (2000)

Wania, F., and D. Mackay; *A Comparison of Overall Persistence Values and Atmospheric Travel Distances calculated by various Multimedia Models*, WECC-Report 2/2000, July, 42 pages (2000)

Webster, E., D. Mackay, and F. Wania; Evaluating Environmental Persistence, *Environ. Toxicol. Chem.*, 17, 2148-2158 (1998)

Wen, Y.H., J. Kalff, and R.H. Peters; Pharmokinetic Modeling in Toxicology: A Critical Perspective, *Environ. Rev.*, 7, 1-18 (1999)

Wienke, G., and J. Gmehling; Prediction of Octanol-Water Partition Coefficients, Henry Coefficients and Water Solubilities using UNIFAC, *Toxicol. Environ. Chem.*, 65, 57-86 (1998)

Wilson, G.M.; Vapor-Liquid Equilibrium. XI. A New Expression for the Excess Free Energy of Mixing, *J. Am. Chem. Soc.*, 86, 127-130 (1964)

Whitby, K.T.; The Physical Characteristic of Sulfate Aerosols, *Atmos. Environ.*, 12, 135-159, (1978)

Wisniak, J., G. Embon, R. Shafir, H. Segura, and R. Reich; Isobaric Vapor-Liquid Equilibria in the systems Methyl 1,1-Dimethylethyl Ether + Octane and Heptane + Octane, J. *Chem. Eng. Data*, 42, 1191-1194 (1997)

Woodburn, K.B., W.J. Doucette, and A.W. Andren; Generator Column Determination of Octanol/Water Partition Coefficients for Selected Polychlorinated Biphenyl Cogeners, *Environ. Sci. Technol.*, 18, 457-459 (1984)

Woodfine, D.G., M. MacLeod, D. Mackay, and J.R. Brimacombe; Development of Continental Scale Multimedia Contaminant Fate Models: Integrating GIS, *Environ. Sci. Pollut. Res.*, 8, 164-172 (2001)

Woodrow, B.N., and J.G. Dorsey; Thermodynamics of Micelle-Water Partitioning in Micellar Electrokinetic Chromatography: Comparisons with 1-Octanol-Water Partitioning and Biopartitioning, *Environ. Sci. Technol.*, 31, 2812-2820 (1997)

Wright, D.A., S. I. Sandler, and D. DeVoll; Infinite Dilution Activity Coefficients and Solubilities of Halogenated Hydrocarbons in Water at Ambient Temperatures, *Environ. Sci. Technol.*, 26, 1828-1831 (1992)

Wu, H.S., and S.I. Sandler; Use of Ab Initio Quantum Mechanics Calculations in Group Contribution Methods. 1. Theory and the Basis for Group Identifications, *Ind. Eng. Chem. Res.*, 30, 881-889 (1991)

Wu, H.S., and S.I. Sandler; Use of Ab Initio Quantum Mechanics Calculations in Group Contribution Methods. 2. Test of New Groups in UNIFAC, *Ind. Eng. Chem. Res.*, 30, 889-897 (1991a)

Yalkowshy, S.H., and F.-M. Dannenfesler; *AQUASOL DATABASE of Aqueous Solubility*, 5th edition, University of Arizona, Tuscon, AZ (1991)

Yeh, C.K., and J.T. Novak; Anaerobic Biodegradation of Gasoline Oxygenates in Soils, *Water Environ. Res.*, 66, 744-752 (1994)

Yeh, C.K., and J.T. Novak; The Effect of Hydrogen Peroxide on the Degradation of Methyl and Ethyl tert-Butyl Ether in Soils, *Water Environ. Res.*, 67, 828-834 (1995)

Zhang, S., T. Hiaki, and K. Kojima; Prediction of Infinite Dilution Activity Coefficients for Systems including Water based on the Group Contribution Model with Mixture-Type Groups 1. Alkane-H_2O and Alkanol-H_2O Mixtures, *Fluid Phase Equilibria*, 149, 27-40 (1998)

Zhang, X., K.-W. Shramm, B. Henkelmann, C. Klimm, A. Kaune, A. Dettrup, and P. Lu; A Method to Estimate the Octanol-Air Partition Coefficient of Semivolatile Organic Compounds, *Anal. Chem.*, 71, 3834-3838 (1999)

Zikmundová, D., J. Matouš, J.P. Novák, V. Kubiček, and J. Pick; Liquid-Liquid and Vapour-Liquid Equilibria in the System Methyl tert-Butyl Ether + Tetrahydrofuran + Water, *Fluid Phase Equilibria*, 54, 93-110 (1990)

APPENDIX A

A-1 Solution techniques for PDE's

Equations (3-1) and (3-2) are partial differential equations corresponding to the Trapp and Matthies (1998) hydrodynamic or flow mechanistic models. In order to solve for the behaviour of a chemical within a single compartment, either Equation (3-1) or (3-2) must be solved. The equations can be solved analytically or numerically. Due to the PDE's implicit spatial complexity, it is normally only solved over a single compartment.

The interpretation of the numerical accuracy and physical realism of models will assume an increased importance in years to come due to the financial and political ramifications of backing a "wrong" environmental policy decision (Thomann, 1998). Consequently, model complexities are spiralling upwards as understanding of the underlying physical, chemical and biological processes increases, allowing the formulation of more complex models (Somlyody et al., 1998). Only certain cases can be solved analytically, imposing limitations on the applicability of the simulation to non-uniform real-world scenarios. Recourse is, therefore, to numerical solution methods, which although are capable of dealing with complex, non-linear environmental models, are nonetheless, subject to numerical errors. Numerical methods for the solutions of PDE's include the finite difference method and the Crank-Nicholson method (Rice and Do, 1994).

The accuracy of a numerical technique depends on the magnitude of the displacement and time steps. The smaller the time step, the more computationally intensive the calculation and hence, the more time required to obtain a solution. Upper limits for integration steps exist in terms of the stability of the techniques. Mathematical criteria like the Courant-condition and the Neumann-criterion (Trapp and Matthies, 1998) define limits for numerical integration steps regarding solution stability. Accordingly, an optimum integration step can be found, taking into consideration the computational time, the accuracy of the solution and the stability of the numerical method.

A-2 Solution techniques for ODE's

A system of ODE's must be solved in order to obtain the distribution profile of a chemical between the n compartments of a multi-compartment system. The system of ODE's represented by Equation (3-5) can be solved either analytically or numerically.

Analytical solutions exist but only for a restricted number of scenarios. Two analytical cases commonly dealt with are the initial condition problem and the steady state problem. Although the latter is not an ODE problem, its solution can be calculated using the same analytical technique.

Initial value problem: $\underline{C}(0) = \underline{C}_0$ and $\underline{B} = \underline{0}$; thus, Equation (3-5) becomes:

$$\frac{d\underline{C}(t)}{dt} = \underline{\underline{A}}.\underline{C}(t) \qquad \textbf{(A-1)}$$

Steady state problem: $\frac{d\underline{C}}{dt} = \underline{0}$ and $\underline{B}$ = constant; thus, Equation (3-5) becomes:

$$\underline{\underline{A}}.\underline{C} + \underline{B} = \underline{0} \qquad \textbf{(A-2)}$$

where $\underline{0}$ is the null (n x 1) vector.

The initial value problem corresponds to a scenario where a pulse of chemical is released into the system. Mathematically, Equation (A-1) is the corresponding homogenous form of Equation (3-5). Steady state describes a system, which does not change with respect to time; subsequently, any property differentiated with respect to time is zero. A steady state solution will occur when all fluxes between compartments are in equilibrium and all flows into and out of the system compartments are balanced.

The analytical solutions to the two special cases above can be ascertained using the linear algebraic technique of eigenvalues and eigenvectors.

The eigenvalues (λ_i) are generated by solving Equation (A-3) below:

$$Det(\underline{\underline{A}} - \lambda_i \underline{\underline{I}}) = 0 \tag{A-3}$$

where $\underline{\underline{I}}$ is the (n x n) identity matrix and $\lambda_i \underline{\underline{I}}$ is a (n x n) matrix whose main diagonal houses the n eigenvalues with all other matrix elements containing zeros.

Each eigenvalue corresponds to an associated eigenvector $(\underline{V_i})$, which can be generated by solving Equation (A-4):

$$(\underline{\underline{A}} - \lambda_i \underline{\underline{I}}).\underline{V_i} = \underline{0} \tag{A-4}$$

The mathematical relationship mapping eigenvalues to their corresponding eigenvectors is presented in Equation (A-5). This relationship is used to generate the analytical solutions to both special cases expressed above:

$$\underline{\underline{A}}.\underline{V_i} = \lambda_i \underline{V_i} \tag{A-5}$$

The resulting solutions for the two contrived scenarios are:

Initial value problem:

$$\underline{C}(t) = \sum_{i=1}^{n} \alpha_i \underline{V_i} e^{\lambda_i t} \tag{A-6}$$

where

$$\underline{C}_0 = \sum_i \alpha_i \underline{V_i}$$

Steady state problem:

$$\underline{C}^{ss} = \underline{\underline{A}}^{-1}.(-\underline{B}) = \sum_i \alpha_i^{ss} \underline{V_i}$$

(A-7)

The method of Laplace transforms may also be used to solve the linear ODE systems (Hertwich, 2001). The Laplace transform reduces ODE's to a readily soluble system of linear algebraic equations.

As the ODE system generated from the multi-compartment examples above are linear, superposition theory may be applied to them (Hertwich, 2001). Superposition theory has been used in steady state modelling, as well as in stochastic air pollution modelling (Smith, 1981), inter alia. Superposition theory is a convenient solution technique as the linear combination of the solutions to the ODE systems normalised for a single medium source discharge into each compartment, (i.e. *n* solutions for *n* compartments) may be combined to solve different initial condition problems including multiple mode emission profiles.

Furthermore, exploitation of the linearity of ODE systems allows the analytical solution of dynamic multi-compartment models of greater complexity: This includes the case of a control vector that is permitted to vary with time. The time dependent control vector [$\underline{B}(t)$] will result from an emission profile, which varies with time. Equation (A-8) allows the simulation of this more realistic emission scenario:

$$\frac{d\underline{C}(t)}{dt} = \underline{\underline{A}}.\underline{C}(t) + \underline{B}(t)$$

(A-8)

The analytical solution is facilitated through the convolution of the response to the simple initial value problems using Equation (A-6) solved for each element of a discretised emission profile.

According to Hertwich (2001), any time function can be described as a series of Dirac delta functions [$\delta(t)$]:

$$\underline{B}(t) = \int_{-\infty}^{\infty} \underline{B}(\tau)\delta(t-\tau)d\tau$$

(A-9)

This allows the description of time varying functions as a superposition of a series of initial conditions occurring as a progression of time (Hertwich, 2001). The system response to the emission profile can be facilitated by superposition of the n initial value problem solutions corresponding to each normalised single mode release scenario. Consequently:

$$\underline{C}_B(t) = \int_{-\infty}^{t} \underline{\underline{C}}_I(t-\tau).\underline{E}(\tau)d\tau$$

(A-10)

where $\underline{\underline{C}}_I$ is the solution to the initial value problem, Equation (A-1), with $\underline{\underline{C}}_0 = \underline{\underline{I}}$.

Numerical techniques used to solve the ODE systems of the types represented above [i.e. Equations (A-1) and (A-8)] include the simple Euler numerical integration technique and the more accurate Runge-Kutta scheme (Shampine, 1994). A discretisation based numerical solution, which preserves the stability of the dynamic control system represeneted by the ODE systems has been developed by Bru et al. (1998).

A-3 Criterion for phase equilibrium

The criterion for phase equilibrium, developed below, is derived for a two-phase system, but can be extended to apply to several phases. Consider a closed system consisting of two phases, α and β, in equilibrium. The overall closed system is composed of two individual open phases, between which mass is free to transfer. As the system is in equilibrium, temperature and pressure is uniform throughout the system. The following two thermodynamic equations can be written regarding the free energy of each phase:

$$d(nG)^{\alpha} = (nV)^{\alpha} dP - (nS)^{\alpha} dT + \sum_i \mu_i^{\alpha} dn_i^{\alpha}$$

(A-11)

$$d(nG)^{\beta} = (nV)^{\beta} dP - (nS)^{\beta} dT + \sum_i \mu_i^{\beta} dn_i^{\beta}$$

(A-12)

where G is the molar Gibbs free energy, S is the molar entropy and μ_i is the chemical potential of species i, which is defined in terms of the molar Gibbs free energy as:

$$\mu_i = \left[\frac{\partial(nG)}{\partial n_i}\right]_{T,P,n_j}$$

(A-13)

Upon summation of Equations (A-11) and (A-12) to yield the total system property, it follows that:

$$d(nG) = (nV)dP - (nS)dT + \sum_i \mu_i^{\alpha} dn_i^{\alpha} + \sum_i \mu_i^{\beta} dn_i^{\beta}$$

(A-14)

Equation (A-14) is obtained using the relationship that a total closed system property is the sum of its phase properties:

$$nM = (nM)^{\alpha} + (nM)^{\beta}$$

(A-15)

Since the overall system is closed, the Gibbs free energy of the total system is:

$$d(nG) = (nV)dP - (nS)dT$$

(A-16)

Comparison of Equation (A-14) and (A-16) yields:

$$\sum_i \mu_i^{\alpha} dn_i^{\alpha} + \sum_i \mu_i^{\beta} dn_i^{\beta} = 0$$

(A-17)

As conservation of mass dictates that $dn_i^{\alpha} = -dn_i^{\beta}$, Equation (A-17) reduces to:

$$\sum_i (\mu_i^{\alpha} - \mu_i^{\beta}) dn_i^{\alpha} = 0$$

(A-18)

Since the quantities dn_i are arbitrary, Equation (A-18) can only be satisfied if the terms in parenthesis are equated to zero. Hence:

$$\mu_i^{\alpha} = \mu_i^{\beta}$$

(A-19)

Generalising the result of Equation (A-19) to Π phases consisting of n species:

$$\mu_i^{\alpha} = \mu_i^{\beta} = \ldots = \mu_i^{\Pi} \quad (i = 1,2,\ldots,n)$$

(A-20)

Alternatively, an equivalent criterion for equilibrium can be derived from the definition of fugacity:

$$d\mu_i = RTd \ln \hat{f}_i \tag{A-21}$$

Integration of Equation (A-21) at constant temperature gives:

$$\mu_i = RT \ln \hat{f}_i + \Theta(T) \tag{A-22}$$

Since $\Theta(t)$ is dependent on temperature only and all phases at equilibrium are at the same temperature, combination of Equation (A-20) and Equation (A-22) reveals an alternative, but equivalent, equilibrium criterion:

$$\hat{f}_i^{\alpha} = \hat{f}_i^{\beta} = \ldots = \hat{f}_i^{\Pi} \quad (i = 1,2,\ldots,n) \tag{A-23}$$

A-4 Derivation of pressure-altitude profile

The static force felt by a differential cube of atmosphere is:

$$dF_{pressure} = A\,dP \tag{A-24}$$

The weight force exerted as a result of the mass of the differential cube is:

$$dF_{weight} = -\rho\, g\, dV \tag{A-25}$$

For a non-accelerating cell at equilibrium, Equation (A-24) can be equated to Equation (A-25). Equating these equations and solving in terms of P yields:

$$dP = -\rho\, g\, d\left(\frac{V}{A}\right) = -\rho\, g dz \tag{A-26}$$

The density of an ideal gas is:

$$\rho = \frac{PM}{RT} \tag{A-27}$$

Substituting Equation (A-27) into Equation (A-26) and rearranging with respect to pressure on the left-hand side yields:

$$\frac{dP}{P} = \left(-\frac{gM}{RT}\right)dz \tag{A-28}$$

Integration of Equation (A-28) from $P(z = 0) = P_0$ to $P(z) = P$ yields:

$$P(z) = P_0 \exp\left[-\left(\frac{gM}{RT}\right)z\right] \tag{A-29}$$

A-5 Derivation of compressed troposphere height

The compressed height of the troposphere, as defined by Mackay (2001), is the hypothetical equivalent height of the air compartment, which has the same mass as the actual atmosphere but a uniform pressure equal to ground level pressure.

Assuming:

- P_0 = 101.325 kPa
- M = 28.94 kg/kmol (Molar mass of air)
- g = 9.81m/s2
- R = 8314 J/kmol.K
- T = 25°C = 298.15 K
- Height of troposphere (H_{tropo}) = 10000 m

and converting the definition of Mackay (2001) above to mathematical terms yields:

$$P_o H = \int_0^{H_{tropo}} P_0 \exp\left[-\left(\frac{gM}{RT}\right)z\right] dz \qquad \textbf{(A-30)}$$

Upon substitution of the parameters listed above into Equation (A-30), solving for the height of the compressed atmosphere (H) yields:

$$\begin{aligned} H &= \left(\frac{RT}{gM}\right)\left(1-\exp\left[-\frac{gM}{RT}H_{tropo}\right]\right) \\ &= 5953.6 \text{ m} \\ &\approx 6 \text{ km} \end{aligned}$$

Graphically this calculation is represented in Figure A-1 below with:

Area (ABCD) = Area (AEFD)

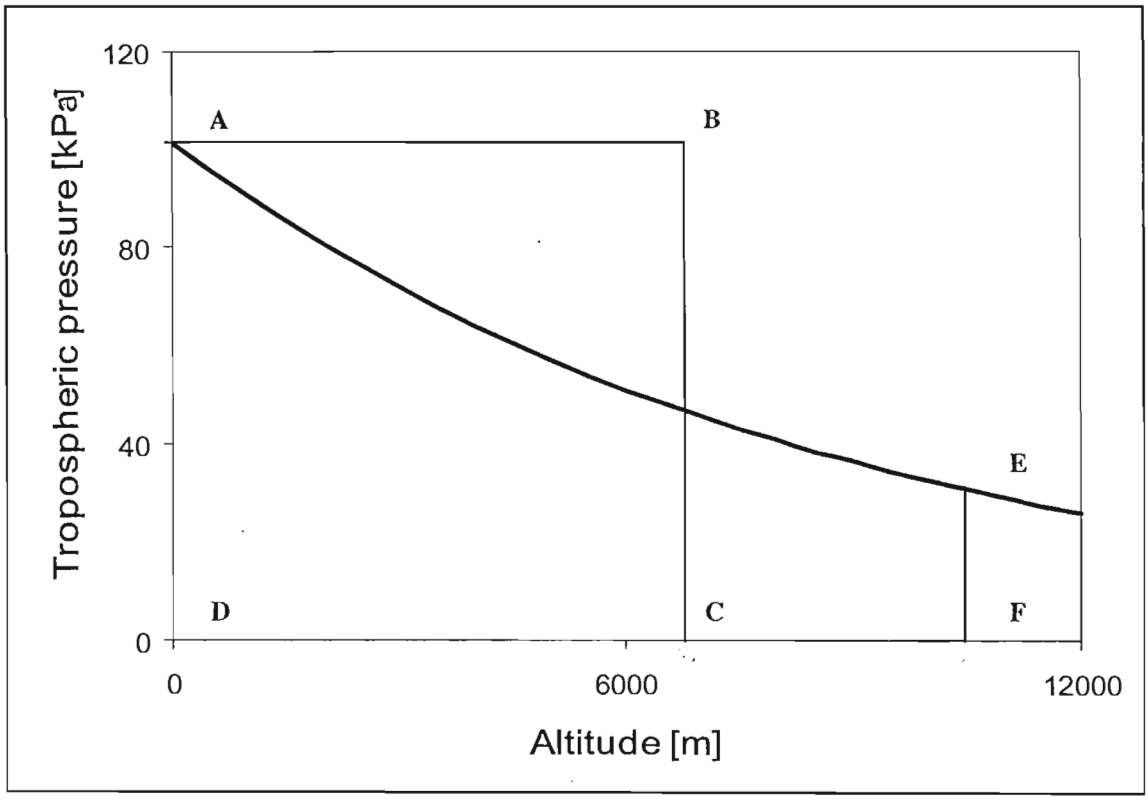

Figure A-1: Graphical representation of Mackay (2001) defined compressed troposphere height

A-6 Derivation of Thomann (1989) four-tiered food chain model

Considering a steady state mass balance over a species (η) in a food chain yields:

Rate of elimination of chemical by decomposition and excretion	=	Rate of uptake of chemical from water	+	Rate of uptake of chemical from prey species

(A-31)

Equation (A-31) can be written for each species in the food chain. Restricting the feeding patterns of each tier to that of the tier below it and converting Equation (A-31) into explicit mathematical terms yields:

$$k_{\eta,e}C_{\eta} = k_{\eta,w}C_{\eta} + \alpha_{\eta}F_{\eta}C_{\eta-1}$$

(A-32)

where $k_{\eta,e}$ is the rate constant for decomposition and excretion of chemical, $k_{\eta,w}$ is the rate constant for the uptake of chemical from water, α_{η} is the assimilation efficiency of food consumed by the biota species and F_{η} is the rate of consumption of prey species by the predator species. Manipulating Equation (A-32) by dividing by $k_{\eta,e}C_1$, where the subscript 1 indicates the primary producer species in the food chain, results in:

$$\frac{C_{\eta}}{C_1} = \frac{k_{\eta,w}C_{\eta}}{k_{\eta,e}C_1} + \frac{\alpha_{\eta}F_{\eta}C_{\eta-1}}{k_{\eta,e}C_1}$$

(A-33)

Assuming equilibrium between excretion/decomposition processes and the uptake of chemical from water, the first term on the right-hand side of Equation (A-33) may be set to one for any trophic level of the food chain. Hence, Equation (A-33) becomes:

$$\frac{C_{\eta}}{C_1} = 1 + \frac{\alpha_{\eta}F_{\eta}C_{\eta-1}}{K_{\eta}C_1}$$

(A-34)

Definition of a baseline biomagnification factor relating the chemical concentration in any species to that in the primary producer species yields:

$$\theta_\eta = \frac{C_\eta}{C_1}$$

(11-2)

Applying the definition in Equation (11-2) to Equation (A-33) yields:

$$\theta_\eta = 1 + \left(\frac{\alpha_\eta F_\eta}{k_{\eta,e}} \right) \theta_{\eta-1}$$

(A-35)

The bracketed term in Equation (A-35) represents a food assimilation coefficient. Thomann (1989) fitted data to the bracketed term for each predator species generating:

$$\delta_\eta = \frac{\alpha_\eta F_\eta}{K_\eta}$$

(A-36)

where

$$\delta_\eta = \frac{a_\eta}{b_\eta + \frac{c_\eta}{K_{ow}}}$$

(11-1)

The parameters required for Equation (11-1) cab be found in Table (11-1).

Combining Equation (A-36) with Equation (A-35) yields:

$$\theta_\eta = 1 + \delta_\eta \theta_{\eta-1}$$

(A-10)

From the combination of Equation (A-39) with Equation (A-36), the concentration of any tier can be calculated from:

$$C_{\eta} = \left(1 + \delta_{\eta}\theta_{\eta-1}\right)C_1 \tag{11-3}$$

APPENDIX B

B-1 Details of model formulation for EQC and ChemSA

The EQC and ChemSA models are formulated using Equation (8-1) and incorporating the fugacity capacity factors of the seven sub-compartments outlined in Table B-1. The four bulk compartment inter-media transport coefficients are generated from transport and mass transfer coefficients defined in Table B-2 and Table B-3 respectively.

Table B-1: Definition of fugacity capacity factors for the EQC and ChemSA models

Phase	Fugacity capacity factor [mol/m^3.Pa]
Air (1)	$Z_1 = \frac{1}{RT}$
Water (2)	$Z_2 = \frac{1}{H}$
Soil (3)	$Z_3 = \frac{Z_2 \rho_3 y_3 K_{oc}}{1000}$
Sediment (4)	$Z_4 = \frac{Z_2 \rho_4 y_4 K_{oc}}{1000}$
Suspended sediment (5)	$Z_5 = \frac{Z_2 \rho_5 y_5 K_{oc}}{1000}$
Fish (6)	$Z_6 = \frac{Z_2 \rho_6 y_6 K_{oc}}{1000}$
Aerosol (7)	$Z_7 = \frac{Z_1 \, 6x10^6}{P^{sat}}$

Table B-2: Inter-media transport and mass transfer coefficients used in the EQC and ChemSA models

Transport Coefficient (U_i)	EQC [m/h]	ChemSA [m/h]
U_1, air-film air-water mass transfer coefficient	5	5
U_2, water-film air-water mass transfer coefficient	0.05	0.05
U_3, Rainfall rate	10^{-4}	5.27×10^{-5}
U_4, Aerosol wet and dry deposition velocity	6×10^{-10}	6×10^{-10}
U_5, Soil-air diffusion mass transfer coefficient	0.02	0.02
U_6, Soil-water phase transport mass transfer coefficient	10^{-5}	10^{-5}
U_7, Soil surface -air mass transfer coefficient	5	5
U_8, Sediment water mass transfer coefficient	10^{-4}	10^{-4}
U_9, Sediment deposition rate	5×10^{-7}	5×10^{-7}
U_{10}, Sediment resuspension rate	2×10^{-7}	2×10^{-7}
U_{11}, Soil-water runoff rate	5×10^{-5}	5×10^{-5}
U_{12}, Soil-solids runoff rate	10^{-8}	10^{-8}

The transport parameters presented in Table B-2 above represent typical values exhibited by chemicals found in the respective environmental compartments. These values have been previously utilised by several researchers investigating environmental fate behaviour (Mackay and Paterson, 1991; Mackay et al., 1996a; Scheringer, 1996).

The mathematical system of ordinary differential equations generated from Equation (8-1) can be written in the following matrix notation:

$$\underline{\dot{f}} = \underline{\underline{A}}\,\underline{f} + \underline{B} \qquad \textbf{(B-1)}$$

where

$\underline{\dot{f}} = \underline{\dot{f}}(t)$ is the fugacity derivative vector with components $[\dot{f}_i] = \left[\frac{d\,\hat{f}_i}{dt}\right]$

$\underline{f} = \underline{f}(t)$ is the fugacity state vector with components $[f_i] = \left[\hat{f}(t)\right]$

$\underline{B}$ is the control vector with components $[b_i] = \dfrac{E_i}{V_i Z_i}$

$$\underline{\underline{A}} = [a_{ij}] = \begin{cases} a_{ki} = \dfrac{-\left(D_{r,i} + D_{ad,i} + \sum_{j \in J_i} D_{ij}\right)}{V_i Z_i} & \text{if } k = i \\ a_{ki} = \dfrac{D_{ji}}{V_i Z_i} & \text{if } k \in J_i \\ a_{ki} = 0 & \text{if } k \notin J_i \end{cases}$$

$\underline{\underline{A}}$, above, is an n x n state matrix.

The D values (subscripts ij or ji) are inter-media transfer coefficients relating fugacity to the molar transfer rate. The D values bearing the subscripts r and ad represent reactive and advective terms respectively.

The inter-media transport coefficients accounting for various transport processes, including non-reversible processes, are list in Table B-3 below:

Table B-3: Inter-media transport coefficients for the EQC and ChemSA model

Environmental Media		Process	Equation
From	To		
Air	Water	TOTAL	$D_{12} = D_{12}^{abs} + D_{12}^{rain} + D_{12}^{dep}$
		Absorption	$D_{12}^{abs} = \frac{A_{12}}{1/U_1Z_1 + 1/U_2Z_2}$
		Rain dissolution	$D_{12}^{rain} = U_3 A_{12} Z_2$
		Aerosol deposition	$D_{12}^{dep} = U_4 A_{12} Z_7$
Water	Air	TOTAL	$D_{21} = D_{21}^{vol}$
		Volatilisation	$D_{21}^{vol} = D_{12}^{abs}$
Air	Soil	TOTAL	$D_{13} = D_{13}^{abs} + D_{13}^{rain} + D_{13}^{dep}$
		Absorption	$D_{13}^{abs} = \frac{A_{13}}{1/U_7Z_1 + 1/(U_5Z_2 + U_6Z_2)}$
		Rain dissolution	$D_{13}^{rain} = U_3 A_{13} Z_1$
		Aerosol deposition	$D_{13}^{dep} = U_4 A_{13} Z_7$
Soil	Air	TOTAL	$D_{31} = D_{31}^{vol}$
		Volatilisation	$D_{31}^{vol} = D_{13}^{abs}$
Water	Sediment	TOTAL	$D_{24} = D_{24}^{diff} + D_{24}^{dep}$
		Diffusion	$D_{24}^{diff} = U_8 A_{12} Z_2$
		Deposition	$D_{24}^{dep} = U_9 A_{12} Z_5$
Sediment	Water	TOTAL	$D_{42} = D_{42}^{diff} + D_{42}^{resusp}$
		Diffusion	$D_{42}^{diff} = U_8 A_{12} Z_2$
		Resuspension	$D_{42}^{resusp} = U_{10} A_{12} Z_5$
Soil	Water	TOTAL	$D_{32} = D_{32}^{w} + D_{32}^{solids}$
		Soil water run-off	$D_{32}^{w} = U_{11} A_{13} Z_2$
		Soil Solids run-off	$D_{32}^{solids} = U_{12} A_{13} Z_5$

B-2 Model equations and definitions for Level III investigation

Level III model equations:

$$0 = \frac{-\left(D_{r,1} + D_{ad,1} + D_{12} + D_{13}\right)}{V_1 Z_1} \hat{f}_1 + \frac{D_{21}}{V_1 Z_1} \hat{f}_2 + \frac{D_{31}}{V_1 Z_1} \hat{f}_3 + \frac{E_1}{V_1 Z_1}$$

$$0 = \frac{D_{12}}{V_2 Z_2} \hat{f}_1 + \frac{-\left(D_{r,2} + D_{ad,2} + D_{21} + D_{24}\right)}{V_2 Z_2} \hat{f}_2 + \frac{D_{32}}{V_2 Z_2} \hat{f}_3 + \frac{D_{42}}{V_2 Z_2} \hat{f}_4 + \frac{E_2}{V_2 Z_2}$$

$$0 = \frac{D_{13}}{V_3 Z_3} \hat{f}_1 + \frac{-\left(D_{r,3} + D_{ad,3} + D_{31} + D_{32}\right)}{V_3 Z_3} \hat{f}_3 + \frac{E_3}{V_3 Z_3}$$

$$0 = \frac{D_{24}}{V_4 Z_4} \hat{f}_2 + \frac{-\left(D_{r,4} + D_{ad,4} + D_{42}\right)}{V_4 Z_4} \hat{f}_4$$

where

$$Z_j = \sum_i v_i^j Z_i \text{ for } i \in [1,7]; j \in [1,4]$$

In matrix notation, the steady state solution is:

$$\underline{f} = \underline{\underline{A}}^{-1}(-\underline{B}) \qquad \textbf{(B-2)}$$

Advection persistence:

$$\tau_{ad} = \frac{\sum_i Z_i \hat{f}_i V_i}{\sum_i D_{ad,i} \hat{f}_i} \qquad \textbf{(B-3)}$$

Reaction persistence:

$$\tau_r = \frac{\sum_i Z_i \hat{f}_i V_i}{\sum_i D_{r,i} \hat{f}_i}$$

(B-4)

Overall persistence:

$$\tau = \left(1/\tau_{ad} + 1/\tau_r \right)^{-1}$$

(B-5)

B-3 Model equations and definitions for Level IV investigation

Level IV model equations:

$$\frac{d\hat{f}_1}{dt} = \frac{-\left(D_{r,1} + D_{ad,1} + D_{12} + D_{13}\right)}{V_1 Z_1}\hat{f}_1 + \frac{D_{21}}{V_1 Z_1}\hat{f}_2 + \frac{D_{31}}{V_1 Z_1}\hat{f}_3 + \frac{E_1}{V_1 Z_1}$$

$$\frac{d\hat{f}_2}{dt} = \frac{D_{12}}{V_2 Z_2}\hat{f}_1 + \frac{-\left(D_{r,2} + D_{ad,2} + D_{21} + D_{24}\right)}{V_2 Z_2}\hat{f}_2 + \frac{D_{32}}{V_2 Z_2}\hat{f}_3 + \frac{D_{42}}{V_2 Z_2}\hat{f}_4 + \frac{E_2}{V_2 Z_2}$$

$$\frac{d\hat{f}_3}{dt} = \frac{D_{13}}{V_3 Z_3}\hat{f}_1 + \frac{-\left(D_{r,3} + D_{ad,3} + D_{31} + D_{32}\right)}{V_3 Z_3}\hat{f}_3 + \frac{E_3}{V_3 Z_3}$$

$$\frac{d\hat{f}_4}{dt} = \frac{D_{24}}{V_4 Z_4}\hat{f}_2 + \frac{-\left(D_{r,i} + D_{ad,i} + D_{42}\right)}{V_4 Z_4}\hat{f}_4$$

where

$$Z_j = \sum_i v_i^j Z_i \text{ for } i \in [1,7]; j \in [1,4]$$

Definition of fugacity settling time:

Time required for the fugacity of a compartment to settle to its steady state value (Bru et al., 1998; Paraiba et al., 1999).

B-4 Uncertainty analyses for Level III EQC and ChemSA studies

The uncertainty analysis technique has been discussed and outlined in Chapter 6. Table B-4 shows the input confidence factors applied in this study to the relevant chemical properties and environment landscape parameters. Default values from MacLeod (2002) were used for most of the parameters.

Justification for changing the default values relied upon knowing the accuracy, or perceived inaccuracy, of the input parameters. Upon customisation of EQC model parameters to ChemSA, the confidence factors were doubled if no source could be found to estimate a value for South African conditions. This is the case for all the organic carbon contents of the organic phases. This is also relevant to the sediment and water compartmental residence times. As air-water partitioning data were measured directly in this study, the confidence factors were lower than those suggested by MacLeod (2002). The confidence factor for the octanol-water partition coefficient reflected the spread of experimental values found in literature for MTBE. The reaction half-life confidence factors were estimated from the high and low values quoted in Howard et al. (1991). As the organic carbon-water partition coefficient correlation, as formulated by Seth et al. (1999), was employed [opposed to the Karickhoff (1981) correlation used by MacLeod (2002) and others (Mackay et al., 1996a)], the subsequent confidence factor suggested by Seth et al. (1999) was used. It was assumed in all the sensitivity analyses performed in this study that, within the context of the evaluative environments investigated, the emission data and the model surface area have confidence factors of one.

Although the Matlab programs written [See Appendix B-6 and B-7 below] investigated the sensitivity and uncertainty of all 51 program input variables, only 37 variables were found to contribute significantly to the variance in the outputs. Seven model outputs were examined in the input sensitivity analysis: the four bulk media concentrations, the reaction persistence, the advection persistence and the overall persistence. The overall percentage contribution to variance, presented in Table B-5 below, is the normalised equal weighted sum of the contributions of each of the input variables to the 7 output variables.

Table B-4: Assumed input confidence factors (*Cf*) for the chemical and environmental properties used in the EQC and ChemSA uncertainty analyses

Input variable	Assumed input confidence factors					
	EQC			ChemSA		
	MTBE	TAME	Ethanol	MTBE	TAME	Ethanol
Area fraction of water of total surface area	1.1	1.1	1.1	1.1	1.1	1.1
Area fraction of soil of total surface area	1.1	1.1	1.1	1.1	1.1	1.1
Atmospheric height [m]	1.5	1.5	1.5	1.5	1.5	1.5
Water depth [m]	1.5	1.5	1.5	1.5	1.5	1.5
Soil depth [m]	1.5	1.5	1.5	1.5	1.5	1.5
Sediment depth [m]	1.5	1.5	1.5	1.5	1.5	1.5
Volume fraction of air phase in bulk soil	1.1	1.1	1.1	1.5	1.5	1.5
Volume fraction of water phase in bulk soil	1.1	1.1	1.1	1.5	1.5	1.5
Volume fraction of water phase in bulk sediment	1.1	1.1	1.1	1.5	1.5	1.5
Density of air [kg/m^3]	1.05	1.05	1.05	1.05	1.05	1.05
Density of water [kg/m^3]	1.05	1.05	1.05	1.05	1.05	1.05
Density of soil [kg/m^3]	1.5	1.5	1.5	1.5	1.5	1.5
Density of sediment [kg/m^3]	1.5	1.5	1.5	1.5	1.5	1.5
Density of suspended sediment [kg/m^3]	1.5	1.5	1.5	1.5	1.5	1.5
Organic carbon content (m/m) of soil	1.5	1.5	1.5	3	3	3
Organic carbon content (m/m) of sediment	1.5	1.5	1.5	3	3	3
Organic carbon content (m/m) of suspended sediment	1.5	1.5	1.5	3	3	3
Air advection residence time [h]	1.5	1.5	1.5	1.5	1.5	1.5
Water advection residence time [h]	1.5	1.5	1.5	3	3	3
Sediment advection residence time [h]	1.5	1.5	1.5	3	3	3
Organic carbon-water partition coefficient [L/kg]	2.5	2.5	2.5	2.5	2.5	2.5
Henry's constant [Pa.m^3/mol]	1.05	1.05	1.05	1.05	1.05	1.05
Half-life in air [h]	4	4	3	4	4	3
Half-life in surface water [h]	3	3	2	3	3	2
Half-life in soil [h]	2	2	3	2	2	3
Half-life in sediment [h]	3	3	2	3	3	2
Air-film (air/water) mass transfer coefficient [m/h]	3	3	3	3	3	3
Water-film (air/water) mass transfer coefficient [m/h]	3	3	3	3	3	3
Rain rate [m/h]	3	3	3	3	3	3
Soil particle-air mass transfer coefficient [m/h]	3	3	3	3	3	3
Soil particle-water mass transfer coefficient [m/h]	3	3	3	3	3	3
Surface soil-air mass transfer coefficient [m/h]	3	3	3	3	3	3
Sediment-water mass transfer coefficient [m/h]	3	3	3	3	3	3
Sediment deposition rate [m/h]	3	3	3	3	3	3
Soil water run-off rate [m/h]	3	3	3	3	3	3

Table B-5: Overall percentage contribution of input variables to model output variance for MTBE, TAME and ethanol in the EQC and ChemSA simulations

Input variable	Percentage contribution to overall model variance					
	EQC			ChemSA		
	MTBE	TAME	Ethanol	MTBE	TAME	Ethanol
Area fraction of water of total surface area	0.7	0.6	0.3	0.1	0.1	0.1
Area fraction of soil of total surface area	0.1	0.1	0.1	0.1	0.1	0.1
Atmospheric height [m]	3.5	1.9	3.4	5.0	2.6	4.6
Water depth [m]	4.5	4.1	4.7	0.2	0.2	2.6
Soil depth [m]	1.1	1.3	1.5	1.8	1.8	2.1
Sediment depth [m]	0.0	0.0	0.8	0.0	0.0	0.6
Volume fraction of air phase in bulk soil	0.0	0.0	0.0	0.1	0.1	0.0
Volume fraction of water phase in bulk soil	0.0	0.0	0.0	0.8	0.1	0.6
Volume fraction of water phase in bulk sediment	0.0	0.0	0.0	0.1	0.0	0.0
Density of air [kg/m^3]	0.1	0.0	0.1	0.1	0.0	0.1
Density of water [kg/m^3]	0.1	0.1	0.1	0.0	0.0	0.0
Density of soil [kg/m^3]	1.3	0.9	1.5	1.1	0.9	1.6
Density of sediment [kg/m^3]	4.1	2.9	1.1	0.9	0.7	0.8
Density of suspended sediment [kg/m^3]	0.0	0.0	0.0	0.0	0.0	0.0
Org carbon content (m/m) of soil	0.3	0.8	0.0	2.8	6.2	0.0
Org carbon content (m/m) of sediment	0.1	0.2	0.0	0.1	0.4	0.0
Org carbon content (m/m) of suspended sediment	0.0	0.0	0.0	0.0	0.0	0.0
Air advection residence time [h]	3.1	1.6	7.1	7.2	2.7	14.9
Water advection residence time [h]	2.4	2.0	0.0	0.7	0.6	0.0
Sediment advection residence time [h]	0.0	0.0	0.0	0.0	0.0	0.0
Organic carbon-water partition coefficient [L/kg]	2.1	5.4	0.0	2.0	4.6	0.0
Henry's constant [Pa.m^3/mol]	0.1	0.1	0.0	0.1	0.1	0.0
Half-life in air [h]	27.9	27.5	33.8	25.0	28.8	34.2
Half-life in surface water [h]	2.7	2.1	19.6	0.1	0.1	7.6
Half-life in soil [h]	0.1	0.1	17.8	0.0	0.0	19.1
Half-life in sediment [h]	0.1	0.1	2.3	0.0	0.0	1.8
Air-film (air/water) mass transfer coefficient [m/h]	3.5	2.3	0.0	0.9	0.6	0.0
Water-film (air/water) mass transfer coefficient [m/h]	20.5	24.7	0.0	5.3	6.4	0.0
Rain rate [m/h]	0.0	0.0	0.0	0.0	0.0	0.0
Soil particle-air mass transfer coefficient [m/h]	20.6	20.6	0.0	34.0	32.0	0.0
Soil particle-water mass transfer coefficient [m/h]	0.0	0.0	0.0	0.0	0.0	0.0
Surface soil-air mass transfer coefficient [m/h]	0.0	0.0	0.0	0.0	0.0	0.0
Sediment-water mass transfer coefficient [m/h]	0.1	0.1	5.8	0.0	0.0	4.4
Sediment deposition rate [m/h]	0.0	0.0	0.0	0.0	0.0	0.0
Soil water run-off rate [m/h]	0.7	0.4	0.0	11.1	10.4	4.7

Table B-6: Output confidence factors and percentage contribution of input variables to the predicted air concentration for MTBE, TAME and ethanol in the EQC and ChemSA simulations

Input variable	Percentage contribution to air concentration variance					
	EQC			ChemSA		
	MTBE	TAME	Ethanol	MTBE	TAME	Ethanol
Area fraction of water of total surface area	0.0	0.0	0.0	0.0	0.0	0.0
Area fraction of soil of total surface area	0.0	0.0	0.0	0.0	0.0	0.0
Atmospheric height [m]	24.2	13.4	23.9	35.1	18.4	32.1
Water depth [m]	0.3	0.2	0.0	0.0	0.0	0.0
Soil depth [m]	0.0	0.0	0.0	0.0	0.0	0.0
Sediment depth [m]	0.0	0.0	0.0	0.0	0.0	0.0
Volume fraction of air phase in bulk soil	0.0	0.0	0.0	0.0	0.0	0.0
Volume fraction of water phase in bulk soil	0.0	0.0	0.0	0.0	0.0	0.0
Volume fraction of water phase in bulk sediment	0.0	0.0	0.0	0.0	0.0	0.0
Density of air [kg/m^3]	0.4	0.2	0.4	0.5	0.3	0.5
Density of water [kg/m^3]	0.0	0.0	0.0	0.0	0.0	0.0
Density of soil [kg/m^3]	0.0	0.0	0.0	0.0	0.0	0.0
Density of sediment [kg/m^3]	0.0	0.0	0.0	0.0	0.0	0.0
Density of suspended sediment [kg/m^3]	0.0	0.0	0.0	0.0	0.0	0.0
Organic carbon content (m/m) of soil	0.0	0.0	0.0	0.0	0.0	0.0
Organic carbon content (m/m) of sediment	0.0	0.0	0.0	0.0	0.0	0.0
Organic carbon content (m/m) of suspended sediment	0.0	0.0	0.0	0.0	0.0	0.0
Air advection residence time [h]	6.5	1.0	3.1	15.3	3.0	8.1
Water advection residence time [h]	0.2	0.1	0.0	0.0	0.0	0.0
Sediment advection residence time [h]	0.0	0.0	0.0	0.0	0.0	0.0
Organic carbon-water partition coefficient [L/kg]	0.0	0.0	0.0	0.0	0.0	0.0
Henry's constant [Pa.m^3/mol]	0.0	0.0	0.0	0.0	0.0	0.0
Half-life in air [h]	66.7	84.1	72.6	48.9	78.2	59.3
Half-life in surface water [h]	0.2	0.1	0.0	0.0	0.0	0.0
Half-life in soil [h]	0.1	0.0	0.0	0.0	0.0	0.0
Half-life in sediment [h]	0.0	0.0	0.0	0.0	0.0	0.0
Air-film (air/water) mass transfer coefficient [m/h]	0.2	0.1	0.0	0.0	0.0	0.0
Water-film (air/water) mass transfer coefficient [m/h]	1.1	0.6	0.0	0.0	0.0	0.0
Rain rate [m/h]	0.0	0.0	0.1	0.0	0.0	0.0
Soil particle-air mass transfer coefficient [m/h]	0.3	0.1	0.0	0.1	0.0	0.0
Soil particle-water mass transfer coefficient [m/h]	0.0	0.0	0.0	0.0	0.0	0.0
Surface soil-air mass transfer coefficient [m/h]	0.0	0.0	0.0	0.0	0.0	0.0
Sediment-water mass transfer coefficient [m/h]	0.0	0.0	0.0	0.0	0.0	0.0
Sediment deposition rate [m/h]	0.0	0.0	0.0	0.0	0.0	0.0
Soil water run-off rate [m/h]	0.0	0.0	0.0	0.0	0.0	0.0
Output confidence factor	1.393	1.820	1.370	1.258	1.548	1.281

Table B-7: Output confidence factors and percentage contribution of input variables to the predicted water concentration for MTBE, TAME and ethanol in the EQC and ChemSA simulations

Input variable	Percentage contribution to water concentration variance					
	EQC			ChemSA		
	MTBE	TAME	Ethanol	MTBE	TAME	Ethanol
Area fraction of water of total surface area	3.0	2.7	1.4	0.5	0.5	0.7
Area fraction of soil of total surface area	0.0	0.0	0.0	0.0	0.0	0.0
Atmospheric height [m]	0.0	0.0	0.0	0.0	0.0	0.0
Water depth [m]	11.1	9.0	25.4	0.7	0.6	12.6
Soil depth [m]	0.0	0.0	0.0	0.0	0.0	3.0
Sediment depth [m]	0.0	0.0	0.0	0.0	0.0	0.0
Volume fraction of air phase in bulk soil	0.0	0.0	0.0	0.0	0.0	0.0
Volume fraction of water phase in bulk soil	0.0	0.0	0.0	0.0	0.0	2.8
Volume fraction of water phase in bulk sediment	0.0	0.0	0.0	0.0	0.0	0.0
Density of air [kg/m^3]	0.0	0.0	0.0	0.0	0.0	0.0
Density of water [kg/m^3]	0.8	0.7	0.4	0.1	0.1	0.2
Density of soil [kg/m^3]	0.0	0.0	0.0	0.0	0.0	0.0
Density of sediment [kg/m^3]	0.0	0.0	0.0	0.0	0.0	0.0
Density of suspended sediment [kg/m^3]	0.0	0.0	0.0	0.0	0.0	0.0
Organic carbon content (m/m) of soil	0.0	0.0	0.0	0.0	0.0	0.0
Organic carbon content (m/m) of sediment	0.0	0.0	0.0	0.0	0.0	0.0
Organic carbon content (m/m) of suspended sediment	0.0	0.0	0.0	0.0	0.0	0.0
Air advection residence time [h]	0.0	0.0	0.0	0.0	0.0	0.0
Water advection residence time [h]	5.6	4.5	0.0	2.5	2.2	0.0
Sediment advection residence time [h]	0.0	0.0	0.0	0.0	0.0	0.0
Organic carbon-water partition coefficient [L/kg]	0.0	0.0	0.0	0.0	0.0	0.0
Henry's constant [Pa.m^3/mol]	0.0	0.0	0.0	0.1	0.1	0.0
Half-life in air [h]	0.0	0.0	0.0	0.0	0.0	0.0
Half-life in surface water [h]	6.8	5.5	72.8	0.4	0.4	36.2
Half-life in soil [h]	0.0	0.0	0.0	0.0	0.0	22.1
Half-life in sediment [h]	0.0	0.0	0.0	0.0	0.0	0.0
Air-film (air/water) mass transfer coefficient [m/h]	10.2	6.4	0.0	3.2	2.2	0.0
Water-film (air/water) mass transfer coefficient [m/h]	58.9	69.1	0.0	18.7	23.3	0.0
Rain rate [m/h]	0.0	0.0	0.0	0.0	0.0	0.0
Soil particle-air mass transfer coefficient [m/h]	1.6	0.9	0.0	33.8	32.5	0.0
Soil particle-water mass transfer coefficient [m/h]	0.0	0.0	0.0	0.0	0.0	0.0
Surface soil-air mass transfer coefficient [m/h]	0.0	0.0	0.0	0.0	0.0	0.0
Sediment-water mass transfer coefficient [m/h]	0.0	0.0	0.0	0.0	0.0	0.0
Sediment deposition rate [m/h]	0.0	0.0	0.0	0.0	0.0	0.0
Soil water run-off rate [m/h]	2.1	1.2	0.0	39.9	38.0	22.3
Output confidence factor	1.157	1.177	1.373	2.342	2.320	1.888

Table B-8: Output confidence factors and percentage contribution of input variables to the predicted soil concentration for MTBE, TAME and ethanol in the EQC and ChemSA simulations

Input variable	Percentage contribution to soil concentration variance					
	EQC			ChemSA		
	MTBE	TAME	Ethanol	MTBE	TAME	Ethanol
Area fraction of water of total surface area	0.0	0.0	0.0	0.0	0.0	0.0
Area fraction of soil of total surface area	0.9	0.8	0.6	0.6	0.6	0.6
Atmospheric height [m]	0.0	0.0	0.0	0.0	0.0	0.0
Water depth [m]	0.0	0.0	0.0	0.0	0.0	0.0
Soil depth [m]	0.1	0.1	10.5	0.0	0.0	10.4
Sediment depth [m]	0.0	0.0	0.0	0.0	0.0	0.0
Volume fraction of air phase in bulk soil	0.0	0.0	0.0	0.4	0.4	0.0
Volume fraction of water phase in bulk soil	0.2	0.0	0.0	0.3	0.3	0.0
Volume fraction of water phase in bulk sediment	0.0	0.0	0.0	0.0	0.0	0.0
Density of air [kg/m^3]	0.0	0.0	0.0	0.0	0.0	0.0
Density of water [kg/m^3]	0.0	0.0	0.0	0.0	0.0	0.0
Density of soil [kg/m^3]	8.2	4.3	10.7	3.0	3.0	10.9
Density of sediment [kg/m^3]	0.0	0.0	0.0	0.0	0.0	0.0
Density of suspended sediment [kg/m^3]	0.0	0.0	0.0	0.0	0.0	0.0
Organic carbon content (m/m) of soil	1.5	3.2	0.0	19.4	19.4	0.0
Organic carbon content (m/m) of sediment	0.0	0.0	0.0	0.0	0.0	0.0
Organic carbon content (m/m) of suspended sediment	0.0	0.0	0.0	0.0	0.0	0.0
Air advection residence time [h]	0.0	0.0	0.0	0.0	0.0	0.0
Water advection residence time [h]	0.0	0.0	0.0	0.0	0.0	0.0
Sediment advection residence time [h]	0.0	0.0	0.0	0.0	0.0	0.0
Organic carbon-water partition coefficient [L/kg]	7.6	16.2	0.0	13.5	13.5	0.0
Henry's constant [Pa.m^3/mol]	0.2	0.1	0.0	0.1	0.1	0.0
Half-life in air [h]	0.0	0.0	0.0	0.0	0.0	0.0
Half-life in surface water [h]	0.0	0.0	0.0	0.0	0.0	0.0
Half-life in soil [h]	0.3	0.3	78.2	0.1	0.1	78.0
Half-life in sediment [h]	0.0	0.0	0.0	0.0	0.0	0.0
Air-film (air/water) mass transfer coefficient [m/h]	0.0	0.0	0.0	0.0	0.0	0.0
Water-film (air/water) mass transfer coefficient [m/h]	0.0	0.0	0.0	0.0	0.0	0.0
Rain rate [m/h]	0.0	0.0	0.0	0.0	0.0	0.0
Soil particle-air mass transfer coefficient [m/h]	80.0	74.5	0.0	62.2	62.2	0.0
Soil particle-water mass transfer coefficient [m/h]	0.0	0.0	0.0	0.0	0.0	0.0
Surface soil-air mass transfer coefficient [m/h]	0.0	0.0	0.0	0.0	0.0	0.0
Sediment-water mass transfer coefficient [m/h]	0.0	0.0	0.0	0.0	0.0	0.0
Sediment deposition rate [m/h]	0.0	0.0	0.0	0.0	0.0	0.0
Soil water run-off rate [m/h]	0.9	0.4	0.0	0.4	0.4	0.0
Output confidence factor	1.624	1.735	2.123	2.058	2.058	2.090

Table B-9: Output confidence factors and percentage contribution of input variables to the predicted sediment concentration for MTBE, TAME and ethanol in the EQC and ChemSA simulations

Input variable	Percentage contribution to sediment concentration variance					
	EQC			ChemSA		
	MTBE	TAME	Ethanol	MTBE	TAME	Ethanol
Area fraction of water of total surface area	2.0	1.8	0.4	0.5	0.5	0.3
Area fraction of soil of total surface area	0.0	0.0	0.0	0.0	0.0	0.0
Atmospheric height [m]	0.0	0.0	0.0	0.0	0.0	0.0
Water depth [m]	7.4	6.1	7.7	0.6	0.5	5.9
Soil depth [m]	0.0	0.0	0.0	0.0	0.0	1.4
Sediment depth [m]	0.1	0.1	5.5	0.0	0.0	4.2
Volume fraction of air phase in bulk soil	0.0	0.0	0.0	0.0	0.0	0.0
Volume fraction of water phase in bulk soil	0.0	0.0	0.0	0.0	0.0	1.3
Volume fraction of water phase in bulk sediment	0.2	0.1	0.0	1.0	0.3	0.1
Density of air [kg/m^3]	0.0	0.0	0.0	0.0	0.0	0.0
Density of water [kg/m^3]	0.0	0.0	0.0	0.0	0.0	0.0
Density of soil [kg/m^3]	0.0	0.0	0.0	0.0	0.0	0.0
Density of sediment [kg/m^3]	28.6	20.2	7.7	6.6	5.2	5.9
Density of suspended sediment [kg/m^3]	0.0	0.0	0.0	0.0	0.0	0.0
Organic carbon content (m/m) of soil	0.0	0.0	0.0	0.0	0.0	0.0
Organic carbon content (m/m) of sediment	0.5	1.7	0.0	0.9	3.1	0.0
Organic carbon content (m/m) of suspended sediment	0.0	0.0	0.0	0.0	0.0	0.0
Air advection residence time [h]	0.0	0.0	0.0	0.0	0.0	0.0
Water advection residence time [h]	3.7	3.0	0.0	2.2	2.0	0.0
Sediment advection residence time [h]	0.0	0.0	0.0	0.0	0.0	0.0
Organic carbon-water partition coefficient [L/kg]	3.1	9.8	0.0	0.6	2.2	0.0
Henry's constant [Pa.m^3/mol]	0.0	0.0	0.0	0.1	0.1	0.0
Half-life in air [h]	0.0	0.0	0.0	0.0	0.0	0.0
Half-life in surface water [h]	4.5	3.7	22.0	0.4	0.3	16.8
Half-life in soil [h]	0.0	0.0	0.0	0.0	0.0	10.2
Half-life in sediment [h]	0.5	0.6	16.1	0.1	0.2	12.4
Air-film (air/water) mass transfer coefficient [m/h]	6.8	4.3	0.0	2.9	1.9	0.0
Water-film (air/water) mass transfer coefficient [m/h]	39.3	46.6	0.0	16.9	20.7	0.0
Rain rate [m/h]	0.0	0.0	0.0	0.0	0.0	0.0
Soil particle-air mass transfer coefficient [m/h]	1.0	0.6	0.0	30.6	28.9	0.0
Soil particle-water mass transfer coefficient [m/h]	0.0	0.0	0.0	0.0	0.0	0.0
Surface soil-air mass transfer coefficient [m/h]	0.0	0.0	0.0	0.0	0.0	0.0
Sediment-water mass transfer coefficient [m/h]	0.5	0.5	40.6	0.1	0.1	31.1
Sediment deposition rate [m/h]	0.0	0.1	0.0	0.0	0.0	0.0
Soil water run-off rate [m/h]	1.4	0.8	0.0	36.2	33.8	10.3
Output confidence factor	1.244	1.274	2.859	2.558	2.574	3.938

Table B-10: Output confidence factors and percentage contribution of input variables to the predicted advection persistence for MTBE, TAME and ethanol in the EQC and ChemSA simulations

Input variable	Percentage contribution to advection persistence variance					
	EQC			ChemSA		
	MTBE	TAME	Ethanol	MTBE	TAME	Ethanol
Area fraction of water of total surface area	0.0	0.0	0.0	0.0	0.0	0.0
Area fraction of soil of total surface area	0.0	0.0	0.0	0.0	0.0	0.0
Atmospheric height [m]	0.0	0.0	0.0	0.0	0.0	0.0
Water depth [m]	3.1	1.3	0.0	0.2	0.1	0.0
Soil depth [m]	2.8	2.4	0.0	5.5	4.7	0.0
Sediment depth [m]	0.0	0.0	0.0	0.0	0.0	0.0
Volume fraction of air phase in bulk soil	0.0	0.0	0.0	0.1	0.2	0.0
Volume fraction of water phase in bulk soil	0.0	0.0	0.0	1.2	0.2	0.0
Volume fraction of water phase in bulk sediment	0.0	0.0	0.0	0.0	0.0	0.0
Density of air [kg/m^3]	0.0	0.0	0.0	0.0	0.0	0.0
Density of water [kg/m^3]	0.0	0.0	0.0	0.0	0.0	0.0
Density of soil [kg/m^3]	0.3	0.6	0.0	0.6	1.2	0.0
Density of sediment [kg/m^3]	0.0	0.0	0.0	0.0	0.0	0.0
Density of suspended sediment [kg/m^3]	0.0	0.0	0.0	0.0	0.0	0.0
Organic carbon content (m/m) of soil	0.3	0.6	0.0	4.3	8.7	0.0
Organic carbon content (m/m) of sediment	0.0	0.0	0.0	0.0	0.0	0.0
Organic carbon content (m/m) of suspended sediment	0.0	0.0	0.0	0.0	0.0	0.0
Air advection residence time [h]	11.5	8.4	43.4	26.3	14.3	84.6
Water advection residence time [h]	3.7	4.0	0.2	0.2	0.1	0.0
Sediment advection residence time [h]	0.0	0.0	0.0	0.0	0.0	0.0
Organic carbon-water partition coefficient [L/kg]	1.5	3.1	0.0	3.0	6.1	0.0
Henry's constant [Pa.m^3/mol]	0.1	0.0	0.0	0.1	0.1	0.0
Half-life in air [h]	43.3	56.5	30.5	12.2	27.9	3.2
Half-life in surface water [h]	0.2	0.1	10.6	0.0	0.0	0.0
Half-life in soil [h]	0.0	0.0	15.2	0.0	0.0	12.2
Half-life in sediment [h]	0.0	0.0	0.0	0.0	0.0	0.0
Air-film (air/water) mass transfer coefficient [m/h]	1.8	0.5	0.0	0.1	0.0	0.0
Water-film (air/water) mass transfer coefficient [m/h]	10.6	5.7	0.0	0.7	0.3	0.0
Rain rate [m/h]	0.0	0.0	0.0	0.0	0.0	0.0
Soil particle-air mass transfer coefficient [m/h]	20.8	16.7	0.0	45.2	36.1	0.0
Soil particle-water mass transfer coefficient [m/h]	0.0	0.0	0.0	0.0	0.0	0.0
Surface soil-air mass transfer coefficient [m/h]	0.0	0.0	0.0	0.0	0.0	0.0
Sediment-water mass transfer coefficient [m/h]	0.0	0.0	0.0	0.0	0.0	0.0
Sediment deposition rate [m/h]	0.0	0.0	0.0	0.0	0.0	0.0
Soil water run-off rate [m/h]	0.0	0.0	0.0	0.3	0.1	0.0
Output confidence factor	1.184	1.307	1.131	1.174	1.412	1.088

Table B-11: Output confidence factors and percentage contribution of input variables to the predicted reaction persistence for MTBE, TAME and ethanol in the EQC and ChemSA simulations

Input variable	Percentage contribution to reaction persistence variance					
	EQC			ChemSA		
	MTBE	TAME	Ethanol	MTBE	TAME	Ethanol
Area fraction of water of total surface area	0.0	0.0	0.0	0.0	0.0	0.0
Area fraction of soil of total surface area	0.0	0.0	0.0	0.0	0.0	0.0
Atmospheric height [m]	0.0	0.0	0.0	0.0	0.0	0.0
Water depth [m]	2.3	4.9	0.0	0.0	0.1	0.0
Soil depth [m]	0.8	2.1	0.0	1.0	2.4	0.0
Sediment depth [m]	0.0	0.0	0.0	0.0	0.0	0.0
Volume fraction of air phase in bulk soil	0.0	0.0	0.0	0.0	0.1	0.0
Volume fraction of water phase in bulk soil	0.0	0.0	0.0	0.2	0.1	0.0
Volume fraction of water phase in bulk sediment	0.0	0.0	0.0	0.0	0.0	0.0
Density of air [kg/m^3]	0.0	0.0	0.0	0.0	0.0	0.0
Density of water [kg/m^3]	0.0	0.0	0.0	0.0	0.0	0.0
Density of soil [kg/m^3]	0.1	0.5	0.0	0.1	0.6	0.0
Density of sediment [kg/m^3]	0.0	0.0	0.0	0.0	0.0	0.0
Density of suspended sediment [kg/m^3]	0.0	0.0	0.0	0.0	0.0	0.0
Organic carbon content (m/m) of soil	0.1	0.5	0.0	0.7	4.5	0.0
Organic carbon content (m/m) of sediment	0.0	0.0	0.0	0.0	0.0	0.0
Organic carbon content (m/m) of suspended sediment	0.0	0.0	0.0	0.0	0.0	0.0
Air advection residence time [h]	2.3	1.5	0.6	0.7	0.6	0.5
Water advection residence time [h]	0.2	0.3	0.0	0.0	0.0	0.0
Sediment advection residence time [h]	0.0	0.0	0.0	0.0	0.0	0.0
Organic carbon-water partition coefficient [L/kg]	0.4	2.7	0.0	0.5	3.1	0.0
Henry's constant [Pa.m^3/mol]	0.0	0.1	0.0	0.0	0.0	0.0
Half-life in air [h]	74.4	45.0	71.8	88.0	69.0	96.0
Half-life in surface water [h]	3.1	2.8	14.1	0.0	0.0	0.0
Half-life in soil [h]	0.2	0.2	13.5	0.1	0.1	3.4
Half-life in sediment [h]	0.0	0.0	0.0	0.0	0.0	0.0
Air-film (air/water) mass transfer coefficient [m/h]	1.4	1.9	0.0	0.0	0.0	0.0
Water-film (air/water) mass transfer coefficient [m/h]	7.9	20.7	0.0	0.1	0.2	0.0
Rain rate [m/h]	0.0	0.0	0.0	0.0	0.0	0.0
Soil particle-air mass transfer coefficient [m/h]	6.7	16.7	0.0	8.3	19.1	0.0
Soil particle-water mass transfer coefficient [m/h]	0.0	0.0	0.0	0.0	0.0	0.0
Surface soil-air mass transfer coefficient [m/h]	0.0	0.0	0.0	0.0	0.0	0.0
Sediment-water mass transfer coefficient [m/h]	0.0	0.0	0.0	0.0	0.0	0.0
Sediment deposition rate [m/h]	0.1	0.1	0.0	0.1	0.1	0.0
Soil water run-off rate [m/h]	0.0	0.0	0.0	0.0	0.0	0.0
Output confidence factor	1.445	1.272	1.156	2.108	1.851	1.371

Table B-12: Output confidence factors and percentage contribution of input variables to the predicted overall persistence for MTBE, TAME and ethanol in the EQC and ChemSA simulations

Input variable	Percentage contribution to overall persistence variance					
	EQC			ChemSA		
	MTBE	TAME	Ethanol	MTBE	TAME	Ethanol
Area fraction of water of total surface area	0.0	0.0	0.0	0.0	0.0	0.0
Area fraction of soil of total surface area	0.0	0.0	0.0	0.0	0.0	0.0
Atmospheric height [m]	0.0	0.0	0.0	0.0	0.0	0.0
Water depth [m]	7.5	7.1	0.0	0.2	0.1	0.0
Soil depth [m]	4.3	4.5	0.0	5.8	5.7	0.0
Sediment depth [m]	0.0	0.0	0.0	0.0	0.0	0.0
Volume fraction of air phase in bulk soil	0.0	0.0	0.0	0.1	0.2	0.0
Volume fraction of water phase in bulk soil	0.1	0.0	0.0	1.3	0.2	0.0
Volume fraction of water phase in bulk sediment	0.0	0.0	0.0	0.0	0.0	0.0
Density of air [kg/m^3]	0.0	0.0	0.0	0.0	0.0	0.0
Density of water [kg/m^3]	0.0	0.0	0.0	0.0	0.0	0.0
Density of soil [kg/m^3]	0.5	1.2	0.0	0.6	1.5	0.0
Density of sediment [kg/m^3]	0.0	0.0	0.0	0.0	0.0	0.0
Density of suspended sediment [kg/m^3]	0.0	0.0	0.0	0.0	0.0	0.0
Organic carbon content (m/m) of soil	0.5	1.2	0.0	4.5	10.7	0.0
Organic carbon content (m/m) of sediment	0.0	0.0	0.0	0.0	0.0	0.0
Organic carbon content (m/m) of suspended sediment	0.0	0.0	0.0	0.0	0.0	0.0
Air advection residence time [h]	1.1	0.1	2.6	8.1	1.0	11.1
Water advection residence time [h]	3.4	2.4	0.0	0.1	0.1	0.0
Sediment advection residence time [h]	0.0	0.0	0.0	0.0	0.0	0.0
Organic carbon-water partition coefficient [L/kg]	2.3	5.9	0.0	3.1	7.5	0.0
Henry's constant [Pa.m^3/mol]	0.1	0.1	0.0	0.1	0.1	0.0
Half-life in air [h]	11.1	6.8	61.6	25.9	26.8	81.0
Half-life in surface water [h]	4.1	2.9	17.9	0.0	0.0	0.0
Half-life in soil [h]	0.3	0.2	17.9	0.1	0.1	7.9
Half-life in sediment [h]	0.0	0.0	0.0	0.0	0.0	0.0
Air-film (air/water) mass transfer coefficient [m/h]	4.5	2.8	0.0	0.1	0.0	0.0
Water-film (air/water) mass transfer coefficient [m/h]	25.9	30.1	0.0	0.8	0.5	0.0
Rain rate [m/h]	0.0	0.0	0.0	0.0	0.0	0.0
Soil particle-air mass transfer coefficient [m/h]	34.2	34.7	0.0	48.5	45.3	0.0
Soil particle-water mass transfer coefficient [m/h]	0.0	0.0	0.0	0.0	0.0	0.0
Surface soil-air mass transfer coefficient [m/h]	0.0	0.0	0.0	0.0	0.0	0.0
Sediment-water mass transfer coefficient [m/h]	0.0	0.0	0.0	0.0	0.0	0.0
Sediment deposition rate [m/h]	0.0	0.0	0.0	0.0	0.0	0.0
Soil water run-off rate [m/h]	0.2	0.1	0.0	0.4	0.2	0.0
Output confidence factor	1.092	1.127	1.115	1.152	1.305	1.145

B-5 Parameterisation of ChemSA model to South African conditions

The surface area of South Africa and the average national rainfall rate are reported in Schulze et al. (1997). A stable mixing atmospheric height was estimated from Piketh et al. (1999). This was taken as the altitude difference between the reported 700 hPa stable air layer and the interior plateau of the country. The active soil depth was changed to 10 cm, which has been utilised by other authors on parameterisation of fate models to national conditions (Mackay et al., 1991; Kawamoto et al., 2001).

The water fraction of the total surface area was estimated by summing up the total surface area of all documented dams in South Africa. Individual dam surface areas are reported in Midgley et al. (1994). Dam volumetric capacities are also reported in Midgley et al. (1994). The average water depth was estimated from the quotient of the summed dam capacities divided by the summed surface areas.

An estimate of the air residence time was calculated from Piketh et al. (1999). This reference quotes a net re-circulation rate of aerosols over South Africa of 60 Tg per annum. On assuming the height of the troposphere to be 10 km and assuming an average background aerosol concentration of 30 μg/m^3, as suggested by Mackay (2001), the air residence time was estimated as follows:

$$\text{Air residence time} = \frac{(\text{Surface area of South Africa})(\text{Troposphere height})}{(\text{aerosol loading})/TSP}$$

$$= \left(\frac{(1267676x10^{6})(10x10^{3})}{60x10^{12}/30x10^{-6}} \right) \left(\frac{365\,days}{1\,year} \right) = 2.3\,days$$

B-6 Program written for computation of Level III models

The following program was written in the Matlab programming language for solution of the Level III simulations. The program displayed below is for the ChemSA MTBE simulation and includes the uncertainty analysis. (Comments are denoted with a "%' in the program code).

```
%SA LEVEL III
%With numerical sensitivity analysis centered around MacLeod(2002)
parameters

%Compartment dimensions
%This is accepted as representing a suitably sized evaluative
environment
%Mackay (1991)

%Environment composed of 4 compartments and 7 sub-compartments
% 1. Air: bulk and sub-compartment
% 2. Water: bulk and sub-compartment
% 3. Soil: bulk and sub-compartment
% 4. Sediment Solids: bulk and sub-compartment
% 5. Suspended sediment: sub-compartment
% 6. Fish: sub-compartment
% 7. Aerosol: sub-compartment

%Compartment Dimensions and Properties
clear all
clc


for i=1:1:52

%Variables
%Declaration of variables for sensitivity analysis


% Landscape parameters
s(2)=1.267676E+12;      %Area of model (m2)*
s(3)=0.0023;            %Area fraction of water (=sed) of total
surface area*
s(4)=0.9977;            %Area fraction of soil of total surface area*
s(5)=1500;              %Atmospheric height (m)*
s(6)=9;                 %Water depth (m)*
s(7)=0.1;               %Soil depth (m)*
s(8)=0.05;              %Sediment depth (m)


s(9)=2e-11;     %Volume fraction of aerosol in bulk air
s(10)=5e-6;     %Volume fraction of suspended sediment in bulk water
s(11)=1e-6;     %Volume fraction of fish in bulk water
s(12)=0.2;      %Volume fraction of air phase in bulk soil
s(13)=0.3;      %Volume fraction of water phase in bulk soil
s(14)=0.8;      %Volume fraction of water phase in bulk sediment

s(15)=1.185;    %Density of air (kg/m3)
s(16)=1000;     %Density of water (kg/m3)
```

```
s(17)=2400;     %Density of soil (kg/m3)
s(18)=2400;     %Density of sediment (kg/m3)
s(19)=1500;     %Density of susp. sediment(kg/m3)
s(20)=1000;     %Density of fish (kg/m3)

s(21)=0.02;     %Org C. content (m/m) of soil
s(22)=0.04;     %Org C. content (m/m) of sediment
s(23)=0.2;      %Org C. content (m/m) of susp. sediment
s(24)=0.05;     %Lipid volume fraction of fish
s(25)=56;       %Air advection res. time (h)*
s(26)=1000;     %Water advection res. time (h)
s(27)=50000;    %Sediment advection res. time (h)


%Chemical Parameters
s(28)=42000;    %Water mass solubility (g/m3)
s(29)=33360;    %Vapour pressure (Pa);
s(30)=1.24;     %Log Octanol-water partition coefficient
s(31)=6.1;      %Organic carbon-water partition coefficient (L/kg)
s(32)=59.5;     %Henry's constant (Pa.m3/mol)

MM=88.150;      %Molecular mass in g/mol;
T_C=25;         %Temperature of parameters (degrees C)

s(33)=74;       %Half-life in air (h)
s(34)=1700;     %Half-life in surface water (h)
s(35)=1270;     %Half-life in soil (h)
s(36)=6815;     %Half-life in sediment (h)

%Emission rates (kg/h)
s(37)=19015.14;   %Air emission
s(38)=131.2;      %Water emission
s(39)=7026.4;     %Soil emission
s(40)=0;          %Sediment emission

%Transport parameters
s(41)=5;          %Air-film (air/water)MTC (m/h)
s(42)=0.05;       %Water-film (air/water)MTC (m/h)
s(43)=5.2740e-5;  %Rain rate (m/h) [corresponds to 0.462 m/a]*
s(44)=6e-10;      %Aerosol deposition rate(m/h)
s(45)=0.02;       %Soil particle-air MTC (m/h)
s(46)=1e-5;       %Soil particle-water MTC (m/h)
s(47)=5;          %Surface soil-air MTC (m/h)
s(48)=1e-4;       %Sediment-water MTC (m/h)
s(49)=5e-7;       %Sediment deposition rate (m/h)
s(50)=2e-7;       %Sediment resuspension rate (m/h)
s(51)=5e-5;       %Soil water runoff rate (m/h)
s(52)=1e-8;       %Soil solids runoff rate (m/h)


%%%%%%%%%%%%%%%%%%%%%%%%%%%%%%%%%%%%%%%%%%%%%%%%%%%%%%%%%%%%%%%%%%%%%%%%%%%%
%Forward Bias

s(i)=1.01*s(i);


%%%%%%%%%%%%%%%%%%%%%%%%%%%%%%%%%%%%%%%%%%%%%%%%%%%%%%%%%%%%%%%%%%%%%%%%%%%%
```

```
%Air Compartment
V1=s(2)*s(5);          %Bulk air volume(m3)
theta17=s(9);          %Volume fraction of aerosol in bulk air

theta11=1-theta17;     %Volume fraction of air phase in bulk air
V11=theta11*V1;        %Volume of air phase in bulk air (m3)
V17=theta17*V1;        %Volume of aerosol in bulk air (m3)


%Water Compartment
Aw=s(2)*s(3);              %Interfacial area of water (m2)
V2=Aw*s(6);                %Bulk water volume(m3)
theta25=s(10);             %Volume fraction of suspended sediment in bulk
water
theta26=s(11);             %Volume fraction of fish in bulk water

theta22=1-theta25-theta26; %Volume fraction of water phase in bulk
water
V22=theta22*V2;                %Volume of water phase in bulk water (m3)
V25=theta25*V2;                %Volume of suspended sediment in bulk water
(m3)
V26=theta26*V2;                %Volume of fish in bulk water (m3)


%Soil Compartment
As=s(2)*s(4);                  %Interfacial area of soil (m2)
V3=As*s(7);                    %Bulk soil volume (m3)
theta31=s(12);                 %Volume fraction of air phase in bulk soil
theta32=s(13);                 %Volume fraction of water phase in bulk
soil

theta33=1-theta31-theta32; % Volume fraction of soil solids in bulk
soil
V31=theta31*V3;                %Volume of air phase in bulk soil (m3)
V32=theta31*V3;                %Volume of water phase in bulk soil (m3)
V33=theta33*V3;                %Volume of soil solids in bulk soil (m3)


%Sediment compartmnet
V4=s(2)*s(3)*s(8);             %Bulk sediment (m3)
theta42=s(14);                 %Volume fraction of water phase in bulk
sediment

theta44=1-theta42;             %Volume fraction of sediment solids in bulk
sediment
V42=theta42*V4;                %Volume of water phase in bulk sediment
V44=theta44*V4;                %Volume of sediment solids in bulk sediment


%Compartmental densities (kg/m3)
rho1=s(15);    %Density of air
rho2=s(16);    %Density of water
rho3=s(17);    %Density of soil
rho4=s(18);    %Density of sediment
rho5=s(19);    %Density of susp. sediment
rho6=s(20);    %Density of fish

%Fraction organic carbon content of sub-compartments (m/m)
y3=s(21);      %Org C. content (m/m) of soil
y4=s(22);      %Org C. content (m/m) of sediment
y5=s(23);      %Org C. content (m/m) of susp. sediment
```

```
%Fraction lipid content of sub-compartment (v/v)
y6=s(24);       %Lipid Volume fraction of fish


%Advection parameters
tau1=s(25);     %Air advection res. time (h)
tau2=s(26);     %Water advection res. time (h)
tau4=s(27);     %Sediment advection res. time (h)

G1=V1/tau1;     %Air advection flow (m3/h)
G2=V2/tau2;     %Water advection flow (m3/h)
G3=0;
G4=V4/tau4;     %Sediment advection flow (m3/h)

%Chemical Properties
MassWS=s(28);           %Water mass solubility (g/m3)
VP=s(29);               %Vapour pressure (Pa)
LogKow=s(30);           %Log Octanol Water partition coefficient
Koc=s(31);              %Alternative: Koc=0.41*10^(LogKow)
H=s(32);                %Henry's constant (Pa.m3/mol)

half_t1=s(33);          %half life in air (h)
half_t2=s(34);          %half life in water (h)
half_t3=s(35);          %half life in soil (h)
half_t4=s(36);          %half life in sediment (h)

Emission1=s(37);        %Air emission in kg/h
Emission2=s(38);        %Water emission in kg/h
Emission3=s(39);        %Soil emission in kg/h
Emission4=s(40);        %Sediment emission in kg/h

E1=Emission1*1000/MM;   %Air emission in mol/h
E2=Emission2*1000/MM;   %Water emission in mol/h
E3=Emission3*1000/MM;   %Soil emission in mol/h
E4=Emission4*1000/MM;   %Sediment emission in mol/h


%Calculated:
Cs=MassWS/MM;         %Molar water solubility (mol/m3)
k1=log(2)/half_t1;    %First order reaction rate in air (h)
k2=log(2)/half_t2;    %First order reaction rate in water (h)
k3=log(2)/half_t3;    %First order reaction rate in soil (h)
k4=log(2)/half_t4;    %First order reaction rate in sediment (h)


%Z values (mol/Pa.m3)
R=8.314; % Gas constant in J/mol.K
T=T_C+273.15; % temp in Kelvin

Z1=1/(R*T);
Z2=1/H;
Z3=Z2*rho3*y3*Koc/1000;
Z4=Z2*rho4*y4*Koc/1000;
Z5=Z2*rho5*y5*Koc/1000;
Z6=Z2*rho6*y6*(10^LogKow)/1000;
Z7=Z1*6e6/VP; %Mackay 2001 recommended
```

```
%Bulk Z values (mol/Pa.m3)
ZB1=theta11*Z1+theta17*Z7;
ZB2=theta22*Z2+theta25*Z5+theta26*Z6;
ZB3=theta31*Z1+theta32*Z2+theta33*Z3;
ZB4=theta42*Z2+theta44*Z4;


%Intermedia transport properties (m/h)
U1=s(41);
U2=s(42);
U3=s(43);
U4=s(44);
U5=s(45);
U6=s(46);
U7=s(47);
U8=s(48);
U9=s(49);
U10=s(50);
U11=s(51);
U12=s(52);


%Intermedia D values (mol/Pa.h)
D12=1/(1/(U1*Aw*Z1)+1/(U2*Aw*Z2)) +(U3*Aw*Z2)+(U4*Aw*Z7);
D21=1/(1/(U1*Aw*Z1)+1/(U2*Aw*Z2));
D13=1/(1/(U7*As*Z1)+1/(U6*As*Z2+U5*As*Z1))+(U3*As*Z2)+(U4*As*Z7);
D31=1/(1/(U7*As*Z1)+1/(U6*As*Z2+U5*As*Z1));
D24=U8*Aw*Z2+U9*Aw*Z5;
D42=U8*Aw*Z2+U10*Aw*Z4;
D32=U11*As*Z2+U12*As*Z3;


%Reaction D values (mol/Pa.h)
Dr1=V1*k1*ZB1;
Dr2=V2*k2*ZB2;
Dr3=V3*k3*ZB3;
Dr4=V4*k4*ZB4;


%Advection D values (mol/Pa.h)
Da1=G1*ZB1;
Da2=G2*ZB2;
Da3=G3*ZB3;
Da4=G4*ZB4;


%MATRIX NOTATION
%State matrix
SM=[-(Dr1+Da1+D12+D13)./(V1*ZB1)     D21./(V1*ZB1)   D31./(V1*ZB1)
   0;...
D12./(V2*ZB2) -(Dr2+Da2+D21+D24)./(V2*ZB2)
D32./(V2*ZB2)D42./(V2*ZB2);...
D13./(V3*ZB3)      0      (Dr3+Da3+D31+D32)./(V3*ZB3)       0;...
0      D24./(V4*ZB4)   0      -(Dr4+Da4+D42)./(V4*ZB4)];

%Forcing atrix
FM=[E1./(V1*ZB1);E2./(V2*ZB2);E3./(V3*ZB3);E4./(V4*ZB4)];


fugacity=inv(SM)*(-FM);
```

```
Dr=[Dr1;Dr2;Dr3;Dr4];
Da=[Da1;Da2;Da3;Da4];
ZB=[ZB1;ZB2;ZB3;ZB4];
V=[V1;V2;V3;V4];


holdup=  sum(V.*ZB.*fugacity);      %holdup in environment of chemical
based on calculated concentrations
tau_adv(i)=holdup/sum(Da.*fugacity);
tau_reac(i)=holdup/sum(Dr.*fugacity);
tau(i)=1/((1/tau_adv(i))+(1/tau_reac(i)));


dtau_a(i)=(tau_adv(i)-tau_adv(1))./tau_adv(1);
dtau_r(i)=(tau_reac(i)-tau_reac(1))./tau_reac(1);
dtau(i)=(tau(i)-tau(1))./tau(1);


rhob1=theta11*rho1+theta17*1.5;
rhob2=theta22*rho2+theta25*rho5+theta26*rho6;
rhob3=theta31*rho1+theta32*rho2+theta33*rho3;
rhob4=theta42*rho2+theta44*rho4;


%mass based part per million (ug/g)
ppm_air(i)=1000*fugacity(1)*MM*ZB1/rho1;
ppm_water(i)=1000*fugacity(2)*MM*ZB2/rho2;
ppm_soil(i)=1000*fugacity(3)*MM*ZB3/rho3;
ppm_sediment(i)=1000*fugacity(4)*MM*ZB4/rho4;


da(i)=(ppm_air(i)-ppm_air(1))./ppm_air(1);
dw(i)=(ppm_water(i)-ppm_water(1))./ppm_water(1);
dsoil(i)=(ppm_soil(i)-ppm_soil(1))./ppm_soil(1);
dsed(i)=(ppm_sediment(i)-ppm_sediment(1))./ppm_sediment(1);


end


%Print base case results
ppm_air(1)
ppm_water(1)
ppm_soil(1)
ppm_sediment(1)

tau_adv(1)
tau_reac(1)
tau(1)


sensitivty_da=da(2:52)'./(0.01);
sensitivty_dw=dw(2:52)'./(0.01);
sensitivty_dsoil=dsoil(2:52)'./(0.01);
sensitivty_dsed=dsed(2:52)'./(0.01);
sensitivty_dtau_a=dtau_a(2:52)'./(0.01);
sensitivty_dtau_r=dtau_r(2:52)'./(0.01);
sensitivty_dtau=dtau(2:52)'./(0.01);
```

```
%%%%%%%%%%%%%%%%%%%%%%%%%%%%%%%%%%%%%%%%%%%%%%%%%%%%%%%%%%%
%Uncertainty analysis begins

%CFinputs=GetConfidenceFactors

CFinputs(1,1)=1;          %Area of model (m2)
CFinputs(2,1)=1.1;        %Area fraction of water (=sed) of total
surface area
CFinputs(3,1)=1.1;        %Area fraction of soil of total surface area
CFinputs(4,1)=1.5;        %Atmospheric height (m)
CFinputs(5,1)=1.5;        %Water depth (m)
CFinputs(6,1)=1.5;        %Soil depth (m)
CFinputs(7,1)=1.5;        %Sediment depth (m)


CFinputs(8,1)=3;          %Volume fraction of aerosol in bulk air
CFinputs(9,1)=3;          %Volume fraction of suspended sediment in bulk
water
CFinputs(10,1)=3;         %Volume fraction of fish in bulk water
CFinputs(11,1)=1.5;       %Volume fraction of air phase in bulk soil [
1.5 for SA as no source]
CFinputs(12,1)=1.5;       %Volume fraction of water phase in bulk soil [
1.5 for SA as no source]
CFinputs(13,1)=1.5;       %Volume fraction of water phase in bulk
sediment [ 1.5 for SA as no source]

CFinputs(14,1)=1.05;      %Density of air (kg/m3)
CFinputs(15,1)=1.05;      %Density of water (kg/m3)
CFinputs(16,1)=1.5;       %Density of soil (kg/m3)
CFinputs(17,1)=1.5;       %Density of sediment (kg/m3)
CFinputs(18,1)=1.5;       %Density of susp. sediment(kg/m3)
CFinputs(19,1)=1.5;       %Density of fish (kg/m3)

CFinputs(20,1)=3;      %Org C. content (m/m) of soil
CFinputs(21,1)=3;      %Org C. content (m/m) of sediment
CFinputs(22,1)=3;      %Org C. content (m/m) of susp. sediment
CFinputs(23,1)=3;      %Lipid volume fraction of fish [Variation in fish
from Campfens and Mackay]

CFinputs(24,1)=1.5;       %Air advection res. time (h)
CFinputs(25,1)=3;         %Water advection res. time (h) [ 3 for SA as
no source]
CFinputs(26,1)=3;         %Sediment advection res. time (h) [ 3 for SA
as no source]


%Chemical Parameters
CFinputs(27,1)=1.5 ;      %Water mass solubility (g/m3)
CFinputs(28,1)=1.05;      %Vapour pressure (Pa) [Accuracy high]
CFinputs(29,1)=1.4;       %Log Octanol-water partition coefficient[
Variation in MTBE eperimental scatter]
CFinputs(30,1)=2.5;       %Organic carbon-water partition coefficient
(L/kg) [Seth et al. 1997]
CFinputs(31,1)=1.05;      %Henry's cosntant (Pa.m3/mol) [Measured in
this study]

CFinputs(32,1)=4;         %Half-life in air (h) [Estimated from Howard
et al 1991]
CFinputs(33,1)=3;         %Half-life in surface water (h) [Estimated
from Howard et al 1991]
```

```
CFinputs(34,1)=2;        %Half-life in soil (h) [Estimated from Howard
et al 1991]
CFinputs(35,1)=3;        %Half-life in sediment (h) [Estimated from
Howard et al 1991]


%Emission rates (kg/h) [Within evaluative framework not an important]
CFinputs(36,1)=1;        %Air emission
CFinputs(37,1)=1;        %Water emission
CFinputs(38,1)=1;        %Soil emission
CFinputs(39,1)=1;        %Sediment emission

%Transport parameters
CFinputs(40,1)=3;     %Air-film (air/water)MTC (m/h)
CFinputs(41,1)=3;     %Water-film (air/water)MTC (m/h)
CFinputs(42,1)=3;     %Rain rate (m/h) [corresponds to 0.876 m.a]
CFinputs(43,1)=3;     %Aerosol deposition rate(m/h)
CFinputs(44,1)=3;     %Soil particle-air MTC (m/h)
CFinputs(45,1)=3;     %Soil particle-water MTC (m/h)
CFinputs(46,1)=3;     %Surface soil-air MTC (m/h)
CFinputs(47,1)=3;     %Sediment-water MTC (m/h)
CFinputs(48,1)=3;     %Sediment deposition rate (m/h)
CFinputs(49,1)=3;     %Sediment resuspension rate (m/h)
CFinputs(50,1)=3;     %Soil water runoff rate (m/h)
CFinputs(51,1)=3;     %Soil solids runoff rate (m/h)


%CFoutputs

CF_da=(exp(sum(((sensitivty_da.^2).* ((log(CFinputs)).^2)))))^(0.5)
CF_dw=exp(sum(((sensitivty_dw.^2).* ((log(CFinputs)).^2)))))^(0.5)
CF_dsoil=exp(sum(((sensitivty_dsoil.^2).*
((log(CFinputs)).^2)))))^(0.5)
CF_dsed=exp(sum(((sensitivty_dsed.^2).* ((log(CFinputs)).^2)))))^(0.5)
CF_dtau_a=exp(sum(((sensitivty_dtau_a.^2).*
((log(CFinputs)).^2)))))^(0.5)
CF_dtau_r=exp(sum(((sensitivty_dtau_r.^2).*
((log(CFinputs)).^2)))))^(0.5)
CF_dtau=exp(sum(((sensitivty_dtau.^2).* ((log(CFinputs)).^2)))))^(0.5)


%Contribution to variance

Denominator_da=sum(((sensitivty_da.^2).* ((log(CFinputs)).^2)));
Denominator_dw=sum(((sensitivty_dw.^2).* ((log(CFinputs)).^2)));
Denominator_dsoil=sum(((sensitivty_dsoil.^2).* ((log(CFinputs)).^2)));
Denominator_dsed=sum(((sensitivty_dsed.^2).* ((log(CFinputs)).^2)));
Denominator_dtau_a=sum(((sensitivty_dtau_a.^2).*
((log(CFinputs)).^2)));
Denominator_dtau_r=sum(((sensitivty_dtau_r.^2).*
((log(CFinputs)).^2)));
Denominator_dtau=sum(((sensitivty_dtau.^2).* ((log(CFinputs)).^2)));
```

```
for count=1:1:length(CFinputs)

Contribution_to_variance_da(count,1)=100*((sensitivty_da(count)^2)*
((log(CFinputs(count)))^2))/Denominator_da;
Contribution_to_variance_dw(count,1)=100*((sensitivty_dw(count)^2)*
((log(CFinputs(count)))^2))/Denominator_dw;
Contribution_to_variance_dsoil(count,1)=100*((sensitivty_dsoil(count)^
2)* ((log(CFinputs(count)))^2))/Denominator_dsoil;
Contribution_to_variance_dsed(count,1)=100*((sensitivty_dsed(count)^2)
* ((log(CFinputs(count)))^2))/Denominator_dsed;
Contribution_to_variance_dtau_a(count,1)=100*((sensitivty_dtau_a(count
)^2)* ((log(CFinputs(count)))^2))/Denominator_dtau_a;
Contribution_to_variance_dtau_r(count,1)=100*((sensitivty_dtau_r(count
).^2)* ((log(CFinputs(count)))^2))/Denominator_dtau_r;
Contribution_to_variance_dtau(count,1)=100*((sensitivty_dtau(count)^2)
* ((log(CFinputs(count)))^2))/Denominator_dtau;
end


Contribution_to_variance_da
Contribution_to_variance_dw
Contribution_to_variance_dsoil
Contribution_to_variance_dsed
Contribution_to_variance_dtau_a
Contribution_to_variance_dtau_r
Contribution_to_variance_dtau
```

B-7 Program written for computation of Level IV models

The following program was written in the Matlab programming language for solution of the Level IV simulations. The program displayed below is for the ChemSA MTBE simulation. (Comments are denoted with a "%' in the program code). This model included a fugacity settling time algorithm different from the method suggested by Bru et al. (1998).

```
%Level IV model customised to SA conditions

clf
clc
clear

global SM


% Landscape parameters
s(2)=1.267676E+12;      %Area of model (m2)*
s(3)=0.0023;            %Areal fraction of water (=sed) of total
surface area*
s(4)=0.9977;            %Areal fraction of soil of total surface area*
s(5)=1500;              %Atmospheric height (m)*
s(6)=9;                 %Water depth (m)*
s(7)=0.1;               %Soil depth (m)*
s(8)=0.05;              %Sediment depth (m)


s(9)=2e-11;     %Volume fraction of aerosol in bulk air
s(10)=5e-6;     %Volume fraction of suspended sediment in bulk water
s(11)=1e-6;     %Volume fraction of fish in bulk water
s(12)=0.2;      %Volume fraction of air phase in bulk soil
s(13)=0.3;      %Volume fraction of water phase in bulk soil
s(14)=0.8;      %Volume fraction of water phase in bulk sediment

s(15)=1.185;    %Density of air (kg/m3)
s(16)=1000;     %Density of water (kg/m3)
s(17)=2400;     %Density of soil (kg/m3)
s(18)=2400;     %Density of sediment (kg/m3)
s(19)=1500;     %Density of susp. sediment(kg/m3)
s(20)=1000;     %Density of fish (kg/m3)

s(21)=0.02;     %Org C. content (m/m) of soil
s(22)=0.04;     %Org C. content (m/m) of sediment
s(23)=0.2;      %Org C. content (m/m) of susp. sediment
s(24)=0.05;     %Lipid volume fraction of fish
s(25)=56;       %Air advection res. time (h)*
s(26)=1000;     %Water advection res. time (h)
s(27)=50000;    %Sediment advection res. time (h)


%Chemical Parameters
s(28)=42000;    %Water mass solubility (g/m3)
s(29)=33360;    %Vapour pressure (Pa);
s(30)=1.24;     %Log Octanol-water partition coefficient
s(31)=6.1;      %Organic carbon-water partition coefficient (L/kg)
```

```
s(32)=59.5;     %Henry's constant (Pa.m3/mol)

MM=88.150;      %Molecular mass in g/mol;
T_C=25;         %Temperature of parameters (degrees C)

s(33)=74;       %Half-life in air (h)
s(34)=1700;     %Half-life in surface water (h)
s(35)=1270;     %Half-life in soil (h)
s(36)=6815;     %Half-life in sediment (h)

%Emission rates (kg/h)
s(37)=19015.14;   %Air emission
s(38)=131.2;      %Water emission
s(39)=7026.4;     %Soil emission
s(40)=0;          %Sediment emission

%Transport parameters
s(41)=5;          %Air-film (air/water)MTC (m/h)
s(42)=0.05;       %Water-film (air/water)MTC (m/h)
s(43)=5.2740e-5;  %Rain rate (m/h) [corresponds to 0.462 m/a]*
s(44)=6e-10;      %Aerosol deposition rate(m/h)
s(45)=0.02;       %Soil particle-air MTC (m/h)
s(46)=1e-5;       %Soil particle-water MTC (m/h)
s(47)=5;          %Surface soil-air MTC (m/h)
s(48)=1e-4;       %Sediment-water MTC (m/h)
s(49)=5e-7;       %Sediment deposition rate (m/h)
s(50)=2e-7;       %Sediment resuspension rate (m/h)
s(51)=5e-5;       %Soil water runoff rate (m/h)
s(52)=1e-8;       %Soil solids runoff rate (m/h)


%%%%%%%%%%%%%%%%%%%%%%%%%%%%%%%%%%%%%%%%%%%%%%%%%%%%%%%%%%%%%%%%%%%%%%%%


%Air Compartment
V1=s(2)*s(5);         %Bulk air volume(m3)
theta17=s(9);         %Volume fraction of aerosol in bulk air

theta11=1-theta17;    %Volume fraction of air phase in bulk air
V11=theta11*V1;       %Volume of air phase in bulk air (m3)
V17=theta17*V1;       %Volume of aerosol in bulk air (m3)


%Water Compartment
Aw=s(2)*s(3);               %Interfacial area of water (m2)
V2=Aw*s(6);                 %Bulk water volume(m3)
theta25=s(10);              %Volume fraction of suspended sediment in
bulk water
theta26=s(11);              %Volume fraction of fish in bulk water

theta22=1-theta25-theta26; %Volume fraction of water phase in bulk
water
V22=theta22*V2;             %Volume of water phase in bulk water (m3)
V25=theta25*V2;             %Volume of suspended sediment in bulk water
(m3)
V26=theta26*V2;             %Volume of fish in bulk water (m3)
```

```
%Soil Compartment
As=s(2)*s(4);                 %Interfacial area of soil (m2)
V3=As*s(7);                   %Bulk soil volume (m3)
theta31=s(12);                %Volume fraction of air phase in bulk soil
theta32=s(13);                %Volume fraction of water phase in bulk
soil

theta33=1-theta31-theta32; %Volume fraction of soil solids in bulk
soil
V31=theta31*V3;               %Volume of air phase in bulk soil (m3)
V32=theta31*V3;               %Volume of water phase in bulk soil (m3)
V33=theta33*V3;               %Volume of soil solids in bulk soil (m3)


%Sediment compartmnet
V4=s(2)*s(3)*s(8);            %Bulk sediment (m3)
theta42=s(14);                %Volume fraction of water phase in bulk
sediment

theta44=1-theta42;            %Volume fraction of sediment solids in bulk
sediment
V42=theta42*V4;               %Volume of water phase in bulk sediment
V44=theta44*V4;               %Volume of sediment solids in bulk sediment


%Compartmental densities (kg/m3)
rho1=s(15);     %Density of air
rho2=s(16);     %Density of water
rho3=s(17);     %Density of soil
rho4=s(18);     %Density of sediment
rho5=s(19);     %Density of susp. sediment
rho6=s(20);     %Density of fish

%Fraction organic carbon content of sub-compartments (m/m)
y3=s(21);       %Org C. content (m/m) of soil
y4=s(22);       %Org C. content (m/m) of sediment
y5=s(23);       %Org C. content (m/m) of susp. sediment

%Fraction lipid content of sub-compartment (v/v)
y6=s(24);       %Lipid Volume fraction of fish

%Advection parameters
tau1=s(25);     %Air advection res. time (h)
tau2=s(26);     %Water advection res. time (h)
tau4=s(27);     %Sediment advection res. time (h)

G1=V1/tau1;     %Air advection flow (m3/h)
G2=V2/tau2;     %Water advection flow (m3/h)
G3=0;
G4=V4/tau4;     %Sediment advection flow (m3/h)

%Chemical Properties
MassWS=s(28);           %Water mass solubility (g/m3)
VP=s(29);               %Vapour pressure (Pa)
LogKow=s(30);           %Log Ocyanol Water partition coefficient
Koc=s(31);              %Alternative: Koc=0.41*10^(LogKow)
H=s(32);                %Henry's constant (Pa.m3/mol)
```

```
half_t1=s(33);          %half life in air (h)
half_t2=s(34);          %half life in water (h)
half_t3=s(35);          %half life in soil (h)
half_t4=s(36);          %half life in sediment (h)

Emission1=s(37);        %Air emission in kg/h
Emission2=s(38);        %Water emission in kg/h
Emission3=s(39);        %Soil emission in kg/h
Emission4=s(40);        %Sediment emission in kg/h


E1=Emission1*1000/MM;   %Air emission in mol/h
E2=Emission2*1000/MM;   %Water emission in mol/h
E3=Emission3*1000/MM;   %Soil emission in mol/h
E4=Emission4*1000/MM;   %Sediment emission in mol/h


%Calculated:
Cs=MassWS/MM;         %Molar water solubility (mol/m3)
k1=log(2)/half_t1;    %First order reaction rate in air (h)
k2=log(2)/half_t2;    %First order reaction rate in water (h)
k3=log(2)/half_t3;    %First order reaction rate in soil (h)
k4=log(2)/half_t4;    %First order reaction rate in sediment (h)


%Z values (mol/Pa.m3)
R=8.314;          %Gas constant in J/mol.K
T=T_C+273.15;     %Temperature in kelvin

Z1=1/(R*T);
Z2=1/H;
Z3=Z2*rho3*y3*Koc/1000;
Z4=Z2*rho4*y4*Koc/1000;
Z5=Z2*rho5*y5*Koc/1000;
Z6=Z2*rho6*y6*(10^LogKow)/1000;
Z7=Z1*6e6/VP;     %Mackay 2001 recommended

%Bulk Z values (mol/Pa.m3)
ZB1=theta11*Z1+theta17*Z7;
ZB2=theta22*Z2+theta25*Z5+theta26*Z6;
ZB3=theta31*Z1+theta32*Z2+theta33*Z3;
ZB4=theta42*Z2+theta44*Z4;


%Intermedia transport properties (m/h)
U1=s(41);
U2=s(42);
U3=s(43);
U4=s(44);
U5=s(45);
U6=s(46);
U7=s(47);
U8=s(48);
U9=s(49);
U10=s(50);
U11=s(51);
U12=s(52);

%Intermedia D values (mol/Pa.h)
D12=1/(1/(U1*Aw*Z1)+1/(U2*Aw*Z2)) +(U3*Aw*Z2)+(U4*Aw*Z7);
D21=1/(1/(U1*Aw*Z1)+1/(U2*Aw*Z2));
```

```
D13=1/(1/(U7*As*Z1)+1/(U6*As*Z2+U5*As*Z1))+(U3*As*Z2)+(U4*As*Z7);
D31=1/(1/(U7*As*Z1)+1/(U6*As*Z2+U5*As*Z1));
D24=U8*Aw*Z2+U9*Aw*Z5;
D42=U8*Aw*Z2+U10*Aw*Z4;
D32=U11*As*Z2+U12*As*Z3;

%Reaction D values (mol/Pa.h)
Dr1=V1*k1*ZB1;
Dr2=V2*k2*ZB2;
Dr3=V3*k3*ZB3;
Dr4=V4*k4*ZB4;

%Advection D values (mol/Pa.h)
Da1=G1*ZB1;
Da2=G2*ZB2;
Da3=G3*ZB3;
Da4=G4*ZB4;


%MATRIX NOTATION
%State matrix
SM=[  -(Dr1+Da1+D12+D13)./(V1*ZB1)  D21./(V1*ZB1)D31./(V1*ZB1)
   0;...
D12./(V2*ZB2)-(Dr2+Da2+D21+D24)./(V2*ZB2) D32./(V2*ZB2)
   D42./(V2*ZB2);...
D13./(V3*ZB3)  0  -(Dr3+Da3+D31+D32)./(V3*ZB3)  0;...
   0  D24./(V4*ZB4)     0        -(Dr4+Da4+D42)./(V4*ZB4)];


%Forcing atrix
FM=[E1./(V1*ZB1);E2./(V2*ZB2);E3./(V3*ZB3);E4./(V4*ZB4)];


fugacity=inv(SM)*(-FM);
f0=fugacity';

[t,f]=ode45('Comp3Model2',[0 5000], f0);
[rowkow column]=size(f);
i=1;
j=2;


limit=0.00005e-3;

%%%%%%%%%%%%%%%%%%%%%%%%%%%%%%%%%%%%%%
% Fugacity Settling time algorithm %
%%%%%%%%%%%%%%%%%%%%%%%%%%%%%%%%%%%%%%

for i=1:1:column
   criterion=limit+1;
   j=2;
   while criterion > limit

    criterion = f(j,i);
      if criterion < limit
         fugset(i)=j;

      end

         j=j+1;
```

```
      if j >= rowkow
         criterion =limit-1;
      fugset(i)=rowkow;
      end
   end
end


fugset


for counter1=1:column
   tsettling(counter1)=t(fugset(counter1));
end

tsettling'


%Graphing of results

figure(1)
plot(t,f(:,1))
hold on
plot(t,f(:,2))
hold on
plot(t,f(:,3))
hold on
plot(t,f(:,4))


figure(2)
func1=f(:,1)*ZB1*V1;
subplot(2,2,1)
plot(t,func1)
title('A')

func2=f(:,2)*ZB2*V2;
subplot(2,2,2)
plot(t,func2)
title('W')

func3=f(:,3)*ZB3*V3;
subplot(2,2,3)
plot(t,func3)
title('soil')

func4=f(:,4)*ZB4*V4;
subplot(2,2,4)
plot(t,func4)
title('sed')


%%%%%%%%%%%%%%%%%%%%%%%%%%%%%%%%%%%%%%%%
%Printing of results

%Inventory in moles
N_air=f(:,1)*ZB1*V1;
N_water=f(:,2)*ZB2*V2;
N_soil=f(:,3)*ZB3*V3;
N_sed=f(:,4)*ZB4*V4
t;
```

APPENDIX C

C-1 Program written for computation of TaPL3 model

The following program was written in Matlab for solution of the TaPL3 simulation. The program displayed below is for the MTBE simulation. The program simulates two modes of entry into the environment including separate emissions into the air and water compartments. (Comments are denoted with a "%' in the program code).

```
%TaPL3 Model
%Based on papers by Webster et al. (1998) and Beyer et al. (2000)

%Compartment dimensions
%This is accepted as representing a suitably sized evaluative
environment
% Mackay (1991)

%Environment composed of 4 compartments and 7 sub-compartments
% 1. Air: bulk and sub-compartment
% 2. Water: bulk and sub-compartment
% 3. Soil: bulk and sub-compartment
% 4. Sediment Solids: bulk and sub-compartment
% 5. Suspended sediment: sub-compartment
% 6. Fish: sub-compartment
% 7. Aerosol: sub-compartment

%Compartment Dimensions and Properties
clear all
clc


for i=1:1:2
Emission(1)=0;          %Air emission in kg/h
Emission(2)=0;          %Water emission in kg/h

Emission(i)=1000;

%Air Compartment
V1=1e11*1000;           %Bulk air volume(m3)
theta17=2e-11;          %Volume fraction of aerosol in bulk air

theta11=1-theta17;   %Volume fraction of air phase in bulk air
V11=theta11*V1;      %Volume of air phase in bulk air (m3)
V17=theta17*V1;      %Volume of aerosol in bulk air (m3)


%Water Compartment
Aw=1e10;             %Interfacial area of water (m2)
V2=Aw*20;            %Bulk water volume(m3)
theta25=5e-6;        %Volume fraction of suspended sediment in bulk
water
theta26=1e-6;        %Volume fraction of fish in bulk water
```

```
theta22=1-theta25-theta26; %Volume fraction of water phase in bulk
water
V22=theta22*V2;            %Volume of water phase in bulk water (m3)
V25=theta25*V2;            %Volume of suspended sediment in bulk water
(m3)
V26=theta26*V2;            %Volume of fish in bulk water (m3)


%Soil Compartment
As=9e10;                 %Interfacial area of soil (m2)
V3=As*0.2;               %Bulk soil volume (m3)
theta31=0.2;             %Volume fraction of air phase in bulk soil
theta32=0.3;             %Volume fraction of water phase in bulk soil

theta33=1-theta31-theta32; % Volume fraction of soil solids in bulk
soil
V31=theta31*V3;            %Volume of air phase in bulk soil (m3)
V32=theta31*V3;            %Volume of water phase in bulk soil (m3)
V33=theta33*V3;            %Volume of soil solids in bulk soil (m3)


%Sediment compartment
V4=1e10*0.05;         %Bulk sediment (m3)
theta42=0.8;          %Volume fraction of water phase in bulk sediment

theta44=1-theta42;    %Volume fraction of sediment solids in bulk
sediment
V42=theta42*V4;       %Volume of water phase in bulk sediment
V44=theta44*V4;       %Volume of sediment solids in bulk sediment


%Compartmental densities (kg/m3)
rho1=1.19;  %Density of air
rho2=1000;  %Density of water
rho3=2400;  %Density of soil solids
rho4=2400;  %Density of sediment solids
rho5=1500;  %Density of susp. sediment solids
rho6=1000;  %Density of fish
rho7=2000;  %Density of aerosol solids

%Fraction organic carbon content of sub-compartments (m/m)
y3=0.02;        %Org C. content (m/m) of soil
y4=0.04;        %Org C. content (m/m) of sediment
y5=0.2;         %Org C. content (m/m) of susp. sediment

%Fraction lipid content of sub-compartment (v/v)
y6=0.05;        %Lipid Volume fraction of fish

%Advection parameters
v1=14.4;     %Wind speed (km/h)
v2=3.60;     %Water velocity (km/h)
tau1=((Aw+As)^(0.5))/(v1*1000);  %Air residence time (h)


%Chemical Properties
T_C=25; % temp in degrees Celsius
MM=88.150;               %Molecular mass in g/mol;
MassWS=42000;            %Water mass solubility (g/m3)
VP=33360;                %Vapour pressure (Pa)
LogKow=1.24;             %Log Octanol Water partition coefficient
Koc=0.41*10^(LogKow);    %[L/kg]
```

```
Cs=MassWS/MM;              %Molar water solubility in mol/m3
H=VP/Cs;                   %Henry's constant (Pa.m3/mol)


half_t1=74;            %half life in air (h)
half_t2=1700;          %half life in water (h)
half_t3=1270;          %half life in soil (h)
half_t4=6815;          %half life in sediment (h)

Emission3=0;           %Soil emission in kg/h
Emission4=0;           %Sediment emission in kg/h

E1=Emission(1)*1000/MM;     %Air emission in mol/h
E2=Emission(2)*1000/MM;     %Water emission in mol/h
E3=Emission3*1000/MM;       %Soil emission in mol/h
E4=Emission4*1000/MM;       %Sediment emission in mol/h


%Calculated:
Cs=MassWS/MM;          %Molar water solubility (mol/m3)
k1=log(2)/half_t1;     %First order reaction rate in air (h)
k2=log(2)/half_t2;     %First order reaction rate in water (h)
k3=log(2)/half_t3;     %First order reaction rate in soil (h)
k4=log(2)/half_t4;     %First order reaction rate in sediment (h)


%Z values (mol/Pa.m3)
R=8.314; % Gas constant in J/mol.K
T=T_C+273.15; %Temperature in Kelvin

Z1=1/(R*T);
Z2=1/H;
Z3=Z2*rho3*y3*Koc/1000;
Z4=Z2*rho4*y4*Koc/1000;
Z5=Z2*rho5*y5*Koc/1000;
Z6=Z2*rho6*y6*(10^LogKow)/1000;
Z7=Z1*6e6/VP;  %Mackay 2001 recommended

%Bulk Z values (mol/Pa.m3)
ZB1=theta11*Z1+theta17*Z7;
ZB2=theta22*Z2+theta25*Z5+theta26*Z6;
ZB3=theta31*Z1+theta32*Z2+theta33*Z3;
ZB4=theta42*Z2+theta44*Z4;


%Intermedia transport properties (m/h)
U1=5;
U2=0.05;
U3=1e-4;
U4=6e-10;
U5=0.02;
U6=1e-5;
U7=5;
U8=1e-4;
U9=5e-7;
U10=2e-7;
U11=5e-5;
U12=1e-8;
```

```
%Intermedia D values (mol/Pa.h)
D12=1/(1/(U1*Aw*Z1)+1/(U2*Aw*Z2)) +(U3*Aw*Z2)+(U4*Aw*Z7);
D21=1/(1/(U1*Aw*Z1)+1/(U2*Aw*Z2));
D13=1/(1/(U7*As*Z1)+1/(U6*As*Z2+U5*As*Z1))+(U3*As*Z2)+(U4*As*Z7);
D31=1/(1/(U7*As*Z1)+1/(U6*As*Z2+U5*As*Z1));
D24=U8*Aw*Z2+U9*Aw*Z5;
D42=U8*Aw*Z2+U10*Aw*Z4;
D32=U11*As*Z2+U12*As*Z3;

%Reaction D values (mol/Pa.h)
Dr1=V1*k1*ZB1;
Dr2=V2*k2*ZB2;
Dr3=V3*k3*ZB3;
Dr4=V4*k4*ZB4;

%Advection D values (mol/Pa.h)
Da1=0;
Da2=0;
Da3=0;
Da4=0;


%MATRIX NOTATION
   %State matrix
   SM=[  -(Dr1+Da1+D12+D13)./(V1*ZB1)  D21./(V1*ZB1) D31./(V1*ZB1)
   0;
D12./(V2*ZB2)  -(Dr2+Da2+D21+D24)./(V2*ZB2)  D32./(V2*ZB2)
D42./(V2*ZB2);
D13./(V3*ZB3)     0     -(Dr3+Da3+D31+D32)./(V3*ZB3)  0;...
0     D24./(V4*ZB4)  0  -(Dr4+Da4+D42)./(V4*ZB4)];

%Forcing matrix
FM=[E1./(V1*ZB1);E2./(V2*ZB2);E3./(V3*ZB3);E4./(V4*ZB4)];



fugacity=inv(SM)*(-FM)

Dr=[Dr1;Dr2;Dr3;Dr4];
Da=[Da1;Da2;Da3;Da4];
ZB=[ZB1;ZB2;ZB3;ZB4];
V=[V1;V2;V3;V4];

holdup(i)=  sum(V.*ZB.*fugacity);      %holdup in environment of
chemical based on calculated concentrations
tau(i)=holdup(i)/sum(Dr.*fugacity)

rhob1=theta11*rho1+theta17*1.5;
rhob2=theta22*rho2+theta25*rho5+theta26*rho6;
rhob3=theta31*rho1+theta32*rho2+theta33*rho3;
rhob4=theta42*rho2+theta44*rho4;


%mass based part per million (ug/g)
ppm_air=1000*fugacity(1)*MM*ZB1/rho1
ppm_water=1000*fugacity(2)*MM*ZB2/rho2
ppm_soil=1000*fugacity(3)*MM*ZB3/rho3
ppm_sediment=1000*fugacity(4)*MM*ZB4/rho4
```

```
%Percentage mass distribution
MassDistr(:,i)=(V.*ZB.*fugacity)./holdup(i)
end


%Beyer et al (2000)
CTDa1=v1*tau(1)*MassDistr(1,1)
CTDw1=v2*tau(1)*MassDistr(2,1)
tau(1)
CTDa2=v1*tau(2)*MassDistr(1,2)
CTDw2=v2*tau(2)*MassDistr(2,2)
tau(2)


%Hertwich and Mckone (2001)
mobility=(v1*MassDistr(1,1)+v2*MassDistr(2,1))
LRT=mobility*holdup(1)/(1000*1000/MM)
persistence=LRT/mobility
mobility=(v1*MassDistr(1,2)+v2*MassDistr(2,2))
LRT=mobility*holdup(2)/(1000*1000/MM)
persistence=LRT/mobility
```

C-2 Program written for computation of the Thomann (1989) bioaccumulation food chain model

The following program was written in Matlab for solution of the Thomann (1989) food web model. The program displayed below is for the MTBE simulation. The water concentration was taken from the ChemSA simulation. (Comments are denoted with a "%' in the program code).

```
% Bioaccumulation/Biomagnification model based on Thomann (1989)
% Four level food chain
% Only successive level feeds on level below
%1. phytoplankton
%2. zoo plankton
%3. small fish
%4. large fish

clear all

ppmw=[0.08960  0.08260  0.00820] %Ppm in water from ChemSA model
rhob=1000                        %Density of aquatic biota [kg/m3]
rhow=1000                        %Density of water [kg/m3]
f=0.05                           %Volume fraction lipid content

MM=[88.150 102.177 46.069];    %Molar masses of oxygenates [g/mol]
logKow= [1.24 1.57 -0.31];     % Log Octanol-water partition
coefficients
Kow=10.^(logKow);

Cw=(rhow*ppmw/MM)*1e-6         % Water concentration [mol/m3]


%Overall food assimilation factors
delta2=0.18./(0.04+2e5./Kow)
delta3=0.024./(0.0046+9e3./Kow)
delta4=0.012./(0.0025+2.5e3./Kow)


%Concentrations in each tier [mol/m3]
Cb1=f.*Kow.*Cw;
Cb2=f*Kow.*Cw.*(1+delta2);
Cb3=f*Kow.*Cw.*(1+delta3.*(1+delta2));
Cb4=f*Kow.*Cw.*(1+delta4.*(1+delta3.*(1+delta2)));


%Concentrations in each tier [ppm]
ppmb1=((1e6/rhob)*(Cb1.*MM))
ppmb2=((1e6/rhob)*(Cb2.*MM))
ppmb3=((1e6/rhob)*(Cb3.*MM))
ppmb4=((1e6/rhob)*(Cb4.*MM))
```

```
for i=-0.5:0.1:8

   count= ((i+0.5)/0.1)+1;
   x_axis(count)=i;
   logKow=i;
   Kow=10^(logKow);

   Cw=(rhow*ppmw/MM)*1e-6;

   delta2=0.18./(0.04+2e5./Kow);
   delta3=0.024./(0.0046+9e3./Kow);
   delta4=0.012./(0.0025+2.5e3./Kow);


   Cb1=f.*Kow.*Cw;
   Cb2=f*Kow.*Cw.*(1+delta2);
   Cb3=f*Kow.*Cw.*(1+delta3.*(1+delta2));
   Cb4=f*Kow.*Cw.*(1+delta4.*(1+delta3.*(1+delta2)));

% Biomagnification factor
BMF2(count)=Cb2/Cb1;
BMF3(count)=Cb3/Cb2;
BMF4(count)=Cb4/Cb3;

%Bioconcentration factor
BCF2(count)=Cb2/Cw;
BCF3(count)=Cb3/Cw;
BCF4(count)=Cb4/Cw;

end


%Graphing of biomagnification and bioconcentration factors with
increasing %Kow

figure(1)
plot(x_axis,BMF2)
hold on
plot(x_axis,BMF3)
hold on
plot(x_axis,BMF4)

figure(2)
plot(x_axis,BCF2)
hold on
plot(x_axis,BCF3)
hold on
plot(x_axis,BCF4)
```

C-3 Program written for computation of groundwater mobility

The following program was written in the Matlab programming language to simulate an equilibrium groundwater model. The program displayed below is for the MTBE simulation. (Comments are denoted with a "%' in the program code).

```
%Equilibrium groundwater model
%
%Three heterogeneous phase single compartment model
%Soil consists of:
%1. Air
%2. Water
%3. Soil particles

clear all
clc


for i=1:1:8


   %Declaration of variables for sensitivity analysis
   s(2)=59.5;      %Henry's constant (Pa.m3/mol)
   s(3)=1.24;      %Log Octanol-water partition coefficient
   s(4)=6.9;       %Organic carbon-water partition coefficient
   s(5)=0.02;      %Organic carbon content of soil
   s(6)=0.2;       %Air volumetric fraction of soil
   s(7)=0.3;       %Water volumetric fraction of soil
   s(8)=1500;      %Dry density of soil


   %Forward Bias
   s(i)=1.01*s(i);


   H=s(2);
   LogKow=s(3);
   Koc=s(4);
   yoc=s(5);
   y13=s(6);
   y23=s(7);
   rhos=s(8);

   y33=1-y13-y23;
   T_C=25;  %Temperature of parameters in degrees C

   %Calculated parameters
   R=8.314; % Gas constant J/mol.K
   K12=H/(R*(T_C+273.15));
   K32=rhos*yoc*Koc/1000;

   Groundwater_mobility(i)=(y23+y13*K12+y33*K32);
   dm(i)=(Groundwater_mobility(i)-
Groundwater_mobility(1))./Groundwater_mobility(1);
end
```

```
Groundwater_mobility(1)
dm;
sensitivty_dm=dm(2:8)'./(0.01);

%%%%%%%%%%%%%%%%%%%%%%%%%%%%%%%%%%%%%%%%%%%%%%%%%%%%%%%%%%%%%%%%%%%%%%%%
%Uncertainty analysis


%Confidence factors for input variables
CFinputs(1,1)=1.05;      %Henry's constant (Pa.m3/mol)
CFinputs(2,1)=1.5;       %Log Octanol-water partition coefficient
CFinputs(3,1)=2.5;       %Organic carbon-water partition coefficient
CFinputs(4,1)=3;         %Organic carbon content of soil
CFinputs(5,1)=1.5;       %Air volumetric fraction of soil
CFinputs(6,1)=1.5;       %Water volumetric fraction of soil
CFinputs(7,1)=1.5;       %Dry density of soil)


%%Confidence factors for output variables
CF_dm=exp(sum(((sensitivty_dm.^2).* ((log(CFinputs)).^2))))

%Contribution to variance
Denominator_dm=sum(((sensitivty_dm.^2).* ((log(CFinputs)).^2)));

for count=1:1:length(CFinputs)
   Contribution_to_variance_dm(count,1)=100*((sensitivty_dm(count)^2)*
((log(CFinputs(count)))^2))/Denominator_dm;
end
Contribution_to_variance_dm
```

C-4 Derivation of activity coefficient based selectivity factor

The selectivity factor is defined as the ratio of the mole fraction of solute in one liquid phase (*I*) to the mole fraction in another liquid phase (*II*):

$$\beta_{I,II} = \frac{x_i^I}{x_i^{II}}$$

(C-1)

The selectivity factor is a mole fraction based partition coefficient. The equilibrium criterion for LLE is the same for that of VLE, namely constant temperature, pressure and fugacity for each species in each phase of the system. Considering an LLE system containing two liquid phases at uniform pressure and temperature, the equivalence of fugacity criteria yields:

$$\hat{f}_i^I = \hat{f}_i^{II} \qquad \text{at constant } T \text{ and } P$$

(C-2)

If the phases, *I* and *II*, represent water and fuel respectively, an equilibrated oxygenate solute in both phases must satisfy:

$$x_{oxy}^w \gamma_{oxy}^w P_{oxy}^{sat} = x_{oxy}^{fuel} \gamma_{oxy}^{fuel} P_{oxy}^{sat}$$

(C-3)

As the saturated vapour pressures on either side of Equation (C-3) are equal, they cancel out, and the equivalence of fugacity criterion reduces to the equivalence of activity criterion. Rearranging Equation (C-3) and including the definition of selectivity [Equation (C-1) above] yields:

$$\beta_{w,fuel} = \frac{x_{oxy}^w}{x_{oxy}^{fuel}} = \frac{\gamma_{oxy}^{fuel}}{\gamma_{oxy}^w}$$

(C-4)

The resulting ratio of activity coefficients is often expressed in terms of the limiting activity coefficients of the solute in each phase. Thus:

$$\beta_{w,fuel}^{\infty} = \frac{\gamma_{oxy}^{fuel,\infty}}{\gamma_{oxy}^{w,\infty}} \qquad \textbf{(C-5)}$$

APPENDIX D

D-1 Vapour-liquid equilibria measurements of MTBE and TAME with toluene

In this work, isothermal vapour liquid equilibrium (VLE) data were measured in a computer controlled dynamic still for two ether-toluene systems. The ethers investigated were 2-methoxy-2-methylpropane (Methyl Tertiary Butyl Ether, MTBE) and 2-methoxy-2-methylbutane (Tertiary Amyl Methyl Ether, TAME) in response to a call from world environmental agencies, the petroleum industry and other concerned organisations (Marsh et al., 1999) to develop a set of recommended values for ether oxygenates. Although the slow phasing out of MTBE on a regional scale has begun, thermodynamic data for this chemical and its behaviour in mixtures is still relevant in the capacity of a benchmarking tool. This data will allow the comparison of MTBE with possible substitute chemicals, hoping to replace the oxygenate as an anti-knocking, octane-enhancing agent with clean burning capabilities.

P-x-y data were collected for MTBE(1)-Toluene(2) at 308.15 K, 318.15 K and 323.15 K adding three new isothermal set to the single isotherm at 333.15 K currently available in literature (Plura et al., 1979). P-x-y data at an unmeasured temperature of 318.15 K was measured for TAME(1)-Toluene(2), enabling a direct comparison with the isotherm generated from the lighter ether-aromatic system.

Experimental

Materials

All chemicals were purchased from Riedel-de-Haën. Although the minimum purity percentage guaranteed by the supplier for TAME was relatively poor, gas chromatographic analysis of all reagents failed to show any significant impurities. After comparison of the measured refractive indices of the reagents with literature values [Table D-1], as well as a comparison of measured vapour pressure points with literature values [Table D-2], it was decided to use the reagents without further purification.

Table D-1: Refractive indices and reagent purities

Reagent	Refractive index (293.15 K)		Minimum purity [%]
	Experimental	Literature*	
MTBE	1.3698	1.3690	99.8
TAME	1.3862	1.3855	97.0
Toluene	1.4965	1.4961	99.8

Reference:

* POC (2002)

Measured vapour pressure data for TAME from this work was correlated to a four-parameter equation [Equation (7-1)], as used by Reid et al. (1987), and compared with three-parameter Antoine equations found in Antosik and Sandler (1994), and the DDB (1999) [See Table D-2].

$$\ln\left(\frac{P^{sat}}{P_c}\right) = (1-x)^{-1}\left[VP_1 x + VP_2 x^{1.5} + VP_3 x^3 + VP_4 x^6\right], \; (P^{sat}\,[\text{bar}]) \qquad \textbf{(D-1)}$$

where

$$x = 1 - \frac{T}{T_c}, \; (\text{T[K]}$$

T_c = 536.3 K; P_c = 31.91 bar; VP_1 = -7.8714; VP_2 = 2.4416; VP_3 = -5.1738; VP_4 = 2.9644

Table D-2: Vapour pressure measurements for TAME and comparison with predictive correlations

$P_{measured}$ [kPa]	$P_{calculated}$ [kPa]			T [K]	$\lvert\Delta P\rvert$ [kPa]		
	This work	DDB (1999)	Antosik and Sandler (1994)		This work	DDB (1999)	Antosik and Sandler (1994)
10.00	10.00	9.98	10.00	298.02	0.00	0.02	0.00
15.00	15.00	15.00	15.00	306.98	0.00	0.00	0.00
25.00	25.00	25.02	24.99	319.20	0.00	0.02	0.01
35.00	34.99	35.03	34.98	327.90	0.01	0.03	0.02
45.00	45.00	45.03	44.99	334.78	0.00	0.03	0.01
55.00	55.01	55.01	54.99	340.52	0.01	0.01	0.01
65.00	65.01	64.99	65.00	345.48	0.01	0.01	0.00
75.00	74.98	74.92	74.97	349.85	0.02	0.08	0.03
85.00	85.01	84.92	85.03	353.81	0.01	0.08	0.03
90.00	89.99	89.99	90.02	355.64	0.01	0.12	0.02

disengaged vapour moves upward around the equilibrium chamber, thermally insulating the latter. The vapour flows through the insulated tubing to the condenser where it condenses into a condensate trap, the overflow of which moves to the standpipe leg feeding the bottom of the equilibrium chamber.

Temperature and pressure measurement and control

The HP multimeter was used to display the resistance measured by the PT-100 sensor. The pressure was monitored with the pressure transducer. The accuracies of temperature and pressure measurement are estimated to be ± 0.02 K and ± 0.03 kPa, respectively. Pressure control in the still was to within 0.01 kPa with the temperature control varying between 0.01 K and 0.05 K depending on the composition region of the charge. The computer control strategy was based upon pulse-width modulation of two solenoid valves fixed to the vacuum and atmospheric lines.

Composition analysis

Samples of equilibrium phases were analysed by a HP 5890 Series II model gas chromatograph (GC) equipped with a thermal conductivity detector (TCD) and a Poropak Q packed column. The analysis method was based on the GC area ratio method as discussed by Raal and Mühlbauer (1998). The estimated uncertainty in the determined mole fractions is ± 0.002 mole fraction. The GC settings are indicated in Table D-3 below.

Table D-3: Gas chromatograph settings for VLE measurement

GC make	Hewlett-Packard
GC type	5890 Series II
Detector type	TCD
Column type	Packed (Poropak Q)
Column length [m]	2
Column outer diameter [inch]	1/8
Injection temperature [°C]	270
Column temperature [°C]	200
Detector temperature [°C]	250
Carrier gas flow rate [mL/min]	30

disengaged vapour moves upward around the equilibrium chamber, thermally insulating the latter. The vapour flows through the insulated tubing to the condenser where it condenses into a condensate trap, the overflow of which moves to the standpipe leg feeding the bottom of the equilibrium chamber.

Temperature and pressure measurement and control

The HP multimeter was used to display the resistance measured by the PT-100 sensor. The pressure was monitored with the pressure transducer. The accuracies of temperature and pressure measurement are estimated to be ± 0.02 K and ± 0.03 kPa, respectively. Pressure control in the still was to within 0.01 kPa with the temperature control varying between 0.01 K and 0.05 K depending on the composition region of the charge. The computer control strategy was based upon pulse-width modulation of two solenoid valves fixed to the vacuum and atmospheric lines.

Composition analysis

Samples of equilibrium phases were analysed by a HP 5890 Series II model gas chromatograph (GC) equipped with a thermal conductivity detector (TCD) and a Poropak Q packed column. The analysis method was based on the GC area ratio method as discussed by Raal and Mühlbauer (1998). The estimated uncertainty in the determined mole fractions is ± 0.002 mole fraction. The GC settings are indicated in Table D-3 below.

Table D-3: Gas chromatograph settings for VLE measurement

GC make	Hewlett-Packard
GC type	5890 Series II
Detector type	TCD
Column type	Packed (Poropak Q)
Column length [m]	2
Column outer diameter [inch]	1/8
Injection temperature [°C]	270
Column temperature [°C]	200
Detector temperature [°C]	250
Carrier gas flow rate [mL/min]	30

Results and discussion

The four sets of P-T-x-y data were regressed according to the gamma/phi formulation. Three activity coefficient models, including the Wilson (1964), the NRTL (Renon and Prausnitz, 1968) and UNIQUAC (Abrams and Prausnitz, 1975), were fitted using the Marquadt (1963) algorithm minimising the pressure residual. Non-ideality in the vapour phase was accounted for using the second virial coefficient correlation of Tsonopoulos and Dymond (1997). Ignoring vapour phase non-idealities would have induced a 3.5% error at worst in the low-pressure systems measured in this work.

All systems measured exhibited ideal vapour-liquid equilibria, as no azeotropes were observed in the isotherms, as illustrated by Figures D-2, D-3 and D-4 below. The measured VLE data are presented in Tables D-4 and D-5 below. Activity coefficient parameters and mean residuals for both pressure and vapour mole fraction are presented in Table D-6.

Table D-4: Vapour liquid equilibrium measurements for MTBE(1)-Toluene(2) at 308.15, 318.15 and 323.15 K

MTBE(1)-Toluene(2)								
308.15 K			318.15 K			323.15 K		
x_1	y_1	P [kPa]	x_1	y_1	P [kPa]	x_1	y_1	P [kPa]
0.000	0.000	6.18	0.000	0.000	9.88	0.000	0.000	12.28
0.018	0.147	7.12	0.015	0.114	10.99	0.011	0.080	13.20
0.024	0.185	7.44	0.023	0.165	11.57	0.028	0.181	14.65
0.037	0.251	8.04	0.036	0.234	12.46	0.043	0.254	15.89
0.082	0.434	10.32	0.088	0.435	16.05	0.071	0.366	18.18
0.212	0.698	16.50	0.224	0.693	25.27	0.158	0.584	25.19
0.433	0.86	26.28	0.417	0.841	37.36	0.393	0.820	42.78
0.671	0.936	36.06	0.656	0.929	51.24	0.594	0.901	56.76
0.859	0.977	43.60	0.839	0.970	61.73	0.826	0.966	72.55
0.921	0.988	46.14	0.926	0.987	66.87	0.931	0.987	79.92
0.966	0.995	48.05	0.971	0.995	69.61	0.977	0.996	83.21
0.984	0.997	48.83	0.989	0.998	70.74	0.985	0.997	83.80
1.000	1.000	49.48	1.000	1.000	71.41	1.000	1.000	84.91

Table D-5: Vapour-liquid equilibrium measurements for TAME(1)-Toluene(2) at 318.15 K

TAME(1)-Toluene(2) at 318.15 K		
x_1	y_1	P [kPa]
0.000	0.000	12.28
0.011	0.080	13.20
0.028	0.181	14.65
0.043	0.254	15.89
0.071	0.366	18.18
0.158	0.584	25.19
0.393	0.820	42.78
0.594	0.901	56.76
0.826	0.966	72.55
0.931	0.987	79.92
0.977	0.996	83.21
0.985	0.997	83.80
1.000	1.000	84.91

Table D-6: Correlated activity coefficient model parameters, and mean pressure and vapour mole fraction residuals

Activity Coefficient Model	Binary VLE system			
	MTBE(1)-Toluene(2)			TAME(1)-Toluene(2)
	308.15 K	318.15 K	323.15 K	318.15 K
Wilson				
$\lambda_{12} - \lambda_{11}$ [J/mol]	-373.1	-222.5	-209.0	-1496.6
$\lambda_{12} - \lambda_{22}$ J/mol]	999.4	847.3	818.2	2268.5
Average Δy_1	0.002	0.001	0.002	0.005
Average ΔP [kPa]	0.04	0.03	0.01	0.04
UNIQUAC				
$u_{12} - u_{11}$ [J/mol]	1566.0	1483.8	1500.5	1962.7
$u_{12} - u_{22}$ [J/mol]	-1211.3	-1166.6	-1185.3	-1456.6
Average Δy_1	0.002	0.001	0.002	0.005
Average ΔP [kPa]	0.04	0.03	0.02	0.04
NRTL				
$g_{12} - g_{11}$ [J/mol]	1761.2	1577.8	1514.6	1521.0
$g_{12} - g_{22}$ [J/mol]	-1019.7	-855.7	-856.6	-994.1
α	0.3	0.3	0.3	0.3
Average Δy_1	0.001	0.001	0.001	0.005
Average ΔP [kPa]	0.04	0.04	0.03	0.05

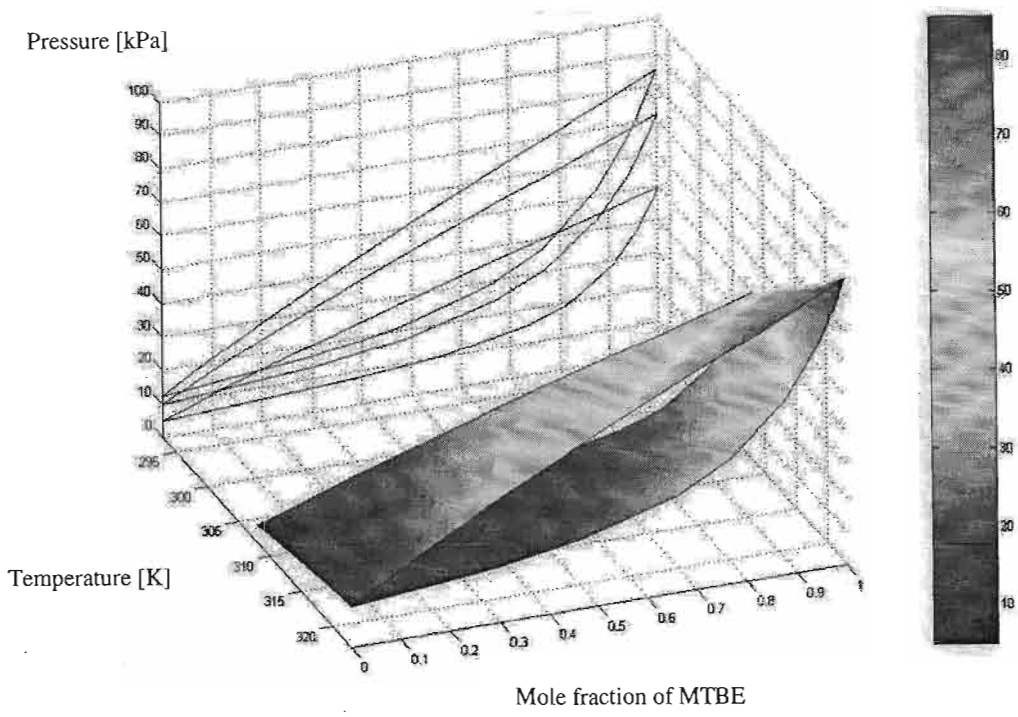

Figure D-2: P-T-x-y data for MTBE(1)-Toluene(2)

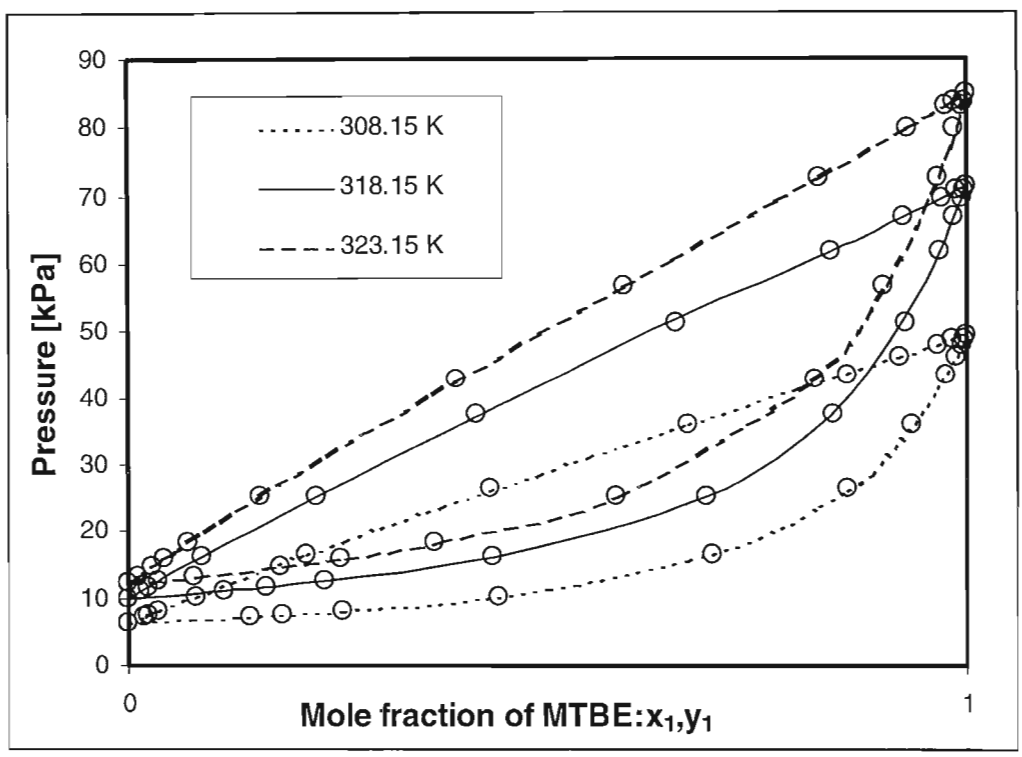

Figure D-3: Experimental P-x-y data and parameterised Wilson Activity coefficient fitted curves for MTBE(1)-Toluene(2) at 308.15, 318.15 and 323.15 K (Circles indicate experimental points)

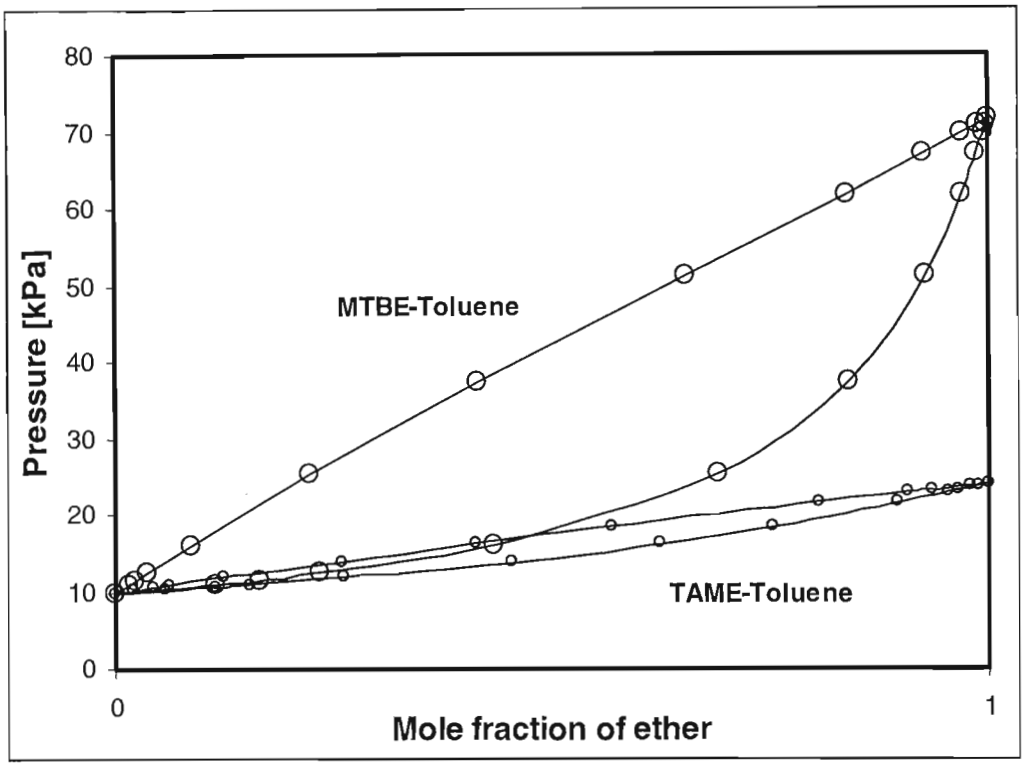

Figure D-4: Experimental P-x-y data and parameterised Wilson activity coefficient model fitted curves for MTBE and TAME in toluene at 318.15 K (Circles indicate experimental points)

Thermodynamic consistency

The thermodynamic consistency of the isothermal data was checked using the point-to-point test of van Ness et al. (1973), which advocates that thermodynamic consistency of data can be judged by the difference between the predicted and experimental vapour compositions. Danner and Gess (1990) stipulate that the absolute deviation between calculated and experimental vapour phase mole fraction must be less than 0.01. The experimental mean residuals, calculated and presented in Table D-6 above, indicate that the experimental isothermal data is thermodynamically consistent.

Although small additions of MTBE have a very small effect on the total equilibrium pressure (Bennett et al., 1993) [and consequently on the Reid vapour pressure], TAME is expected to have less of an effect judging from the P-x-y curves in Figure D-4 above.

Infinite dilution activity coefficients

For systems at low to moderate pressures, the equation of the infinite dilution activity coefficient is related to the partial derivative of the system pressure with respect to liquid mole fraction by the following equation, as suggested by Pividal et al. (1992):

$$\gamma_i^{j,\infty} = \varepsilon_i^{\infty} \frac{P_j^{sat}}{P_i^{sat}} \left(1 + \frac{\beta_j}{P_j^{sat}} \left[\frac{\partial P}{\partial x_1} \right]_{T, x_1 \to 0} \right) \tag{D-2}$$

where

$$\varepsilon_i^{\infty} = \exp\left(\frac{\left(B_{ii} - V_i^L\right)\left(P_j^{sat} - P_i^{sat}\right) + \delta_{ij} P_j^{sat}}{RT} \right)$$

$$\beta_j = 1 + P_j^{sat} \left(\frac{B_{jj} - V_j^L}{RT} \right)$$

$$\delta_{ij} = 2B_{ij} - B_{ii} - B_{jj}$$

The accuracy of the infinite dilution activity coefficient is dependent on the accuracy of the pressure-composition derivative. The partial derivative dependency of pressure on liquid composition was generated by fitting the pressure data in the dilute region to Equation (D-3), as previously used by Sandler and others (Pividal et al., 1992; Wright et al., 1992). A linear equation was regressed owing to the linear nature of the measured P-x data curves:

$$P = a + bx_1 \tag{D-3}$$

The partial derivative is equal to b, the gradient of Equation (D-3).

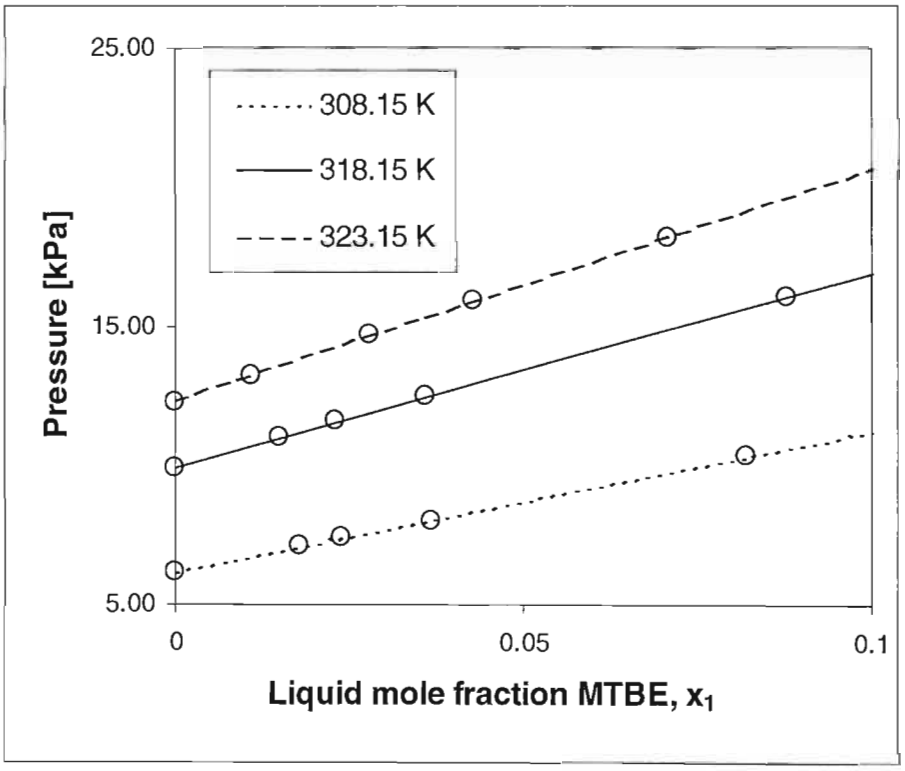

Figure D-5: Linear P-x curves for MTBE(1)-Toluene(2) at 308.15, 318.15 and 323.15 K

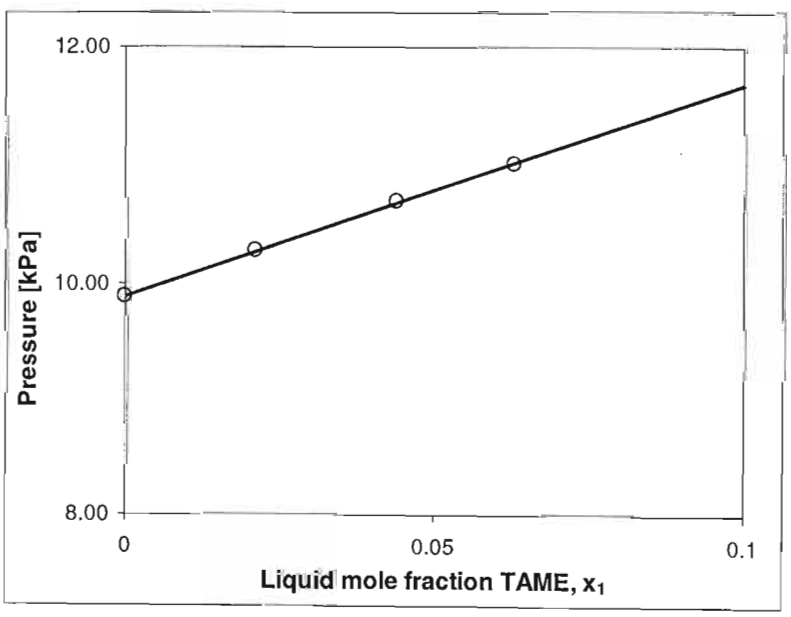

Figure D-6: Linear P-x curve for TAME(1)-Toluene(2) at 318.15K

Only the infinite dilution coefficients of oxygenate in toluene were regressed, as these are pertinent in assessing the environmental behaviour of the oxygenate in gasoline. The limiting activity coefficients are presented in Table D-7 below:

Table D-7: Limiting activity coefficients of the ethers, MTBE and TAME, in toluene, pure ether vapour pressures and ether Henry's constants in toluene

Oxygenate property	**Temperature [K]**		
	308.15	318.15	323.15
Infinite dilution activity coefficient, $\gamma_i^{2,\infty}$			
MTBE(1)-Toluene(2)	1.18	1.15	1.14
TAME(1)-Toluene(2)	-	1.13	-
Vapour pressure, P_i^{sat} [kPa]			
MTBE	49.48	71.41	84.91
TAME	-	23.99	-
Henry's constant in toluene, $\hat{H}_i^2$ [kPa]			
MTBE(1)-Toluene(2)	58.37	82.12	96.80
TAME(1)-Toluene(2)	-	27.11	-

Conclusions

TAME, when compared with MTBE, has a lower Henry's constant, which reflects its reduced tendency to equilibrate into air from an aromatic mixture. Both ether-aromatic systems display ideal behaviour containing no azeotropes. The binary systems were fitted satisfactorily by all the activity coefficient models employed (Wilson, NRTL and UNIQUAC), with the Wilson model showing a marginally superior fit.

APPENDIX E

E-1 Octanol-water partition coefficient measurements

In this work, octanol-water partition coefficients were measured for several fuel related chemicals using a liquid-liquid equilibrium (LLE) cell. This direct contact equilibrium method showed rapid equilibration and accurate results on comparison of the measured values with literature sources. The solutes measured include MTBE, TAME, ethanol, heptane (n-heptane), TMP (i-octane) and toluene. The estimation methods used to predict the octanol-water partition coefficients include GCSKOW, ClogP and KOWWIN, which were compared with the experimental results.

Experimental

Materials

All chemicals were purchased from Riedel-de-Haën. On compositional analysis of the reagents, using a gas chromatograph (GC) installed with a thermal conductivity detector (TCD), no major impurities were found; even though the minimum purity percentage guaranteed by the supplier for TAME was relatively poor (97.0 %). All other solutes had supplier guaranteed minimum purity percentages of greater than 99.8 %. Deionised water from a Milli-Q millipore water purification unit was used in the experiment.

Apparatus and procedure

An equilibrium cell, as modified by Raal (Raal and Mühlbauer, 1998) was used. The apparatus consisted of a single piece 30 mL glass cell and jacket and a stainless steel teflon lined end-piece through which water from a temperature bath could be circulated. The glass cell and the end-piece were sealed by teflon o-rings. This set-up ensured an isothermal environment, which completely encased the contents of the cell. A double paddle, linked to a magnetic capsule by a common support shaft was fitted inside the glass cell. The paddle was driven by magnetic coupling with an external horseshoe magnet and DC motor. The stirring of the cell contents by the double paddle facilitated rapid mass transfer and quick equilibration rates. Sampling was performed via a sampling point in the end-piece through which a syringe needle could be

inserted to draw a sample from either phase. The sampling point was sealed with a plug during operation. The end-piece housed a stainless steel temperature well, in which a PT-100 temperature sensor was inserted. This temperature sensor was attached to a Hewlett-Packard (HP) model 34401 multimeter to measure the temperature of the cell contents. The sensor extended into the mid portion of the cell.

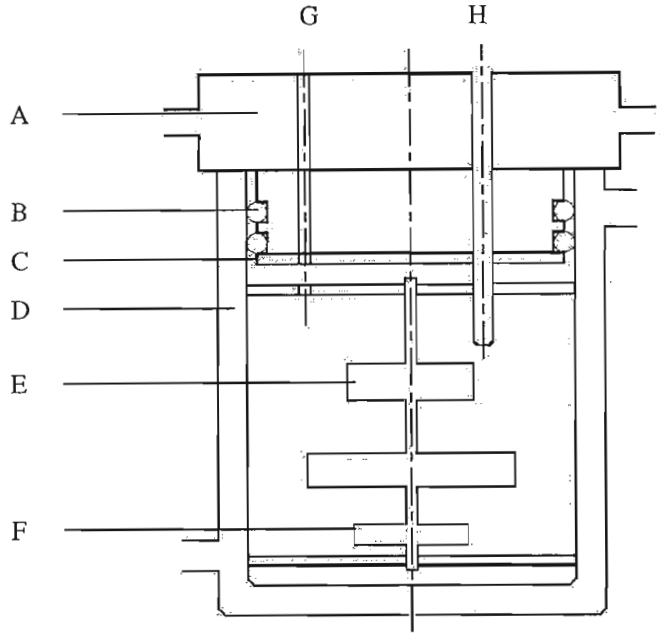

A: End-piece
B: Teflon o-rings
C: Teflon lining
D: Glass cell jacket
E: Double paddle
F: Magnetic capsule
G: Sampling point
H: Temperature sensor well

Figure E-1: Schematic diagram of glass liquid-liquid equilibrium cell used for octanol-water partition coefficient measurement

The equilibrium cell was charged with octanol and water in a specified volume ratio. A small amount of solute was added and the DC motor was powered stirring the cell contents. The cell was left mixing at a moderate shaft speed (30 to 40 rpm) for 1 hour. The stirrer was than disengaged and the cell contents were left to settle for another 30 minutes. Compositional analysis of both the organic and aqueous phases were than performed by withdrawing a sample of known volume and injecting into a gas chromatograph. Each sample was analysed at least three times.

Temperature measurement and control

The temperature of the cell was monitored using a PT-100 sensor attached to a HP multimeter to display the resistance of the temperature sensor. The linear relationship between temperature

and the resistance of the sensor is displayed below in Figure E-2. The temperature control of the cell contents was maintained by the temperature of the water bath. The temperature controller in the water bath is a bang-bang controlled unit. The perturbation of the temperature inside the cell, affected by this controller was observed: The cell temperature oscillated approximately 0.2°C about the set point. The accuracy of the temperature measurement is estimated to be ± 0.02°C.

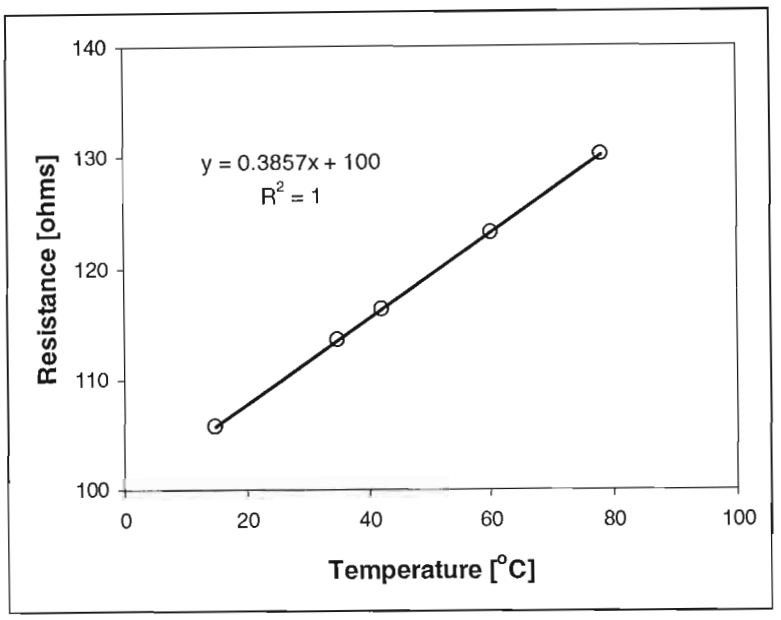

Figure E-2: Temperature calibration of the PT-100 sensor showing its temperature profile with resistance

Composition analysis

The samples obtained from both equilibrium phases were analysed using a Pye Unicam Series 104 gas chromatograph (GC) equipped with a flame ionisation detector (FID) and a Poropak Q packed column. The analysis method was based on the GC response volume method, as used by Sandler and co-workers (Peschke and Sandler, 1995; Wagner and Sandler, 1995) in their LLE measurements. From density data concerning the various solutes, the injected volumes could be translated into amounts of solute. The GC calibration curve for MTBE is displayed below in Figure E-3 as an illustration. The estimated uncertainty in the determined mole fractions is ± 0.002 mole fraction. The GC settings are indicated in Table E-1 below.

Table E-1: Gas chromatograph settings for octanol-water partition coefficient measurements

GC make	Pye Unicam
GC type	Series 104
Detector type	FID
Column type	Packed (10 % Carbowax)
Column length [m]	2.5
Column inner diameter [inch]	1/4
Injection/column/detector temperature [°C]	190
Carrier gas flow rate [mL/min]	25

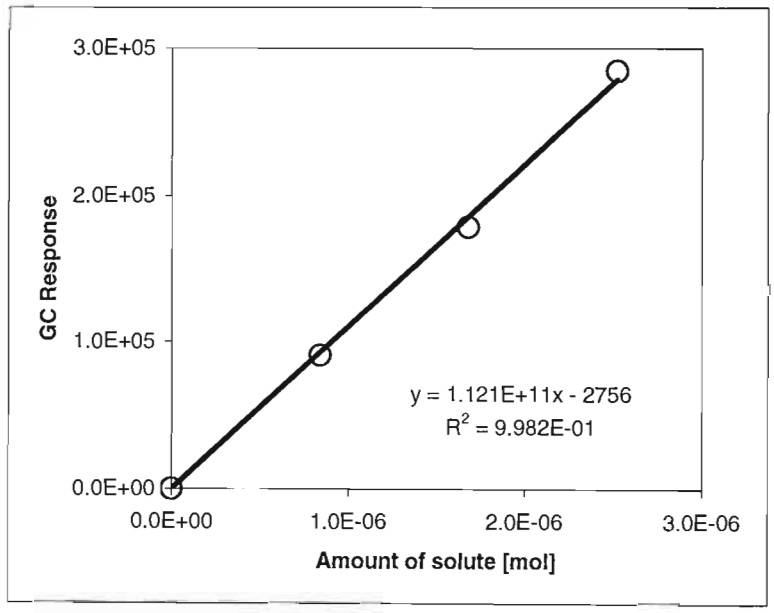

Figure E-3: Composition analysis calibration for octanol-water partition coefficient measurement using the method advocated by Sandler and co-workers (Illustrated for MTBE)

Results and discussion

Table E-2 includes measured values, reported literature values and estimated partition coefficients using the methods delineated above:

Table E-2: Measured and predicted octanol-water partition coefficients for MTBE, TAME, ethanol, heptane, TMP and toluene

Solute	log K_{ow}				
	Experimental	**Literature**	**GCSKOW**	**CLogP**	**KOWWIN**
MTBE	1.19	1.24[†]	1.12	1.049	1.4292
TAME	1.57	1.55[†]	1.65	1.578	1.9203
Ethanol	-0.30	-0.31[††]	-0.17	-0.235	-0.1412
Heptane	4.58	4.66[†††]	4.46	4.397	3.7791
TMP	4.59	-	4.49	4.536	4.0856
Toluene	2.60	2.69[†]	2.68	3.873	2.5403

References:

[†] Huttunen et al. (1997)

[††] Hansch and Leo (1985)

[†††] Leo et al. (1975)

The ease of measurement of the dilute aqueous layer concentration was improved by choosing a favourable layer volume ratio upon charging the clean cell with octanol and water. As distribution coefficients are concentration defined, by reducing the amount of solvent added, and subsequently lowering the respective phase volume, less solute will be drawn into the phase.

One of the many advantages derived from the use of a glass equilibrium cell is that it is transparent and does not have to be submerged in a water bath owing to its built-in temperature jacket and end-piece. Consequently, the cell contents can be observed and formation of micelle can be avoided through careful control of the paddle stirring rate. Thus, care was taken, especially when measuring the more hydrophobic solutes and no micelle were observed at the stirring rates used in this experiment.

As infinite dilution is a necessary assumption in the derivation of most of the K_{ow} prediction techniques (especially regarding the GCSKOW method), it was necessary to ensure that the distributed solute in both phases approached infinitely dilution. Practical infinitely dilution of solute in each phase, according to the mole fractions suggested by Alessi et al. (1991), was ensured through an iterative procedure, which was used to quantify the amount of solute to be

added to the cell. Using the ClogP prediction method, which requires structure only as an input, the octanol-water partition coefficients were estimated. Imposing the Alessi et al. (1991) suggested mole fractions, representing infinite dilution in each phase, and upon setting of a favourable volume ratio, the amount of solute required was calculated. This iterative approach, thus, ensured that infinitely dilute conditions were set up in both the organic and aqueous phases.

The most difficult partition coefficients to measure were those of heptane and TMP, which are the most hydrophobic of all the solutes measured; consequently, GC analysis of the aqueous phase for these solutes was difficult when using the amount of solute as calculated by the iterative technique discussed above. The small equilibrium cell did not provide much play with the volume ratio of the phases; consequently, greater quantities of solute than those calculated from the iterative method were added for these chemicals. This altered the assumption of infinite dilution in the octanol-rich phase. Nonetheless, the increased accuracy of the measurement of the water-rich phase facilitated by addition of extra solute allowed the accurate K_{ow} measurement of these chemicals. Remarkably, the GCSKOW predictive technique, which uses the assumption of infinite dilution in both phases, adequately estimated the K_{ow} for these hydrophobic solutes.

Conclusions

The liquid-liquid equilibrium cell accurately reproduced K_{ow} literature data for several fuel type chemicals. Furthermore, an octanol-water partition coefficient for TAME was measured, increasing the small set of environmentally relevant data available for this oxygenate. No literature measurement could be found for the K_{ow} of TMP; hence, the measurement above represents its first reported experimental value. The GCSKOW and ClogP methods were found to be the best predict the compounds housed in the limited database investigated. GSCKOW showed its least accuracy for ethanol and ClogP was least accurate in predicting toluene.

APPENDIX F

F-1 Relative gas liquid chromatography

Relative gas liquid chromatography [RGLC] (Orbey and Sandler, 1991) was used to measure the infinite dilution activity coefficients of several solutes in water. Among the list of organic solutes investigated, TAME, a possible oxygenate additive was investigated. No previously published measurements are available for this additive.

The work presented here was performed at the University of Delaware (USA), using the same equipment utilised by Sandler and co-workers in the derivation and explication of the RGLC method (Orbey and Sandler, 1991; Tse et al., 1992). The experimental measurements performed in this work are essentially a continuation of data published by Tse et al. (1992).

RGLC is particularly apt for the measurement of infinite dilution activity coefficients in water for several reasons:

- Water is a relatively volatile solvent; RGLC does not require exact knowledge of the amount of water in the column owing to the relative nature of the technique. Thus, water stripped from the column is of no significance provided that the amount of water remaining in the column is sufficient to ensure infinite dilution of the injected solute.
- This technique is relatively quick and easy.
- Exact control of flow rate and column pressure is not necessary owing to the relative nature of the technique.

The RGLC method uses the ratio of retention times for a known solute and unknown solute with respect to an inert solute. This technique alleviates the importance of knowing the weight of solvent in the column, compressibility of the gas in the column, the carrier gas flow rate, and the pressure at the entrance and exit of the column. All of the above factors are otherwise integral control parameters necessary in the absolute measurement of infinite dilution activity coefficients using regular gas-liquid chromatography.

Details of the theory and derivation of the RGLC method are available in Orbey and Sandler (1991). For reasons of brevity, the two equations required to calculate infinite dilution activity coefficients from the RGLC method are presented below:

$$\frac{\gamma_A^\infty}{\gamma_B^\infty} = \frac{P_B^{sat}}{P_A^{sat}} \alpha_{BA} \qquad \textbf{(F-1)}$$

where

$$\alpha_{BA} = \frac{t_B - t_{ref}}{t_A - t_{ref}} \qquad \textbf{(F-2)}$$

Hence, on knowing the infinite dilution activity coefficient of a solute (B) in a given solvent (γ_B^∞), and vapour pressures for both solutes (P_B^{sat}, P_A^{sat}) at the column temperature, the infinite dilution of an unknown solute (A) in the same solvent (γ_A^∞) can be calculated, if the GC retention times of both solutes (t_B, t_A) with respect to an inert species (t_{ref}, normally butane gas) are measured.

Experimental

Materials

All chemicals used in this experiment were supplied by Aldrich. Owing to the nature of GLC methods, it was not necessary for chemicals to be purified before use (Tse et al., 1992).

Apparatus and procedure

A schematic diagram of the equipment can be found below in Figure F-1. In all measurements a Hewlett-Packard Model 5890A gas chromatograph equipped with a flame ionisation detector (FID) linked to an integrator was used. The FID was utilised, as it does not respond to water, which was continuously stripped off the column. Thus, accurate detection of solute peaks was facilitated. A five metre long, 1/8-inch stainless steel column, packed with solid support

(Chromosorb GHP, 80/100 mesh) loaded with approximately 3 g of water, was used. It was found that this amount of water was enough to run the column for approximately 4 h, depending on the carrier gas flow rate and the column temperature and head pressure. As the GC runs continued, small amounts of water were added to the column periodically to reload the stationary phase with this relatively volatile solvent. An attempt was made to modify the RGLC technique of Tse et al. (1992) by adding a water pre-saturator to the apparatus. This addition was made to saturate the helium carrier gas with water; thus, reducing the stripping rate of water off the column.

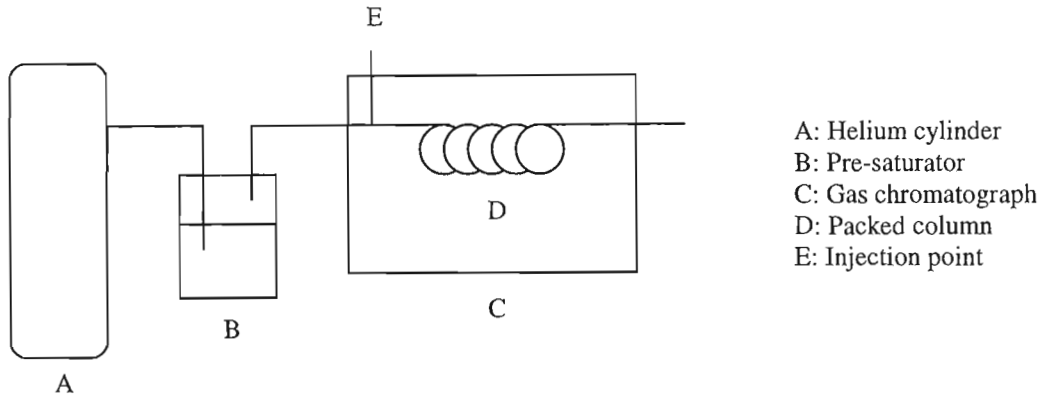

Figure F-1: Schematic of gas-liquid chromatography apparatus

Accurate measurements of carrier gas flow rates and column inlet and exit pressures were not made, as they are not necessary in the RGLC technique. Typical runs consisted of a head pressure of less than 2 bar (gauge) and a helium carrier gas flow rate of between 30 and 40 mL/min. The residence time of injected butane gas was used to determine t_{ref}. The butane gas was injected periodically to maintain a record of changing conditions in the system. Chloroform and carbon tetrachloride were used as standard solutes, as their activity coefficients in water are available in literature. Choice of which standard to use depended on the residence time of the unknown solute. Each chemical was injected separately into the gas chromatograph to determine approximate retention times for identification purposes. Next, chemicals were injected in groups together with the selected standard solute. The injection volume, which ranged between 0.1 and 0.5 μL, was determined by observing the response of the FID to the solute injections. The runs were performed over three temperatures.

Results and discussion

Six organic chemicals were investigated at the temperatures of 25, 35, and 45°C. This temperature range was selected as it reflects ambient conditions associated with environmental studies. Chloroform and carbon tetrachloride were used as the standard reagents. Tse et al. (1992) has previously reported limiting activity coefficients for chloroform in water, while Wright et al. (1992) has measured aqueous infinite dilution activity coefficients for carbon tetrachloride. As the temperatures investigated in this work differed from those in the literature references, the activity coefficients of the standard reagents were linearly interpolated from the results reported by Wright et al. (1992) and Tse et al. (1992) using the following relationship:

$$\left[\frac{\partial \ln \gamma_i^{\infty}}{\partial(1/T)}\right]_P = \frac{H_i^{E,\infty}}{R} \qquad \textbf{(F-3)}$$

where $H_i^{E,\infty}$ is the infinite dilution excess partial molar enthalpy of the solute. Interpolation of activity coefficient data using this temperature dependency has been suggested and used by several authors (Tse and Sandler. 1992; Eckert and Sherman, 1996).

For each solute, at each given temperature, at least 9 runs were performed in order to obtain a representative average for the solutes' retention time. The average retention time ratios from these measurements can be found in Table F-1 below. All solute vapour pressures were estimated from the parameters and suggested correlation as found in Reid et al. (1987); except for TAME, which was estimated using the correlation and parameters found in Appendix D of this dissertation.

An attempt was made to improve the procedure as developed by Tse et al. (1992) through the addition of a pre-saturator cell to the helium carrier gas line. The pre-saturator consisted of an airtight cell with an inlet line connected to a one-way valve. The inlet line extended below the water level in the cell. An exit line, which was suspended above the water line was connected to another one-way valve. This valve was closed at start-up to allow pressure to build up in the pre-saturator cell. It was hoped that the introduction of the pre-saturator would allow the number of GC runs to be extended by slowing solvent stripping. Although this objective was

accomplished, it came at the expense of a much longer start-up time. The column pressure took longer to build-up as a result of the large pressure drop, which was affected over the pre-saturator cell. It was, therefore, decided that the pre-saturator did not merit significant improvement to the experimental set-up. It was subsequently, removed towards the end of the solute runs. Its addition or removal did not seem to affect the retention ratios measured.

Table F-1: Infinite dilution activity coefficients of several solutes in water obtained from relative gas-liquid chromatography results

Solute	Temperature [ºC]	Vapour pressure [bar]	α_{BA}	γ_i^{∞}
Chloroform†	25	0.2623	-	827
	35	0.3955	-	847
	45	0.5787	-	853
Carbon tetrachloride†	25	0.1525	-	9485
	35	0.2335	-	8999
	45	0.3464	-	8431
Heptane†	25	0.0607	4.40	15723
	35	0.0981	5.03	17185
	45	0.1528	5.26	17001
Cyclohexane†	25	0.1304	5.50	9144
	35	0.2011	5.06	8431
	45	0.3003	3.98	6549
MTBE‡	25	0.3336	0.05	207
	35	0.4952	0.06	271
	45	0.7151	0.06	242
Benzene‡	25	0.1266	0.30	3478
	35	0.1973	0.32	3395
	45	0.2974	0.25	2483
TAME†	25	0.1006	0.21	447
	35	0.1579	0.25	536
	45	0.2397	0.31	641
Heptene†	25	0.0748	5.22	15111
	35	0.1191	4.19	11784
	45	0.1833	4.24	11425

Note: † Chloroform used as reference solute

‡ - Carbon tetrachloride used as reference solute

Acknowledgements

Acknowledgement is made of Prof. S.I Sandler's input into the above work; as well as, Cory Mulcahy, an undergraduate student at the University of Delaware. Mr. Mulcahy served as a laboratory technician and assisted in the measurement of the above solutes.

APPENDIX G

G-1 Regression of P-x data to obtain infinite dilution activity coefficients

Several methods for the extraction of limiting activity coefficients from VLE data have been proposed (Gautreaux and Coates, 1955). Ellis and Jonah (1962) have proposed a successful regression method, which has been extended by Maher and Smith (1979) to regress systems, which are non-linear according to the Ellis and Jonah (1962) method. The Gautreaux and Coates (1955) expression for isothermal total-pressure-composition measurements has already been presented in this dissertation and can be found in Appendix D. For convenience, it is reproduced below. This method has been used previously, by Pividal et al. (1992) and Wright et al. (1992), to regress infinite dilution activity coefficients from isothermal data.

$$\gamma_i^{j,\infty} = \varepsilon_i^{\infty} \frac{P_j^{sat}}{P_i^{sat}} \left(1 + \frac{\beta_j}{P_j^{sat}} \left[\frac{\partial P}{\partial x_1} \right]_{T, x_1 \to 0} \right)$$

(D-1)

where

$$\varepsilon_i^{\infty} = \exp\left(\frac{\left(B_{ii} - V_i^L\right)\left(P_j^{sat} - P_i^{sat}\right) + \delta_{ij} P_j^{sat}}{RT} \right)$$

$$\beta_j = 1 + P_j^{sat} \left(\frac{B_{jj} - V_j^L}{RT} \right)$$

$$\delta_{ij} = 2B_{ij} - B_{ii} - B_{jj}$$

Wright et al. (1992) suggests an approximation of Equation (D-2) if measurements are performed at sufficiently low pressures at which vapour phase non-idealities are negligible:

$$\gamma_i^{j,\infty} = \frac{1}{P_i^{sat}} \left(P_j^{sat} + \left[\frac{\partial P}{\partial x_1} \right]_{T, x_1 \to 0} \right)$$

(G-1)

Wright et al. (1992) have reported an error of 1-2 % upon using Equation (G-1) to regress P-x-y data. Appendix D of this dissertation contains measured isothermal P-x-y data, which has been regressed to obtain limiting activity coefficients. The systems investigated showed errors of about 3.5 % on using Equation (G-1) to regress infinite dilution activity coefficients.

Limiting activity coefficients for MTBE, TAME and ethanol were required in both water and hydrocarbons (heptane, toluene and TMP) to calculate selectivity factors for the oxygenates with respect to water and a pseudo-fuel phase. Most of the required infinite dilution activity coefficients for oxygenate in the respective hydrocarbon solvents were not found in literature; however, the relevant isothermal P-x data sets were available. As all the relevant P-x-y data sets for the oxygenate-hydrocarbon system were sub-atmospheric, consequently approaching ideal gas conditions, Equation (G-1) was used to regress the data.

As the accuracy of infinite dilution activity coefficient regression depends on the pressure-liquid composition relationship [as indicated in Equations (D-2) and (G-1) above], the experimental P-x data were fitted using the regression method, which demonstrated the best fitment correlation coefficient. The linear correlation coefficients obtained from the regression technique, as used by Wright et al. (1992), were closer to one than those regressed using the methods of Ellis and Jonah (1962) and Maher and Smith (1979). Accordingly, Equation (D-2) was used to fit the P-x data; Thus, the constant, b, is equal to the pressure-composition derivative required for insertion into Equation (G-1):

$$P = a + bx_1 \qquad \textbf{(D-2)}$$

Table G-1, below, contains information regarding the several oxygenate-hydrocarbon systems investigated including their literature references, their regressed pressure-composition derivatives and their linear correlation coefficients (R^2), as fitted to Equation (D-2). The vapour pressures required in Equation (G-1) were estimated using the correlation reported in Reid et al. (1987); except for TAME, which was estimated using the correlation and fitted parameters found in Appendix D of this dissertation.

Table G-1: Infinite dilution activity coefficients, limiting pressure-liquid composition derivatives and linear correlation coefficients for MTBE, TAME, and ethanol in heptane, TMP and toluene as regressed using the method of Wright et al. (1992)

System	P-x-y data reference	Temperature [°C]	Linear correlation coefficient, R^2	$\left[\frac{\partial P}{\partial x_1}\right]_{T,x_1\to 0}$ [kPa]	γ_i^{∞}
TAME(1)-	Moessner et al.	25	0.9996	5.76	1.18
Heptane(2)	(1997)	35	0.9998	8.50	1.13
TAME(1)-	Antosik and	20	0.9977	6.20	1.15
Toluene(2)	Sandler (1994)	38	0.9994	13.14	1.13
		60	0.9999	28.54	1.11
TAME(1)-	Antosik and	20	0.9985	3.85	1.14
TMP(2)	Sandler (1994)	38	0.9999	8.41	1.13
		60	0.9999	18.76	1.12
MTBE(1)-	Wu et al. (1991)	15	0.9615	29.10	1.51
TMP(2)		25	0.9985	41.34	1.43
		38	0.9946	59.85	1.29
		60	0.9999	110.3	1.18

G-2 Interpolation of infinite dilution activity coefficients with respect to temperature

The interpolation of infinite dilution activity coefficient data was performed using the temperature dependency relationship suggested by Tse and Sandler. (1992) and Eckert and Sherman (1996).

$$\left[\frac{\partial \ln \gamma_i^{\infty}}{\partial(1/T)}\right]_P = \frac{H_i^{E,\infty}}{R} \qquad \textbf{(F-3)}$$

Tables G-2, G-3 and G-4 display limiting activity coefficients for the oxygenates in heptane, toluene and TMP respectively at various temperatures. Included in the tables are the limiting activity coefficients interpolated at the environmentally significant temperature of 25°C.

Table G-2: Infinite dilution activity coefficients of oxygenates in heptane at various temperatures

System	Reference	Temperature [°C]	γ_i^{∞}	$H_i^{E,\infty}$ [kJ/mol]
MTBE	Pividal et al. (1992a)	40	1.31	
	Pividal et al. (1992a)	50	1.22	
	(interpolated)	25	1.47	5.99
Ethanol	Thomas et al. (1982)	20	51	
	Pividal et al. (1992a)	40	39.94	
	Pividal et al. (1992a)	50	16.27	
	(interpolated)	25	47.3	26.59

Table G-3: Infinite dilution activity coefficients of oxygenates in toluene at various temperatures

System	Reference	Temperature [°C]	γ_i^{∞}	$H_i^{E,\infty}$ [kJ/mol]
MTBE	Appendix D	35	1.18	
	Appendix D	45	1.15	
	Appendix D	50	1.14	
	(interpolated)	25	1.21	1.93
TAME	Antosik and Sandler (1994)	20	1.15	
	Antosik and Sandler (1994)	38	1.13	
	Appendix D	45	1.13	
	Antosik and Sandler (1994)	60	1.11	
	(interpolated)	25	1.14	0.739
Ethanol	Thomas et al. (1982)	20	18.4	
	Brandani et al. (1991)	55	9.58	
	(interpolated)	25	16.6	14.9

Table G-4: Infinite dilution activity coefficients of oxygenates in TMP at various temperatures

System	Reference	Temperature [°C]	γ_i^{∞}	$H_i^{E,\infty}$ [kJ/mol]
TAME	Antosik and Sandler (1994)	20	1.14	
	Antosik and Sandler (1994)	38	1.13	
	Antosik and Sandler (1994)	60	1.12	
	(interpolated)	25	1.14	0.359
Ethanol	Thomas et al. (1982)	20	46	
	Thomas et al. (1982)	40	27	
	(interpolated)	25	40.0	20.3